### EUMETSAT Satellite Application Facility on Support to Operational Hydrology and Water Management



# Product Validation Report (PVR-02) for product H02 (PR-OBS-2)

# Precipitation rate at ground by MW cross-track scanners (with indication of phase)

Reference Number: SAF/HSAF/PVR-02/1.1

Issue/Revision Index: 1.1

Last Change: 30 September 2011

Validation Cluster Leader, with the support of the Project Management Team and of the Validation and Development Teams of the Precipitation

Cluster



(Product H02 – PR-OBS-2)

Doc.No: SAF/HSAF/PVR-02/1.1 Issue/Revision Index: 1.1

Date: 30/09/2011

Page: 2/177

### **DOCUMENT CHANGE RECORD**

| Issue / Revision | Date       | Description   |
|------------------|------------|---|
| 1.0              | 16/05/2011 | Baseline version prepared for ORR1 Part 2. Obtained by PVR-01 delivered during the Development Phase. |
| 1.1              | 30/09/2011 | Updates, acknowledging ORR1 Part 2 review board recommendation  |
| 1.2              | 16/01/2012 | Minor adjustments:  • Document reference number as "PVR-01" instead of "PVR"                          |



(Product H02 – PR-OBS-2)

Doc.No: SAF/HSAF/PVR-02/1.1 Issue/Revision Index: 1.1

Date: 30/09/2011

Page: 3/177

# Index

| 1 | The   | EUMETSAT Satellite Application Facilities and H-SAF                            | 14 |
|---|-------|--|----|
| 2 | Intro | oduction to product PR-OBS-1   | 15 |
|   | 2.1   | Sensing principle  | 15 |
|   | 2.2   | Algorithm principle  |    |
|   | 2.3   | Main operational characteristics   | 17 |
| 3 | Valid | dation strategy, methods and tools   | 18 |
|   | 3.1   | Validation team and work plan  | 18 |
|   | 3.2   | Validation objects and problems  | 20 |
|   | 3.3   | Validation methodology   | 20 |
|   | 3.4   | Ground data and tools used for validation                                      | 21 |
|   | 3.5   | Spatial interpolation for rain gauges  | 24 |
|   | 3.6   | Techniques to make observation comparable: up-scaling technique for radar data | 24 |
|   | 3.6.2 | 1 Average of hi-res ground validation data                                     | 25 |
|   | 3.6.2 | 2 Smoothing of radar precipitation   | 26 |
|   | 3.7   | Temporal comparison of precipitation intensity                                 | 27 |
|   | 3.8   | Large statistic: Continuous and multi-categorical                              | 27 |
|   | 3.9   | Case study analysis  | 31 |
|   | 3.10  | Next steps   | 31 |
| 4 | Gro   | und data used for validation activities  | 32 |
|   | 4.1   | Introduction   | 32 |
|   | 4.2   | Rain Gauge in PPVG   | 32 |
|   | 4.2.  | 1 The networks   | 32 |
|   | 4.2.2 | 2 The instruments  | 34 |
|   | 4.2.3 | 3 Data processing  | 35 |
|   | 4.2.4 | 4 Some conclusions   | 36 |
|   | 4.3   | Radar data in PPVG   | 36 |
|   | 4.3.3 | 1 The networks   | 36 |
|   | 4.3.2 | 2 The instruments  | 38 |
|   | 4.3.3 | 3 Data processing  | 39 |
|   | 4.3.4 | 4 Some conclusions   | 40 |
|   | 4.4   | Rain gauge and radar data integrated products in PPVG                          | 42 |
|   | 4.4.  | 1 INCA system  | 43 |
|   | 4.4.2 | 2 RADOLAN system   | 44 |
|   | 4.4.3 | 3 Some conclusions   | 46 |
|   | 4.5   | Ground data in Belgium (IRM)   | 47 |
|   | 4.5.3 | 1 Radar data   | 47 |
|   | 4.6   | Ground data in Bulgaria (NIMH)   | 48 |
|   | 4.6.3 | 1 Rain gauge   | 48 |
|   | 4.7   | Ground data in Germany (BfG)   | 50 |
|   | 4.7.  | 1 Rain gauge   | 50 |
|   | 4.7.2 | 2 Radar data   | 51 |
|   | 4.8   | Ground data in Hungary (OMSZ)  | 53 |
|   | 4.8.3 | 1 Radar data   | 53 |
|   |       |  |    |



(Product H02 – PR-OBS-2)

Doc.No: SAF/HSAF/PVR-02/1.1 Issue/Revision Index: 1.1

Date: 30/09/2011 Page: 4/177

|     | A.O. Convert data in Natur (DDC Uni Fa)  |     |
|-----|--|-----|
| 4   | 4.9 Ground data in Italy (DPC, Uni Fe)   |     |
|     | 4.9.1 Rain gauge   |     |
|     | 4.9.2 Radar data   |     |
| 4   | 4.10 Ground data in Poland (IMWM)  |     |
|     | 4.10.1 Rain gauge  |     |
| 4   | 4.11 Ground data in Slovakia (SHMU)  | 67  |
|     | 4.11.1 Rain gauge  | 67  |
|     | 4.11.2 Radar data  | 68  |
| 4   | 4.12 Ground data in Turkey   | 71  |
|     | 4.12.1 Rain gauge  | 71  |
| 4   | 4.13 Conclusions   | 75  |
| 5   | Validation results: case study analysis  | 76  |
| į   | 5.1 Introduction   | 76  |
|     | 5.2 Case study analysis in Belgium (IRM)   | 77  |
|     | 5.2.1 Case study: August 14 <sup>th</sup> -17 <sup>th</sup> , 2010                             |     |
|     | 5.2.2 Case study: August 22 <sup>th</sup> -24 <sup>th</sup> , 2010                             |     |
|     | 5.2.3 Case study: November 12 <sup>th</sup> - 15 <sup>th</sup> , 2010                          |     |
|     | 5.3 Case study analysis in Germany (BfG)   |     |
|     | 5.3.1 Case study: August 7 <sup>th</sup> , 2010 (River Neiße, Oder, Spree and Elbe catchments) |     |
|     | 5.3.2 Case study: June 3 <sup>rd</sup> , 2010 (River Danube catchment)                         |     |
|     | 5.3.3 Case study: December 5 <sup>th</sup> /6 <sup>th</sup> , 2010 (River Rhine catchment)     |     |
|     | 5.4 Case study analysis in Hungary (OMSZ)  |     |
| •   | 5.4.1 Case study: July 18 <sup>th</sup> , 2010   |     |
|     | 5.4.2 Case study: September 2010   |     |
|     | 5.4.2 Case study. September 2010   |     |
|     |  |     |
|     |  |     |
|     | 5.6 Case study analysis in Poland (IMWM)   |     |
|     | 5.6.1 Case study: August 15 <sup>th</sup> , 2010   |     |
|     | 5.6.2 Case study: September 27 <sup>th</sup> , 2010  |     |
|     | 5.7 Case study analysis in Slovakia  |     |
|     | 5.7.1 Case study: August 15 <sup>th</sup> , 2010   |     |
| į   | 5.8 Case study analysis in Turkey (ITU)  | 112 |
|     | 5.8.1 Case study: October 20 <sup>th</sup> , 2010  |     |
| !   | 5.9 Conclusions  |     |
| 6   | Validation results: long statistic analysis  |     |
| (   | 6.1 Introduction   |     |
| (   | 6.2 The continuous statistic   | 116 |
| (   | 6.3 The multi-categorical statistic  | 122 |
| (   | 6.4 User requirement compliance  | 124 |
| 7   | Conclusions  | 124 |
| -   | 7.1 Summary conclusions on the status of product validation                                    | 124 |
| •   | 7.2 Next steps   | 125 |
| 8   | Annex 1: Status of working group   | 127 |
| 9   | Annex 2: Working Group 1 "Rain gauge data"   |     |
| 10  |  |     |
| 11  |  |     |
| vis | ibility  | 143 |



(Product H02 – PR-OBS-2)

Doc.No: SAF/HSAF/PVR-02/1.1 Issue/Revision Index: 1.1

Date: 30/09/2011 Page: 5/177

| 12 | Annex 5: Working Group 3 "INCA Precipitation for PPV"                                    | . 149 |
|----|--|-------|
|    | Annex 6: Working Group 4 "PR-ASS-1 (COSMO grid) validation"                              |       |
|    | Annex 7: Working Group 5 "Geographical maps – distribution of error"                     |       |
| 15 | Annex 8: Comments on the Validation Results for Products PR-ORS-1, PR-ORS-2 And PR-ORS-3 | 171   |



(Product H02 – PR-OBS-2)

Doc.No: SAF/HSAF/PVR-02/1.1 Issue/Revision Index: 1.1

Date: 30/09/2011

Page: 6/177

### List of tables

| Table 1 H-SAF Product List   | 15    |
|--|-------|
| Table 2 List of the people involved in the validation of H-SAF precipitation products                    | 19    |
| Table 3 Number and density of raingauges within H-SAF validation Group                                   | 22    |
| Table 4 Summary of the raingauge characteristics   | 22    |
| Table 5 Data pre-processing strategies   | 24    |
| Table 6 Left) Original Gaussian matrix – Right)Reduced matrix to dimensions M xK                         | 26    |
| Table 7 Classes for evaluating Precipitation Rate products   |       |
| Table 8 Number and density of raingauges within H-SAF validation Group                                   | 34    |
| Table 9 Summary of the raingauge characteristics   |       |
| Table 10 Data pre-processing strategies  | 35    |
| Table 11 Matching strategies for comparison with H01 and H02   | 36    |
| Table 12 Inventory of the main radar data and products characteristics in Belgium, Italy, Hungary        |       |
| Table 13 Inventory of the main radar data and products characteristics in Poland, Slovakia, Turkey.      |       |
| Table 14 INCA Questionnaire  | 46    |
| Table 15 Precipitation data used at BfG for validation of H-SAF products                                 | 50    |
| Table 16 Location of the 16 meteorological radar sites of the DWD  | 52    |
| Table 17 Main characteristics of the Hungarian radar network   | 54    |
| Table 18 Characteristics of the three radar instruments in Hungary                                       | 54    |
| Table 19 Characteristics of the SHMÚ radars  | 69    |
| Table 20 QA flags descriptions (modified from Shafer et al., 1999)                                       | 72    |
| Table 21 Scores obtained with the comparison with radar data (* in mm h <sup>-1</sup> )h                 | 79    |
| Table 22 Scores obtained with the comparison with radar data (* in mm h <sup>-1</sup> )                  | 82    |
| Table 23 Scores obtained with the comparison with radar data (* in mm h <sup>-1</sup> )h                 | 85    |
| Table 24 Results of the categorical statistic of the validation for 7th August 2010                      | 88    |
| Table 25 Results of the categorical statistic of the validation for whole August 2010                    | 88    |
| Table 26 Continuous statistic  | 90    |
| Table 27 Results of the categorical statistic of the validation for 3rd June 2010                        | 92    |
| Table 28 Results of the categorical statistic of the validation for whole June 2010                      | 92    |
| Table 29 Continuous statistic  | 93    |
| Table 30 Results of the categorical statistic of the validation for 5/6th December 2010                  | 96    |
| Table 31 Results of the categorical statistic of the validation for whole December 2010                  | 96    |
| Table 32 Continuous statistic  |       |
| Table 33 Results of the categorical statistics obtained for PR-OBS-1 on the base of all data available   | on e  |
| the 15 <sup>th</sup> August 2010   |       |
| Table 34 Results of the categorical statistics obtained for H02 on the base of all data available on the |       |
| 27 <sup>th</sup> September 2010  |       |
| Table 35 Scores for continuous statistics for precipitation threshold of 0,25 mm/h                       |       |
| Table 36 Scores for dichotomous statistics for precipitation threshold of 0,25 mm/h                      |       |
| Table 37 Statistic scores for H02  |       |
| Table 38 Accuracy requirements for product PR-OBS-1 [RMSE (%)]   | . 115 |
| Table 39 split in four sections, one for each season, reports the Country/Team results side to side      | . 116 |
| Table 40 The main statistical scores evaluated by PPVG for H02 during the winter period. The rain        |       |
| rates lower than 0.25 mm/h have been considered as no rain   |       |
| Table 41 The main statistical scores evaluated by PPVG for H02 during the spring period. The rain        |       |
| lower than 0.25 mm/h have been considered as no rain   | . 118 |
|  |       |



(Product H02 - PR-OBS-2)

Doc.No: SAF/HSAF/PVR-02/1.1 Issue/Revision Index: 1.1

Date: 30/09/2011 Page: 7/177

| Table 42 The main statistical scores evaluated by PPVG for H02 during the summer period. The rain             |     |
|---|-----|
| rates lower than 0.25 mm/h have been considered as no rain  |     |
| Table 43 The main statistical scores evaluated by PPVG for H02 during the autumn period. The rain             | 1   |
| rates lower than 0.25 mm/h have been considered as no rain  |     |
| Table 44 The main statistical scores evaluated by PPVG for H02 during one year of data 1 <sup>st</sup> Decemb |     |
| 2009- 30 <sup>th</sup> November 2010 . The rain rates lower than 0.25 mm/h have been considered as no rain    | 121 |
| Table 45 The averages POD, FAR and CSI deduced comparing H02 with radar data                                  | 122 |
| Table 46 The contingency table for the three precipitation classes defined in table 7 evaluated by            |     |
| comparing H02 with radar data   | 122 |
| Table 47 The averages POD, FAR and CSI deduced comparing H02 with rain gauge data                             | 123 |
| Table 48 The contingency table for the three precipitation classes defined in table 7 evaluated by            |     |
| comparing H02 with rain gauge data  | 123 |
| Table 49 User requirement and compliance analysis for product H02   | 124 |
| Table 53 Summary of the raingauge characteristics   | 130 |
| Table 54 Number and density of raingauges within H-SAF validation Group                                       | 131 |
| Table 55 Data pre-processing strategies   | 132 |
| Table 56 Matching strategies for comparison with H01 and H02  | 133 |
| Table 57 Matching strategies for comparison with H03 and H05  | 133 |
| Table 58 List of products used  | 142 |
| Table 59 List of contact persons  | 151 |
| Table 60 Questionnaire  | 154 |
| Table 61 List of precipitation events selected for statistical analysis                                       | 158 |
| Table 62 Mean Residual and Mean Absolute Residual values obtained for three algorithms for spat               | ial |
| interpolation using cross-validation approach   | 170 |
| Table 63 Simplified compliance analysis for product PR-OBS 1-2-3  | 171 |
| Table 64 Errors of the ground reference provided by all validation groups                                     | 172 |
| Table 65 RMSE% and standard deviation of interpolation algorithms for 3 different regular grids               | 175 |
|   |     |
|   |     |
| List of figures   |     |
| Figure 1 Conceptual scheme of the EUMETSAT application ground segment   | 14  |
| Figure 2 Current composition of the EUMETSAT SAF network (in order of establishment)                          |     |
| Figure 3 Geometry of cross-track scanning for AMSU  |     |
| Figure 4 Flow chart of the AMSU-MHS precipitation rate processing chain                                       |     |
| Figure 5 Structure of the Precipitation products validation team  |     |
| Figure 6 The network of 3500 rain gauges used for H-SAF precipitation products validation                     |     |
| Figure 7 The networks of 54 C-band radars available in ther H-SAF PPVG  |     |
| Figure 8 Geometry - Geometry of cross-track scanning for AMSU   | 25  |
| Figure 9 Left) Gaussian filter – Right) section of gaussian filter  | 25  |
| Figure 10 Main steps of the validation procedure in the PPVG  | 28  |
| Figure 11 Rain gauge networks in PPVG   |     |
| Figure 12 Correlation coefficient between raingauge pairs as function of the distances between the            |     |
| gauges. Colours refer to the months of the year 2009  |     |
| Figure 13 Radar networks in PPVG  | 37  |



(Product H02 – PR-OBS-2)

Doc.No: SAF/HSAF/PVR-02/1.1 Issue/Revision Index: 1.1

Date: 30/09/2011

Page: 8/177

| Figure 15 Coverage of Europe by the INCA and RADOLAN systems                                       | 43     |
|--|--------|
| Figure 16 Procedure of the RADOLAN online adjustment (hourly precipitation amount on 7 August      | :      |
| 2004 13:50 UTC)  | 45     |
| Figure 17 Meteorological radar in Belgium  | 47     |
| Figure 18 Distribution of the raingauge stations of Iskar River Basin                              | 48     |
| Figure 19 Distribution of the raingauge stations of Chepelarska River Basin                        |        |
| Figure 20 Distribution of the raingauge stations of Varbica River Basin                            | 49     |
| Figure 21 Network of rain gauges in Germany  | 51     |
| Figure 22 Pluvio with Remote Monitoring Module   | 51     |
| Figure 23 Left: radar compound in Germany (March 2011); Right: location of ombrometers for on      | line   |
| calibration in RADOLAN; squares: hourly data provision (about 500), circles: event-based hourly d  | ata    |
| provision (about 800 stations)   | 52     |
| Figure 24 Flowchart of online calibration RADOLAN (DWD, 2004)                                      | 53     |
| Figure 25 The location and coverage of the three meteorological Doppler radars in Hungary          | 53     |
| Figure 26 Correlation between rainrates detected by two close by stations as function of the dista | nce    |
| between the two stations. Colors refer to the month along 2009                                     | 56     |
| Figure 27 Distribution of the raingauge stations of the Italian network collected by DPC           | 57     |
| Figure 28 Italian radar network coverage   | 58     |
| Figure 29 Graphical mosaic of reflectivity (CAPPI at 2000 m) for the event of 04/18/08 at 0015 U.T | .C. 59 |
| Figure 30 Architecture of the Italian radar network  | 60     |
| Figure 31 Schematic representation of radar data processing chain                                  | 61     |
| Figure 32 Measured (upper panel) and attenuation corrected (lower panel) PPI (1.0 deg) of reflect  | ivity  |
| observed on 09/14/08 at 0500 U.T.C. by the polarimetric radar operated by Piemonte and Liguria     |        |
| regions  | 62     |
| Figure 33 Hydrometeor classes as detected by the classification algorithm starting from the radar  |        |
| variables observed on 09/14/08 at 0500 U.T.C. by the polarimetric radar operated by Piemonte an    | d      |
| Liguria regions  |        |
| Figure 34 Measured (upper panel) and VPR corrected (lower panel) PPI of reflectivity observed on   |        |
| 03/25/07 at 0930 U.T.C. by the polarimetric radar located in Gattatico (Emilia Romagna, Italy)     | 64     |
| Figure 35 Cumulated radar rainfall estimates versus gage measurements for the event observed o     |        |
| 06/01/2006 by the dualpolarized radar located in Settepani (Liguria, Italy)                        | 65     |
| Figure 36 ATS national network in Poland   |        |
| Figure 37 Map of SHMÚ rain gauge stations: green – automatic (98), blue – climatological (586), re |        |
| hydrological stations in H-SAF selected test basins (37)   |        |
| Figure 38 Map of SHMÚ radar network; the rings represent maximum operational range – 240 km        |        |
| radar at Maly Javornik (left), 200 km for radar at Kojsovska hola (right)                          |        |
| Figure 39 Map of relative RMSE (left) and Mean Error (right) over the SHMÚ radar composite         |        |
| Figure 40 Automated Weather Observation System (AWOS) station distribution in western part of      |        |
| Turkey   |        |
| Figure 41 H01 and H02 products footprint centers with a sample footprint area as well as the Awo   |        |
| ground observation sites   |        |
| Figure 42 Meshed structure of the sample H01 and H02 products footprint                            |        |
| Figure 43 Synoptic situation on 15 August 2010 at 6 UTC (zoom in the surface map)                  |        |
| Figure 44 H02 image of August 15, 2010 at 12.08 (left) compared with upscaled radar at 12.10 (rig  | •      |
| The scale corresponds to thresholds of 0.1, 1., and 10. mm h-1h-1                                  | 78     |



(Product H02 – PR-OBS-2)

Doc.No: SAF/HSAF/PVR-02/1.1 Issue/Revision Index: 1.1

Date: 30/09/2011 Page: 9/177

| Figure 45 H02 image of August 15th, 2010 at 12.09 (left) compared with upscaled radar at 12.10 (right                    |   |
|--|---|
| – the same radar image as above, but upscaled on a different grid). The scale corresponds to                             |   |
| thresholds of 0.1, 1., and 10. mm h-1  | 3 |
| Figure 46 H02 image of August 16th, 2010 at 2.07 (left) compared with upscaled radar at 2.05 (right).                    |   |
| The scale corresponds to thresholds of 0.1, 1., and 10. mm h-1   | ) |
| Figure 47 Time evolution of fraction area with rain, average rain rate over this area (threshold 0.25                    |   |
| mm/h), RMSE and ETS during the present case study80  | ) |
| Figure 48 Surface map on 22 August 2010 at 06 UTC (MSLP and synoptic observations)                                       | ) |
| Figure 49 H02 image of August 23th, 2010 at 2.35 (left) compared with upscaled radar at the same                         |   |
| time (right). The scale corresponds to thresholds of 0.1, 1., and 10. mm h-1   | L |
| Figure 50 H02 image of August 23th, 2010 at 12.23 (left) compared with upscaled radar at 12.25                           |   |
| (right). The scale corresponds to thresholds of 0.1, 1., and 10. mm h-1  | L |
| Figure 51 H02 image of August 23th, 2010 at 12.23 (left) compared with upscaled radar at 12.25                           |   |
| (right). The scale corresponds to thresholds of 0.1, 1., and 10. mm h-1  | ) |
| Figure 52 Time evolution of fraction area with rain, average rain rate over this area (threshold 0.25                    |   |
| mm/h), RMSE and ETS during the present case study83  | } |
| Figure 53 Surface map on 13 November 2010 at 06 UTC (MSLP and synoptic observations)                                     |   |
| Figure 54 H02 image of November 13th, 2010 at 12.53 (left) compared with upscaled radar at 12.55                         |   |
| (right). The scale corresponds to thresholds of 0.1, 1., and 10. mm h-1  | ļ |
| Figure 55 H02 image of November 15th, 2010 at 1.29 (left) compared with upscaled radar at 1.30                           |   |
| (right). The scale corresponds to thresholds of 0.1, 1., and 10. mm h-1  | ļ |
| Figure 56 Time evolution of fraction area with rain, average rain rate over this area (threshold 0.25                    |   |
| mm/h), RMSE and ETS during the present case study85  | ; |
| Figure 57 Synopsis for Central Europe for 07th August 2010 (FU Berlin, http://wkserv.met.fu-berlin.de)                   |   |
| 86   | j |
| Figure 58 two-day totals (ending at 9th August, 0 UTC) interpolated on a 1°x1° evaluation grid as                        |   |
| derived from SYNOP messages (Global Precipitation Climatology Centre, GPCC operated by DWD) 86                           | j |
| Figure 59 Hourly precipitation sum [mm] for H02 satellite data (crosses, time stamp 2010-08-07 11:58                     |   |
| UTC, station Rome) and for RADOLAN-RW (left, filled raster, 2010-08-07 12:50 UTC) and station data                       |   |
| (right, dots, 2010-08-07 13:00 UTC)  | 1 |
| Figure 60 Contingency table statistic of rain rate [mmh h <sup>-1</sup> ] for H02 vs. radar data. Left: for 7th August   |   |
| 2010, Right: for whole August 2010   | ) |
| Figure 61 Contingency table statistic of rain Rate [mm h <sup>-1</sup> ] for H02 vs. rain gauge data. Left: for 7th      |   |
| August 2010, Right: for whole August 2010  | ) |
| Figure 62 Synopsis for Central Europe for 03rd June 2010 (FU Berlin, http://wkserv.met.fu-berlin.de)                     |   |
| 90   |   |
| Figure 63 12h totals of precipitation(ending (FU at 3rd June 2010, 7 UTC)  | _ |
| Figure 64 Hourly precipitation sum [mm] for H02 satellite data (crosses, time stamp 2010-06-03 01:50                     |   |
| UTC, station Athens) and for RADOLAN-RW (left, filled raster, 2010-06-03 01:50 UTC) and station data                     |   |
| (right, dots 2010-06-03 02:00 UTC)   | _ |
| Figure 65 Contingency table statistic of Rain Rate [mm h <sup>-1</sup> ] for H02 vs. radar data Left: for 3rd June       |   |
| 2010, Right: for whole June 2010   |   |
| Figure 66 Contingency table statistic of rain rate [mm h <sup>-1</sup> ] for H02 vs. rain gauge data. Left: for 3rd June |   |
| 2010; Right: for whole June 2010   | , |
| Figure 67 Synopsis for Central Europe for 05th December 2010 (FU Berlin, http://wkserv.met.fu-                           |   |
| berlin.de)   |   |
| Figure 68 96h totals of precipitation94  | ŀ |



(Product H02 – PR-OBS-2)

Doc.No: SAF/HSAF/PVR-02/1.1 Issue/Revision Index: 1.1

Date: 30/09/2011 Page: 10/177

| Figure 69 Hourly precipitation sum [mm] for H02 satellite data (crosses, time stamp 2010-12-05 (   | ງ2:29    |
|--|----------|
| UTC) and for RADOLAN-RW (left, filled raster, 2010-12-05 02:50 UTC) and station data (right, dot   | S        |
| 2010-12-05 03:00 UTC)  | 95       |
| Figure 70 Hourly precipitation sum [mm] for H02 satellite data (crosses, time stamp 2010-12-06 (   | )2:18    |
| UTC) and for RADOLAN-RW (left, filled raster, 2010-12-06 02:50 UTC) and station data (right, dot   | S        |
| 2010-12-06 03:00 UTC)  | 95       |
| Figure 71 Contingency table statistic of Rain Rate [mm h <sup>-1</sup> ] for H02 vs. radar data. Left: for 5/6th   |          |
| December, Right: for whole December 2010   | 96       |
| Figure 72 Contingency table statistic of rain rate [mm h <sup>-1</sup> ] for H02 vs. rain gauge data. Left: for 5/   | 6th      |
| December; Right: for whole December 2010   | 97       |
| Figure 73 Synoptic chart at 00 UTC on 18 July 2010   | 98       |
| Figure 74 H02 product (left panel), Precipitation rate from the Hungarian radar network at its original radar network at its o | ginal    |
| resolution (right panel) at 00:30 UTC, at 2:15 UTC and at 12 UTC   | 99       |
| Figure 75 Synoptic chart at 00 UTC on 10 September 2010  | 100      |
| Figure 76 Precipitation rate from the Hungarian radar network at its original resolution at 11 UTC   | C (right |
| panel), H02 product at 11 UTC (left panel)   | 100      |
| Figure 77 H02 precipitation map at 12:16 UTC (top-left), at 12:27 (top-right) and raingauges hour  | ly       |
| precipitation cumulated at 13:00 UTC (bottom panel) of 06 July 2010  | 102      |
| Figure 78 Synoptic chart at 1200 UTC on 15th of August 2010  | 103      |
| Figure 79 Total lighting map of Poland showing electrical activity between 1145 and 1215 UTC or  | ո 15th   |
| of August 2010   | 104      |
| Figure 80 H02 at 1208 UTC on the 15th of August 2010 (right panel) and 10 minute precipitation   |          |
| interpolated from RG data from 1210 UTC (left panel)   | 104      |
| Figure 81 Scatter plot for measured (RG) and satellite derived (H-02) rain rate obtained for all H0  |          |
| on the 15 <sup>th</sup> of August 2010   |          |
| Figure 82 Percentage distribution of H02 precipitation classes in the rain classes defined using rain  |          |
| gauges (RG) data on the 15 <sup>th</sup> of August 2010  |          |
| Figure 83 Synoptic chart at 1200 UTC on 27th of September 2010   | 107      |
| Figure 84 PR-OBS-1 at 1251 UTC on the 27 <sup>th</sup> of September 2010 (right panel) and 10 minute   |          |
| precipitation interpolated from RG data from 1250 UTC (left panel)   |          |
| Figure 85 Scatter plot for measured (RG) and satellite derived (H-02) rain rate obtained for all H0  |          |
| on the 27 <sup>th</sup> of September 2010  |          |
| Figure 86 Percentage distribution of PR-OBS-1 precipitation classes in the rain classes defined usi  | -        |
| rain gauges (RG) data on the 27th of September 2010  |          |
| Figure 87 Synoptic situation on 15 August 2010 at 0:00 UTC   | 109      |
| Figure 88 Instantaneous precipitation fields from 15 August 2010 observed by H02 product (left   |          |
| column) and SHMU radar network (right column) corresponding to NOAA18 passage at 12:07 UT  |          |
| row) and NOAA19 passage at 12:08 UTC (second row)  |          |
| Figure 89 Atmospheric condition (20.10.2010; 06:00 GMT)  |          |
| Figure 90 Atmospheric condition (20.10.2010; 12:00 GMT)  |          |
| Figure 91 Comparison of H02 product and rain gauge   |          |
| Figure 92 Scatter diagram of rain gauge and H02 product (Red line is 45 degree line)   | 114      |
| Figure 96 Rain gauge networks in PPVG  |          |
| Figure 97 Correlation coefficient between raingauge pairs as function of the distances between t   |          |
| gauges. Colours refer to the months of the year 2009   |          |
| Figure 98 Volume scan procedure  |          |
| Figure 99 Distribution of rain gauges according their altitude above the sea level   | 143      |



(Product H02 – PR-OBS-2)

Doc.No: SAF/HSAF/PVR-02/1.1 Issue/Revision Index: 1.1

Date: 30/09/2011 Page: 11/177

| Figure 100 Radar horizon model output for Malý Javorník (left) and Kojšovská hoľa (right) radar site   |       |
|--|-------|
| Figure 101 Composite picture of minimum visible height above the surface over the whole radar  | . 144 |
| network. Compositing algorithm selects the minimum value from both radar sites   | . 145 |
| Figure 102 Distribution of rain gauges according to the minimum visible height of radar beam Figure 103 Scatterplot of log(R/G) versus station altitude shows general underestimation of                 |       |
| precipitation by radar   | . 146 |
| Figure 104 Scatterplot of log(R/G) versus radar beam altitude shows increased underestimation of radar for high and close to zero radar beam elevations  | 146   |
| Figure 105 Relative RMSE (left) and Mean Error (right) computed independently for each rain gaug   |       |
| station in radar range and corresponding trend lines extrapolated for beam elevation up to 1500m Figure 106 Final relative root mean square error map of radar measurements with regard to terrain       | 147   |
| visibility by current radar network of SHMÚ  |       |
| Figure 107 Final mean error map of radar measurements with regard to terrain visibility by current   |       |
| radar network of SHMÚ. General underestimation of precipitation by radars is observed  |       |
| Figure 108 Coverage of Europe by the INCA and RADOLAN systems  |       |
| Figure 109 Procedure of the RADOLAN online adjustment (hourly precipitation amount on 7 Augus  | t     |
| 2004 13:50 UTC)  | . 153 |
| Figure 110 Precipitation intensity field from 15 August 2010 15:00 UTC obtained by a) radars, b)   |       |
| interpolated raingauge data, c) INCA analysis and d) PR-OBS-1 product  | . 155 |
| Figure 111 Precipitation intensity field from 15 August 2010 6:00 UTC obtained by a) radars, b)  |       |
| interpolated raingauge data, c) INCA analysis and d) PR-OBS-3 product (5:57 UTC) supplemented w  | ith   |
| map of minimum visible height above surface level (SHMU radar network)   |       |
| Figure 112 Precipitation intensity field as in previous figure, except for 8:00 UTC  |       |
| Figure 113 Comparison of selected statistical scores for the PR-OBS-2 product obtained by differen   |       |
| "ground reference" data; valid for event 1 (convective)  | . 159 |
| Figure 114 Comparison of selected statistical scores for the PR-OBS-2 product as in previous figure  |       |
| except for event 4 (stratiform)  | . 160 |
| Figure 115 The Wideumont radar image of 1/2/2010 (cumulated rainfall in the previous 24 hours,   | 464   |
| raingauge-adjusted)  |       |
| Figure 116 The Wideumont radar image of 1/2/2010 upscaled to the COSMO grid  | . 164 |
| Figure 117 The Wideumont radar image of 2/2/2010 (cumulated rainfall in the previous 24 hours,   | 1.05  |
| raingauge-adjusted)  |       |
| Figure 118 The Wideumont radar image of 2/2/2010 upscaled to the COSMO grid  | . 105 |
| raingauge-adjusted)  | 165   |
| Figure 120 The Wideumont radar image of 4/2/2010 upscaled to the COSMO grid  |       |
| Figure 121 Distribution of the monthly average H-05 3 h cumulated precipitation Mean Error   | . 100 |
| calculated for July 2010 using three methods: a) Ordinary Kriging, b) Natural Neighbour, and c) IDW  | 1 (2) |
| Calculated for July 2010 using three methods. a) Ordinary Krighig, b) Natural Neighbour, and c) IDW  |       |
| Figure 122 Cross validation results obtained for three different methods for spatial interpolation   |       |
| Figure 123 Example of sampled data for a regular grid. In right on the upper part a detail of field studied, below the original grid of field for step 2. From the field the white circles mean the data |       |
| removed from the map. The black squares mean the position of perfect measurement. The  | 4     |
| techniques of up/down scaling reproduce the field only from the perfect measurements   |       |
| Figure 124 randomly distribution of perfect measurement to remap the field on a regular grid   |       |
| Figure 125 STD vs. RMSE% for interpolations by step 2  | . т/б |



(Product H02 – PR-OBS-2)

Doc.No: SAF/HSAF/PVR-02/1.1 Issue/Revision Index: 1.1

Date: 30/09/2011

Page: 12/177

# Acronyms

| AMSU             | Advanced Microwave Sounding Unit (on NOAA and MetOp)  |
|------------------|---|
| AMSU-A           | Advanced Microwave Sounding Unit - A (on NOAA and MetOp)  |
| AMSU-B           | Advanced Microwave Sounding Unit - B (on NOAA up to 17)   |
| ATDD             | Algorithms Theoretical Definition Document  |
| AU               | Anadolu University (in Turkey)  |
| BfG              | Bundesanstalt für Gewässerkunde (in Germany)  |
| CAF              | Central Application Facility (of EUMETSAT)  |
| CDOP             | Continuous Development-Operations Phase   |
| CESBIO           | Centre d'Etudes Spatiales de la BIOsphere (of CNRS, in France)  |
| CM-SAF           | SAF on Climate Monitoring   |
| CNMCA            | Centro Nazionale di Meteorologia e Climatologia Aeronautica (in Italy)  |
| CNR              | Consiglio Nazionale delle Ricerche (of Italy)   |
| CNRS             | Centre Nationale de la Recherche Scientifique (of France)   |
| DMSP             | Defense Meteorological Satellite Program  |
| DPC              | Dipartimento Protezione Civile (of Italy)   |
| EARS             | EUMETSAT Advanced Retransmission Service  |
| ECMWF            | European Centre for Medium-range Weather Forecasts  |
| EDC              | EUMETSAT Data Centre, previously known as U-MARF  |
| EUM              | Short for EUMETSAT  |
| EUMETCast        | EUMETSAT's Broadcast System for Environmental Data  |
| EUMETSAT         | European Organisation for the Exploitation of Meteorological Satellites   |
| FMI              | Finnish Meteorological Institute  |
| FTP              | File Transfer Protocol  |
| GEO              | Geostationary Earth Orbit   |
| GRAS-SAF         | SAF on GRAS Meteorology   |
| HDF              | Hierarchical Data Format  |
| HRV              | High Resolution Visible (one SEVIRI channel)  |
| H-SAF            | SAF on Support to Operational Hydrology and Water Management  |
| IDL <sup>©</sup> | Interactive Data Language   |
| IFOV             | Instantaneous Field Of View   |
| IMWM             | Institute of Meteorology and Water Management (in Poland)   |
| IPF              | Institute of Meteorology and Water Management (IT Folding)  Institut für Photogrammetrie und Fernerkundung (of TU-Wien, in Austria) |
| IPWG             | International Precipitation Working Group   |
| IR               | Infra Red   |
| IRM              | Institut Royal Météorologique (of Belgium) (alternative of RMI)   |
| ISAC             | Istituto di Scienze dell'Atmosfera e del Clima (of CNR, Italy)  |
| ITU              | istanbul Technical University (in Turkey)   |
| LATMOS           | Laboratoire Atmosphères, Milieux, Observations Spatiales (of CNRS, in France)   |
| LEO              |   |
| LSA-SAF          | Low Earth Orbit   |
| Météo France     | SAF on Land Surface Analysis  National Meteorological Service of France   |
| METU             |   |
| MHS              | Middle East Technical University (in Turkey)  Migray and Humidity Soundar (on NOAA 18 and 10, and on MetOn)                         |
| MSG              | Microwave Humidity Sounder (on NOAA 18 and 19, and on MetOp)  |
|                  | Meteosat Second Generation (Meteosat 8, 9, 10, 11)  |
| MVIRI<br>MW      | Meteosat Visible and Infra Red Imager (on Meteosat up to 7)  Micro Wave   |
|                  |   |
| NESDIS           | National Environmental Satellite, Data and Information Services   |
| NMA              | National Meteorological Administration (of Romania)   |
| NOAA<br>NWC-SAF  | National Oceanic and Atmospheric Administration (Agency and satellite)  |
|                  | SAF in support to Nowcasting & Very Short Range Forecasting   |
| NWP<br>NWD SAE   | Numerical Weather Prediction  |
| NWP-SAF          | SAF on Numerical Weather Prediction   |



(Product H02 – PR-OBS-2)

Doc.No: SAF/HSAF/PVR-02/1.1 Issue/Revision Index: 1.1

Date: 30/09/2011

Page: 13/177

| O3M-SAF         | SAF on Ozone and Atmospheric Chemistry Monitoring                           |
|-----------------|---|
| OMSZ            | Hungarian Meteorological Service  |
| ORR             | Operations Readiness Review   |
| OSI-SAF         | SAF on Ocean and Sea Ice  |
| PDF             | Probability Density Function  |
| PEHRPP          | Pilot Evaluation of High Resolution Precipitation Products                  |
| Pixel           | Picture element   |
| PMW             | Passive Micro-Wave  |
| PP              | Project Plan  |
| PR              | Precipitation Radar (on TRMM)   |
| PUM             | Product User Manual   |
| PVR             | Product Validation Report   |
| RMI             | Royal Meteorological Institute (of Belgium) (alternative of IRM)            |
| RR              | Rain Rate   |
| RU              | Rapid Update  |
| SAF             | Satellite Application Facility  |
| SEVIRI          | Spinning Enhanced Visible and Infra-Red Imager (on Meteosat from 8 onwards) |
| SHMÚ            | Slovak Hydro-Meteorological Institute                                       |
| SSM/I           | Special Sensor Microwave / Imager (on DMSP up to F-15)                      |
| SSMIS           | Special Sensor Microwave Imager/Sounder (on DMSP starting with S-16)        |
| SYKE            | Suomen ympäristökeskus (Finnish Environment Institute)                      |
| T <sub>BB</sub> | Equivalent Blackbody Temperature (used for IR)                              |
| TKK             | Teknillinen korkeakoulu (Helsinki University of Technology)                 |
| TMI             | TRMM Microwave Imager (on TRMM)   |
| TRMM            | Tropical Rainfall Measuring Mission UKMO                                    |
| TSMS            | Turkish State Meteorological Service  |
| TU-Wien         | Technische Universität Wien (in Austria)                                    |
| U-MARF          | Unified Meteorological Archive and Retrieval Facility                       |
| UniFe           | University of Ferrara (in Italy)  |
| URD             | User Requirements Document  |
| UTC             | Universal Coordinated Time  |
| VIS             | Visible   |
| ZAMG            | Zentralanstalt für Meteorologie und Geodynamik (of Austria)                 |



(Product H02 - PR-OBS-2)

Doc.No: SAF/HSAF/PVR-02/1.1 Issue/Revision Index: 1.1

Date: 30/09/2011 Page: 14/177

### 1 The EUMETSAT Satellite Application Facilities and H-SAF

The "EUMETSAT Satellite Application Facility on Support to Operational Hydrology and Water Management (H-SAF)" is part of the distributed application ground segment of the "European Organisation for the Exploitation of Meteorological Satellites (EUMETSAT)". The application ground segment consists of a "Central Application Facility (CAF)" and a network of eight "Satellite Application Facilities (SAFs)" dedicated to development and operational activities to provide satellite-derived data to support specific user communities. See fig. 1.

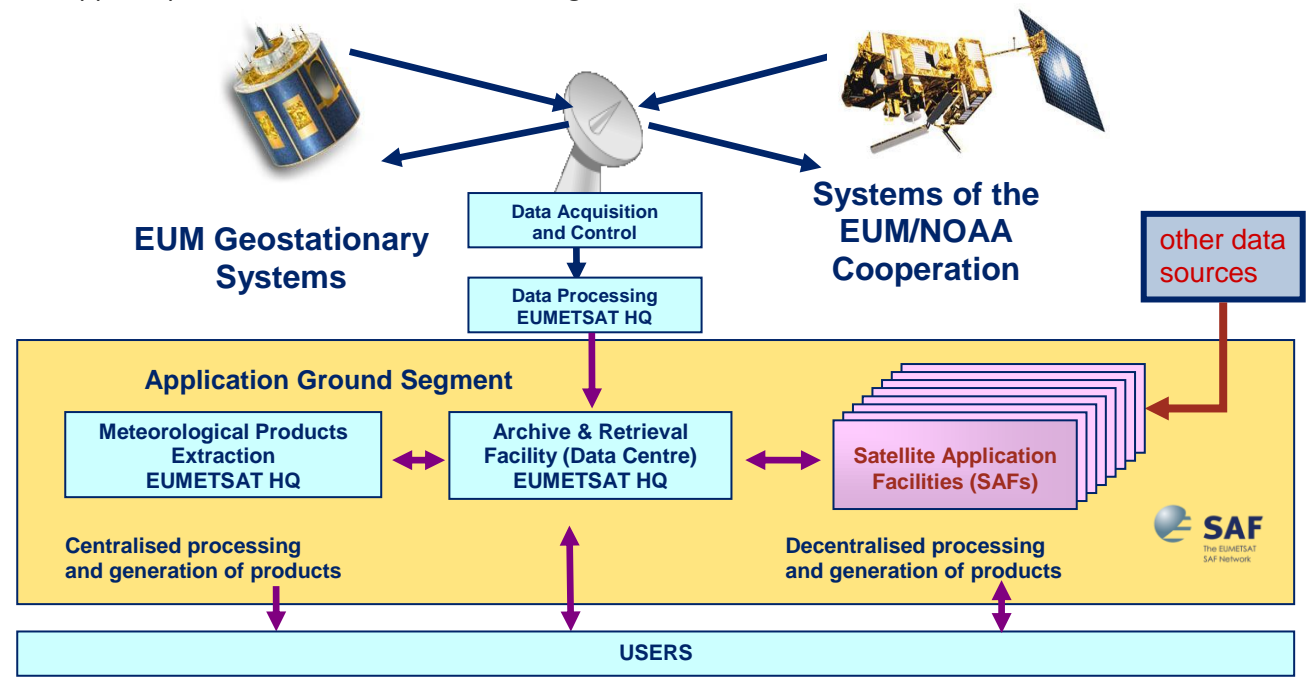


Figure 1 Conceptual scheme of the EUMETSAT application ground segment

Next figure reminds the current composition of the EUMETSAT SAF network (in order of establishment).



Figure 2 Current composition of the EUMETSAT SAF network (in order of establishment)

Conceptual scheme of the EUMETSAT application ground segment

The H-SAF was established by the EUMETSAT Council on 3 July 2005; its Development Phase started on 1<sup>st</sup> September 2005 and ended on 31 August 2010. The SAF is now in its first Continuous Development and Operations Phase (CDOP) which started on 28 September 2010 and will end on 28 February 2012 The list of H-SAF products is shown in Table 1:



(Product H02 – PR-OBS-2)

Doc.No: SAF/HSAF/PVR-02/1.1 Issue/Revision Index: 1.1

Date: 30/09/2011 Page: 15/177

| Acronym  | Identifier | Name   |
|----------|------------|--|
| PR-OBS-1 | H-01       | Precipitation rate at ground by MW conical scanners (with indication of phase)     |
| PR-OBS-2 | H-02       | Precipitation rate at ground by MW cross-track scanners (with indication of phase) |
| PR-OBS-3 | H-03       | Precipitation rate at ground by GEO/IR supported by LEO/MW                         |
| PR-OBS-4 | H-04       | Precipitation rate at ground by LEO/MW supported by GEO/IR (with flag for phase)   |
| PR-OBS-5 | H-05       | Accumulated precipitation at ground by blended MW and IR                           |
| PR-OBS-6 | H-15       | Blended SEVIRI Convection area/ LEO MW Convective Precipitation                    |
| PR-ASS-1 | H-06       | Instantaneous and accumulated precipitation at ground computed by a NWP model      |
| SM-OBS-2 | H-08       | Small-scale surface soil moisture by radar scatterometer                           |
| SM-OBS-3 | H-16       | Large-scale surface soil moisture by radar scatterometer                           |
| SM-DAS-2 | H-14       | Liquid root zone soil water index by scatterometer assimilation in NWP model       |
| SN-OBS-1 | H-10       | Snow detection (snow mask) by VIS/IR radiometry                                    |
| SN-OBS-2 | H-11       | Snow status (dry/wet) by MW radiometry   |
| SN-OBS-3 | H-12       | Effective snow cover by VIS/IR radiometry  |
| SN-OBS-4 | H-13       | Snow water equivalent by MW radiometry   |

Table 1 H-SAF Product List

### 2 Introduction to product PR-OBS-1

### 2.1 Sensing principle

Product PR-OBS-2 is based on the instruments AMSU-A and AMSU-B or MHS flown on NOAA and MetOp satellites. These cross-track scanners provide images with constant angular sampling across track, that implies that the IFOV elongates as the beam moves from nadir toward the edge of the scan (see next figure). The elongation is such that:

- for AMSU-A the IFOV at nadir is: 48 x 48 km<sup>2</sup>, at the edge of the 2250 km swath: 80 x 150 km<sup>2</sup>;
- for AMSU-B and MHS the IFOV at nadir is: 16 x 16 km<sup>2</sup>; at the edge: 27 x 50 km<sup>2</sup>.



(Product H02 - PR-OBS-2)

Doc.No: SAF/HSAF/PVR-02/1.1 Issue/Revision Index: 1.1

Date: 30/09/2011

Page: 16/177

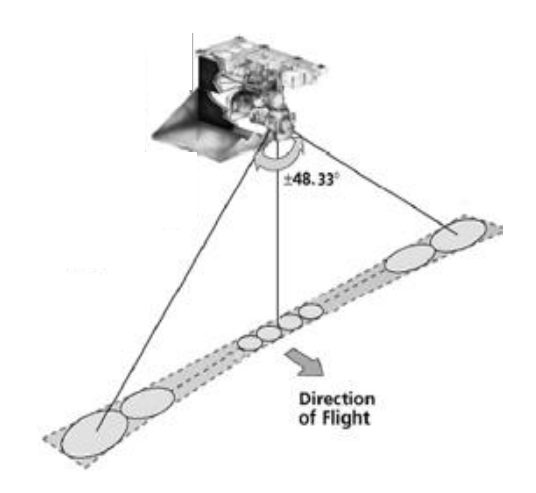


Figure 3 Geometry of cross-track scanning for AMSU

Since the incidence angle changes moving cross-track, the effect of polarisation also changes, thus the information stemming from dual polarisation would be very difficult to be used, and in effect the various frequencies are observed under a single polarisation, V or H. The resolution is constant for all frequencies in AMSU-A (48 km at s.s.p.) and AMSU-B/MHS (16 km at s.s.p.).

The NOAA satellites are managed by NOAA, MetOp by EUMETSAT. Both NOAA and MetOp provide direct-read-out (the real-time transmitter of MetOp suffered of a failure, but now transmission of data over Europe has been resumed).

For more information, please refer to the Products User Manual (specifically, volume PUM-02).

### 2.2 Algorithm principle

The baseline algorithm for PR-OBS-2 processing is described in ATDD-02. Only essential elements are highlighted here.

Next figure illustrates the flow chart of the AMSU-MHS processing chain.



(Product H02 - PR-OBS-2)

Doc.No: SAF/HSAF/PVR-02/1.1 Issue/Revision Index: 1.1

Date: 30/09/2011 Page: 17/177

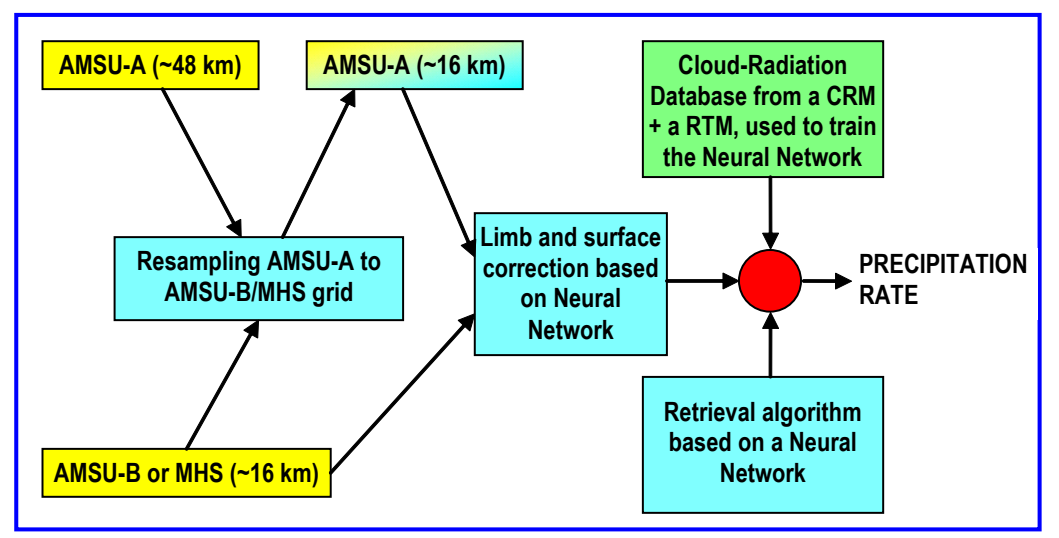


Figure 4 Flow chart of the AMSU-MHS precipitation rate processing chain

The first step is to resample AMSU-A brightness temperature (TB) to AMSU-B/MHS grid using bilinear interpolation. Then AMSU-A and AMUS-B/MHS radiometers are corrected for limb and surface effects, to report the viewing geometry changing across the image, to vertical viewing. This is obtained by applying procedures based on specific Neural Networks (one Net for each channel). The instantaneous rain field is finally retrieved by using a Neural Network on the corrected TBs.

In the initial product release the Neural Network had been trained by selected radars of the NEXRAD network. In the current release the Neural Network is trained by a Cloud-Radiation Database (CRD) built by applying a Radiative Transfer Model (RTM) to simulated cloud systems derived by a Cloud Resolving Model (CRM).

#### 2.3 Main operational characteristics

The operational characteristics of PR-OBS-2 are discussed in PUM-02. Here are the main highlights.

<u>The horizontal resolution ( $\Delta x$ )</u> descends from the instrument Instantaneous Field of View (*IFOV*). AMSU-A and AMSU-B/MHS have constant resolution with frequency (different for AMSU-A, 48 km at nadir, and AMSU-B/MHS, 16 km at nadir), degrading across-scan (80 x 150 and 27 x 50 km<sup>2</sup> respectively, at the very edge of scan). Lower resolution AMSU-A data are resampled over the AMSU-B/MHS grid by means of bilinear interpolation. As a whole, a representative value for the final product could be ~ 40 km. Sampling is made at ~ 16 km intervals, the AMSU-B/MHS resolution at nadir. Thus:

• resolution  $\Delta x \sim 40 \text{ km}$  - sampling distance: 16 km.

The <u>observing cycle ( $\Delta t$ )</u> is defined as the average time interval between two measurements over the same area. In the case of LEO, the observing cycle depends on the instrument swath and the number of satellites carrying the addressed instrument. For PR-OBS-2 there are one MetOp (orbit: 9:30 LST) and up to 5 NOAA satellites. However, AMSU-MHS on NOAA is in a good status only for NOAA-18 and NOAA-19, that follow approximately the same orbit, close to 14:00 LST. Therefore the total service is equivalent to that one of two satellites, around 9:30 and 14:00 LST. In average the observing cycle over Europe is  $\Delta t \sim 6$  h, with actual interval ranging from 4.5 to 7.5 hours. Gaps are filled by product PR-OBS-1, that also has observing cycle  $\Delta t \sim 6$  h, but LST around 7:00 and 18:00, with actual intervals ranging from 2 to 10 hours. The conclusion is:



(Product H02 - PR-OBS-2)

Doc.No: SAF/HSAF/PVR-02/1.1 Issue/Revision Index: 1.1

Date: 30/09/2011 Page: 18/177

- for PR-OBS-2 as stand alone (from NOAA & MetOp satellites): cycle  $\Delta t$  = 6 h, sampling 4.5÷7.5 h;
- for the composite PR-OBS-1 + PR-OBS-2 system: cycle  $\Delta t = 3$  h, sampling 2÷4.5 h.

The  $\underline{timeliness}$  ( $\underline{\delta}$ ) is defined as the time between observation taking and product available at the user site assuming a defined dissemination mean. The timeliness depends on the satellite transmission facilities, the availability of acquisition stations, the processing time required to generate the product and the reference dissemination means. Direct-read-out is provided by all NOAA satellites and, after partial recovery from the AHRPT transmitter failure, also by MetOp-A. After adding the processing time we have:

timeliness δ ~ 0.5 h.

The <u>accuracy (RMS)</u> is the convolution of several measurement features (random error, bias, sensitivity, precision, ...). To simplify matters, it is generally agreed to quote the root-mean-square difference [observed - reference values]. The accuracy of a satellite-derived product descends from the strength of the physical principle linking the satellite observation to the natural process determining the parameter. It is difficult to be estimated a-priori: it is generally evaluated a-posteriori by means of the <u>validation activity</u>.

### 3 Validation strategy, methods and tools

### 3.1 Validation team and work plan

To evaluate the satellite precipitation product accuracy a Validation Group has been established by the beginning of the Validation Phase in the H-SAF project. The Precipitation Product Validation team is composed of experts from the National Meteorological and Hydrological Institutes of Belgium, Bulgaria, Germany, Hungary, Italy, Poland, Slovakia, and Turkey (fig. 5). Hydrologists, meteorologists, and precipitation ground data experts, coming from these countries are involved in the product validation activities (Table 2).

H01 has been submitted to validation in all these countries except Bulgaria. Until now the Bulgarian data are used only for H05 validation activity according to the Project Plan. Their use in the next months is under consideration.

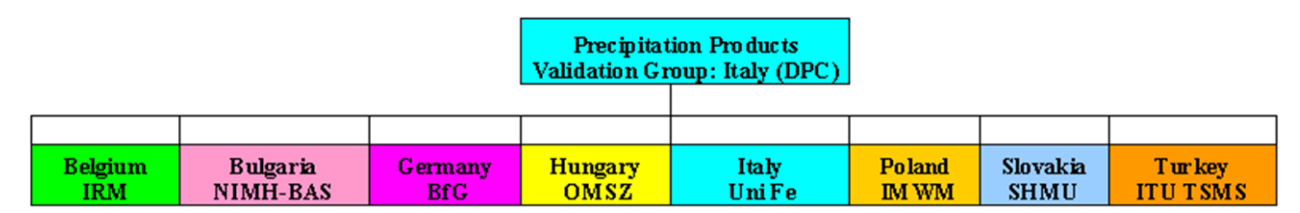


Figure 5 Structure of the Precipitation products validation team

| Validation team for precipitation products |                                      |         |   |  |  |  |
|--|--------------------------------------|---------|---|--|--|--|
| Silvia Puca (Leader)                       | Dipartimento Protezione Civile (DPC) | Italy   | silvia.puca@protezionecivile.it         |  |  |  |
|  |                                      |         | emanuela.campione@protezionecivile.i    |  |  |  |
| Emanuela Campione                          | Dipartimento Protezione Civile (DPC) | Italy   | <u>t</u>                                |  |  |  |
| Gianfranco Vulpiani                        | Dipartimento Protezione Civile (DPC) | Italy   | gianfranco.vulpiani@protezionecivile.it |  |  |  |
| Alexander Toniazzo                         | Dipartimento Protezione Civile (DPC) | Italy   | alexander.toniazzo@protezionecivile.it  |  |  |  |
| Emmanuel Roulin                            | Institut Royal Météorologique (IRM)  | Belgium | Emmanuel.Roulin@oma.be                  |  |  |  |



(Product H02 - PR-OBS-2)

Doc.No: SAF/HSAF/PVR-02/1.1 Issue/Revision Index: 1.1

Date: 30/09/2011

Page: 19/177

| Angelo Rinollo      | Institut Royal Météorologique (IRM)   | Belgium    | angelo.rinollo@oma.be        |
|---------------------|---------------------------------------|------------|------------------------------|
| 7 ingelo ranono     | National Institute of Meteorology and | Deigiani   | ungeron money ornande        |
|                     | Hydrology Bulgarian Academy of        |            |                              |
| Gergana Kozinarova  | Sciences (NIMH-BAS)                   | Bulgaria   | gkozinarova@gmail.com        |
| Gergana Rozmarova   | National Institute of Meteorology and | Daigaria   | grozmarova@gman.com          |
|                     | Hydrology Bulgarian Academy of        |            |                              |
| Georgy Koshinchanov | Sciences (NIMH-BAS)                   | Bulgaria   | georgy.koshinchanov@meteo.bg |
|                     |                                       | _ sgs. rs. | Beergye                      |
| Claudia Rachimow    | Bundesanstalt für Gewässerkunde (BfG) | Germany    | rachimow@bafg.de             |
| Peter Krahe         | Bundesanstalt für Gewässerkunde (BfG) | Germany    | krahe@bafg.de                |
|                     | Hungarian Meteorological Service      |            |                              |
| Eszter Lábó         | (OMSZ)                                | Hungary    | labo.e@met.hu                |
|                     | Hungarian Meteorological Service      |            |                              |
| Judit Kerenyi       | (OMSZ)                                | Hungary    | kerenyi@met.hu               |
|                     | Ferrara University, Department of     |            |                              |
| Federico Porcu'     | Physics (UniFe)                       | Italy      | porcu@fe.infn.it             |
|                     | Ferrara University, Department of     |            |                              |
| Lisa Milani         | Physics (UniFe)                       | Italy      | milani@fe.infn.it            |
|                     | Institute of Meteorology and Water    |            |                              |
| Bozena Lapeta       | Management (IMWM)                     | Poland     | Bozena.Lapeta@imgw.pl        |
|                     | Institute of Meteorology and Water    |            |                              |
| Rafal Iwanski       | Management (IMWM)                     | Poland     | Rafal.lwanski@imgw.pl        |
|                     | Slovenský Hydrometeorologický Ústav   |            |                              |
| Ján Kaňák           | (SHMÚ)                                | Slovakia   | jan.kanak@shmu.sk            |
|                     | Slovenský Hydrometeorologický Ústav   |            |                              |
| Ľuboslav Okon       | (SHMÚ)                                | Slovakia   | luboslav.okon@shmu.sk        |
|                     | Slovenský Hydrometeorologický Ústav   |            |                              |
| Mariàn Jurasek      | (SHMÚ)                                | Slovakia   | marian.jurasek@shmu.sk       |
| Ahmet Öztopal       | Istanbul Technical University (ITU)   | Turkey     | oztopal@itu.edu.tr           |
|                     | Turkish State Meteorological Service  |            |                              |
| Ibrahim Sonmez      | (TSMS)                                | Turkey     | isonmez@dmi.gov.tr           |
|                     | Turkish State Meteorological Service  |            |                              |
| Aydin Gurol Erturk  | (TSMS)                                | Turkey     | agerturk@dmi.gov.tr          |

Table 2 List of the people involved in the validation of H-SAF precipitation products

The Precipitation products validation programme started with a first workshop in Rome, 20-21 June 2006, soon after the H-SAF Requirements Review (26-27 April 2006). The first activity was to lay down the Validation plan, that was finalised as first draft early as 30 September 2006. After the first Workshop, other ones followed, at least one per year to exchange experiences, problem solutions and to discuss possible improvement of the validation methodologies. Often the Precipitation Product Validation workshop are joined with the Hydrological validation group.

The results of the Product Validation Programme are reported in this Product Validation Report (PVR) and are published in the validation section of the H-SAF web page. A new structure and visualization of the validation section of H-SAF web page is in progress to take into account the user needs. This validation web section is continuously updated with the last validation results and studies coming from the Precipitation Product Validation Group (PPVG).

In the last Validation Workshop hosted by Slovenský Hydrometeorologický Ústav in Bratislava, 20-22 October 2010 it has been decided to introduce several Working Groups to solve specific items of validation procedure and to develop software used by all members of the validation cluster. The coordinators and the participants of the working groups are members of the PPVG or external experts



(Product H02 - PR-OBS-2)

Doc.No: SAF/HSAF/PVR-02/1.1 Issue/Revision Index: 1.1

Date: 30/09/2011 Page: 20/177

of the institutes involved in the validation activities. The first results obtained by the Working Groups are here reported.

#### 3.2 Validation objects and problems

The products validation activity has to serve multiple purposes:

- to provide input to the product developers for improving calibration for better quality of baseline products, and for guidance in the development of more advanced products;
- to characterise the product error structure in order to enable the Hydrological validation programme to appropriately use the data;
- to provide information on product error to accompany the product distribution in an open environment, after the initial phase of distribution limited to the so-called "beta users".

Validation is obviously a hard work in the case of precipitation, both because the sensing principle from space is very much indirect, and because of the natural space-time variability of the precipitation field (sharing certain aspects with fractal fields), that places severe sampling problems.

It is known that an absolute 'ground reference' does not exist. In the H-saf project the validation is based on comparisons of satellite products with ground data: radar, rain gauge and radar integrated with rain gauge. During the Development phase some main problems have been pointed out. First of all the importance to characterize the error associated to the ground data used by PPVG. Secondly to develop software for all steps of the Validation Procedure, a software available to all the members of the PPVG. Three months ago the radar and rain gauge Working Group (WG) have been composed in order to solve these problems. The first results obtained by the working groups are reported in the following sections and a complete documentation is available as annex 1-7 of this document. In addition to the radar and rain gauge WG other WG have been composed on: integrate various sets of precipitation data sources — raingauge network, radar network, NWP models outputs and climatological standards into common precipitation product, which can describe the areal instantaneous and cumulated precipitation fields (*INCA -WG*) and to investigate the opportunity to create geographical maps of error distribution for providing information on test catchments to the Hydrological Validation Group (*GEO MAP -WG*).

### 3.3 Validation methodology

From the beginning of the project it was clear the importance to define a common validation procedure in order to make the results obtained by several institutes comparable and to better understand their meanings. The main steps of this methodology have been identified during the development phase inside the validation group, in collaboration with the product developers, and with the support of ground data experts. The common validation methodology is based on ground data (radar and rain gauge) comparisons to produce <a href="Iarge statistic">Iarge statistic</a> (multi-categorical and continuous), and <a href="Case study analysis">Case study analysis</a>) are considered complementary in assessing the accuracy of the implemented algorithms. Large statistics helps in identifying existence of pathological behaviour, selected case studies are useful in identifying the roots of such behaviour, when present.

The main steps of the validation procedure are:

- ground data error analysis: radar and rain gauge;
- point measurements (rain gauge) spatial interpolation;



### Product Validation Report - PVR-02 (Product H02 – PR-OBS-2)

Doc.No: SAF/HSAF/PVR-02/1.1 Issue/Revision Index: 1.1

Date: 30/09/2011 Page: 21/177

- up-scaling of radar data versus SSMI grid;
- temporal comparison of precipitation products (satellite and ground);
- statistical scores (continuous and multi-categorical) evaluation;
- case study analysis.

#### 3.4 Ground data and tools used for validation

Both rain gauge and radar data have been used until now for H01 validation. As said in the previous section during the last Precipitation Product Validation Workshop held in Bratislava, 20-22 October 2010 it has been decided to set up Working Groups to solve specific items of the validation procedure and to develop software used by all members of the validation cluster. A complete knowledge of the ground data characteristics used inside the PPVG has been the first item of the working groups; this is necessary to understand the validation results and to define the procedure to select the most reliable data to represent a "ground reference". A complete report on the results obtained by the Working Group on rain gauge, radar and ground data integration are reported in the Chapter 4 with a complete inventory of the ground data used within the PPVG.

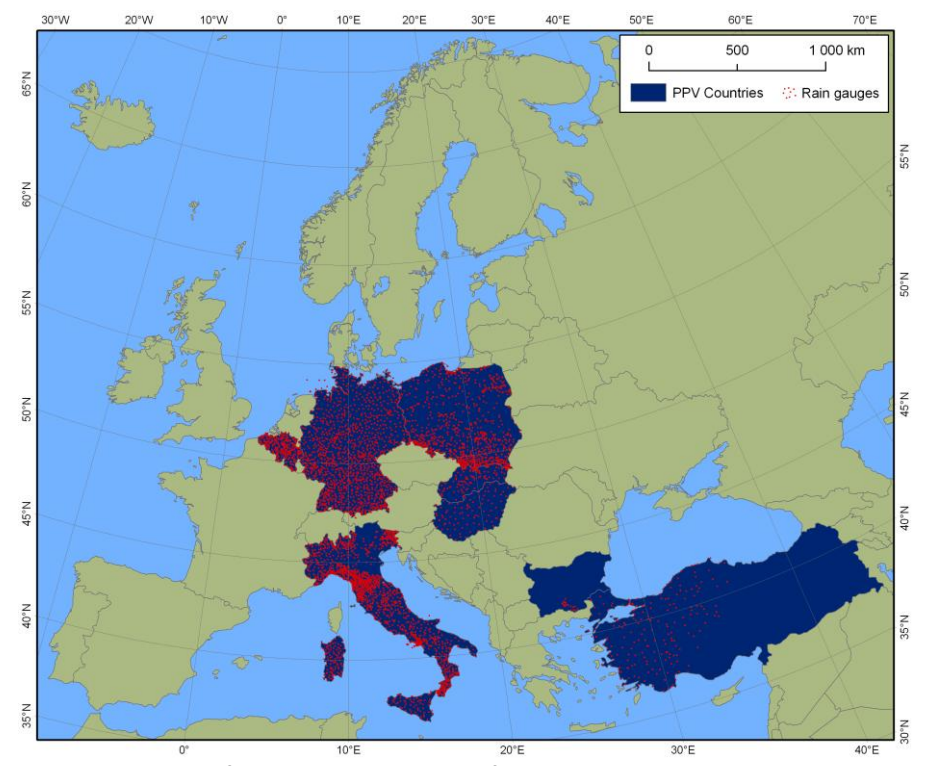


Figure 6 The network of 3500 rain gauges used for H-SAF precipitation products validation

The rain gauge networks of PPVG is composed of approximately 3500 stations across 6 Countries (Figure 6). A key characteristic of such networks is the distance between each raingauge and the closest one, averaged over all the instruments considered in the network and it is a measure of the raingauge density. Instruments number and density are summarized in Table 3.

| Country | Total number of gauges * | Average minimum |
|---------|--------------------------|-----------------|
|         |                          | distance (km)   |



(Product H02 – PR-OBS-2)

Doc.No: SAF/HSAF/PVR-02/1.1 Issue/Revision Index: 1.1

Date: 30/09/2011 Page: 22/177

| Belgium  | 89**    | 11.2 |
|----------|---------|------|
| Bulgaria | 37***   | 7    |
| Germany  | 1300    | 17   |
| Italy    | 1800    | 9.5  |
| Poland   | 330-475 | 13.3 |
| Turkey   | 193**** | 27   |

Table 3 Number and density of raingauges within H-SAF validation Group

- \* the number of raingauges could vary from day to day due to operational efficiency within a maximum range of 10-15%.
- \*\* only in the Wallonia Region
- \*\*\* only in 3 river basins
- \*\*\*\* only covering the western part of Anatolia

Most of the gauges used in the National networks by the PPVG Partners are of the tipping bucket type, and hourly cumulated (see Table 4).

The rain gauge inventory (Chapter 4) proposed by *rain gauge-WG* (annex 2) on the instruments, the operational network and the approach to match gauge data with the satellite estimates in the PPVG, has pointed out that the rain gauge networks available in the PPVG are surely appropriated for the validation of cumulated products (1 hour and higher), but probably not for instantaneous estimates. The comparison of satellite rain rate with hourly cumulated ground measurements surely introduces intrinsic errors in the matching scores, that can be estimated as very large. The validation of instantaneous estimates should be carried on only when gauges cumulation interval is 10 to 15 minutes (as in Poland). Values cumulated over shorter intervals (5 or even one minute, as it is done in Turkey) are affected by large relative errors in cases of low/moderate rain rates. Studies are undertaken in order to quantitatively estimate the errors introduced in the validation procedure comparing the instantaneous satellite precipitation estimation with the rain gauge precipitation cumulated on different intervals.

Moreover the revisiting time (3,4 hours) of H01 makes impossible or not reasonable to validate the product for 1-24 hours cumulated interval.

The WG has also pointed out that different approaches for the estimates matching are considered in the PPVG. One of the next step of the WG will be to define in collaboration with the *GeoMap-WG* (Annex 7) the spatial interpolation technique and to develop the related software to be used in side the PPVG.

| Country  | Minimum detectable             | Maximum detectable             | Heating system | cumulation     |
|----------|--------------------------------|--------------------------------|----------------|----------------|
|          | rainrate (mm h <sup>-1</sup> ) | rainrate (mm h <sup>-1</sup> ) | (Y/N)          | interval (min) |
| Belgium  | 0.1                            | N/A                            | N              | 60             |
| Bulgaria | 0.1                            | 2000                           | Υ              | 120, 1440      |
| Germany  | 0.05                           | 3000                           | Υ              | 60             |
| Italy    | 0.2                            | 300                            | Y/N*           | 60             |
| Poland   | 0.1                            | 300                            | Υ              | 10             |
| Turkey   | 0.2                            | 288                            | Υ              | 1              |

**Table 4 Summary of the raingauge characteristics** 

<sup>\*</sup> only 300 out of 1800 gauges are heated



### Product Validation Report - PVR-02 (Product H02 – PR-OBS-2)

Doc.No: SAF/HSAF/PVR-02/1.1 Issue/Revision Index: 1.1

Date: 30/09/2011 Page: 23/177

An inventory on radar data, networks and products used in PPVG (Chapter 4), has pointed out that all the institutes involved in the PPVG declared the system are kept in a relatively good status and all of them apply some correction factors in their processing chain of radar data. In Figure 7 there is the map of the 54 C-band radars available in their H-SAF PPVG. Only the radar data which pass the quality control of the owner Institute are used by the PPVG for validation activities. However, these correction factors are diverse in the countries, depending on their capacities and main sources of error in the radar measurements. This also means that the corresponding rainfall estimates are different products in nature, and the estimation of their errors cannot be homogenized for all the countries of the PPVG. However, each county can provide useful information of the error structure of its rainfall products based on its own resources. The Radar-WG (Annex 3) is now working to define quality index (static or dynamic) in order to select the more reliable radar fields and to associate an error structure to the radar data. Quality information should take into account the radar site/geographical areas/event type/radar products. The study performed by the Slovakian team (Annex 4) and the scheme published by J. Szturcn et all 2008, on the quality index evaluation are under consideration by the Radar-WG. In the future the satellite product testing will be carried out using only the data having a sufficient quality but the validation results showed in this document have been obtained using radar data which passed only data owner institute controls.

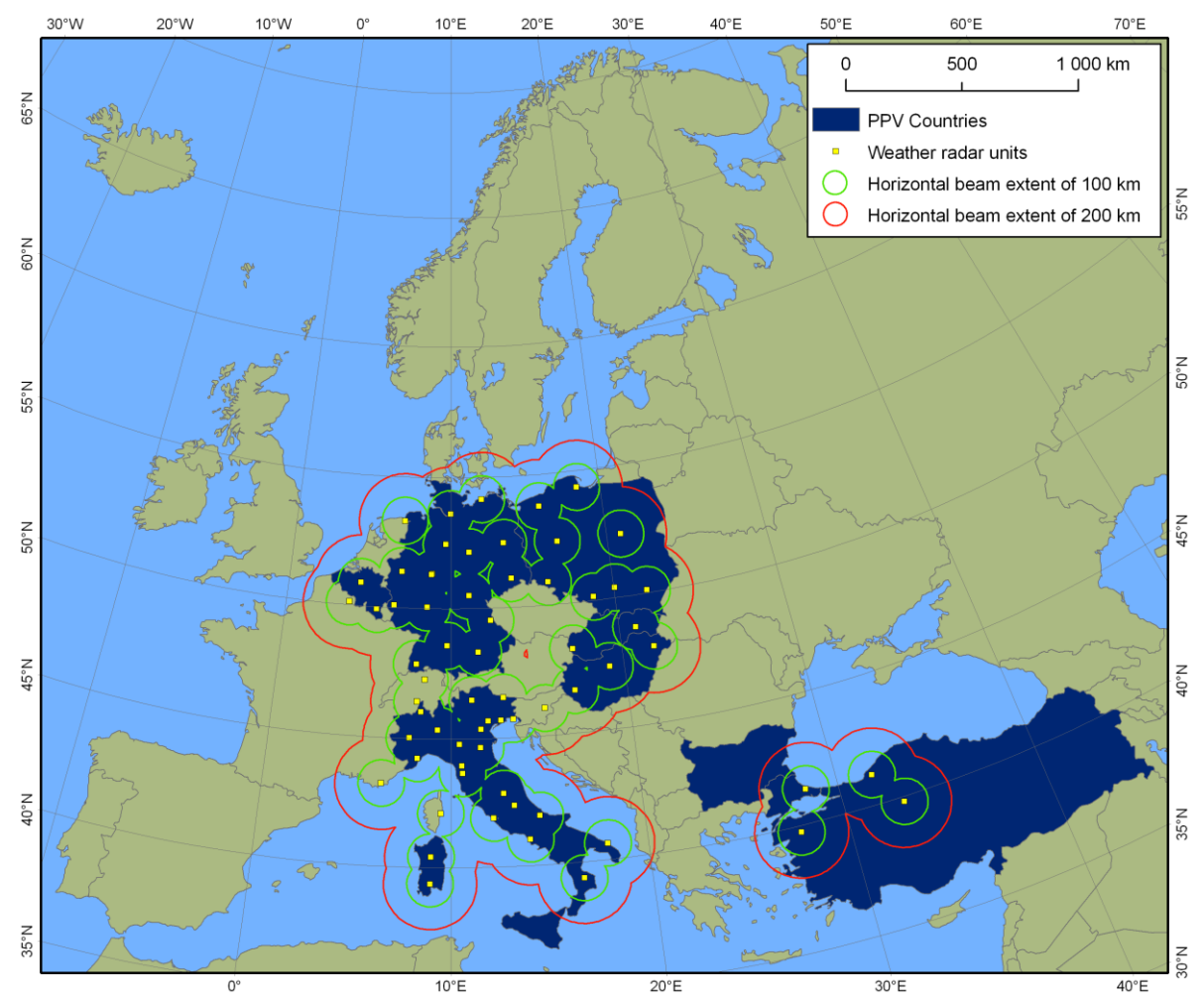


Figure 7 The networks of 54 C-band radars available in ther H-SAF PPVG



(Product H02 – PR-OBS-2)

Doc.No: SAF/HSAF/PVR-02/1.1 Issue/Revision Index: 1.1

Date: 30/09/2011 Page: 24/177

The studies that have been carried out in the PPVG on comparison of radar data with rain gauge data have shown that RMSE error associated with radar fields depends considerably on radar minimum visible height above the rain gauge in mountainous terrains like Slovakia, but less importantly in flat terrains like Hungary. In Slovakia, the RMSE% error (see Section 3.7) of radar accumulated fields is between 70-90%, whereas in Hungary, it is slightly lower, between 60-80%. Dataset for May-September 2010 have been used to derive these parameters.

In PPVG it is under investigation (*INCA-WG annex 5*) the possibility to use ground data integrated software to produce precipitation field. The results obtained by *INCA-WG* are reported in the chapter 4.

### 3.5 Spatial interpolation for rain gauges

The partners of the Validation Group have been using a variety of different strategies to treat gauge data. Some are using interpolation algorithms to get spatially continuous rainfall maps, while others process directly the measurements of individual gauges (Table 5). The first approach seems to be more convenient, especially when the "large" IFOV of H01 are concerned.

| Country  | Type of interpolation   |  |
|----------|-------------------------|--|
| Belgium  | Barnes over 5x5 km grid |  |
| Bulgaria | Co kriging              |  |
| Germany  | Inverse square distance |  |
| Italy    | Barnes over 5x5 km grid |  |
| Poland   | No                      |  |
| Turkey   | No                      |  |

Table 5 Data pre-processing strategies

One of the next step of the *Rain Gauge-WG* will be to harmonize the different spatial interpolation techniques among partners developing a common software for the validation, collaborating with the *GeoMap-WG* (Annex 7).

### 3.6 Techniques to make observation comparable: up-scaling technique for radar data

From the first Validation Workshop in 2006 it has been decided that the <u>comparison between satellite</u> <u>product and ground data has to be on satellite native grid</u>. Generally one or two rain gauges are in a SSMI pixel, but radar instruments provide many measurements within a single SSMI pixel. For this reason an up-scaling technique is necessary to compare radar data with the H01 precipitation estimations on the satellite native grid.

The precipitation data in the retrieval product (H02) is based on the instruments AMSU-A and AMSU-B or MHS flown on NOAA and MetOp satellites. These cross-track scanners provide images with constant angular sampling across track, that implies that the IFOV elongates as the beam moves from nadir toward the edge of the scan. The elongation is such that:

- for AMSU-A the IFOV at nadir is: 48 x 48 km<sup>2</sup>, at the edge of the 2250 km swath: 80 x 150 km<sup>2</sup>;
- for AMSU-B and MHS the IFOV at nadir is: 16 x 16 km<sup>2</sup>; at the edge: 27 x 50 km<sup>2</sup>.



(Product H02 - PR-OBS-2)

Doc.No: SAF/HSAF/PVR-02/1.1 Issue/Revision Index: 1.1

Date: 30/09/2011 Page: 25/177

H02 follows the scanning geometry and IFOV resolution of AMSU-B scan, so that each pixel along the scan has a precipitation value representative for an elliptical region next figure.

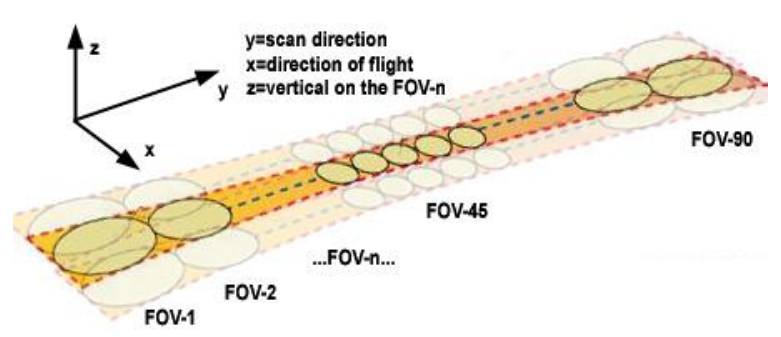


Figure 8 Geometry - Geometry of cross-track scanning for AMSU

#### 3.6.1 Average of hi-res ground validation data

Radar instruments provide many measurements within a single AMSU pixel. Those measurements should be averaged following the AMSU-B antenna pattern.

- Establish the size in km of the axis for each elliptic FOV. You will have N=90 couples of values  $(\mathbf{Fx}_n, \mathbf{Fy}_n)$
- Define a 2-dimensional Gaussian surface (matrix **G(NxN)**), having resolution **R** (pixel size) **R≤radar resolution**, and elliptical section at half high having axis (**Ex**<sub>n</sub>, **Ey**<sub>n</sub>) equal to the correspondent FOV (i.e. **Ex**<sub>n</sub> = **Fx**<sub>n</sub> and **Ey**<sub>n</sub> = **Fy**<sub>n</sub>, see figures below; note that if the Radar resolution is 1km, 1px=1km)

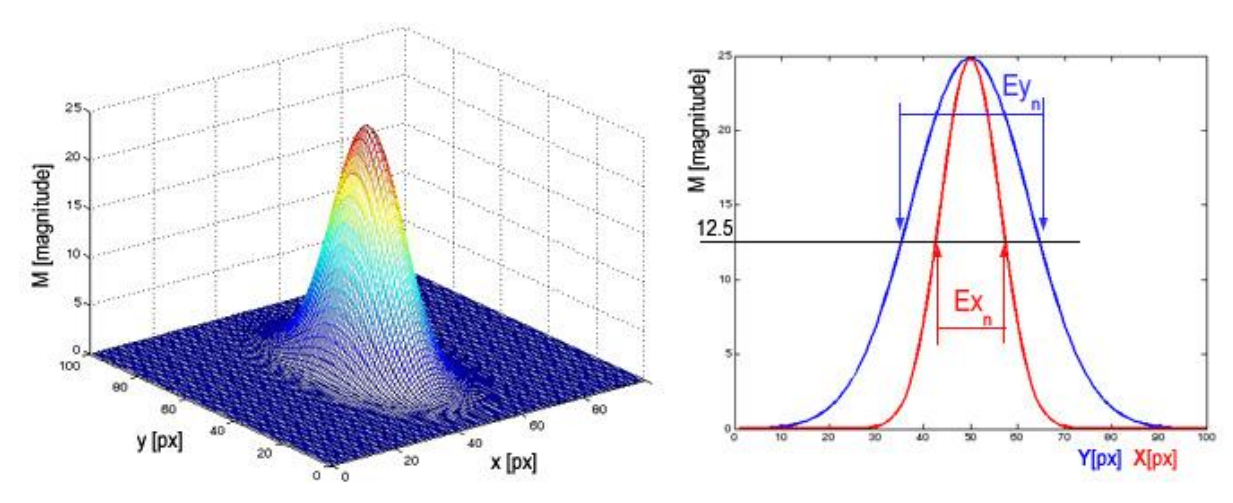


Figure 9 Left) Gaussian filter - Right) section of gaussian filter

— If the matrix NxN is too large, it can be reduced to a **MxK** matrix until the pixels (1,C), (C,1), (N,C), (C,N) are less than (C,C)/100



(Product H02 – PR-OBS-2)

Doc.No: SAF/HSAF/PVR-02/1.1 Issue/Revision Index: 1.1

Date: 30/09/2011

Page: 26/177

| (1,1) | () | (1,C) | () | (1,N) |
|-------|----|-------|----|-------|
| ( )   |    |       |    |       |
| ()    |    |       |    |       |
| (C,1) |    | (C,C) |    | (C,N) |
| ( )   |    |       |    |       |
| ()    |    |       |    |       |
| (N,1) | () | (N,C) | () | (N,N) |

|      |      | 0.24   |          |      |  |
|------|------|--------|----------|------|--|
|      |      | 0.25   |          |      |  |
|      |      |        |          |      |  |
|      |      |        |          |      |  |
| 0.23 | 0.25 | <br>25 | <br>0.25 | 0.23 |  |
|      |      |        |          |      |  |
|      |      |        |          |      |  |
|      |      | 0.25   |          |      |  |
|      |      | 0.24   |          |      |  |

Table 6 Left) Original Gaussian matrix - Right)Reduced matrix to dimensions M xK

Normalize the matrix G (MxK) obtaining the matrix G' having the sum of all elements equal to
 1:

$$G'(m,k) = \frac{G(m,k)}{\sum_{m=1}^{M} \sum_{k=1}^{K} G(m,k)}$$

#### 3.6.2 Smoothing of radar precipitation

For each FOV and for each SCANLINE in the file H02, make the gaussian filter overlapping radar data so that the central pixel (C,C) corresponds to (H02<sub>lat</sub>, H02<sub>lon</sub>) and the y axis has the same direction of the scanline.

Multiply each element of G' for the closest radar measurements ( $RR_{high}(lat,lon)$ ), and sum the products:

$$RR_{low} = \sum_{m=1}^{M} \sum_{k=1}^{K} G'(m,k) \cdot RR_{high}$$

Following this procedure it is obtained, for each FOV and SCANLINE, a value RR<sub>low</sub>. RR<sub>low</sub>(FOV,SCANLINE) which represents the matrix of validation used versus AMSU-B estimates.

This scheme has been suggested by the precipitation developers of CNR-ISAC and it has been adopted by the PPVG.

One of the *Radar-WG* and *Rain Gauge-WG* next steps is to develop a common code for the up-scaling of radar data versus AMSU-B grids following this technique. The code will be an evolution and optimization of the code already available by Belgium (Van de Vyver, H., and E. Roulin, 2008) and Italy A. Rinollo. All participants of validation task will use not only the same technique but <u>the same</u> software.



(Product H02 - PR-OBS-2)

Doc.No: SAF/HSAF/PVR-02/1.1 Issue/Revision Index: 1.1

Date: 30/09/2011 Page: 27/177

### 3.7 Temporal comparison of precipitation intensity

Taking to account the revisiting time of the H02 (3,4 hours) it was decided (during the first validation workshop in 2006) to perform a direct comparison between the satellite and radar precipitation intensity maps. The revisiting time of the product does not allow to have a sensible accumulated precipitation map on 1-24 hours.

In the PPVG the satellite product is compared with the closest (up-scaled) radar and rain gauge data in time. The satellite time is considered the time in the BUFR4 file, provided by CNMCA, when validation area is first reached.

### 3.8 Large statistic: Continuous and multi-categorical

The large statistic analysis allows to point out the existence of pathological behaviour in the satellite product performance. It requires the application of the same validation technique step by step in all the institutes take part of the PPVG.

The large statistic analysis in PPVG is based on the evaluation of monthly and seasonal *Continuous verification* and *Multi-Categorical* statistical scores on one year of data (2010) for three precipitation classes (see next figure).

It was decided to evaluate both continuous and multi-categorical statistic to give a complete view of the error structure associated to H02. Since the accuracy of precipitation measurements depends on the type of precipitation or, to simplify matters, the intensity, the verification is carried out on three classes indicated by hydrologists during the development phase (see *next table*).



**Table 7 Classes for evaluating Precipitation Rate products** 

The rain rate lower than 0.25 mm/h is considered no precipitation.

The main steps to evaluate the statistical scores are:

- all the institutes up-scale the national radar and rain gauge data on the satellite native grid using the up-scaling techniques before described;
- all the institutes compare H02 with the radar precipitation intensity and the rain gauge cumulated precipitation;
- all the institutes evaluate the monthly and seasonal continuous scores (below reported) and contingency tables for the precipitation classes producing numerical files called 'CS' and 'MC' files;
- all the institutes evaluate PDF producing numerical files called 'DIST' files and plots;
- the precipitation product validation leader collects all the validation files (MC, CS and DIST files), verifies the consistency of the results and evaluates the monthly and seasonal common statistical results;



(Product H02 - PR-OBS-2)

Doc.No: SAF/HSAF/PVR-02/1.1 Issue/Revision Index: 1.1

Date: 30/09/2011

Page: 28/177

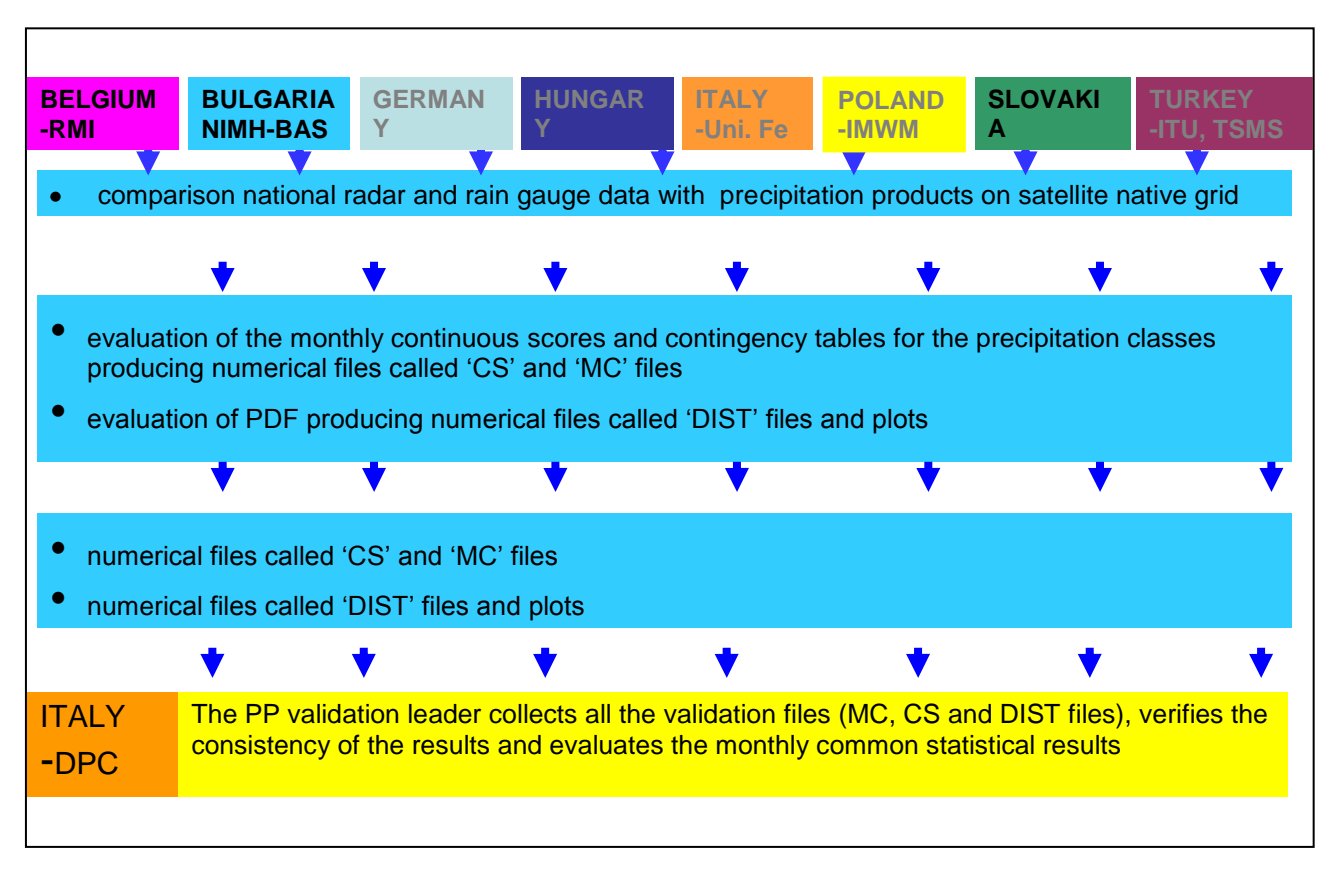


Figure 10 Main steps of the validation procedure in the PPVG

#### **Statistical scores**

The statistical scores evaluated in PPVG for continuous statistics are:

- Mean Error (ME)

$$ME = \frac{1}{N} \sum_{k=1}^{N} (sat_k - true_k)$$

Range:  $-\infty$  to  $\infty$ . Perfect score: 0

Mean Absolute Error (MAE)

$$MAE = \frac{1}{N} \sum_{k=1}^{N} |sat_k - true_k|$$

Range: 0 to ∞. Perfect score: 0

Standard Deviation (SD)

$$SD = \sqrt{\frac{1}{N} \sum_{k=1}^{N} \{ at_k - true_k - ME \}^2}$$

Range: 0 to ∞. Perfect score: 0

- Multiplicative Bias (MBias)



(Product H02 - PR-OBS-2)

Doc.No: SAF/HSAF/PVR-02/1.1

Issue/Revision Index: 1.1 Date: 30/09/2011

Page: 29/177

$$MB = \frac{\frac{1}{N} \sum_{1}^{N} sat_{K}}{\frac{1}{N} \sum_{1}^{N} true_{K}}$$

Range: - ∞ to ∞. Perfect score: 1

Correlation Coefficient (CC)

$$CC = \frac{\sum_{k=1}^{N} \{at_{k} - \overline{sat}\} \{rue_{k} - \overline{true}\}}{\sqrt{\sum_{k=1}^{N} \{at_{k} - \overline{sat}\} \sum_{k=1}^{N} \{rue_{k} - \overline{true}\}}} \quad \text{with } \overline{sat} = \frac{1}{N} \sum_{k=1}^{N} sat_{k} \quad \text{and} \quad \overline{true} = \frac{1}{N} \sum_{k=1}^{N} true_{k};$$

with 
$$\overline{sat} = \frac{1}{N} \sum_{k=1}^{N} sat_k$$
 and  $\overline{true} = \frac{1}{N} \sum_{k=1}^{N} true_k$ 

Range: -1 to 1. Perfect score: 1

Root Mean Square Error (RMSE)

$$RMSE = \sqrt{\frac{1}{N} \sum_{k=1}^{N} \{ at_k - true_k \}^2}$$

Range: 0 to ∞. Perfect score: 0

Root Mean Square Error percent (RMSE %), used for precipitation since error grows with rate.

RMSE %= 
$$\sqrt{\frac{1}{N}\sum_{k=1}^{N}\frac{\text{\$at}_{k}-true_{k}^{2}}{true^{2}_{k}}}*100$$

Range: 0 to ∞. Perfect score: 0

The statistical scores evaluated in PPVG for multi categorical statistic are derived by the following contingency table:

#### **Contingency Table**

|           |              | ground       |                   |              |  |
|-----------|--------------|--------------|-------------------|--------------|--|
|           | yes no total |              |                   |              |  |
|           | yes          | hits         | false alarms      | forecast yes |  |
| satellite | no           | misses       | correct negatives | forecast no  |  |
|           | total        | observed yes | observed no       | total        |  |

- hit: event observed from the satellite, and also observed from the ground
- miss: event not observed from the satellite, but observed from the ground
- false alarm: event observed from the satellite, but not observed from the ground
- correct negative: event not observed from the satellite, and also not observed from the ground.

The scores evaluated from the contingency table are:



(Product H02 - PR-OBS-2)

Doc.No: SAF/HSAF/PVR-02/1.1

Issue/Revision Index: 1.1 Date: 30/09/2011

Page: 30/177

- Probability Of Detection (POD)

$$POD = \frac{hits}{hits + misses} = \frac{hits}{observed \ yes}$$

Range: 0 to 1. Perfect score: 1

- False Alarm Rate (FAR)

$$FAR = \frac{falsealarms}{hits + falsealarms} = \frac{falsealarms}{forecast yes}$$

Range: 0 to 1. Perfect score: 0

- Critical Success Index (CSI)

$$CSI = \frac{hits}{hits + misses + false alarm}$$

Range: 0 to 1. Perfect score: 1

- Equitable Threat Score (ETS)

$$ETS = \frac{hits - hits_{random}}{hits + misses + false alarm - hits_{random}} \quad \text{with} \quad hits_{random} = \frac{observed \ yes * forecast \ yes}{total}$$

$$ETS \ ranges \ from \ -1/3 \ to \ 1. \ 0 \ indicates \ no \ skill. \ Perfect \ score: \ 1.$$

- Frequency Blas (FBI)

$$FBI = \frac{hits + false \, alarms}{hits + misses} = \frac{forecast \, yes}{observed \, yes}$$

Range: 0 to ∞. Perfect score: 1

- Probability Of False Detection (POFD)

$$POFD = \frac{falsealarms}{correct \, negatives \, + falsealarms} = \frac{falsealarms}{observed \, no}$$

Range: 0 to 1. Perfect score: 0

- Fraction correct Accuracy (ACC)

$$ACC = \frac{hits + correct \, negatives}{total}$$

Range: 0 to 1. Perfect score: 1

- Heidke skill score (HSS)

$$HSS = \frac{(hits + correct \, negatives) - (expected \, correct)_{random}}{N - (expected \, correct)_{random}} \qquad \text{with}$$

 $(expected correct)_{random} = \frac{1}{N}$  [observed yes)(forecast yes)+(forecast no)(observed no)]

Range:  $-\infty$  to 1. 0 indicates no skill. Perfect score: 1.

Dry-to-Wet Ratio (DWR).

$$DWR = \frac{false\ alarm + correct\ negative}{hits + misses} = \frac{observed\ no}{observed\ yes}$$
 Range: 0 to  $\infty$ . Perfect score: n/a.



(Product H02 – PR-OBS-2)

Doc.No: SAF/HSAF/PVR-02/1.1 Issue/Revision Index: 1.1

Date: 30/09/2011 Page: 31/177

### 3.9 Case study analysis

Each Institute, in addition to the large statistic verification produces a case study analysis based on **the knowledge and experience of the Institute itself**. Each institute, following a standard format here reported decides whether to use ancillary data such as lightning data, SEVIRI images, the output of numerical weather prediction and nowcasting products.

The main sections of the standard format are:

- description of the meteorological event;
- comparison of ground data and satellite products;
- visualization of ancillary data;
- discussion of the satellite product performances;
- indications to Developers;
- indication on the ground data (if requested) availability into the H-SAF project.

More details on case study analysis will be reported in the Chapter 5.

#### 3.10 Next steps

On the base of the development phase it is possible to say that the ground data error characterization is necessary and that a validation of a common protocol is not enough. Only the use of the same software can guarantee that the results obtained by several institutes are obtained in the same way. To improve the validation methodology and to develop software used by all members of the validation cluster several working groups have been composed during the last Validation Workshop held in Bratislava, 20-22 October 2010 (Annex 1 -7).

On the base of published papers and the characteristics of the ground data available inside the PPVG the main next steps are foreseen in order to improve the validation methodology:

- quantitative estimation of the errors introduced in the validation procedure comparing the instantaneous satellite precipitation estimation with the rain gauge precipitation cumulated on different intervals;
- definition of a rain gauge and radar data quality check;
- application of the data quality check to all radar and rain gauge data used in the PPVG;
- definition of the optimal and minimal spatial density of rain gauge stations to be representative
  of the ground precipitation in the view of satellite product comparison;
- development of the three software for raingauges, radar and INCA products up-scaling vs AMSU-B grids;
- definition and code implementation of the technique for the temporal matching of satellite rain rate with rain gauge and radar data;
- selection of the appropriate methodology for spatial distribution of precipitation products errors taking into consideration spatial and temporal characteristics of each product for selected areas as test catchments.

All these activities will be developed and coordinated inside the Working Groups (Annex 1 -7).



(Product H02 - PR-OBS-2)

Doc.No: SAF/HSAF/PVR-02/1.1 Issue/Revision Index: 1.1

Date: 30/09/2011 Page: 32/177

### 4 Ground data used for validation activities

#### 4.1 Introduction

In the following sections the precipitation ground data networks used in the PPVG are described: radar and rain gauge data of eight countries: Belgium, Bulgaria, Germany, Hungary, Italy, Poland, Slovakia, and Turkey. H02, has been submitted to validation in all these countries except Bulgaria. Until now the Bulgarian data are used only for H05 validation activity according to the Project Plan. Their use in the next months is under consideration.

It is well know that radar and rain gauge rainfall estimation is influenced by several error sources that should be carefully handled and characterized before using these data as reference for ground validation of any satellite-based precipitation products. In the last months working groups (Annex 1, 2, 3, 4, 5 and 7) have been composed in order to provide complete information on the ground data characteristics and to evaluate the associated errors.

In this chapter a complete analysis of the ground data available in the PPVG is reported by the rain gauge and radar data in PPVG summaries (Section 4.2 and 4.3), the Rain gauge and radar data integrated products in PPVG first report (Section 4.4) and a country by country ground data description (Section 4.5- 4.13). The chapter has the object to provide ground data information and to highlight their error sources.

### 4.2 Rain Gauge in PPVG

In this section the complete inventory of the raingauges used in the PPVG with some considerations are reported as first results of the *Rain gauge-WG* (Annex 2).

#### 4.2.1 The networks

The validation work carried on with raingauges uses about 3500 instruments across the 6 Countries: Belgium, Bulgaria, Germany, Italy, Poland, and Turkey, as usual, irregularly distributed over ground. A key characteristic of such networks is the distance between each raingauge and the closest one, averaged over all the instruments considered in the network and it is a measure of the raingauge density. Instruments number and density are summarized in Table 8.

The gauges density ranges between 7 (for Bulgaria, where only 3 river basins are considered) to 27 km (for Turkey). These numbers should be compared with the decorrelation distance for precipitation patterns at mid-latitude. Usually the decorrelation distance is defined as the minimum distance between two measures to get the correlation coefficient (Pearson Coefficient) reduced to e<sup>-1</sup>. A recent study on the H-SAF hourly data for Italy, shows this decorrelation distance varies from about 10 km in warm months (where small scale convection dominates) to 50 km in cold months, when stratified and long lasting precipitation mostly occur. In Figure 12 value of the linear correlation coefficient is computed between each raingauge pair in the Italian hourly 2009 dataset, as function of the distance between the two gauges.



(Product H02 - PR-OBS-2)

Doc.No: SAF/HSAF/PVR-02/1.1 Issue/Revision Index: 1.1

Date: 30/09/2011

Page: 33/177

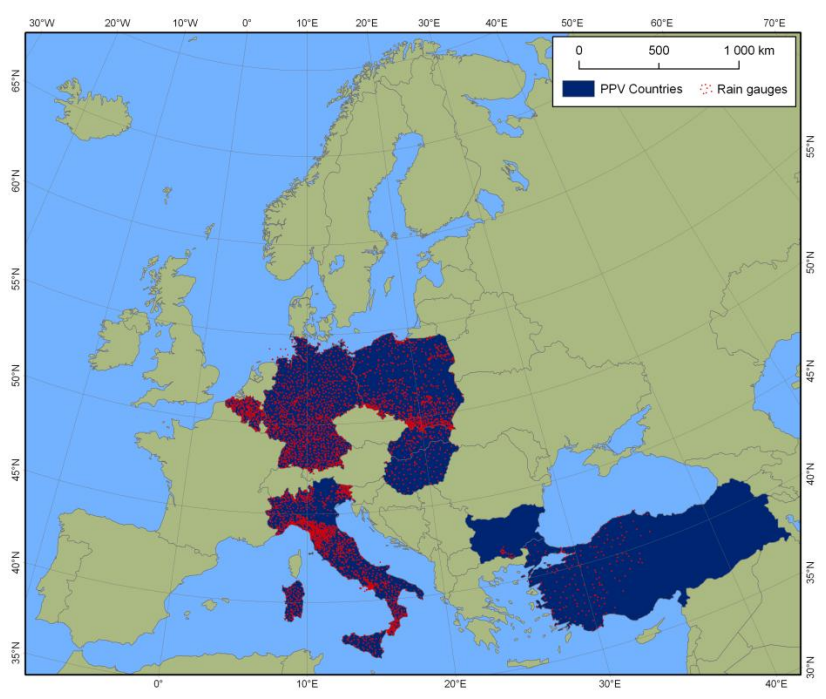


Figure 11 Rain gauge networks in PPVG

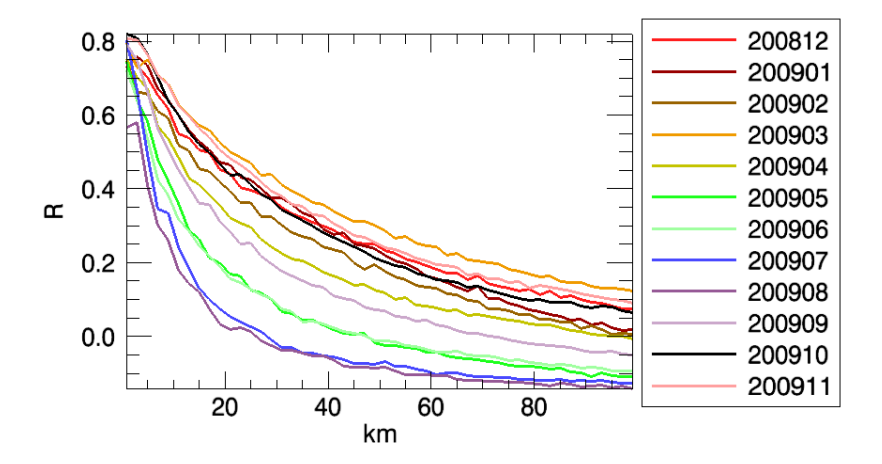


Figure 12 Correlation coefficient between raingauge pairs as function of the distances between the gauges. Colours refer to the months of the year 2009

Assuming these values significant for the other Countries involved in this study, we can conclude that the gauge network in PPVG is capable to resolve the spatial structure of rain patterns only for stratified systems but it is inadequate for small scale convective events.

| Country  | Total number of gauges * | Average minimum distance (km) |  |
|----------|--------------------------|-------------------------------|--|
| Belgium  | 89**                     | 11.2                          |  |
| Bulgaria | 37***                    | 7                             |  |
| Germany  | 1300                     | 17                            |  |
| Italy    | 1800                     | 9.5                           |  |
| Poland   | 330-475                  | 13.3                          |  |



(Product H02 - PR-OBS-2)

Doc.No: SAF/HSAF/PVR-02/1.1 Issue/Revision Index: 1.1

Date: 30/09/2011

Page: 34/177

**Turkey** 193\*\*\*\* 27

Table 8 Number and density of raingauges within H-SAF validation Group

- \* the number of raingauges could vary from day to day due to operational efficiency within a maximum range of 10-15%.
- \*\* only in the Wallonia Region
- \*\*\* only in 3 river basins
- \*\*\*\* only covering the western part of Anatolia

#### 4.2.2 The instruments

Most of the gauges used in the National networks by the PPVG Partners are of the tipping bucket type, which is the most common device used worldwide to have continuous, point-like rainrate measurement. Nevertheless, several source of uncertainty in the measurements are well known but difficult to mitigate. First, very light rainrates (1 mm h<sup>-1</sup> and less) can be incorrectly estimated due to the long time it takes the rain to fill the bucket (Tokay et al., 2003). On the other side, high rainrates (above 50 mm h<sup>-1</sup>) are usually underestimated due to the loss of water during the tips of the buckets (Duchon and Biddle, 2010). Drifting wind can also greatly reduce the size of the effective catching area, if rain does not fall vertically, resulting in a rainrate underestimation quantitatively assessed in about 15% for an average event (Duchon and Essenberg, 2001).

Further errors occur in case of solid precipitation (snow or hail), when frozen particles are collected by the funnel but not measured by the buckets, resulting in a temporal shift of the measurements since the melting (and the measure) can take place several hours (or days, depending on the environmental conditions) after the precipitation event (Leitinger et al, 2010, Sugiura et al, 2003). This error can be mitigated by an heating system that melts the particles as soon as are collected by the funnel. All these errors can be mitigated and reduced, but in general not eliminated, by a careful maintenance of the instrument.

A number of *a posteriori* correction strategies have been developed in order to correct precipitation data measured by raingauges, but mainly apply at longer accumulation intervals, daily to monthly (Wagner, 2009)

| Country  | Minimum detectable rainrate | Maximum detectable rainrate (mm h <sup>-1</sup> ) | Heating system (Y/N) | cumulation interval (min) |
|----------|-----------------------------|---|----------------------|---------------------------|
| Belgium  | 0.1 mm                      | N/A**   | N                    | 60                        |
| Bulgaria | 0.1 mm                      | 2000  | Υ                    | 120, 1440                 |
| Germany  | 0.05 mm h <sup>-1</sup>     | 3000  | Υ                    | 60                        |
| Italy    | 0.2 mm                      | N/A**   | Y/N*                 | 60                        |
| Poland   | 0.1 mm                      | N/A**   | Υ                    | 10                        |
| Turkey   | 0.2 mm                      | 720   | Υ                    | 1                         |

**Table 9 Summary of the raingauge characteristics** 

Most of these shortcomings could be avoided by using instruments based on different principle or mechanisms. The German network, and a part of the Bulgarian network, as an example, are equipped by precipitation weighting gauges, that allow continuous precipitation (both solid and liquid)

<sup>\*</sup> only 300 out of 1800 gauges are heated

<sup>\*\*</sup> information not available at the moment: a value about 300 mmh<sup>-1</sup> can be assumed for tipping bucket raingauges.



(Product H02 – PR-OBS-2)

Doc.No: SAF/HSAF/PVR-02/1.1 Issue/Revision Index: 1.1

Date: 30/09/2011 Page: 35/177

measurements with higher accuracy. Other option could be the use of disdrometers, which give more information about the precipitation structure and a more accurate rainrate measure.

In previous table relevant characteristics of the raingauges used in the different countries are reported.

### 4.2.3 Data processing

The partners of the Validation Group have been using a variety of different strategies to treat gauge data and to compare them with satellite estimates. Some are using interpolation algorithms to get spatially continuous rainfall maps, while others process directly the measurements of individual gauges. All the data in the network (except for cold months in Poland) are quality controlled: there is no information about the techniques used, but usually quality control rejects data larger than a given threshold and in case of too high rainrate difference (exceeding given thresholds) among neighbouring gauges and between subsequent measures of the same instrument. Table 10 summarizes the data preprocessing performed in different Countries, while Table 11 reports the different matching approaches for H01-H02 respectively.

As for the temporal matching, the used approaches are rather homogeneous within the Groups: instantaneous measurements are matched with next ground cumulated values over the different available intervals, ranging from 1 minute (Turkey) to 1 hour (Italy, Germany). Cumulated estimates, obviously, are compared to ground measured rain amounts over the same cumulation intervals.

As for spatial matching, different approaches are considered, also taking into account the different spatial structure of the satellite IFOVs. Two basic ideas are pursued: pixel-by-pixel matching or ground measure averaging inside satellite IFOV. The second approach seems to be more convenient, especially when the "large" IFOV of H01 and H02 are concerned. Probably it is mandatory for H02 also take into account that the size of the IFOV changes across the track and could become very large. The first approach, e.g. nearest neighbour, can be more effective for H03 and H05 products.

| Country  | Type of interpolation   | Quality control (Y/N)  |  |
|----------|-------------------------|------------------------|--|
| Belgium  | Barnes over 5x5 km grid | Υ                      |  |
| Bulgaria | Co kriging              | Υ                      |  |
| Germany  | Inverse square distance | Υ                      |  |
| Italy    | Barnes over 5x5 km grid | N                      |  |
| Poland   | No                      | Y (except cold months) |  |
| Turkey   | No                      | Υ                      |  |

Table 10 Data pre-processing strategies

|           | H                    | 01                | H02                  |                   |
|-----------|----------------------|-------------------|----------------------|-------------------|
| Country   | Spatial matching     | Temporal matching | Spatial matching     | Temporal matching |
| Belgium*  | N/A                  | N/A               | N/A                  | N/A               |
| Bulgaria* | N/A                  | N/A               | N/A                  | N/A               |
| Germany   | matching gauges are  | each overpass is  | matching gauges are  | each overpass is  |
|           | searched on a radius | compared to the   | searched on a radius | compared to the   |
|           | of 2.5 km from the   | next hourly rain  | of 2.5 km from the   | next hourly rain  |
|           | IFOV centre          | amount            | IFOV centre          | amount            |
| Italy     | mean gauges value    | each overpass is  | Gaussian-weighted    | each overpass is  |
|           | over 15x15 km area   | compared to the   | mean gauges value    | compared to the   |
|           | centred on satellite | next hourly rain  | centred on satellite | next hourly rain  |



(Product H02 – PR-OBS-2)

Doc.No: SAF/HSAF/PVR-02/1.1 Issue/Revision Index: 1.1

Date: 30/09/2011

Page: 36/177

|        | IFOV   | amount   | IFOV   | amount   |
|--------|--|--|--|--|
| Poland | mean gauges value<br>over the IFOV area<br>(rectangular)   | each overpass is compared to the next 10-minutes rain amount                           | mean gauges value<br>over the IFOV area<br>(rectangular)   | each overpass is compared to the next 10-minutes rain amount                           |
| Turkey | weighted mean of<br>the gauge values<br>estimated at the<br>3kmX3km grid<br>structure within<br>satellite IFOV by<br>using semi<br>variogram | each overpass is<br>compared to 5<br>minute averaged<br>rain" for Temporal<br>matching | weighted mean of<br>the gauge values<br>estimated at the<br>3kmX3km grid<br>structure within<br>satellite IFOV by<br>using semi<br>variogram | each overpass is<br>compared to 5<br>minute averaged<br>rain" for Temporal<br>matching |

Table 11 Matching strategies for comparison with H01 and H02

#### 4.2.4 Some conclusions

After this inventory some conclusion can be drawn.

First, it seems the raingauge networks used in this validation activities are surely appropriated for the validation of cumulated products (1 hour and higher), while for instantaneous estimates the use of hourly cumulated ground measurements surely introduces intrinsic errors in the matching scores, that can be estimated as very large. The validation of instantaneous estimates should be carried on only when gauges cumulation interval is 10 to 15 minutes (as in Poland). Values cumulated over shorter intervals (5 or even one minute, as it is done in Turkey) are affected by large relative errors in cases of low/moderate rainrates.

Different approaches for the estimates matching are considered, and probably could be a good idea to harmonize them among partners. The ground data up-scaling procedure indicated in Section 3.5 has been already developed by E. Roulin (Van de Vyver, H., and E. Roulin, 2008) and A. Rinollo. An optimization of this code to be used by all the partners of the PPVG represent one of the next step.

Anyway, different approaches over different Countries are leading to very similar values in the considered skill scores, indicating probably two things: 1) none of the considered approaches can be considered as inadequate and (more important) 2) the differences between ground fields and satellite estimates are so large that different views in the data processing do not results in different numbers.

#### 4.3 Radar data in PPVG

In this section the complete inventory of the radar data used in the PPVG with some considerations are reported as first results of the *Radar-WG* (Annex 3).

#### 4.3.1 The networks

In the HSAF project, satellite-based precipitation estimations are compared regularly with the radarderived precipitation fields. However, radar rainfall products are influenced by several error sources that should be carefully analyzed and possibly characterized before using it as a reference for validation purposes.

However, we have to emphasize that the radar data used for validation purposes is not developed by the validation groups themselves. They are developed within specialized radar working teams in many

<sup>\*</sup>Belgium and Bulgaria use raingauges only for cumulated precipitation validation.



(Product H02 - PR-OBS-2)

Doc.No: SAF/HSAF/PVR-02/1.1 Issue/Revision Index: 1.1

Date: 30/09/2011 Page: 37/177

of the countries. It is not the aim of the PPVG to improve the radar data used; however, it is specifically expected from the current activities to characterize radar data and error sources of the ground data coming from the radar networks of the PPVG.

Main error sources of radar rainfall estimations are listed in the Radar Working Group description document (Annex 3):

- 1. system calibration,
- 2. contamination by non-meteorological echoes, i.e. ground clutter, sea clutter, "clear air" echoes (birds, insects), W-LAN interferences,
- 3. partial or total beam shielding,
- 4. rain path attenuation,
- 5. wet radome attenuation,
- 6. range dependent errors (beam broadening, interception of melting snow),
- 7. contamination by dry or melting hail ("hot spots"),
- 8. variability of the Raindrop Size Distribution (RSD) and its impact on the adopted inversion techniques

Moreover, several studies have been on radar quality assessments like *S'* alek *M*, Cheze J-L, Handwerker J, Delobbe L, Uijlenhoet R. 2004.: Radar techniques for identifying precipitation type and estimating quantity of precipitation. COST Action 717, Working Group 1 – A review. Luxembourg, Germany; or Holleman, I., D., Michelson, G. Galli, U. Germann and M. Peura, Quality information for radars and radar data, Technical rapport: 2005, EUMETNET OPERA, OPERA 2005 19, 77p.

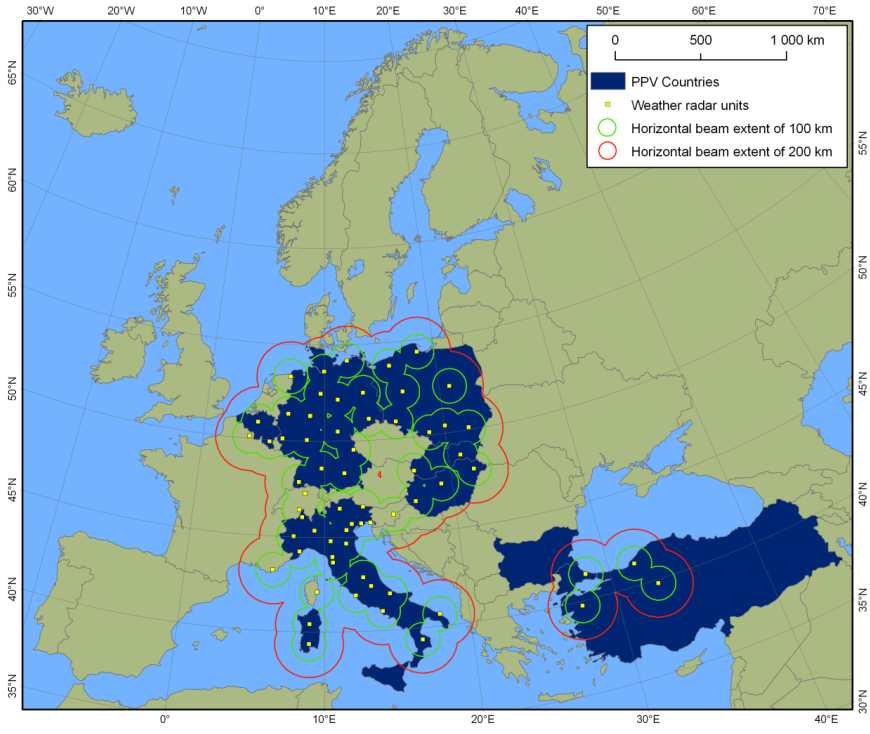


Figure 13 Radar networks in PPVG

The first step was to collect characteristics (polarization, beam width, maximum range, range, resolution, scan frequency, geographical coordinates, scan strategy [elevations]...) of the radar networks which composes the PPVG adopted processing chain; and the generated products (including



(Product H02 - PR-OBS-2)

Doc.No: SAF/HSAF/PVR-02/1.1 Issue/Revision Index: 1.1

Date: 30/09/2011 Page: 38/177

the quality map, if any). The results of the overview of different radar capacities and instruments in each of the participating countries are here reported.

#### 4.3.2 The instruments

In the PPVG group, there are 54 C-band radars used, or in the plan to be used. Their distribution in the countries is:

- Belgium (1 radar)
- Germany (16 radars not BfG products)
- Hungary (3 radars)
- > Italy (18 radars)
- Slovakia (2 radars)
- Poland (8 radars)
- Turkey (6 radars)

These radars cover wide range of geographical area: from the longitude 5.50562 in Wideumont, Belgium to the most Eastern area with longitude 32°58'15" in Ankara, Turkey; and from the Northern latitude of 54°23′03,17" in Gdańsk, Poland to the latitude of 36°53'24" in Mugla, Turkey and lat 37,462 in Catania, Italy. The Radars are built at different elevations above the sea level. In mountainous countries, they are placed at elevations more than 1000m above sea level; whereas in flat countries like Hungary or Belgium, their height position is not exceeding 400m. This information collected will be useful in the future steps of the Working Group to assess the partial or total beam shielding by mountains in the propagation way of the radar signals.

All radars are C-band radars, working at frequency in C-band, at 5.6 GHz. All radars are equipped by Doppler capacity which means that ground clutters can be removed from the radar data measurements effectively; however, not all of them have dual polarization which would be important to correct rain path attenuation.

The scan strategy for each of the radars used has been investigated. In this matter, all countries have shared their information on the number of elevations, minimum and maximum elevations, scan frequency, maximum nominal range distance, and range resolution.

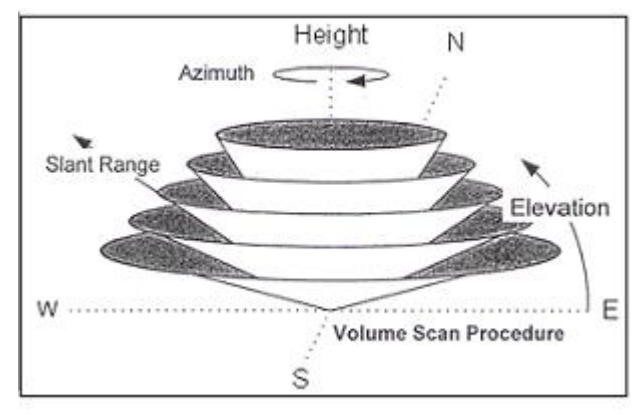


Figure 14 Radar scan procedure

In the PPVG the scan frequency ranges from 5 minutes in Belgium, Germany and Slovakia to 10 minutes in Turkey and Poland, and 15 minutes in Hungary; and varying frequency for Italian radars. The number of elevation stays between 4 and 15, in average around 10.



(Product H02 - PR-OBS-2)

Doc.No: SAF/HSAF/PVR-02/1.1 Issue/Revision Index: 1.1

Date: 30/09/2011 Page: 39/177

The range distance used is 240 km in general. But in some places in Italy, and for the Turkish radars, the maximum range distance used is 120 km, or even less, e.g. 80 km.

Range resolution is 250 m in Belgium, 250, 340, 225, and sometimes 500 m for the Italian radars, 500 m for one of the Hungarian radars, and 250m for the other two, Polish radars can work with 125 m and 250 m resolution, and in Turkey it is 250 m for all the radars.

The scan strategies within the PPVG countries are well-balanced and similar to each other; though they vary from one radar to the other, even within countries.

All radars are regularly maintained and calibrated, which is a good indicator of the continuous supervision of quality of radar data, and the important element to sustain radar data quality.

#### 4.3.3 Data processing

The Tab. 08 is provided to summarize the available products generated from radar measurements, and the processing chain used to generate them. Finally, the list of the radar products used for the validation work is included in the last row.

Radar rainfall products are obtained after processing the measured radar reflectivity at different elevations of the radar scan strategy. After each elevation, the PPI (Plan Position Indicator) products and the CAPPI (Constant Altitude PPI) products are calculated. PPI is the measurement of the radar antenna rotating 360 degrees around the radar site at a fixed elevation angle. CAPPI products are derived from this, by taking into account the radar displays which give a horizontal cross-section of data at constant altitude. The CAPPI is composed of data from several different angles that have measured reflectivity at the requested height of CAPPI product.

The PPVG group uses mostly CAPPI products for calculation of rainfall intensities; except for Hungary, which uses the CMAX data (maximum radar reflectivity in each pixel column among all of the radar elevations) for deriving rainfall intensities. However, the rest of the countries have also chosen different elevation angles for the CAPPI product which provides the basis for rain rate estimations. Additionally, we have to say that the countries apply different techniques of composition of radar data that were not specified in this questionnaire. The composition technique is important in areas which are covered by more than one radar measurements. Also, the projection applied is varying from one country to the other.

To sum up, the radar products used are not harmonized, different techniques are applied. However, each of them is capable to grasp rainfall and to estimate rainfall intensity.

As for the accumulated products, we see that Belgium uses 24-hourly accumulations, with rain gauge correction, Italy uses 3, 6, 12, 24h accumulations without gauge-correction; in Hungary 3, 6, 12, 24h data is used, but only the 12h and 24 hourly accumulations are corrected by rain gauges, in Poland and Slovakia no rain gauge correction is applied. Poland has only 6, and 24 hourly data. Turkey has 3,6,12,24h data, and applies rain gauge correction for 1 hourly data. It is important to note that techniques used for accumulation are numerous, even within the same country the can differ from one accumulation period to another. E.g. in Hungary, the 3,6h accumulations are derived from summing up the interpolation of the 15minute-frequent measurements into 1 minute-intervals; whereas the 12, and 24 h accumulations are summed up from 15 minute measurements, but corrected with rain gauge data.

All above implies that more probably the quality and error of rainfall and rain rate accumulations is differing from one country to another; and cannot be homogeneously characterized.



(Product H02 - PR-OBS-2)

Doc.No: SAF/HSAF/PVR-02/1.1 Issue/Revision Index: 1.1

Date: 30/09/2011 Page: 40/177

#### 4.3.4 Some conclusions

#### Maintenance

All the contributors declared the system are kept in a relatively good status.

### <u>Correction factors</u> for error elimination:

These correction factors are diverse in the countries, not homogeneous distribution of correction methods:

- > all contributors compensate for non-meteorological echoes (Clutter)
- RLAN interferences implemented in Hungary, Slovakia- in development.
- > Poland and Slovakia correct attenuation. In other countries, it is not accounted for.
- Some of the countries are testing new procedures for dealing with VPR (Italy) and Partial Beam Blockage, PBB effects. VPR (Vertical Profile of Reflectivity) used in Turkey.

This means that the corresponding rainfall estimates are diverse, and the estimation of their errors cannot be homogenized.

However, each county can provide useful information of the error structure of its rainfall products based on its own resources: e.g. if they have already defined Quality Indicators, or estimations of errors based on studies of comparison of radar and rain gauge data in the country itself. The study performed by the Slovakian team (Annex 4) and the scheme published by J. Szturc, on the quality index evaluation are under consideration by the *Radar-WG*.

In the future, possible separation of reliable and quasi-reliable radar fields would be possible. Separation would be based on radar site/geographical areas/event type/radar products. Selected cases will be suitable enough to be used as a reference for the H-SAF products validation. A study on evaluation of radar measurements quality indicator with regards to terrain visibility has been conducted by the Slovakian team (see Annex 4).

Satellite product testing will be carried out in areas with higher reliability. Statistical results will be evaluated and compared to previous data. As such, the accuracy of statistical results of PPVG with radar data as ground reference will be able to be established.

|                | BELGIUM                    | ITALY                    | HUNGARY                    |
|----------------|----------------------------|--------------------------|----------------------------|
| List of        | Rain rate 240 Km;          |                          | CMAX,                      |
| Available      | rain rate 120 Km; velocity |                          | PPI,                       |
| Products       | (120 Km);                  |                          | CAPPI(2.5 km),             |
|                | MAX (240 Km);              |                          | VIL,                       |
|                | VVP2 Windprofiles;         |                          | ETops,                     |
|                | Hail Probability;          |                          | Base,                      |
|                | Hail Probability 24h       |                          | HailProbability            |
|                | Overview;                  |                          |                            |
|                | 1, 3, 24 Hr Rainrate       |                          |                            |
|                | accumulation;              |                          |                            |
| Is any quality | NO                         | YES                      | NO                         |
| map available? |                            |                          |                            |
| Processing     | Clutter removal (time-     | Clutter suppression by   | RLAN(wifi) filter; Clutter |
| chain          | domain Doppler filtering   | Fuzzy Logic scheme using | removal; atttenuation      |
|                | and static clutter map);   | Clutter map, Velocity,   | correction + beam          |



(Product H02 – PR-OBS-2)

Doc.No: SAF/HSAF/PVR-02/1.1

Issue/Revision Index: 1.1

Date: 30/09/2011

Page: 41/177

|                | Z-R: a=200, b=1.6      | Texture.<br>Z-R: a=200, b=1. | blocking correction => next Year (2012) |
|----------------|------------------------|------------------------------|---|
|                |                        | VPR correction under         | VPR => No                               |
|                |                        | testing.                     | Z-R: a=200, b=1.6                       |
| Description of | PCAPPI-1500m Cartesian | Nationale composite:         | National composite,                     |
| instantaneous  | grid,                  | CAPPI 2 km, CAPPI 3 km,      | (CMAX)                                  |
| radar product  | 600m resolution        | CAPPI 5 km, VMI, SRI         | Projection: stereographic               |
| used in HSAF   |                        | Projection: Mercator         | (S60)                                   |
| Validation     |                        | Resolution: 1 km             | Resolution: 2 km                        |
| Activities     |                        | Threshold: No                | Threshold: 7dBZ                         |
|                |                        |                              | No rain gauge correction                |
| Description of | 24-h accumulation with | Acc. periods: 1, 3, 6, 12,   | Acc.periods: 3,6,12,24h                 |
| accumulated    | range-dependent gauge  | 24h                          | National composite,                     |
| radar product  | adjustment,            | Projection: Mercator         | (CMAX)                                  |
| used in HSAF   | Cartesian grid,        | Resolution: 1 km             | Projection: stereographic               |
| Validation     | 600m resolution        | Threshold: No                | (S60)                                   |
| Activities     |                        | No rain gauge correction     | Resolution: 2 km                        |
|                |                        |                              | Threshold: 7dBZ                         |
|                |                        |                              | Rain gauge correction                   |
|                |                        |                              | applied for 12, 24 hourly               |
|                |                        |                              | data                                    |

Table 12 Inventory of the main radar data and products characteristics in Belgium, Italy, Hungary

|                   | POLAND                   | SLOVAKIA                | TURKEY                 |
|-------------------|--------------------------|-------------------------|------------------------|
| List of Available | PPI, PCAPPI, RHI, MAX,   | CAPPI 2 km,             | MAX,                   |
| Products.         | EHT, SRI, PAC, VIL, VVP, | Etops,                  | PPI,                   |
|                   | HWIND, VSHEAR, HSHEAR,   | PPI 0.2,                | CAPPI,                 |
|                   | LTB, SWI, MESO, WRN.     | Base,                   | VIL,                   |
|                   | List of non-operational  | Cmax,                   | ETOPS,                 |
|                   | products: LMR, CMAX,     | Hmax,                   | EBASE,                 |
|                   | UWT, VAD, SHEAR, SWI,    | VIL,                    | RAIN Accumulation      |
|                   | MESO, ZHAIL, RTR, CTR,   | Precip. Intensity, 1h-, | (1,3,6,12,24h)         |
|                   | WRN.                     | 3h-, 6h-, 24h-acc.      |                        |
|                   |                          | precip., 1h-acc.        |                        |
|                   |                          | SRI 1km, 2km agl        |                        |
| Processing chain  | Doppler method clutter   | Clutter filtering:      | Clutter Removal, VPR   |
|                   | removal; attenuation     | frequency-domain IIR    | Correction, Z-R: A=200 |
|                   | correction - yes;        | filter;                 | b=1.6                  |
|                   | VPR => No                | Atmospheric             |                        |
|                   | Z-R: a=200, b=1.6        | attenuation correction; |                        |
|                   |                          | Z-R: a=200, b=1.6       |                        |
|                   | !                        | RLAN filtering in       |                        |
|                   |                          | development             |                        |
| Is any quality    | NO, in development       | NO                      | NO                     |
| map available?    |                          |                         |                        |



(Product H02 - PR-OBS-2)

Doc.No: SAF/HSAF/PVR-02/1.1 Issue/Revision Index: 1.1

Date: 30/09/2011

Page: 42/177

| Description of        | National composite, (SRI); | National composite      | CAPPI, Projection:        |
|-----------------------|----------------------------|-------------------------|---------------------------|
| instantaneous         | Projection: azimutal       | CAPPI 2 km              | Azimuthal Equidistant     |
| radar product         | equidistant (standard:     | Projection: Mercator    | Resolution: 250 m         |
| used in HSAF          | ellipsoid); Resolution: 1  | Resolution: 1 km        | Threshold: ? Rain Gauge   |
| Validation            | km; Threshold: 5 dBZ; No   | Threshold: -31.5 dBZ    | Correction (with limited  |
| Activities            | rain gauge correction.     | No rain gauge           | number of gauges)         |
|                       |                            | correction              |                           |
| <b>Description</b> of | Acc. Periods: 1, 6, 24h;   | Acc. periods: 3, 6, 12, | Acc.periods: 1,3,6,12,24h |
| accumulated           | National composite (PAC),  | 24h                     | Projection: Azimuthal     |
| radar product         | Projection: azimuthal      | National composite      | Equidistant               |
| used in HSAF          | equidistant (standard:     | CAPPI 2 km              | Resolution: 250 m         |
| Validation            | elipsoid); Resolution: 1   | Projection: Mercator    | Threshold: ?              |
| Activities            | km; Threshold: 0,1 mm;     | Resolution: 1 km        | Rain gauge correction     |
|                       | No rain gauge correction   | Threshold: -31.5 dBZ    | applied for 1h Rain Acc.  |
|                       |                            | No rain gauge           |                           |
|                       |                            | correction              |                           |

Table 13 Inventory of the main radar data and products characteristics in Poland, Slovakia, Turkey

### 4.4 Rain gauge and radar data integrated products in PPVG

In order to investigate the possible improvement of the ground precipitation field estimation a WG "INCA-WG" has been introduced in the validation activities of PPVG. In this section the first results with some considerations of the INCA- WG (Annex 5) are reported.

Within the WG participating countries (Slovakia, Poland and Germany) there are two types of systems providing precipitation analyses usable for H-SAF validation: **INCA** (developed by ZAMG, Austria) and **RADOLAN** (DWD, Germany).

The INCA system is currently under development as INCA-CE (Central Europe) and it is used in preoperational mode in Slovakia and Poland. The RADOLAN system is used in Germany operationally and it is already utilized for the H-SAF products validation. Both systems consist of computational modules which enable to integrate various sets of precipitation data sources — raingauge network, radar network, NWP models outputs and climatological standards into common precipitation product, which can describe well the areal instantaneous and cumulated precipitation fields.

Here below a brief description of the INCA and RADOLAN systems follows. More information on both systems can be found in the documentation which is available on the H-SAF ftp server: /hsaf/WP6000/precipitation/WG\_groups/WG3-inca/documentation .



(Product H02 - PR-OBS-2)

Doc.No: SAF/HSAF/PVR-02/1.1 Issue/Revision Index: 1.1

Date: 30/09/2011 Page: 43/177



Figure 15 Coverage of Europe by the INCA and RADOLAN systems

#### 4.4.1 INCA system

The INCA (Integrated Nowcasting through Comprehensive Analysis) analysis and nowcasting system is being developed primarily as a means of providing improved numerical forecast products in the nowcasting and very short range forecasting. It should integrate, as far as possible, all available data sources and use them to construct physically consistent analyses of atmospheric fields. Among the input data sources belong:

- NWP model outputs in general (P, T, H, clouds ...)
- Surface station observations (T, precipitation)
- Radar measurements (reflectivity, currently 2-d, 3-d in development)
- Satellite data (CLM, Cloud type, in development for use in precipitation analysis)
- Elevation data (high resolution DTM, indication of flat and mountainous terrain, slopes, ridges, peaks)

#### The INCA system provides:

- High-resolution analyses interest of validation WG-3
- Nowcasts
- Improved forecasts

#### of the following variables:

- Temperature (3-d field)
- Humidity (3-d)
- Wind (3-d)
- Precipitation (2-d) interest of validation WG-3
- Cloudiness (2-d)
- Global radiation (2-d)

The INCA precipitation analysis is a combination of station data interpolation including elevation effects, and radar data. It is designed to combine the strengths of both observation types, the accuracy of the point measurements and the spatial structure of the radar field. The radar can detect precipitating cells that do not hit a station. Station interpolation can provide a precipitation analysis in areas not accessible to the radar beam.



(Product H02 - PR-OBS-2)

Doc.No: SAF/HSAF/PVR-02/1.1 Issue/Revision Index: 1.1

Date: 30/09/2011 Page: 44/177

The precipitation analysis consists of the following steps:

- Interpolation of station data into regular INCA grid (1x1 km) based on distance weighting (only nearest 8 stations are taken into account to reduce bull-eyes effect)
- ii. Climatological scaling of radar data by means of monthly precipitation totals of raingauge to radar ratio (partial elimination of the range dependence and orographical shielding)
- iii. Re-scaling of radar data using the latest rain gauge observations
- iv. Final combination of re-scaled radar and interpolated rain gauge data
- Elevation dependence and orographic seeding precipitation ٧.

In the final precipitation field the raingauge observations are reproduced at the raingauge station locations within the limits of resolution. Between the stations, the weight of the radar information becomes larger the better the radar captures the precipitation climatologically.

Important factor affecting the final precipitation analysis is accuracy and reliability of the raingauge stations. In order to eliminate the influence of raingauge stations providing evidently erroneous data, the SHMÚ is developing the blacklisting technique which temporarily excludes such stations from the analysis. Currently, the stations can be put into the blacklist only manually but development of the automated blacklisting is expected in near future.

#### 4.4.2 **RADOLAN system**

RADOLAN is a routine method for the online adjustment of radar precipitation data by means of automatic surface precipitation stations (ombrometers) which has started on a project base at DWD in 1997. Since June 2005, areal, spatial and temporal high-resolution, quantitative precipitation data are derived from online adjusted radar measurements in real-time production for Germany.

The data base for the radar online adjustment is the operational weather radar network of DWD with 16 C-band sites on the one hand, and the joined precipitation network of DWD and the federal states with automatically downloadable ombrometer data on the other hand. In the course of this, the precipitation scan with five-minute radar precipitation data and a maximum range of 125 km radius around the respective site is used for the quantitative precipitation analyses. Currently, from more than 1000 ombrometer station (approx. 450 synoptic stations AMDA I/II-and AMDA III/S-of DWD; approx. 400 automatic precipitation stations AMDA III/N of DWD; approx. 150 stations of the densification measurement network of the federal states) the hourly measured precipitation amount is used for the adjustment procedure.

In advance of the actual adjustment different preprocessing steps of the quantitative radar precipitation data are performed. These steps, partly already integrated in the offline adjustment procedure, contain the orographic shading correction, the refined Z-R relation, the quantitative composite generation for Germany, the statistical suppression of clutter, the gradient smoothing and the pre-adjustment. Further improvements of these procedures are being developed.

rain gauge point measurements

Precipitation distribution of the Precipitation distribution of the areal original radar measurements

RADOLAN precipitation product



(Product H02 - PR-OBS-2)

Doc.No: SAF/HSAF/PVR-02/1.1 Issue/Revision Index: 1.1

Date: 30/09/2011

Page: 45/177

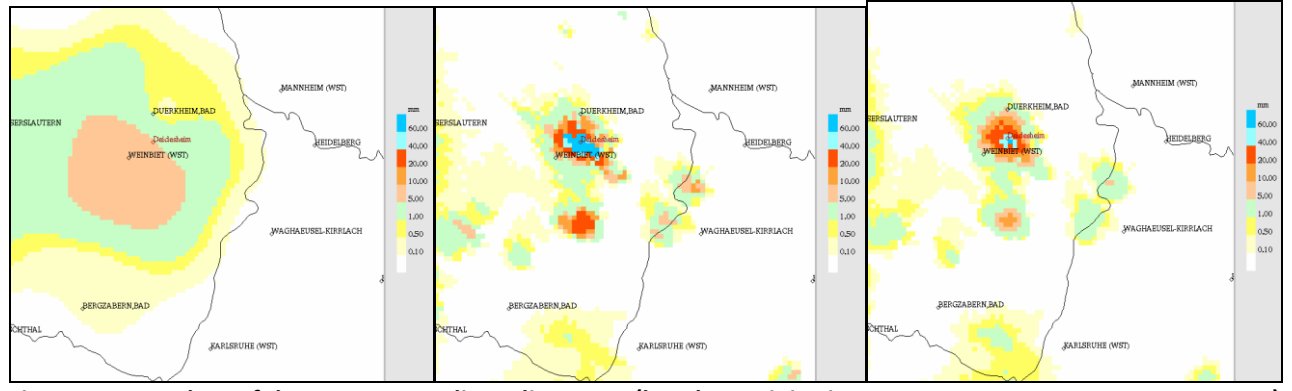


Figure 16 Procedure of the RADOLAN online adjustment (hourly precipitation amount on 7 August 2004 13:50 UTC)

In order to collect more detailed information about both types of systems a questionnaire was elaborated and completed by Slovakia, Poland and Germany. The questionnaire provided details such as geographical coverage (see Fig. 17), input data inventory or availability of different instantaneous and cumulated precipitation products.

The final version of the questionnaire is shown in the next table and is also available as annex 5.



(Product H02 - PR-OBS-2)

Doc.No: SAF/HSAF/PVR-02/1.1 Issue/Revision Index: 1.1

Date: 30/09/2011

Page: 46/177

| Pokumentation received   |                                 |   |                             |                 |                        | I  |
|--|---------------------------------|---|-----------------------------|-----------------|------------------------|--|
| Available   Procedure   Proc   | Group of information            | Item  | GERMANY                     | POLAND          | SLOVAKIA domain1       | SLOVAKIA domain2                         |
| Min longitude  |                                 |   | during Helsinki validation  |                 |                        | Documentation should be issued in future |
| Max longitude  |                                 | Grid size in pixels   | 900x900                     | 741x651         | 501x301                | 1193x951                                 |
| Min latitude  46,95719 N  48,728 N  47,1385 N  45,0027313232 N  50,30057834 N  50,30057834 N  50,30057834 N  50,30057834 N  1 km  1  |                                 | Min longitude   | 3.5943 E                    | 13.82 E         | 15.99231 E             | 8,9953784943 E                           |
| Max latitude   |                                 | Max longitude   | 15.71245 E                  | 25.334 E        | 23.09630 E             | 25,9996967316 E                          |
| Space resolution   1 km  |                                 | Min latitude  | 46.95719 N                  | 48.728 N        | 47.13585 N             | 45,0027313232 N                          |
| Imput data   Number of radars in network   Number of precipitation stations   Number of precipitation based only on raingauge network, time resolution, immellines   Number of precipitation based only on statinaneous   Number of Pea, similar precipitation   Number of Pea, similar precipit |                                 | Max latitude  | 54.73662 N                  | 55.029 N        | 50.14841 N             | 53,000579834 N                           |
| Number of reads in network Number of precipitation stations Number of precipitation stations Number of precipitation stations Neshol Selective for precipitation stations Neshol  |                                 | Space resolution  | 1 km                        | 1 km            | 1 km                   | 1 km                                     |
| Number of precipitation stations   1300   475 (Poland only)   397 (SHML, CHML, ZAMG, MWWM)   TED   | Input data                      | Number of radars in network   |                             |                 |                        |  |
| New Not   New    |                                 | Number of precipitation stations  |                             |                 | 397 (SHMU, CHMI, ZAMG, |  |
| Density of rangauge stations    Yes,No   |                                 |   | ?                           | Yes             | Yes                    | Yes                                      |
| Output data  on raingauge network, time resolution, timelines instantaneous precipitation based only on radar network, time resolution, timelines  Cumulative precipitation based only on raingauge network, time intervals, timelines  Cumulative precipitation based only on raingauge network, time intervals, timelines  Cumulative precipitation based only on raingauge network, time intervals, timelines  Cumulative precipitation based only on raingauge network, time intervals, timelines  Cumulative precipitation based only on radar network, time intervals, timelines  Cumulative precipitation based on combined raingauge and radar network, time intervals, timelines  Dates for selected case studies  Case 1  Case 2  Case 3  Case 4  Case 4  Case 5  No  No  Yes, 5 minute  Yes, 5 minute  Yes, 5 minutes  Yes, 5 minutes  Yes, min 5 min, available 1,3,6,12,24 hours  No 29,3,2009  Yes, min 5 min, available 1,3,6,12,24 hours  No 10 minutes, available 1,3,6,12,24 hours  No 29,3,2009  No 1,3,6,12,18,24 hours  No 29,3,2009  No N  | Density of raingauge stations   |   | ?                           | TBD             | TBD                    | TBD                                      |
| on radar network, time resolution, timelines instantaneous precipitation based on combined raingauge and radar network, time resolution, timelines Cumulative precipitation based only on radar network, time intervals, timelines  Cumulative precipitation based only on radar network, time intervals, timelines  Cumulative precipitation based only on radar network, time intervals, timelines  Cumulative precipitation based only on radar network, time intervals, timelines  Cumulative precipitation based only on radar network, time intervals, timelines  Cumulative precipitation based on combined raingauge and radar network, time intervals, timelines  Dates for selected case studies  Case 1  Case 2  No  Case 3  No  29.3.2009  Case 3  No  20.6.2010  Case 4  No  15.16.8.2010  Availability of own software for upscaling NCA data into native satellite grid  H01  yes  No  No  No  No  No  No  No  No  No  N  | Output data                     | on raingauge network, time resolution,                                    | 5 min                       | No              | Yes, 15 min            | Yes, 15 minute                           |
| Instantaneous precipitation based on combined raingauge and radar network, time resolution, timelines Cumulative precipitation based only on raingauge network, time intervals, timelines  Cumulative precipitation based only on radar network, time intervals, timelines  Cumulative precipitation based only on radar network, time intervals, timelines  Cumulative precipitation based only on radar network, time intervals, timelines  Cumulative precipitation based only on radar network, time intervals, timelines  Cumulative precipitation based on combined raingauge and radar network, time intervals, timelines  Cumulative precipitation based only on radar network, time intervals, timelines  Cumulative precipitation based only on radar network, time intervals, timelines  Smin, 1,3,6,12,18,24 hours  Yes, min 10 minutes, available 1,3,6,12,24 hours  Yes, min 5 min, available 1,3,6,12,24 hours  No 29.3.2009  To ase 2  No 13,6,2010  Case 3  No 29.3.2009  Case 3  No 13,6,2010  Case 4  No 1516.8.2010  Case 5  No No No No  No No  H01  H02  yes No No No No No  No No  No No  H03  H04  No No No No  No No No  No No No  No No No  No No No No  No No No No  No No No No No  No No No No No No No No No No No No No N  |                                 | on radar network, time resolution,  | 5 min                       | No              | Yes, 5 minute          | Yes, 5 minute                            |
| Cumulative precipitation based only on raingauge network, time intervals, timelines  Cumulative precipitation based only on radar network, time intervals, timelines  Cumulative precipitation based on combined raingauge and radar network, time intervals, timelines  Cumulative precipitation based on combined raingauge and radar network, time intervals, timelines  Camulative precipitation based on combined raingauge and radar network, time intervals, timelines  Case 1  Case 1  Case 2  No  Case 2  No  Case 3  No  Case 3  No  Case 4  No  Case 4  No  Case 5  No  Availability of own software for upscaling INCA data into native satellite grid  H01  yes  No  No  Yes, min 5 min, available 1,3,6,12,24 hours  No  Take, min 5 min, available 1,3,6,12,24 hours  No  1,3,6,12,24 hours  Yes, min 5 min, available 1,3,6,12,24 hours  No  1,3,6,12,24 hours  Yes, min 5 min, available 1,3,6,12,24 hours  No  1,3,6,12,24 hours  Yes, min 5 min, available 1,3,6,12,24 hours  No  1 |                                 | Instantaneous precipitation based on combined raingauge and radar         | 5 min                       | Yes, 10 minutes | Yes, 5 minutes         | Yes, 5 minutes                           |
| Tadar network, time intervals, timelines   Smin, 1,3,6,12,18,24 hours   Cumulative precipitation based on combined raingauge and radar network, time intervals, timelines   Smin, 1,3,6,12,18,24 hours   Yes, min 10 minutes, available 1,3,6,12,24 hours   Yes, min 5 min, available 1,3,6,12,24 hours    |                                 | Cumulative precipitation based only on raingauge network, time intervals, | 5 min, 1,3,6,12,18,24 hours | No              |                        |  |
| Cambined raingauge and radar network, time intervals, timelines   5 min, 1,3,6,12,18,24 hours   7 min, available 1,3,6,12,24 hours   7 min, available 1,3,6,1   |                                 |   | 5 min, 1,3,6,12,18,24 hours | No              |                        |  |
| Dates for selected case studies         Case 1         will be set         No         29.3.2009           Case 2         No         13.6.2010         13.6.2010           Case 3         No         20.6.2010           Case 4         No         1516.8.2010           Case 5         No         No           Availability of own software for upscaling INCA data into native satellite grid         H01         yes         No         No         No           H02         yes         No         No         No         No           H03         yes         No         No         No           H04         no         No         No         No   |                                 | combined raingauge and radar  | 5 min, 1,3,6,12,18,24 hours |                 |                        |  |
| Case 3   | Dates for selected case studies | Case 1  | will be set                 | No              | 29.3.2009              |  |
| Case 4         No         1516.8.2010           Case 5         No         No           Availability of own software for upscaling INCA data into native satellite grid         H01         yes         No         No         No           H02         yes         No         No         No         No           H03         yes         No         No         No           H04         no         No         No         No   |                                 | Case 2  |                             | No              | 13.6.2010              |  |
| Case 5   |                                 | Case 3  |                             | No              | 20.6.2010              |  |
| Availability of own software for upscaling   H01   |                                 | Case 4  |                             | No              | 1516.8.2010            |  |
| INCA data into native satellite grid  H02  yes  No  No  No  No  No  No  No  No  No  N  |                                 | Case 5  |                             | No              |                        |  |
| H03 yes No   |                                 | H01   | yes                         | No              | No                     | No                                       |
| H04 no No No No  |                                 | H02   | yes                         | No              | No                     | No                                       |
|  |                                 | Н03   | yes                         | No              | No                     | No                                       |
| H05 yes No No No   |                                 | H04   | no                          | No              | No                     | No                                       |
|  | _                               | Н05   | yes                         | No              | No                     | No                                       |
| H06 yes No No No   |                                 | Н06   | yes                         | No              | No                     | No                                       |

**Table 14 INCA Questionnaire** 

#### 4.4.3 Some conclusions

The INCA system as a potential tool for the precipitation products validation is available in Slovakia and Poland, in both countries being run in pre-operational mode. It is still relatively new system undergoing continuous development. More sophisticated algorithms of the precipitation analysis (e.g. assimilation of the 3-D radar data) can be expected from its development in frame of the ongoing INCA-CE project.

In Germany similar precipitation analysis system called RADOLAN is being run operationally. This tool is already used for validation of the H-SAF precipitation products in this country.

The accuracy and reliability of the raingauge stations significantly affect final precipitation analysis of the INCA or INCA-like systems and therefore need to be checked. In order to solve this problem an



## Product Validation Report - PVR-02 (Product H02 – PR-OBS-2)

Doc.No: SAF/HSAF/PVR-02/1.1 Issue/Revision Index: 1.1

Date: 30/09/2011 Page: 47/177

automated blacklisting technique is going to be developed at SHMÚ (currently blacklisting is used in manual mode).

The software for upscaling the INCA precipitation field into the H-SAF products grid will have to be developed. Since the grids of INCA and RADOLAN have similar horizontal resolution to the common radar grid, the radar upscaling techniques can be applied also on the INCA or RADOLAN data. In frame of the unification of the validation methodologies the same common upscaling software could be shared between both radar and INCA working groups in the future.

### 4.5 Ground data in Belgium (IRM)

#### 4.5.1 Radar data

#### The network

Belgium is well covered with three radars (see *next figure*). Further radar is currently under construction in the coastal region.

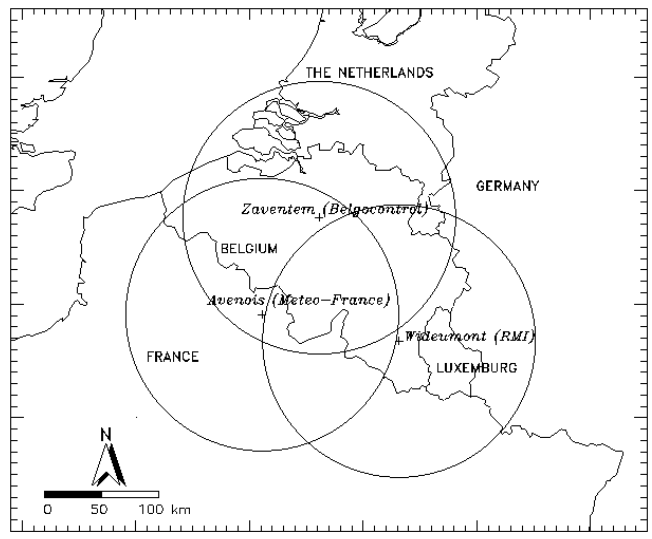


Figure 17 Meteorological radar in Belgium

#### The instruments

These are Doppler, C-band, single polarization radars with beam width of 1° and a radial resolution of 250 m. Data are available at 0.6, 0.66 and 1 km horizontal resolution for the Wideumont, Zaventem and Avesnois radars respectively.

In this report, only the Wideumont radar has been used. The data of this radar are controlled in three steps.

## Data processing

First, a long-term verification is performed as the mean ratio between 1-month radar and gauge accumulation for all gauge stations at less than 120 km from the radar. The second method consists in fitting a second order polynomial to the mean 24 h (8 to 8 h local time) radar / gauge ratio in dB and the range; only the stations within 120 km and where both radar and gauge values exceed 1 mm are taken into account. The third method is the same as the second but is performed on-line using the 90 telemetric stations of the SETHY (Ministry of the Walloon Region). Corrected 24 h images are then



(Product H02 – PR-OBS-2)

Doc.No: SAF/HSAF/PVR-02/1.1 Issue/Revision Index: 1.1

Date: 30/09/2011 Page: 48/177

calculated. New methods for the merging of radar and raingauge data have been recently evaluated (Goudenhoofdt and Delobbe 2009)<sup>1</sup>.In this report, only instantaneous radar images are used.

## 4.6 Ground data in Bulgaria (NIMH)

### 4.6.1 Rain gauge

#### The network

The maximum number of available raingauges for this project is 37, distributed over 3 basins.

The average distance between stations is about 7 km, with a very high variance. Generally in the plain area distance is lower than in the mountainous areas



Figure 18 Distribution of the raingauge stations of Iskar River Basin

-

<sup>&</sup>lt;sup>1</sup> Goudenhoofdt E. and L. Delobbe, 2009: "Evaluation of radar-gauge merging methods for quantitative precipitation estimates". *Hydrol. Earth Syst. Sci.*, 13, 195-203.



(Product H02 - PR-OBS-2)

Doc.No: SAF/HSAF/PVR-02/1.1 Issue/Revision Index: 1.1

Date: 30/09/2011 Page: 49/177

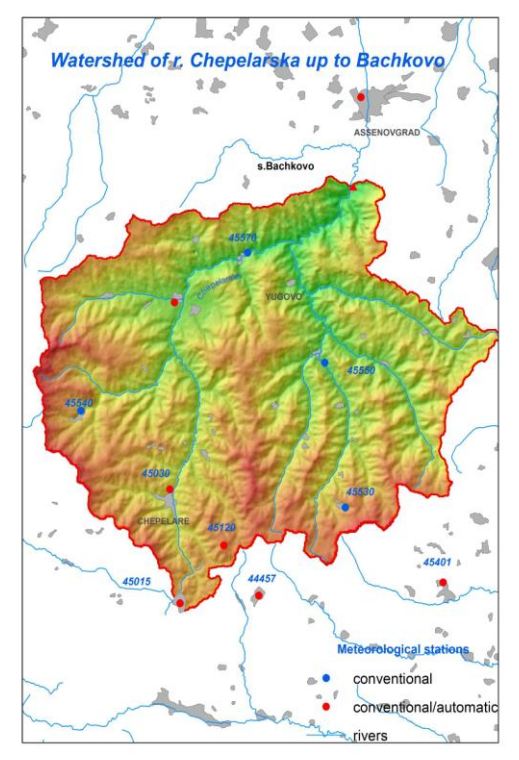


Figure 19 Distribution of the raingauge stations of Chepelarska River Basin

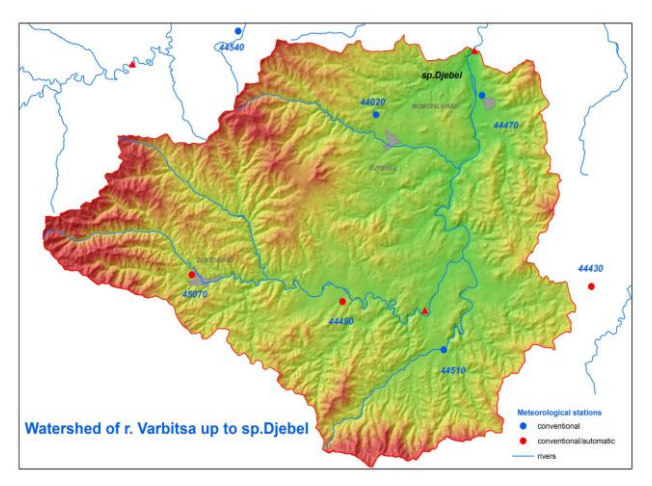


Figure 20 Distribution of the raingauge stations of Varbica River Basin

### The instrument

The following information should be provided in this section:

- Tipping bucket with heating (measures the precipitation with increments of 0.1 mm) quality index of the measurements (between 1 and 10) 7-8.
- Weighing type measurement with heating rim (measures the precipitation with increments of 0.1 mm) quality index of the measurements (between 1 and 10) 8-9.
- Conventional precipitation gauges type Wild measuring 24 hourly totals of precipitation



(Product H02 – PR-OBS-2)

Doc.No: SAF/HSAF/PVR-02/1.1 Issue/Revision Index: 1.1

Date: 30/09/2011 Page: 50/177

The rainrate is given only by the automatic stations for a 60 minutes interval. Those stations are located in Varbica and Chepelarska river basins. There are no automatic stations in Iskar river basin.

#### Data processing

There is quality control on the data.

In this Project the point-like gauges data are interpolated for using Co kriging interpolation of the ground measurements taking into account orography .

### 4.7 Ground data in Germany (BfG)

The H-SAF products are validated for the territory of Germany by use of two observational ground data sets: SYNOP - precipitation data based on the network of synoptical stations, provided by the German Weather Service (DWD) and RADOLAN-RW - calibrated precipitation data based on the radar network of DWD and calibrated by DWD by use of measurements at precipitation stations.

| Data                   | Number/Resolution                          | Time interval | Delay          | Annotation  |
|------------------------|--|---------------|----------------|---|
| Synoptical stations    | ~ 200                                      | 6h / 12h      | Near-real-time |   |
| Precipitation stations | ~ 1100                                     | hourly        | Near-real-time | Automatic precipitation stations  |
| RADOLAN RW             | 16 German radar<br>sites,<br>~1 km x ~1 km | 1 hour,       | Near-real-time | Quantitative radar composite product RADOLAN RW (Radar data after adjustment with the weighted mean of two standard procedures) |

Table 15 Precipitation data used at BfG for validation of H-SAF products

### 4.7.1 Rain gauge

#### The network

The data used are compiled from  $^{\sim}1300$  rain gauges. About 1000 are operated by DWD while about 300 are operated by other German authorities. The average minimum distance between stations is 17 km.

## The instruments

The measurement instruments are precipitation sensors OTT PLUVIO of Company Ott<sup>2</sup> <sup>3</sup>. They continually and precisely measure quantity and intensity of precipitation in any weather, based on balance principle with temperature compensation (heated funnel) and by an electronic weighing cell. The absolute measuring error is less than 0.04 mm for a 10 mm precipitation amount and the long-term (12months) stability is better than 0.06 mm. The operating temperature ranges from –30°C to +45°C. The minimum detected quantity (sensitivity) is 0,05 mmh<sup>-1</sup>. The maximum possible measured rain rate is 3000 mmh<sup>-1</sup>. The operational accumulation interval theoretically is one minute.

### The data processing

Continuous, automatic measurement of liquid and solid precipitation data are collected, accumulated (intervals: from 1hour until 1day) and provided as SYNOP tables by DWD. These data are error

<sup>2</sup> http://www.ott.com/web/ott\_de.nsf/id/pa\_ottpluvio2\_vorteile.html?OpenDocument&Click=

<sup>&</sup>lt;sup>3</sup> Precipitation amount and intensity measurements with the Ott Pluvio, Wiel Wauben, Instrumental Department, INSA-IO, KNMI, August 26, 2004



(Product H02 - PR-OBS-2)

Doc.No: SAF/HSAF/PVR-02/1.1 Issue/Revision Index: 1.1

Date: 30/09/2011 Page: 51/177

corrected and quality controlled in four steps with checks of completeness, climatologic temporal/spatial consistency and marginal checks.

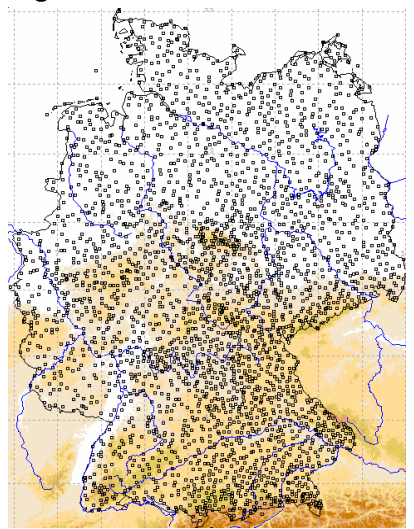


Figure 21 Network of rain gauges in Germany



Figure 22 Pluvio with Remote Monitoring Module

#### 4.7.2 Radar data

Radar-based real-time analyses of hourly precipitation amounts for Germany (RADOLAN) is a quantitative radar composite product provided in near-real time by DWD. Spatial and temporal high-resolution, quantitative precipitation data are derived from online adjusted radar measurements in real-time production for Germany. Radar data are calibrated with hourly precipitation data from automatic surface precipitation stations.<sup>4</sup>

1



(Product H02 - PR-OBS-2)

Doc.No: SAF/HSAF/PVR-02/1.1 Issue/Revision Index: 1.1

Date: 30/09/2011

Page: 52/177

The combination of hourly point measurements at the precipitation stations with the five-minute-interval radar signals of the 16 weather radars (C-Band Doppler) provides gauge-adjusted hourly precipitation sums for a ~1km x ~1km raster for Germany in a polar stereographic projection.

| Radar site | Latitude (N) | Longitude (E) | WMO No. | Radar site    | Latitude (N) | Longitude (E) | WMO No. |
|------------|--------------|---------------|---------|---------------|--------------|---------------|---------|
| München    | 48° 20' 14'' | 11° 36′ 46″   | 10871   | Rostock       | 54° 10′ 35″  | 12° 03′ 33″   | 10169   |
| Frankfurt  | 50° 01' 25"  | 08° 33' 34"   | 10630   | Ummendorf     | 52° 09' 39"  | 11° 10′ 38″   | 10356   |
| Hamburg    | 53° 37' 19'' | 09° 59' 52"   | 10147   | Feldberg      | 47° 52' 28"  | 08° 00' 18"   | 10908   |
| Berlin-    | 52° 28' 43'' | 13° 23 17"    | 10384   | Eisberg       | 49° 32' 29"  | 12° 24' 15"   | 10780   |
| Tempelhof  |              |               |         |               |              |               |         |
| Essen      | 51° 24' 22"  | 06° 58' 05"   | 10410   | Flechtdorf    | 51° 18' 43"  | 08° 48' 12"   | 10440   |
| Hannover   | 52° 27' 47'' | 09° 41' 54''  | 10338   | Neuheilenbach | 50° 06' 38"  | 06° 32' 59"   | 10605   |
| Emden      | 53° 20' 22"  | 07° 01' 30"   | 10204   | Türkheim      | 48° 35' 10"  | 09° 47' 02"   | 10832   |
| Neuhaus    | 50° 30' 03'' | 11° 08' 10"   | 10557   | Dresden       | 51° 07' 31"  | 13° 46′ 11″   | 10488   |

Table 16 Location of the 16 meteorological radar sites of the DWD

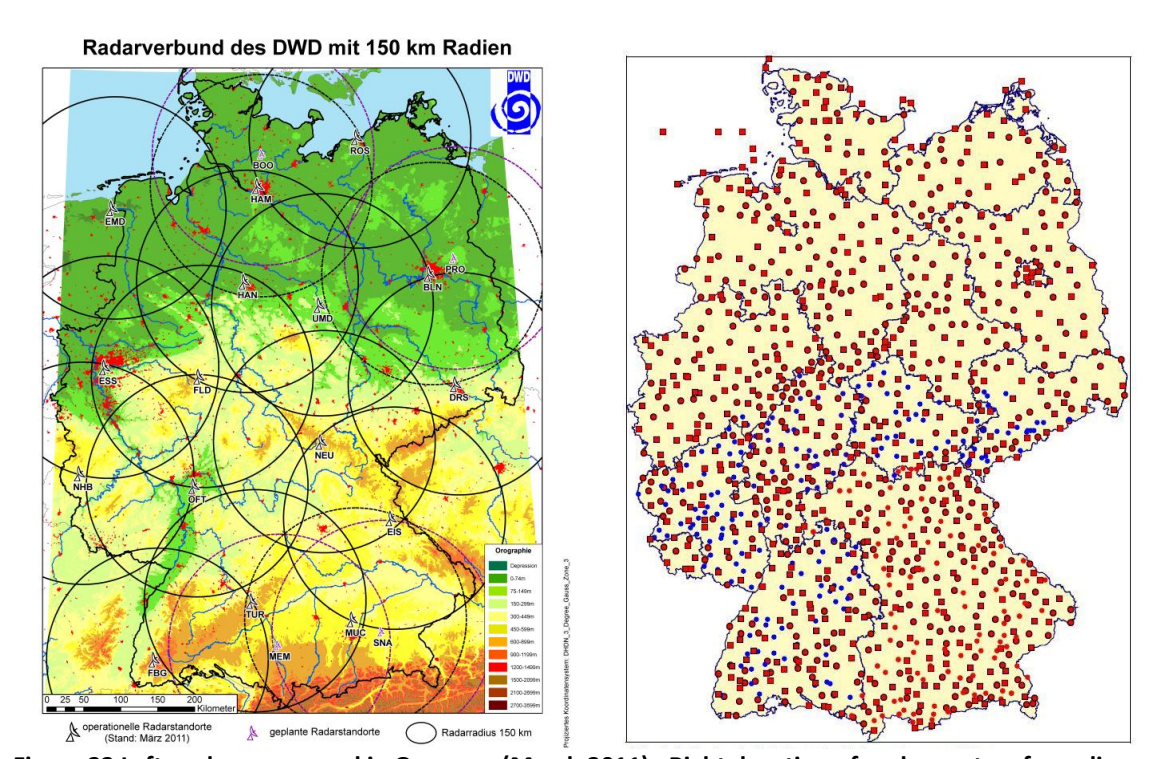


Figure 23 Left: radar compound in Germany (March 2011); Right: location of ombrometers for online calibration in RADOLAN; squares: hourly data provision (about 500), circles: event-based hourly data provision (about 800 stations).



(Product H02 - PR-OBS-2)

Doc.No: SAF/HSAF/PVR-02/1.1

Issue/Revision Index: 1.1

Date: 30/09/2011

Page: 53/177

The flowchart of online calibration method applied in RADOLAN is depicted in next figure.

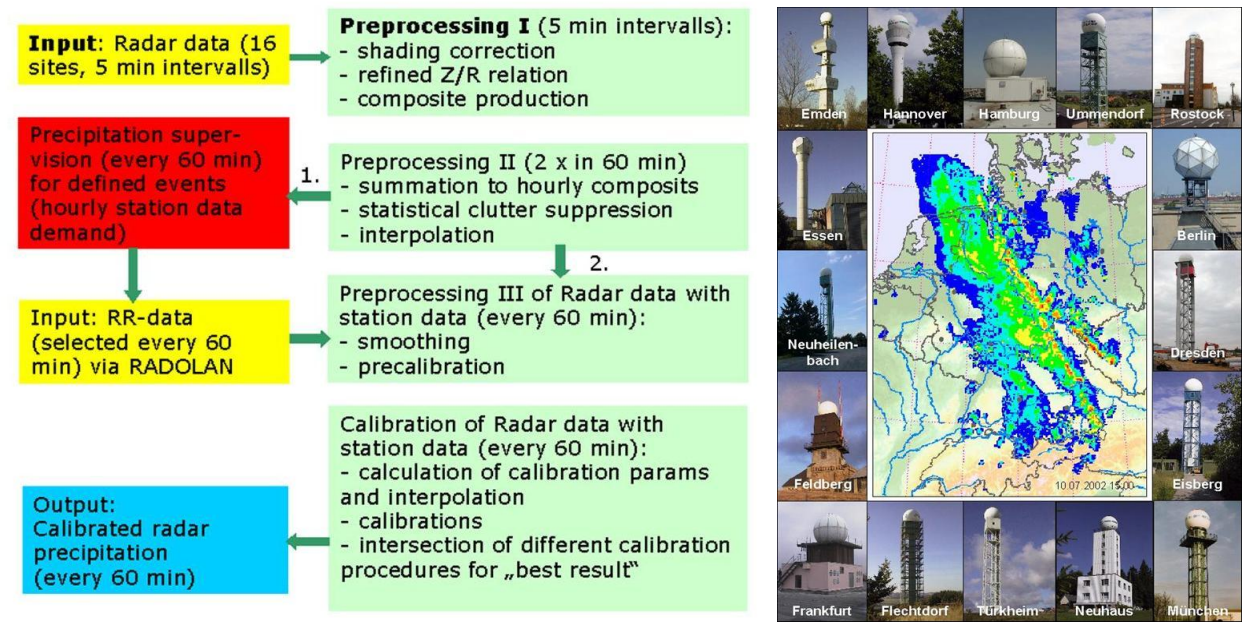


Figure 24 Flowchart of online calibration RADOLAN (DWD, 2004)

### 4.8 Ground data in Hungary (OMSZ)

#### 4.8.1 Radar data

#### The network

The main data used for validation in Hungary would be the data of meteorological radars. There are three C-band dual polarized Doppler weather radars operated routinely by the OMSZ-Hungarian Meteorological Service. The location and coverage of the three Hungarian radars are shown in next figure the measurement characteristics are listed in Table 18.

All three radars are calibrated periodically, with an external (calibrated) TSG, the periodicity is kept every 3 months.

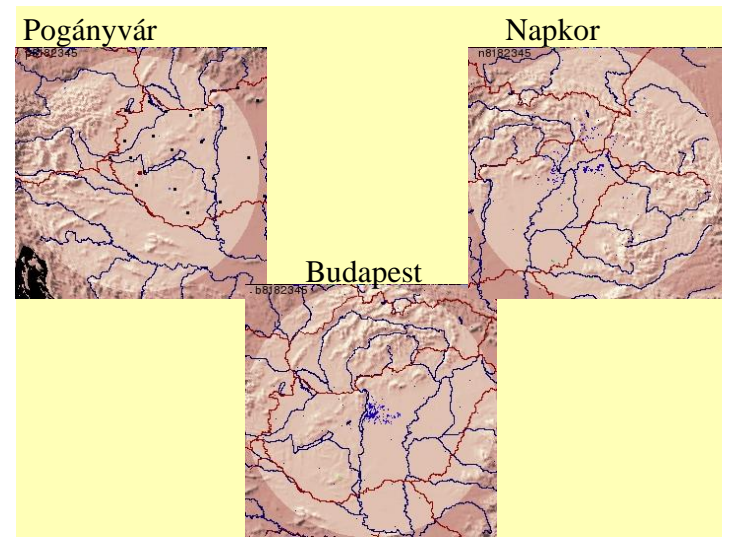


Figure 25 The location and coverage of the three meteorological Doppler radars in Hungary



(Product H02 – PR-OBS-2)

Doc.No: SAF/HSAF/PVR-02/1.1 Issue/Revision Index: 1.1

Date: 30/09/2011

Page: 54/177

| Year of installation | Location  | Radar type                         | Parameters<br>measured                              |
|----------------------|-----------|------------------------------------|---|
| 1999                 | Budapest  | Dual-polarimetric<br>Doppler radar | z, z <sub>DR</sub>                                  |
| 2003                 | Napkor    | Dual-polarimetric<br>Doppler radar | z,z <sub>DR</sub> ,κ <sub>DP</sub> ,Φ <sub>DP</sub> |
| 2004                 | Poganyvar | Dual-polarimetric<br>Doppler radar | Z,Z <sub>DR</sub> ,K <sub>DP</sub> ,Φ <sub>DP</sub> |

Table 17 Main characteristics of the Hungarian radar network

## The instruments

The Hungarian radar network is composed by three Doppler radars, which are measuring in the C-band, mainly at same frequencies. The scan strategy is the same for all the radars, the Budapest radar has a resolution lower than the two other radars which are newer types. The parameters of the instruments and the measurement campaigns are listed in next table.

|   | Budapest  | Napkor  | Poganyvar  |
|---|---|---|--|
| Frequency band  | C-Band, 5625MHz   | C-Band, 5610MHz   | C-Band, 5610MHz  |
| Polarization<br>(Single/Double)   | single  | single  | single   |
| Doppler capability (Yes/No)   | Yes   | Yes   | Yes  |
| Scan strategy: elevations, maximum nominal range distance, range resolution | scan freq: 15 min  Elevaions(deg): 0 0.5 1.1 1.8 2.7 3.8 5.1 6.6 8.5  Range 240 Km  Resolution:500m | scan freq: 15 min  Elevaions(deg): 0 0.5 1.1 1.8 2.7 3.8 5.1 6.6 8.5  Range 240 Km  Resolution:250m | scan freq: 15 min Elevaions(deg): 0 0.5 1.1 1.8 2.7 3.8 5.1 6.6 8.5 Range 240 Km Resolution:250m |

Table 18 Characteristics of the three radar instruments in Hungary

### The data processing

Radar measurements are influenced by many error sources that should be minimized as much as possible. As such, in case of the Hungarian radar data many correction methods are applied, or planned to be applied int he near future to filter out false radar reflectivity measurements. Clutter removal, and WLAN filter is already implemented int he processing chain of all three radar data; and a filter to disregard signals below 7dBz is also applied because in general, these data is not coming from real rain drops, but false targets.

According to experiences, beam blockage can result in serious underestimation of precipitation amounts (e.g. behind the Börzsöny mountains at the north of Budapest). So the bleam blockage



(Product H02 - PR-OBS-2)

Doc.No: SAF/HSAF/PVR-02/1.1 Issue/Revision Index: 1.1

Date: 30/09/2011 Page: 55/177

correction is planned to be implemented during year 2012. Also, the attenuation correction (the attenuation of electromagnetic waves in water environment, water drops) is planned for 2012. Hungary does not apply VPR (Vertical Profile Reflectivity) correction.

Precipitation intensity is derived from radar reflectivity with the help of an empirical formula, the Marshall-Palmer equation (R=a\*Z^b, where a=200, b=1.6). From the three radar images a composite image over the territory of Hungary is derived every 15 minutes applying the maximum reflectivity in one column method, in order to make adjustments in overlapping regions.

# Description of instantaneous and accumulated radar product used in HSAF Validation Activities Rain gauge correction

The non-corrected precipitation field can be corrected by rain gauge measurements. In Hungary, we do not make corrections to instantaneous 15 minutes radar data. In our institute, we only use a correction for the total precipitation for 12 and 24 hour periods.

For the 3h and 6h accumulated products, we use a special method to accumulate rainfalls: we interpolate the 15-minutes measurements for 1-minute grid by the help of displacement vectors also measured by the radar, and then sum up the images which we got after the interpolation. It is more precise especially when we have storm cells on the radar picture, because a storm cell moves a lot during 15 minutes and thus we do not get continuous precipitation fields when we sum up only with 15.minutes periods. This provides satisfying results. However, there is still a need for rain-gauge adjustment because there are obviously places (behind mountains) that the radar does not see.

The radars are corrected with rain gauge data every 12 hours. The correction method using rain gauge data for 12 hour total precipitation consists of two kinds of corrections: the spatial correction which becomes dominant in the case of precipitation extended over a large area, whereas the other factor, the distance correction factor prevails in the case of sparse precipitation. These two factors are weighted according to the actual situation. The weighting factor depends on the actual effective local station density, and also on the variance of the differences of the bias between radar and rain gauge measurements. On the whole, we can say that our correction method is efficient within a radius of 100 km from the radar. In this region, it gives a final underestimation of about 10%, while at bigger distance; the underestimation of precipitation fields slightly increases. Besides, we also produce 12 hour total composite images: first the three radar data are corrected separately, and then the composite is made from them. The compositing technique consists of weighting the intensity of each radar at a given point according to the distance of the given point from the radars. This is also true for the 24-hourly accumulations.

#### Resolution, projection, threshold of detection

The resolution of the radar data used for validation is 2km by 2km. This is true for the accumulated and the instantaneous products as well. As We have already mentioned, the threshold of detection in Hungary is 7dB. Hungarian radar data is available operationally in stereographic (S60) projection.

#### <u>References</u>

Péter Németh: Complex method for quantitative precipitation estimation using polarimetric relationships for C-band radars. Proceed. of 5th European Radar Conference (ERAD), Helsinki (Finland); <a href="http://erad2008.fmi.fi/proceedings/extended/erad2008-0270-extended.pdf">http://erad2008.fmi.fi/proceedings/extended/erad2008-0270-extended.pdf</a>

### 4.9 Ground data in Italy (DPC, Uni Fe)

### 4.9.1 Rain gauge

The network



(Product H02 - PR-OBS-2)

Doc.No: SAF/HSAF/PVR-02/1.1 Issue/Revision Index: 1.1

Date: 30/09/2011 Page: 56/177

The maximum number of available raingauges is about 1800, irregularly distributed over the surface. On the average, however, a number of stations have low quality data, failure or data transmission problems and their data are missing (-9999 recorded). This number of no data stations is highly varying on hourly/daily basis and ranges from few units to a hundred. In case of data acquired but not transmitted/recorded, the first transmitted measure is the cumulated value over the time when the data were not transmitted.

The average minimum distance between closest stations is about 9.5 km, with a very high variance: in some regions (such as Tuscany in central Italy) it is below 5 km, while in Emilia Romagna (Po Valley) it is more than 20 km. A study of the decorrelation distance between stations as function of the mutual distance has been carried out for the 2009 dataset. The decorrelation distance is defined as the minimum distance between two observations that makes the Pearson correlation coefficient between the two measures decrease below e<sup>-1</sup>. Results are shown in next figure, where the decorrelation distance is plotted as function of the distance between stations. It appears that there is a large variability of this parameter from higher values (around 60 km for cold months when large precipitating systems dominate and reduces to roughly 10 km when small scale convection is more likely to occur (warm months).

This points out that the distribution of gauges could be able to describe the spatial structures of precipitation fields in case of wintertime rainfall, while may be inadequate for spring/summer convective events.

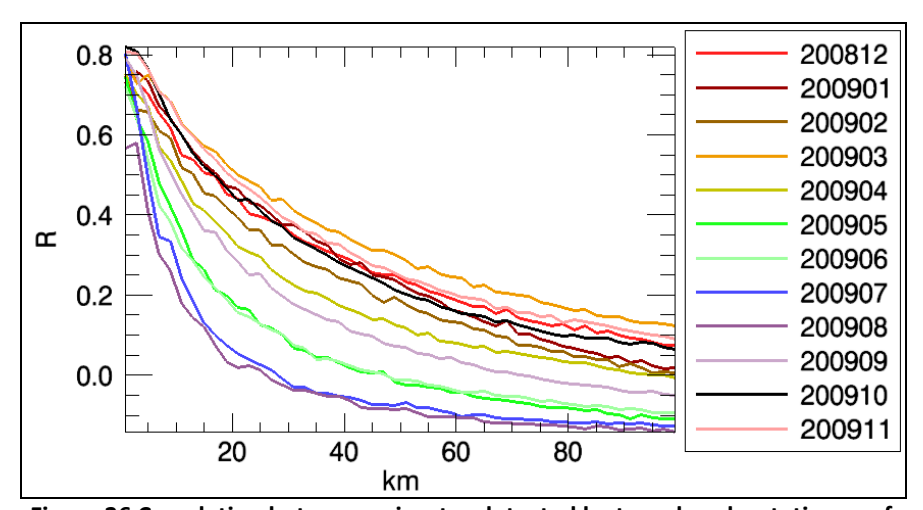


Figure 26 Correlation between rainrates detected by two close by stations as function of the distance between the two stations. Colors refer to the month along 2009

In next figure the distribution of working stations over Italy is shown for a given day.



(Product H02 - PR-OBS-2)

Doc.No: SAF/HSAF/PVR-02/1.1 Issue/Revision Index: 1.1

Date: 30/09/2011 Page: 57/177



Figure 27 Distribution of the raingauge stations of the Italian network collected by DPC

#### The instruments

The following information should be provided in this section:

- All the available raingauge are of tipping bucket type;
- Most of the raingauge have a minimum detected quantity of 0.2 mm, others have 0.1 mm.
- The maximum rainrate that can be measured by the gauges ranges between 300 and 500 mm<sup>-1</sup> over one minute, depending on the manufacturer.

The rainrate is measured over different cumulation intervals by the different local administrations managing the network, but the data disseminated are all integrated over 60 minutes.

At the moment, the National network made available by DPC provides only hourly data, Shorter cumulation times could be available for case studies after specific agreements with local management authorities.

Only a small subset (about 300 stations) of gauges have heated funnel, especially in alpine regions (such as Valle d'Aosta and Piedmont), and this is a clear source of errors in both summer (due to hailfall) and in autumn/winter (due to snowfall).

### The data processing

No quality control is performed on the data right now.

In this Project the point-like gauges data are interpolated by using the Barnes method (Barnes, 1964; Koch et al, 1983) widely used to interpolate station data. It works by defining a regular output grid (5x5 km in our case) and a "radius of influence" of each station (in our case it was 10 km). The point information from a raingauge is "spread" in the neighbour by an exponential function, limited by the influence radius, and the rainfall value for each grid-point is computed as the contribution of all the closest measurements.



(Product H02 - PR-OBS-2)

Doc.No: SAF/HSAF/PVR-02/1.1 Issue/Revision Index: 1.1

Date: 30/09/2011 Page: 58/177

The resulting grid is a 5x5 km regular grid with 240 columns and 288 lines. Moreover, a Digital elevation model is used to provide a mask of Italy in order to: 1) screen out sea-pixels too far from the coastlines and 2) process the pixels with the elevation above sea level.

#### 4.9.2 Radar data

#### The network

The Italian radar data have been not used for the validation of the current version of H01 but the verification of the satellite product with those data is in progress. The results will be presented at the next review of the project.

The Italian Department of Civil Protection (DPC) is the authority leading the national radar coverage project in order to integrate the pre-existent regional systems, made of ten C band fixed regional installations (five of them polarimetric and one transportable X-band polarimetric radar), two systems owned by the Italian company for air navigation services (ENAV), and three managed by the Meteorological Department of the Italian Air Force (AMI).

After its completion, the Italian radar network will include twenty-five C-band radars (including seven polarimetric systems) and five transportable dual-polarized X-band radars (next figure). The Italian Department of Civil Protection is developing the radar network in Southern Italy and, thanks also to the fruitful collaborations with Regional Authorities, ENAV and AMI, integrated all the existing radars in one national network with a clear advantage for both severe weather monitoring and civil protection purposes.

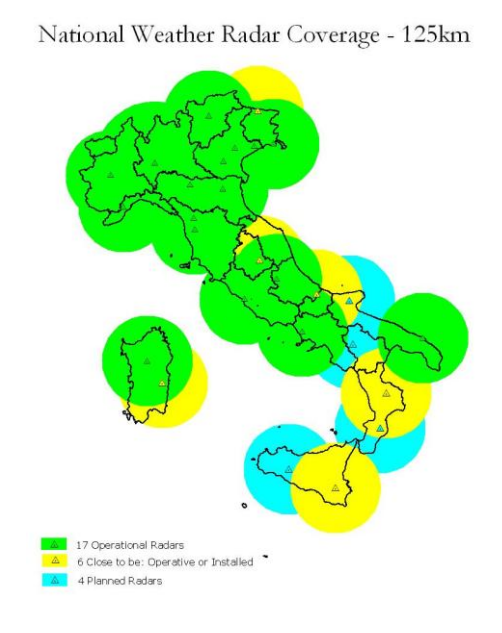


Figure 28 Italian radar network coverage

The existing sixteen C-band weather radars that belong to Regional Authorities ENAV and AMI are listed below:

- · Bric della Croce (Owner: Regione Piemonte; Polarization: on going upgrade to polarimetry)
- · Settepani (Owner: Regione Piemonte and Regione Liguria; Polarization: dual)
- · San Pietro Capofiume and Gattatico (Owner: Regione Emilia Romagna; Polarization: dual)
- . Monte Macaion (Owner: Regione Trentino Alto Adige and Provincia autonoma Trento; Polarization: single)



(Product H02 – PR-OBS-2)

Doc.No: SAF/HSAF/PVR-02/1.1 Issue/Revision Index: 1.1

Date: 30/09/2011 Page: 59/177

- · Teolo and Loncon (Owner: Regione Veneto; Polarization: single)
- · Monte Midia (Owner: Regione Abruzzo; Polarization: single)
- · Monte Rasu (Owner: Regione Sardegna; Polarization: single)
- · Fossolon di Grado (Owner: Regione Friuli Venezia Giulia; Polarization: single)
- · Linate and 12) Fiumicino (Owner: ENAV; Polarization: single)
- · Brindisi (Owner: Italian Air Force; Polarization: single)
- · Grazzanise (Owner: Italian Air Force; Polarization: single)
- · Pisa, (Owner: Italian Air Force; Polarization: single)
- · Istrana, (Owner: Italian Air Force; Polarization: single)

The first C-band radar of new generation, directly managed by DPC (located in Tuscany, Italy), is operational since the beginning of 2008, whereas six C-band radars (including two dual-polarized systems) will be operational by the end of 2008 (see Figure 29). As an example, the national mosaic CAPPI at 2000 m is shown in next figure relatively to the event of 04/18/08 at 0015 U.T.C.

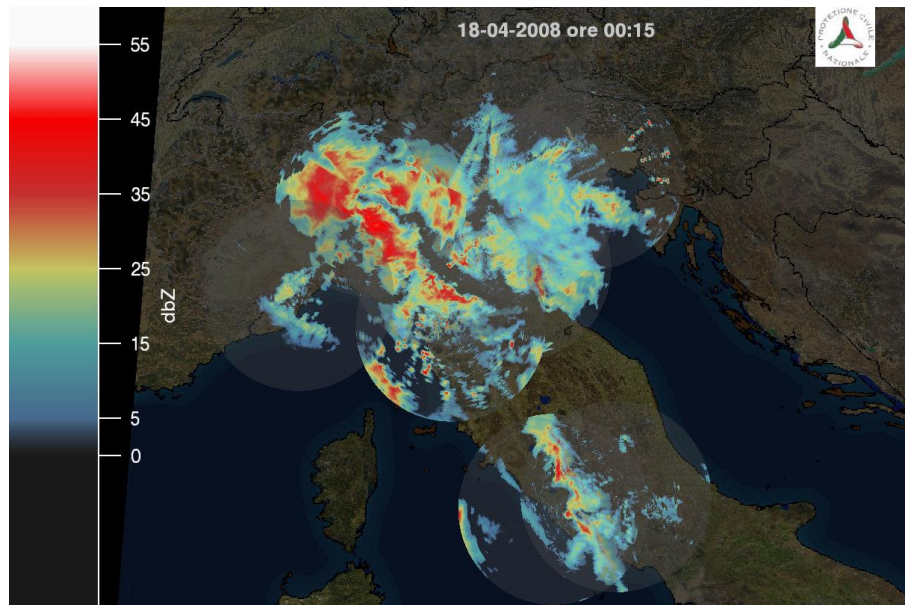


Figure 29 Graphical mosaic of reflectivity (CAPPI at 2000 m) for the event of 04/18/08 at 0015 U.T.C.

As depicted before, each Doppler Radar System either dual or single-polarized (PDRS or DRS) are connected by satellite links to the two National Radar Primary Centres (RPC), located in Roma (DPC) and Savona (CIMA Research Foundation) in order to mainly ensure the remote control (through the RRC server) and products generation (through the RPG server). The RPC located in Savona works as "backup centre" in order to continuously ensure the system functioning. The subsystem RAC (Radar Archive Centre) is devoted to archive and manage radar data and products by means of a relational database. The generated products are then disseminated to all institutions composing the national network.



(Product H02 – PR-OBS-2)

Doc.No: SAF/HSAF/PVR-02/1.1 Issue/Revision Index: 1.1

Date: 30/09/2011 Page: 60/177

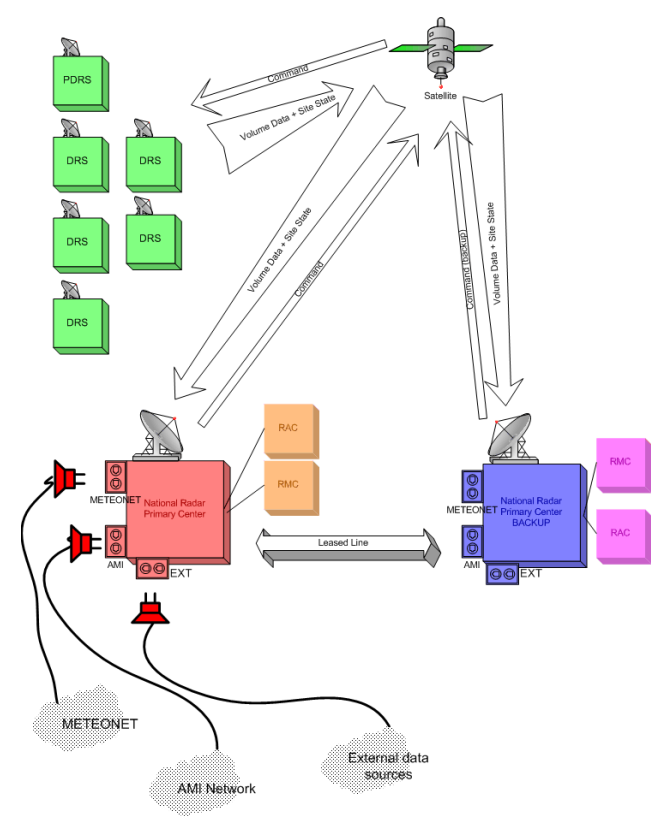


Figure 30 Architecture of the Italian radar network

#### Data processing

Data processing and product generation are here briefly described. In particular, attenuation correction, hydrometeor classification, vertical profile of reflectivity correction and rainfall estimation will be treated in the following sections

#### Radar data quality

As known, any fruitful usage of radar data either for quantitative precipitation estimation or just for operational monitoring, must deal with a careful check of data quality. Figure 31 schematically shows the operational processing chain that is applied within the system DATAMET (software system for radar remote control, product generation, visualization, system maintenance, and data archive) developed by DATAMAT S.P.A. Ground clutter, anomalous propagation, beam blockage effects are routinely mitigated through the application of the decision-tree method proposed by Lee et al., (1995) for single polarized systems. Dual-polarized systems provide additional observables such as differential reflectivity, correlation coefficient (and their texture) that can be used to further reinforce the traditional techniques. Furthermore, as soon as the polarimetric systems directly managed by DPC will be operational (end of summer 2008), the property of the rain medium at vertical incidence are planned to be used for differential reflectivity calibration according to the procedure proposed by Gorgucci et al. (1999). Redundancy of polarimetric variables will also be used for absolute calibration (Gourley et al., 2005).



(Product H02 - PR-OBS-2)

Doc.No: SAF/HSAF/PVR-02/1.1 Issue/Revision Index: 1.1

Date: 30/09/2011

Page: 61/177

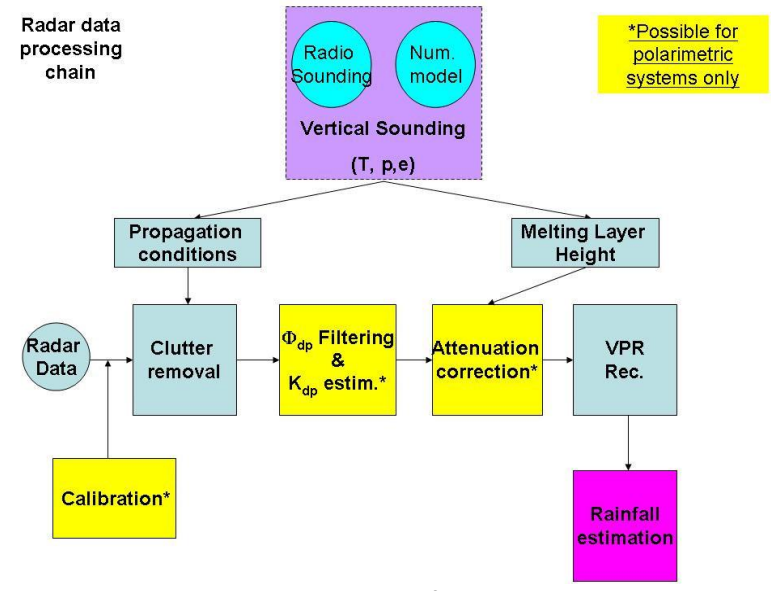


Figure 31 Schematic representation of radar data processing chain

Attenuation correction and hydrometeor classification Polarimetric radar systems enable the use of reliable algorithms for correcting rain path attenuation. Based on the paradigm that specific attenuation ah,dp and specific differential phase Kdp (Kdp=0.5 dFdp/dr) are linearly related in rain (ah,dp =g h,dp Kdp), cumulative attenuation effects can be corrected through the use of Fdp (Carey et al., 2000).



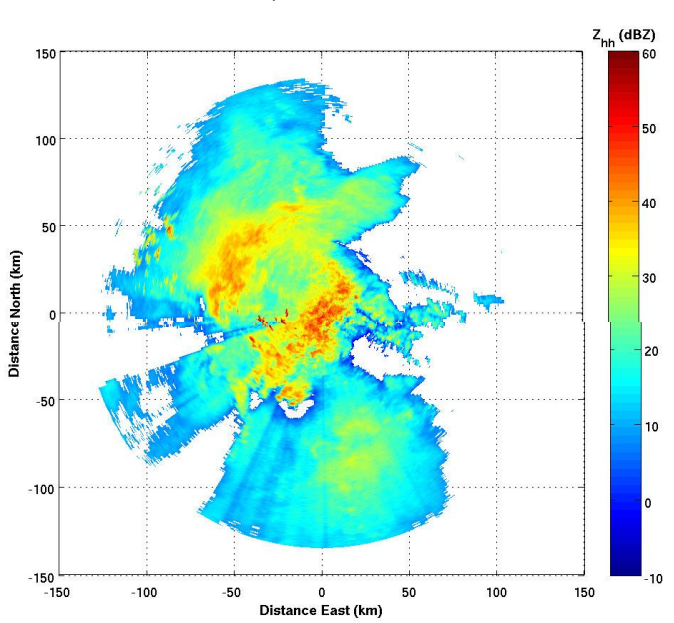
(Product H02 - PR-OBS-2)

Doc.No: SAF/HSAF/PVR-02/1.1 Issue/Revision Index: 1.1

Date: 30/09/2011

Page: 62/177

### a) Observed



## b) Corrected

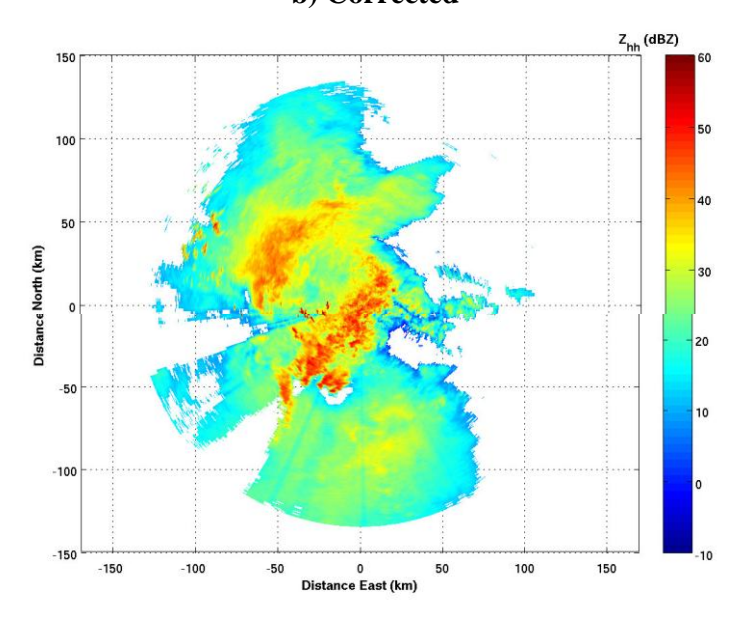


Figure 32 Measured (upper panel) and attenuation corrected (lower panel) PPI (1.0 deg) of reflectivity observed on 09/14/08 at 0500 U.T.C. by the polarimetric radar operated by Piemonte and Liguria regions

Although, several approaches with different degree of sophistication have been proposed in the last years, the procedure (named APDP) proposed in Vulpiani et al. (2007) has been chosen to be implemented for its physical adaptability and operationally-oriented architecture. APDP (Adaptive PhiDP method) is an iterative correction of attenuation, based on the use of Fdp, that taking advantage from the classification of hydrometeors (Marzano et al.,2006, 2007), adapt the coefficients g h,dp.to the observed physical conditions.



(Product H02 - PR-OBS-2)

Doc.No: SAF/HSAF/PVR-02/1.1 Issue/Revision Index: 1.1

Date: 30/09/2011 Page: 63/177

As an example, previous figure shows the 1.0 degree PPI of measured (upper panel) and attenuation corrected (lower panel) reflectivity observed on 09/14/08 at 0500 U.T.C. by the polarimetric radar (located in mount Settepani) operated by Piemonte and Liguria regions. Next figure shows the hydrometeor classes detected by the classification algorithm corresponding to the event illustrated before.

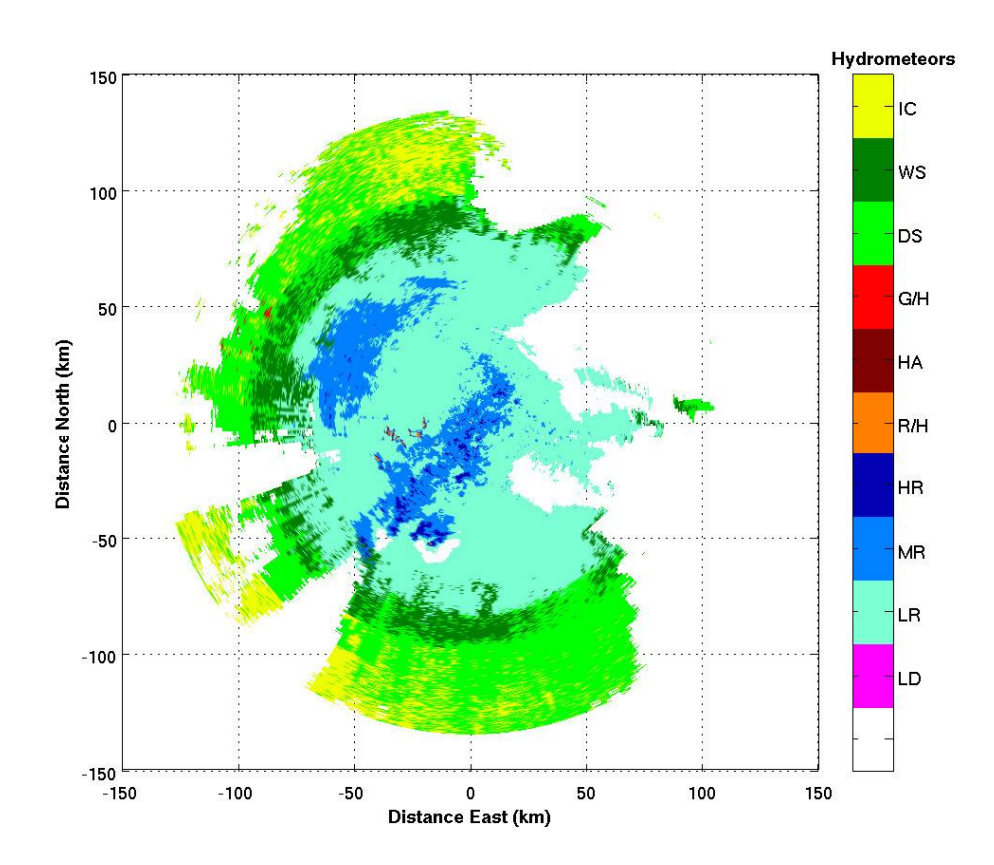


Figure 33 Hydrometeor classes as detected by the classification algorithm starting from the radar variables observed on 09/14/08 at 0500 U.T.C. by the polarimetric radar operated by Piemonte and Liguria regions

Note: LD (Large Drops), LR (Light Rain), MR (Moderate Rain), HR (Heavy Rain), R/H (Rain/ Hail mixture), HA (Hail), G/H (Graupel or small Hail), DS (Dry Snow), WS (Wet Snow), IC (Ice Crystals).

#### Reconstruction of vertical profile of reflectivity

Rainfall estimation might be heavily perturbed by the presence of melting snow due to the enhancement of reflectivity factor (caused by the increase in size and dielectric constant), without a corresponding increase of rain rate. This well known problem is usually handled by retrieving the Vertical Profile of Reflectivity (VPR) and correcting the observed measures.

The algorithm developed by ARPA-SIM for VPR retrieval and correction is currently under test in order to be implemented within the DATAMET system. It is based on the computation of mean VPR shape (Germann and Joss, 2002) and, assuming it to be uniform in the whole radar domain, on the retrieval of the reflectivity at the desired level by the simple adding of a constant quantity (in dBZ units). The original algorithm is modified and integrated with a VPR diagnosis and analysis phase, to handle different operative problems (Fornasiero et al., 2008).



(Product H02 - PR-OBS-2)

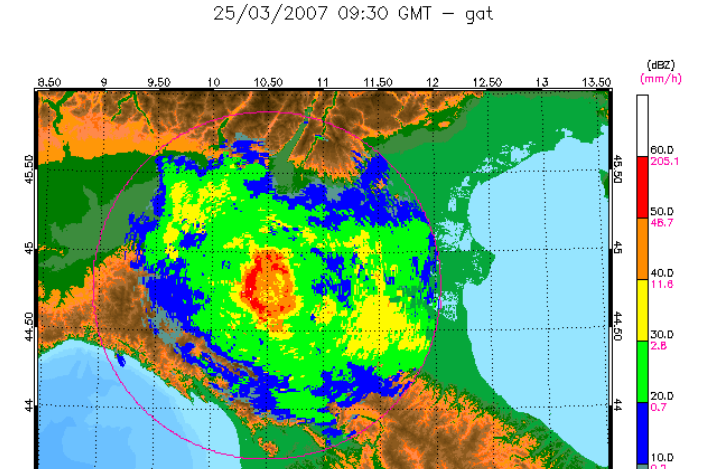
Doc.No: SAF/HSAF/PVR-02/1.1 Issue/Revision Index: 1.1

Date: 30/09/2011

Page: 64/177

As an example, next figure shows the measured (upper panel) and VPR-corrected (lower panel) PPI of reflectivity observed on 03/25/07 at 0930 U.T.C. by the polarimetric radar located in Gattatico (Emilia Romagna, Italy).

.a)



arpa Servizio Idro Meteo

b)

25/03/2007 09:30 GMT - gat

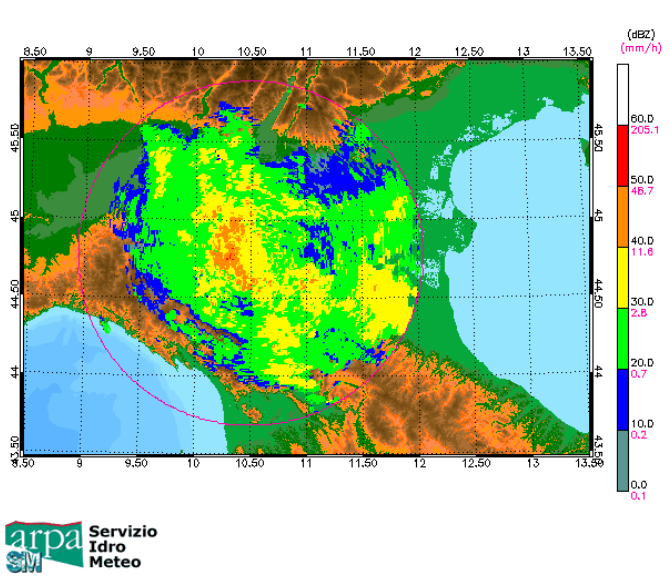


Figure 34 Measured (upper panel) and VPR corrected (lower panel) PPI of reflectivity observed on 03/25/07 at 0930 U.T.C. by the polarimetric radar located in Gattatico (Emilia Romagna, Italy)

### Rainfall estimation

Quantitative rainfall estimation is one of the first application of the radar network. The estimation of rainfall at the ground takes advantage of the dense network of raingauges spread all over Italy. This



(Product H02 - PR-OBS-2)

Doc.No: SAF/HSAF/PVR-02/1.1 Issue/Revision Index: 1.1

Date: 30/09/2011 Page: 65/177

network is one of the most dense in the world with more than 1700 gages and it is used for tuning and correcting the operational Z-R algorithms of non-polarimetric radars.

In order to evaluate the benefits of upgrading the new radar installations to full-polarimetric radars and for considering the benefit of existing polarimetric radars, many studies have been carried on by Research Centres and Regional Authorities belonging to the network (e.g., Silvestro et al 2008). As an example, in next figure is shown the cumulated rainfall estimates versus gage measurements obtained for the event observed on 06/01/2006 by the dualpolarized C-Band radar of Mt. Settepani. The figure shows the comparison between a multi-parameter algorithm that uses polarimetric data (Silvesto et al., 2008) and a simple ZR relationship (Marshall-Palmer).

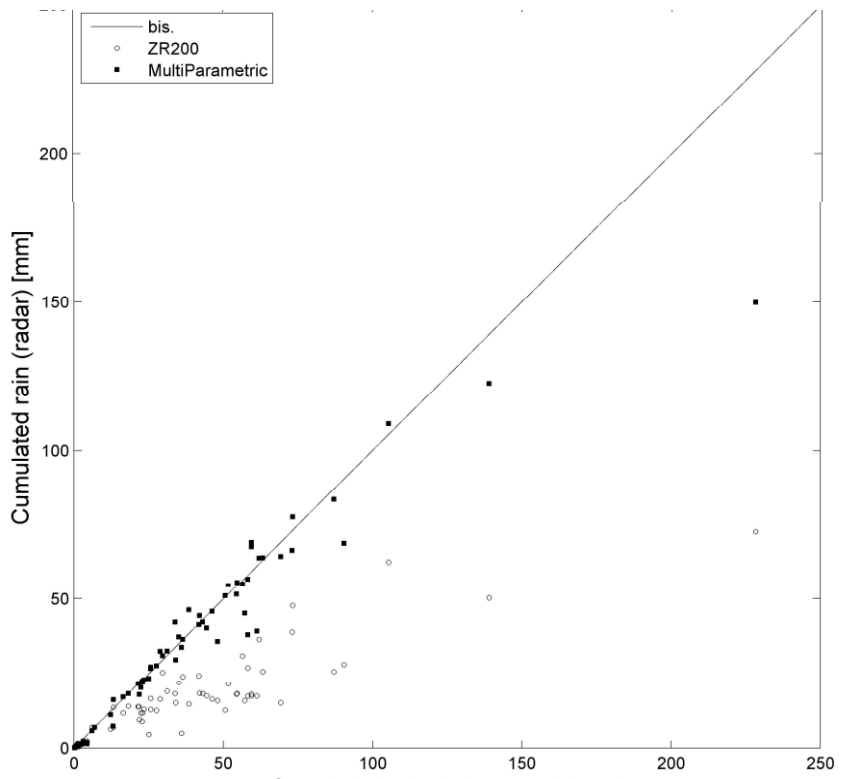


Figure 35 Cumulated radar rainfall estimates versus gage measurements for the event observed on 06/01/2006 by the dualpolarized radar located in Settepani (Liguria, Italy)

#### 4.10 Ground data in Poland (IMWM)

#### 4.10.1 Rain gauge

### The network

The maximum number of rain gauges in the Polish ATS (Automatic Telemetric Station) national network is 950. Each ATS post is equipped with two independent rain gauges of the same sort. One of them is heated during the winter period and the other one is not. Therefore precipitation information is derived from 475 points at the time. Fact that rainfall is measured by two equally sensitive instruments two meters away from each other at the same post, enables to apply simple in situ data quality control during summertime. During winter non-heated rain gauge is covered with a cup to prevent it from being clogged by the ice and damaged. Because of that the precipitation information



(Product H02 - PR-OBS-2)

Doc.No: SAF/HSAF/PVR-02/1.1 Issue/Revision Index: 1.1

Date: 30/09/2011

Page: 66/177

derived from ATS network in winter cannot be verified using this method. It can be stated that during the wintertime precipitation information might be burdened by a slightly bigger measuring error. The number of rain gauges available for H-SAF validation activities varies from day to day due to operational efficiency of ATS network in Poland and depends on large number of independent factors. It can be stated that the number varies between 330 and 475 rain gauges for each day of operational work.

Mean minimum distance between precipitation measuring ATS posts (between each pair of rain gauges) in Polish national network is 13,3 km.

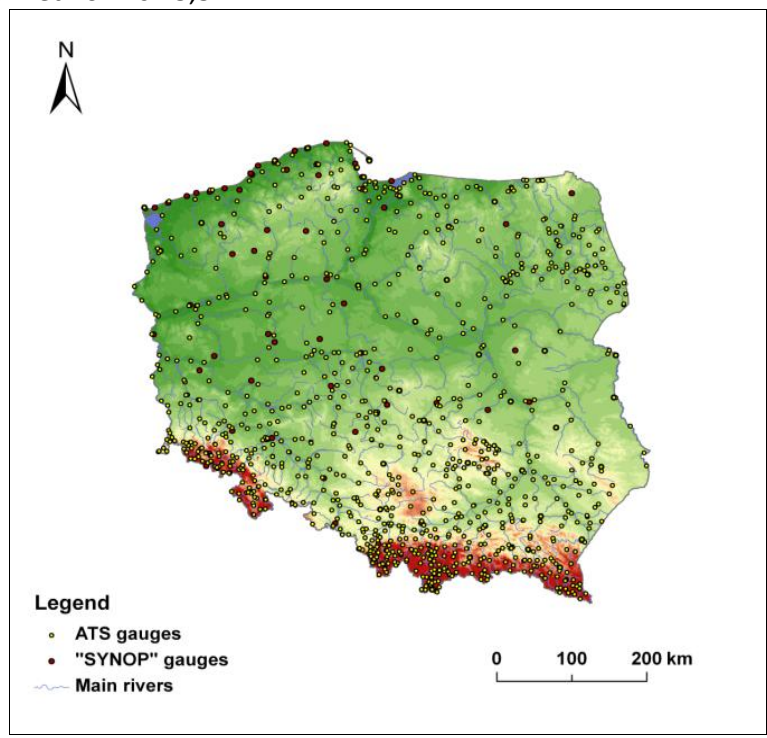


Figure 36 ATS national network in Poland

### The instruments

All rain gauges working within Polish ATS national network are MetOne tipping bucket type instruments. Minimum detected quantity that can be measured by those rain gauges is 0,1 mm/h which means that each tilt of rain gauge bucket adds 0,1mm to the total sum of the measured precipitation. During very heavy precipitation events MetOne rain gauges tend to underestimate real precipitation by factor of 10%. Maximum measured rainrate (mmh<sup>-1</sup>) by MetOne instruments in Poland was recorded in 5.06.2007 at ATSO Koscielisko Kiry at the foot of Tatra Mountains. The recorded values reached 65 mm/h. Operational cumulation interval (min) of ATS network rain gauges is set for 10 minutes and can be adjusted according to given needs. There is possibility to have very short cumulation intervals for case studies - theoretically 1 minute - but not on every given precipitation post. It depends on local DCS settings.

#### The data processing

As stated above the data quality control can be achieved by comparison on two rainfall datasets collected by two independent rain gauges at the same ATS post. It is done operationally during summertime. There is no such possibility during the winter because of lack of non-heated rain gauge



(Product H02 - PR-OBS-2)

Doc.No: SAF/HSAF/PVR-02/1.1 Issue/Revision Index: 1.1

Date: 30/09/2011 Page: 67/177

dataset. In case that one pair of rain gauges at the same ATS post provide two different rainfall readings the higher one is taken into account.

No specialization technique is used for standard validation process. However, for some case studies, the Natural Neighbor technique is applied for satellite and ground precipitation data. To match the precipitation information with satellite data spatial and temporal matching are applied.

- Spatial matching: for each given satellite pixel, the posts situated within that pixel were
  found. The pixel size was taken into account, however, its shape was assumed to be
  rectangular. If more than one rain gauge were found within one satellite pixel, the
  ground rain rate value was calculated as a mean of all rain gauges measurements
  recorded within that pixel;
- <u>Temporal matching</u>: satellite derived product is combined with the next corresponding ground measurement. As the ground measurements are made with 10 minute time resolution, the maximum interval between satellite and ground precipitation is 5 minutes.

### 4.11 Ground data in Slovakia (SHMU)

### 4.11.1 Rain gauge

#### The network

In Slovakia there are overall 98 automatic rain gauge stations potentially available for the H-SAF project. The real number of usable gauges varies with time because on average about 20 of them are out of operation.

Mean minimum distance between rain-gauges in the complete network is 7,74 km. Map of the rain gauge network in Slovakia containing also climatological and selected hydrological stations is shown in next figure.



Figure 37 Map of SHMÚ rain gauge stations: green – automatic (98), blue – climatological (586), red - hydrological stations in H-SAF selected test basins (37)

#### The instruments

Type of all the automatic rain gauges is tipping bucket (without heating of the funnel). The gauges are able to measure precipitation rates ranging from 0,1 to 200 mm/h at 10 min operational accumulation



(Product H02 - PR-OBS-2)

Doc.No: SAF/HSAF/PVR-02/1.1 Issue/Revision Index: 1.1

Date: 30/09/2011 Page: 68/177

interval. Shorter accumulation interval of 1 min is also possible which makes the instruments suitable for case studies in the H-SAF project.

#### The data processing

The rain gauge data are not used at SHMÚ directly for the H-SAF precipitation validation but they are utilized as the input to the INCA precipitation analysis system which is supposed to become a new validation tool. Prior the INCA analysis the rain gauge data are interpolated onto the regular 1x1 km grid using the inverse-distance-squared (IDS) interpolation method. Only the 8 nearest rain gauge stations are taken into account in the interpolation in order to reduce occurrence of precipitation bull-eyes artifact.

SHMÚ performs the offline automatic and manual quality check of the rain gauge data. In frame of the INCA system a quality control technique called blacklisting has been developed which avoids the data from systematically erroneous rain gauges to enter the analysis. Currently the blacklisting is used in manual mode only.

#### 4.11.2 Radar data

### The network

The Slovak meteorological radar network consists of 2 radars (see next figure). One is situated at the top of Maly Javornik hill near city Bratislava and second one is on the top of Kojsovska hola hill close to the city Kosice. Both are Doppler, C-band radars; the newer one at Kojsovska hola is able to measure also the dual polarization variables (non-operational).

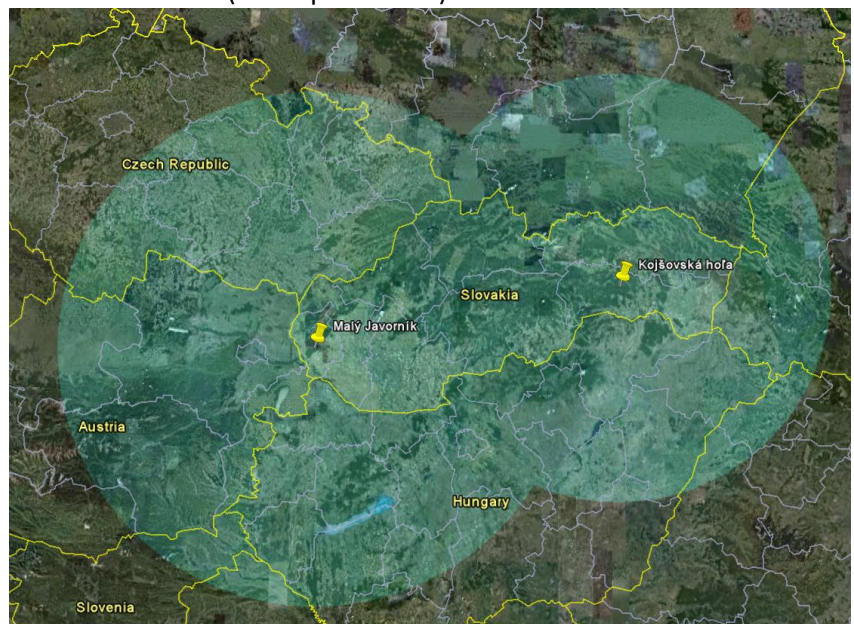


Figure 38 Map of SHMÚ radar network; the rings represent maximum operational range – 240 km for radar at Maly Javornik (left), 200 km for radar at Kojsovska hola (right)

### The instruments

The radars are operated and technically maintained by SHMÚ. Receivers of radars are calibrated regularly by means of internal test signal generator (TSG). In case of radar at Maly Javornik calibration is performed every 3 months and in case of radar at Kojsovska hola every 1 month.



(Product H02 – PR-OBS-2)

Doc.No: SAF/HSAF/PVR-02/1.1 Issue/Revision Index: 1.1

Date: 30/09/2011

Page: 69/177

The basic parameters of both SHMÚ radars are summarized in next table.

|   | Maly Javornik   | Kojsovska hola   |
|---|---|--|
| Frequency band  | C-Band, 5600 MHz  | C-Band, 5617 MHz   |
| Polarization<br>(Single/Double)   | Single  | Double (but so far only single pol. products generated)  |
| Doppler capability (Yes/No)   | Yes   | Yes  |
| Scan strategy: scan frequency, elevations, maximum nominal range distance, range resolution | Scan frequency: 5 min  Elevations (deg): 0.2 0.7 1.4 2.5 3.8 5.4 7.3 9.5 13.0 17.0 25.0  Range: 240 Km  Resolution: 1000m | Scan frequency: 5 min  Elevations (deg): -0.5 0.0 0.5 1.0 1.5 2.5 4.0 6.0 10.0 20.0  Range: 200 Km  Resolution: 125m |

Table 19 Characteristics of the SHMÚ radars

#### The data processing

For ground clutter removal the Doppler filtering is used. In case of radar at Maly Javornik the frequency-domain IIR filter is used, at Kojsovska hola the Doppler filtering is supplemented with moving target identification (MTI) technique. Isolated radar reflectivity and Doppler velocity bins are removed by the Speckle removal filter. The data with signal to noise ratio below the specified threshold are also eliminated.

The measured radar reflectivity is corrected for atmospheric (clear-air) attenuation of the radar beam. Neither beam blocking correction nor vertical profile of reflectivity (VPR) is applied at SHMÚ. However implementation of the beam blocking correction is being considered for the H-SAF validation due to complicated orographical conditions in Slovakia.

Precipitation intensity is derived from radar reflectivity according to the Marshall-Palmer equation (Z=a\*R^b) with constant coefficients valid for stratiform rain (a=200, b=1.6). Polarimetric techniques for quantitative precipitation estimation in case of dual polarization radar at Kojsovska hola are not used because the measured polarimetric data are not operational (calibration would be required). Software filter for the RLAN interference detected by radars is currently in development at SHMÚ.

Radar composite based on CAPPI 2 km products from both radars is used for the H-SAF validation. The composition algorithm used selects the higher value measured by the two radars in the overlapping area.

No raingauge correction of the derived instantaneous precipitation is applied. Effect of elevating radar beam with increasing range and beam attenuation is reduced by limiting the validation area to rain effective range of 120 km for both radars in the composite.

The instantaneous precipitation products are provided in Mercator projection with approximately 1 km resolution. Threshold for precipitation detection is 0,02 mm/h. Time resolution of the current instantaneous products is 5 minutes, for the products prior to April 2010 it was 10 minutes and prior to August 2009 15 minutes.



(Product H02 - PR-OBS-2)

Doc.No: SAF/HSAF/PVR-02/1.1 Issue/Revision Index: 1.1

Date: 30/09/2011 Page: 70/177

Precipitation accumulation in case of 3-hourly interval is based on integration of 5 (10 or 15) minutes instantaneous measurements in time period of 3 hours. Accumulated precipitation for intervals of 6, 12 and 24 hours is calculated as a sum of the 3-hourly accumulated precipitation. At least 92% of instantaneous measurements must exist in relevant time period for the 3-hourly accumulated product to be produced.

No rain gauge correction of the accumulated precipitation is applied but the same limitation of validation area is used as for the instantaneous product. Threshold for precipitation detection of the 3-hourly accumulated product is 0,5 mm. Geographical projection and space resolution of the accumulated products are the same as those of instantaneous product (see above).

For validation of H-SAF precipitation products it is necessary to know errors distribution of used ground reference data — in case of SHMÚ it is precipitation intensity and accumulated precipitation measured by Slovak radar network. For this purpose a study called "SHMU study on evaluation of radar measurements quality indicator with regards to terrain visibility" has been elaborated. To find distribution of errors in radar range next steps had to be done:

- simulations of terrain visibility by radar network using 90m digital terrain model
- statistical comparison of radar data against independent rain gauge data measurements
- derivation of dependence (regression equation) describing the errors distribution in radar range with regard to terrain visibility, based on rain gauge and radar data statistical evaluation computation of error distribution maps using regression equation and terrain visibility

Main results of this study are shown in next figure. It is evident that the best visibility of SHMU radars corresponds to the lowest URD-RMSE of 60% displayed by light violet colors. URD-RMSE is of quite homogeneous distribution with average of 69% in prevalent lowlands of Slovakia displayed by bluish colors. But in central and north-west mountainous areas this error exceeds 100%.

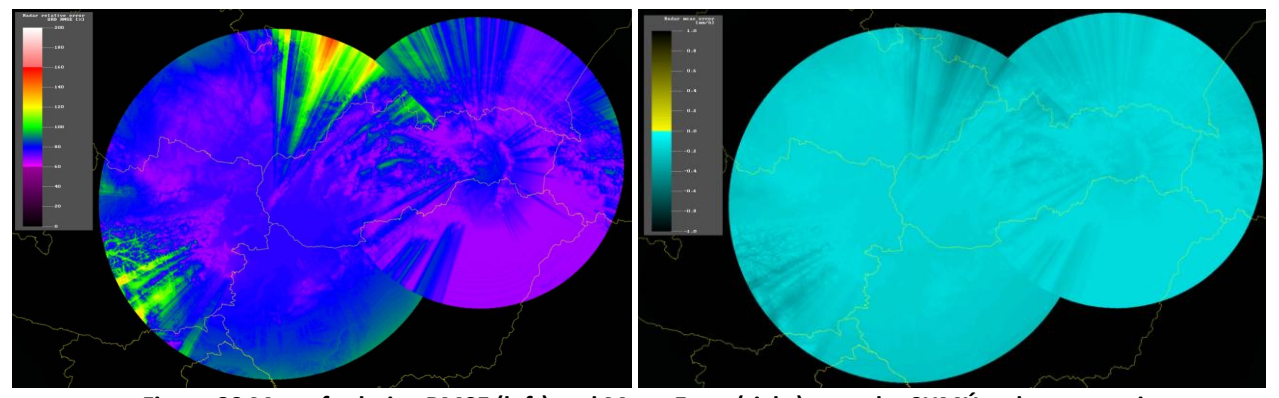


Figure 39 Map of relative RMSE (left) and Mean Error (right) over the SHMÚ radar composite

Similar studies that have been carried out in the PPVG on comparison of radar data with rain gauge data have shown in general that RMSE error associated with radar fields depends considerably on radar minimum visible height above the rain gauge especially in mountainous countries. In lowlands this dependence is not so significant, but no negligible. The reason can be the location of radar sites at the top of hills and impossibility of the lowest elevation to reach the lowland's surface. In case of Slovakia The URD-RMSE error of radar accumulated fields is between 60-90%, with an average URD-RMSE value of 69,3%. Mean Error specified for 24-hours cumulated precipitation is -4,42mm or converted into instantaneous precipitation -0,184 mm/h. RMSE specified for 24-hours cumulated precipitation is 9,48mm or converted into instantaneous precipitation 0,395 mm/h.



(Product H02 – PR-OBS-2)

Doc.No: SAF/HSAF/PVR-02/1.1 Issue/Revision Index: 1.1

Date: 30/09/2011 Page: 71/177

Complete SHMU study is available on the H-SAF ftp server: /hsaf/WP6000/WP6100/precipitation/WG\_groups/WG2-radar/WG-2-3\_radar quality indication\_v1.doc

### 4.12 Ground data in Turkey

## 4.12.1 Rain gauge

### The network

193 Automated Weather Observation Station (AWOS) located in the western part of Turkey are used for the validation of the satellite precipitation products in the HSAF project. The average distance between the AWOS sites is 27 km. The locations of the AWOS sites are shown in next figure.

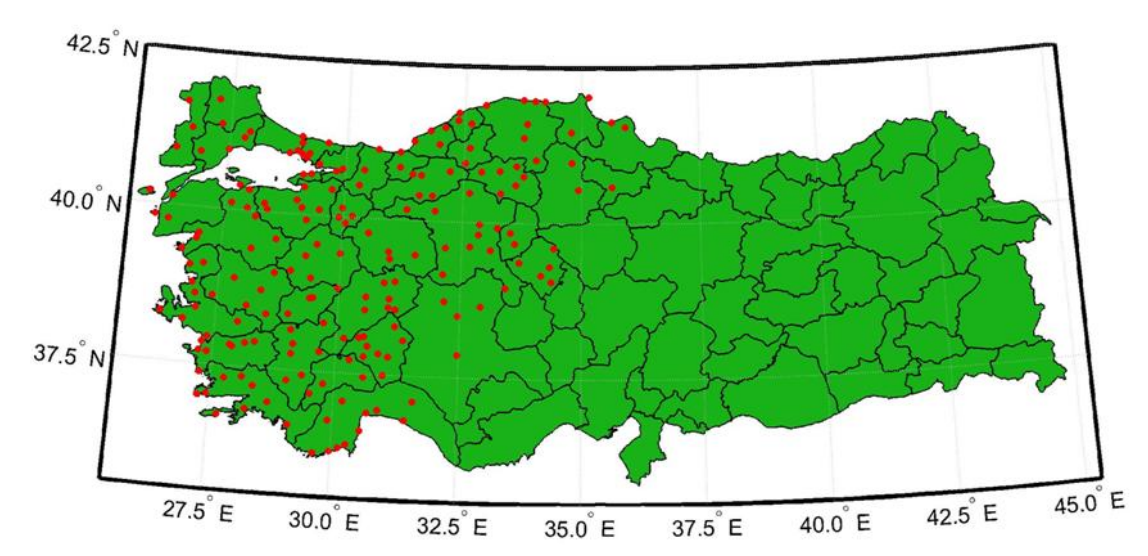


Figure 40 Automated Weather Observation System (AWOS) station distribution in western part of Turkey

#### **The instruments**

The gauge type of the network is tipping bucket where each has a heated funnel. The minimum detection capability of the gauge is 0.2mm per tip. In the maximum capacity of the instrument is 720 mm/h at most. The operational accumulation interval is 1 minute, so that alternative cumulation intervals such as 5, 10, 20, 30 minutes are possible.

#### **Data processing**

Quality control

High quality of the ground data is critical for performing the validation of the precipitation products. The validation results or statistics can provide meaningful feedbacks for the product developers and additionally the products can be used reliably only if there is a confidence present about the ground data at a certain level. For this reason, some predefined quality assurance (QA) tests are considered for the precipitation data in order to define the confidence level. First of all, a flagging procedure is defined as described in next table.

| QA Flag Value | QA Status | Brief Description |
|---------------|-----------|-------------------|
|---------------|-----------|-------------------|



(Product H02 - PR-OBS-2)

Doc.No: SAF/HSAF/PVR-02/1.1 Issue/Revision Index: 1.1

Date: 30/09/2011 Page: 72/177

| 0 | Good    | Datum has passed all QA Test             |
|---|---------|--|
| 1 | Suspect | There is concern about accuracy of datum |
| 2 | Failure | Datum is unstable                        |

Table 20 QA flags descriptions (modified from Shafer et al., 1999)

The precipitation data QA tests are summarized as follows.

#### Range Test

This test is used to see if any individual precipitation observation falls within the climatological lower and upper limits. The test procedures applied in the study are as follows.

```
IF Lim_{Lower} \le Obser_{j,t} \le Lim_{Upper} THEN Obser_{j,t} flag is 'Good'
IF Obser_i > Lim_{Upper} OR Obser_{j,t} < Lim_{Lower} THEN Obser_{j,t} flag is 'Failure'
```

Lim<sub>Lower</sub> and Lim<sub>Upper</sub> thresholds are separately determined for each station on a monthly basis. At any specific site, all the observed monthly data is considered for determination of the upper and lower limits. By applying this test, each observation is flagged either by 'Good' or 'Failure' label depending on the comparison tests mentioned above.

#### Step Test

It is used to see if increment/decrement between sequential observations in time domain is in acceptable range or not. The applied test procedure is,

```
IF |Obser_{j,t}-Obser_{j,t-1}| < Step_j THEN Obser_{j,t} flag is 'Good'
IF |Obser_{j,t}-Obser_{j,t-1}| > Step_j THEN Obser_{j,t} flag is 'Suspect'
```

Step<sub>j</sub> threshold is determined again for each site on a monthly basis. For each site, the dataset containing the absolute difference of the sequential observations is determined by considering the observations for the matching month. The 99.9 % cumulative histogram value of the dataset is set as the Step<sub>j</sub> threshold for the related site and month.

### Persistence Test

Persistence test is used to determine if any group of observations are due to instrument failures. The test procedure applied is defined as,

```
IF T < \Delta THEN Flag for all Obser in T: 'Good'
IF T > \Delta THEN Flag for all Obser in T: 'Suspect'
```

where T is the total number of the sequentially repeating observations forward in time and  $\Delta$  is the possible maximum number of sequentially repeating observations. As in the other two tests,  $\Delta$  threshold is determined for each site on a monthly basis. For any site, the data belonging to the same month is taken into account to determine the repeating number of the sequential observations. Then, 99.9 % cumulative histogram value of the repeating number dataset is assigned as the  $\Delta$  amount for the corresponding site and month. Since there is a high possibility of no-precipitation data (zero), the sequential zero observations are excluded in this test during the determination of the  $\Delta$  threshold amount and application of the test.

#### **QA Test procedure**



(Product H02 - PR-OBS-2)

Doc.No: SAF/HSAF/PVR-02/1.1 Issue/Revision Index: 1.1

Date: 30/09/2011 Page: 73/177

By applying the control procedures of the QA test mentioned above, each individual precipitation observation receives three flags referring to the corresponding test. For the corresponding observation if all the test flag is not 'Good' then the observation is excluded from the validation process.

### Use of spatialization technique

Due to the time and space structure of precipitation and to the sampling characteristics of both the precipitation products and observations used for validation, care has to be taken to bring data into comparable and acceptable range. At a given place, precipitation occurs intermittently and at highly fluctuating rates. Various maps, time series analysis, statistical and probabilistic methodologies are employed in the validation procedure classically, but some additional new aspects such as the spatial coverage verification model of point cumulative semivariogram (PCSV) approach (Şen and Habib, 1998) are proposed for usage in this work.

Each precipitation product within the H-SAF project represents a foot print geometry. Among these, H01 and H02 products represent an elliptical geometry while H03 and H05 have a rectangular geometry. On the other hand, the ground observation (rain gauge) network consists of point observations. The main problem in the precipitation product cal/val activities occurs in the dimension disagreement between the product space (area) and the ground observation space (point). To be able to compare both cases, either area to point (product to site) or point to area (site to product) procedure has to be defined. However, the first alternative seems easier. The basic assumption in such an approach is that the product value is homogenous within the product footprint. Next figure presents satellite foot print (FOV) centers of the H01 and H02 products, an elliptical footprint for the corresponding center (area within the yellow dots) and Awos ground observation sites. The comparison statistic can be performed by considering just the sites in the footprint area. Although this approach is reasonable on the average but it is less useful in spatial precipitation variability representation. The comparison is not possible when no site is available within the footprint area.

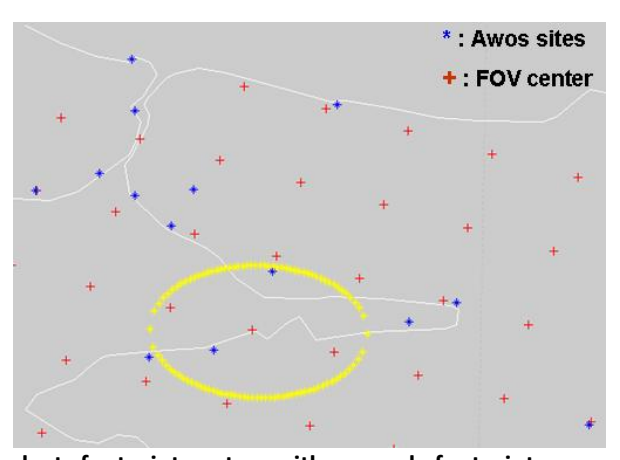


Figure 41 H01 and H02 products footprint centers with a sample footprint area as well as the Awos ground observation sites

Alternatively, the point to area approach is more appealing for the realistic comparison of the precipitation product and the ground observation. This approach is simply based on the determination of the reference precipitation field underneath the product footprint area. To do so, the footprint area is meshed and precipitation amounts are estimated at each grid point by using the precipitation observations at the neighboring Awos sites as shown in next figure. A 3x3 km grid spacing is



(Product H02 - PR-OBS-2)

Doc.No: SAF/HSAF/PVR-02/1.1 Issue/Revision Index: 1.1

Date: 30/09/2011 Page: 74/177

considered for the products with elliptical geometry while 2x2 km spacing is considered for the products with rectangular geometry. For any grid point, Awos sites within the 45 km for the time period of April-September (convective type) and 125km for the rest(stratiform type) are taken into consideration. At each grid point, the precipitation amount is estimated by,

$$\mathbf{Z_{m}} = \frac{\sum_{i=1}^{n} \mathbf{W}(\mathbf{r_{i,m}}) \mathbf{Z_{i}}}{\sum_{i=1}^{n} \mathbf{W}(\mathbf{r_{i,m}})}$$
(4.13.1)

where  $Z_m$  is the estimated value and  $W(r_{i,m})$  is the spatially varying weighting function between the i-th site and the grid point m.

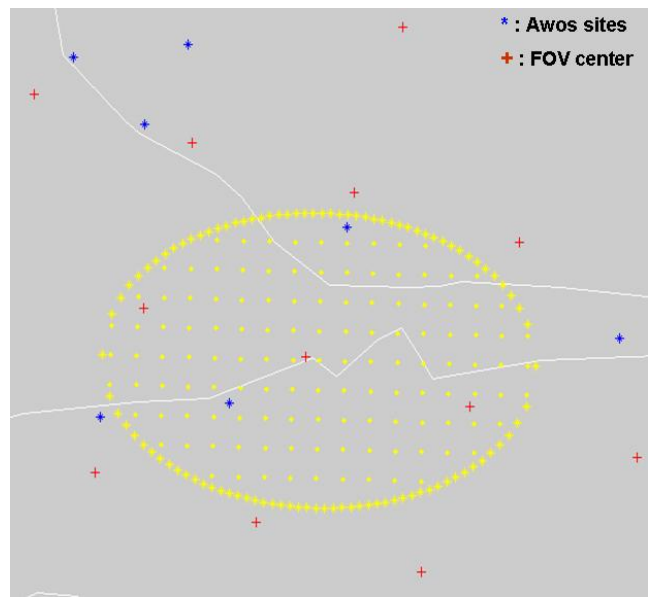


Figure 42 Meshed structure of the sample H01 and H02 products footprint

Determination of the  $W(r_{i,m})$  weighting function in Equation 1 is crucial. In open literature, various approaches are proposed for determining this function. For instance, Thiebaux and Pedder (1987) suggested weightings in general as,

$$W(\mathbf{r}_{i,m}) = \begin{cases} \left(\frac{\mathbf{R}^2 - \mathbf{r}_{i,m}^2}{\mathbf{R}^2 + \mathbf{r}_{i,m}^2}\right)^{\alpha} & \text{for } \mathbf{r}_{i,m} \leq \mathbf{R} \\ \mathbf{0} & \text{for } \mathbf{r}_{i,m} \geq \mathbf{R} \end{cases}$$
(4.13.2)

where R is the radius of influence,  $r_{i,m}$  is the distance from point i to point m to the point and  $\alpha$  is a power parameter that reflects the curvature of the weighting function. Another form of geometrical weighting function was proposed by Barnes (1964) as,

$$\mathbf{W}(\mathbf{r}_{i,m}) = \exp \left[ -4 \left( \frac{\mathbf{r}_{i,m}}{\mathbf{R}} \right)^{\alpha} \right]$$
 (4.13.3)

Unfortunately, none of these functions are observation dependent but suggested on the basis of the logical and geometrical conceptualizations only. They are based only on the configuration, i.e. geometry of the measurement stations and do not take into consideration the natural variability of the



(Product H02 - PR-OBS-2)

Doc.No: SAF/HSAF/PVR-02/1.1 Issue/Revision Index: 1.1

Date: 30/09/2011 Page: 75/177

meteorological phenomenon concerned. In addition, the weighting functions are always the same from site to site and time to time. However, in reality, it is expected that the weights should reflect to a certain extent the regional and temporal dependence behavior of the phenomenon concerned.

For the validation activities, the point cumulative semi-variogram technique proposed by Şen and Habib (1998) is used to determine the spatially varying weighting functions. In this approach, the weightings not only vary from site to site, but also from time to time since the observed data is used. In this way, the spatial and temporal variability of the parameter is introduced more realistically to the validation activity.

### Matching approach

The temporal and spatial matching approaches are applied separately in the validation of the satellite products. As for the temporal matching, the product time is taken into account and 5 minute window(t-2 to t+3) is considered for estimation of the average rainrate for each site.

For the spatial matching, the mesh grid size of 3kmX3km is constructed for each IFOV area. For each grid point, the rainrate is estimated by taking the 5 minute averaged rainrate amounts observed at the nearby AWOS sites within the radius distance of 45 km(for convective type) or 125 km(for stratiform type) considering the weighting of each site with respect to the grid point(Equation 1). The weighting amounts are derived from the spatially varying weighting functions obtained by using the semi-variogram approach(Şen and Habib,1998). Finally, the Gaussian filter is applied to the estimations at the mesh grid of the IFOV area to get the average rainrate. Then, this amount is compared with the satellite precipitation product amount for the validation purposes.

#### 4.13 Conclusions

After these inventories some conclusions can be drawn.

The rain gauge in PPVG is composed by 3500 instruments across the 6 Countries: Belgium, Bulgaria, Germany, Italy, Poland, and Turkey. These data are, as usual, irregularly distributed over ground and are generally deduced by tipping bucket type instruments. Moreover most of the measurements are hourly cumulated. So probably the raingauge networks used in this validation activities are surely appropriated for the validation of cumulated products (1 hour and higher), while for the validation of instantaneous estimates the use of hourly cumulated ground measurements could introduce a large error. Moreover the revisiting time (3,4 hours) of H02 makes impossible or not reasonable to validate the product for 1-24 hours cumulated interval. The first object of PPVG (Rain Gauge- WG) in the next future it will be to quantitatively estimate the errors introduced in the validation procedure comparing the instantaneous satellite precipitation estimation with the rain gauge precipitation cumulated on different intervals (the Polish and Turkish data will be used for this purpose).

The rain gauge inventory has also pointed out that different approaches for the estimates matching are considered in the PPVG. The second steps in the next future will be to define the rain gauge spatial interpolation technique and to develop the related software.

The radar data in the PPVG is composed by 54 C-band radars across the 7 countries: Belgium, Germany, Hungary, Italy, Slovakia, Poland, Turkey. The rain gauge network responsible declared that the systems are kept in a relatively good status. The rain gauge inventory pointed out that different correction factors are applied. This means that the corresponding rainfall estimates are diverse, and



(Product H02 - PR-OBS-2)

Doc.No: SAF/HSAF/PVR-02/1.1 Issue/Revision Index: 1.1

Date: 30/09/2011 Page: 76/177

the estimation of their errors cannot be homogenized. The first step in PPVG (Radar –WG) will be to define a quality index on the base of the study performed by the Slovakian team (Annex 4) and the scheme published by J. Szturc *et all* 2008. The main difficulty consists on the definition of a quality index computable for every radar networks of PPVG. The evaluation of this quality index will allow to evaluate the rain gauge error in the same way and to select the more reliable radar data in the PPVG.

In this chapter the first example of precipitation fields integration has been provided (Section 4.4.3): INCA and RADOLAN products. The INCA system, a tool for the precipitation products validation, is available in Slovakia and Poland, in both countries being run in pre-operational mode. In Germany similar precipitation analysis system called RADOLAN is being run operationally. This tool is already used for validation of the H-SAF precipitation products in Germany. The study performed in the PPVG (INCA-WG) showed that the accuracy and reliability of the raingauge stations significantly affect final precipitation analysis of the INCA or INCA-like systems. In order to solve this problem an automated blacklisting technique is going to be developed at SHMÚ (currently blacklisting is used in manual mode). The next step will be to develop the software for up-scaling the INCA precipitation field into the satellite product grid. The grids of INCA and RADOLAN have similar horizontal resolution to the common radar grid. The up-scaling software will allow to provide case study analysis and statistical score evaluation for future considerations on the opportunity to use these precipitation integration products in the H-saf validation programme.

### 5 Validation results: case study analysis

### 5.1 Introduction

As reported in the Chapter 3 the common validation methodology is composed of large statistic (multi-categorical and continuous), and case study analysis. Both components (large statistic and case study analysis) are considered complementary in assessing the accuracy of the implemented algorithms. Large statistics helps in identifying existence of pathological behaviour, selected case studies are useful in identifying the roots of such behaviour, when present.

This Chapter collects the case study analysis performed by PPVG on H02 for the year 2010. The Chapter is structured by Country / Team, one section each. The analysis has been conducted to provide information to the User of the product on the variability of the performances with climatological and morphological conditions, as well as with seasonal effects.

Each section presents the case studies analysed giving the following information:

- description of the meteorological event;
- comparison of ground data and satellite products;
- visualization of ancillary data deduced by nowcasting products or lightning network;
- discussion of the satellite product performances;
- indications to satellite product developers;
- indication on the ground data (if requested) availability into the H-SAF project.

In the future the PPVG will test the possibility to present case study analysis in the test sites, indicated by the hydrological validation team, in order to provide a complete product accuracy and hydrological validation analysis to the users.



(Product H02 - PR-OBS-2)

Doc.No: SAF/HSAF/PVR-02/1.1 Issue/Revision Index: 1.1

Date: 30/09/2011 Page: 77/177

### 5.2 Case study analysis in Belgium (IRM)

### 5.2.1 Case study: August 14<sup>th</sup> -17<sup>th</sup>, 2010

### Description

This event has been select because convective precipitation occurred during 14 - 17 August and covering large parts of the study area during 15 and 16 August. A low was moving from Germany to The Netherlands (next figure). Warm air from Central Europe was lifted over oceanic cold air over the study area.

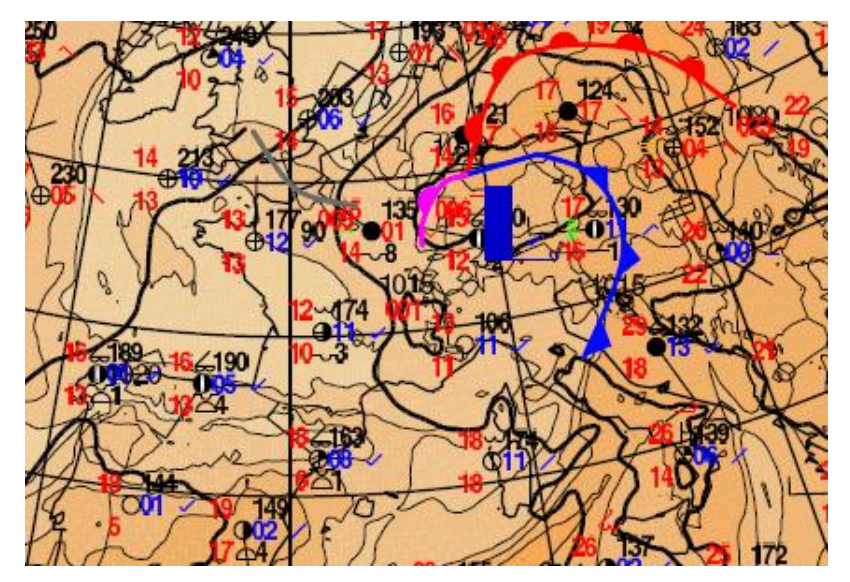


Figure 43 Synoptic situation on 15 August 2010 at 6 UTC (zoom in the surface map)

### Data used

Products (H02) from August 14<sup>th</sup> at 6.00 UTC to August 17<sup>th</sup> at 18.00 UTC have been considered in this study. The total is 32 satellite passages, distributed as follows:

- 4 in the afternoon of August 14<sup>th</sup>;
- 4 in the morning of August 15<sup>th</sup>;
- 7 in the afternoon of August 15<sup>th</sup>;
- 8 in the morning of August 16<sup>th</sup>;
- 3 in the afternoon of August 16<sup>th</sup>;
- 6 in the morning of August 17<sup>tn</sup>;

The ground data used for validation are the Wideumont radar instantaneous measurements, without rain-gauge adjustment. Radar data are available within 5 minutes around the satellite passage.

### Comparison

Here are three examples of H02 files, compared with radar data upscaled to the same grid. The first two examples are observing the same scene from different satellites at noon of August 15<sup>th</sup>, while the third one refers to the early morning of August 16<sup>th</sup>.

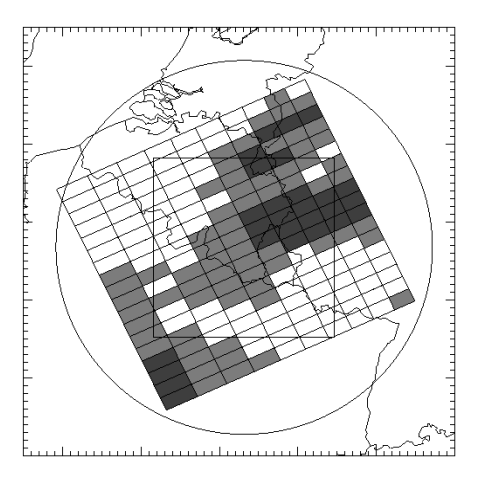


(Product H02 - PR-OBS-2)

Doc.No: SAF/HSAF/PVR-02/1.1

Issue/Revision Index: 1.1 Date: 30/09/2011

Page: 78/177



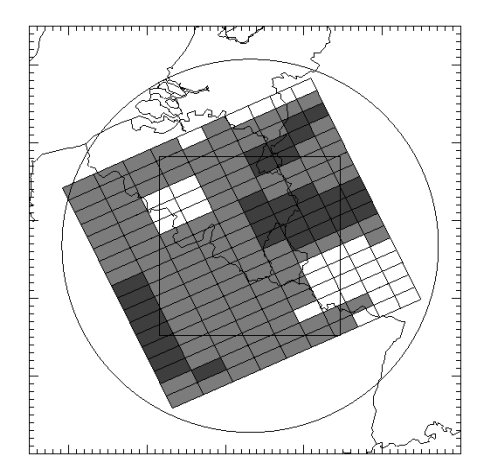
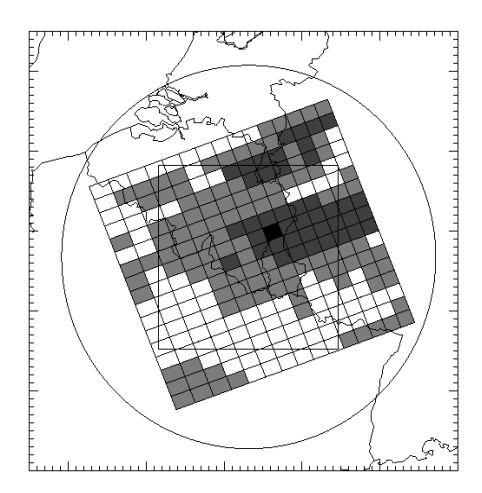


Figure 44 H02 image of August 15, 2010 at 12.08 (left) compared with upscaled radar at 12.10 (right). The scale corresponds to thresholds of 0.1, 1., and 10. mm h-1



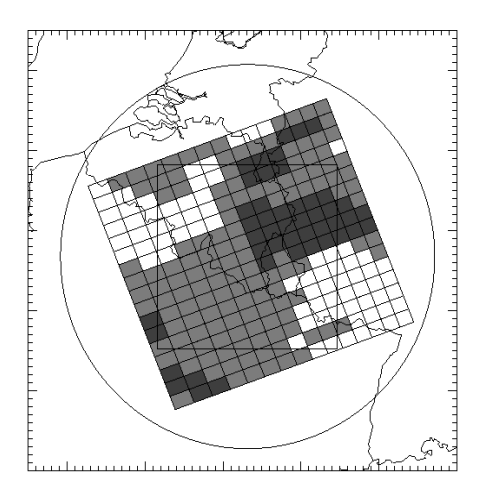


Figure 45 H02 image of August 15th, 2010 at 12.09 (left) compared with upscaled radar at 12.10 (right – the same radar image as above, but upscaled on a different grid). The scale corresponds to thresholds of 0.1, 1., and 10. mm h-1

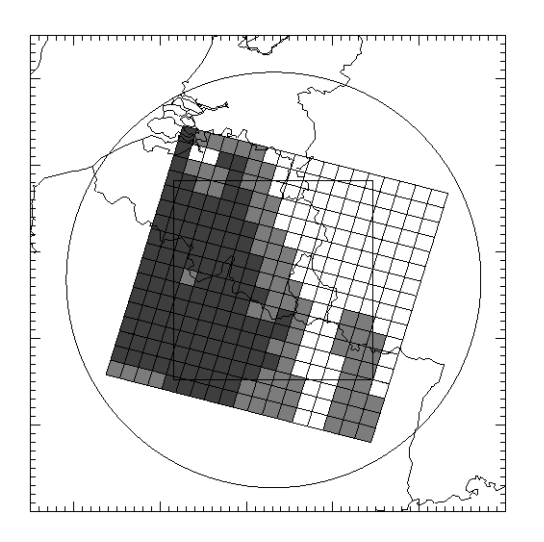


(Product H02 - PR-OBS-2)

Doc.No: SAF/HSAF/PVR-02/1.1 Issue/Revision Index: 1.1

Date: 30/09/2011

Page: 79/177



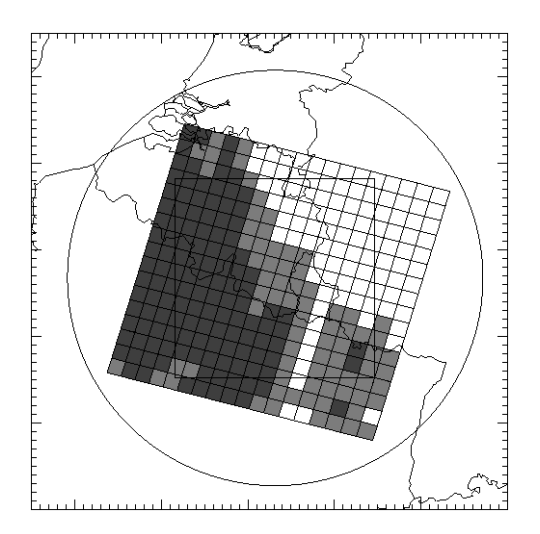


Figure 46 H02 image of August 16th, 2010 at 2.07 (left) compared with upscaled radar at 2.05 (right). The scale corresponds to thresholds of 0.1, 1., and 10. mm h-1

We can see that in the noon case the matching is rather good and the images from two satellites are consistent in particular in detecting the precipitation cells in the North of the validation area. There is just a slight underestimation. In the morning case it is quite good.

### Scores evaluation

The score evaluation results (Table 21) are quite good if compared to long period statistics, especially for what concerns correlation, POD and FAR. A slight underestimation is reported over all the case study (consistently with the long period statistics).

| Sample                  | 32    |
|-------------------------|-------|
| Mean error*             | -0.43 |
| Standard deviation*     | 1.37  |
| Mean absolute error*    | 0.98  |
| Multiplicative bias     | 0.72  |
| Correlation coefficient | 0.49  |
| Root mean square error* | 1.45  |
| URD-RMSE                | 1.56  |
| POD                     | 0.62  |
| FAR                     | 0.22  |
| CSI                     | 0.52  |

Table 21 Scores obtained with the comparison with radar data (\* in mm h<sup>-1</sup>)



(Product H02 - PR-OBS-2)

Doc.No: SAF/HSAF/PVR-02/1.1 Issue/Revision Index: 1.1

Date: 30/09/2011

Page: 80/177

The time evolution of the fraction area with rain, the average rain rate over this area, the Equitable Threat Score (ETS), and the root mean square error (RMSE) is reported in the following figure:

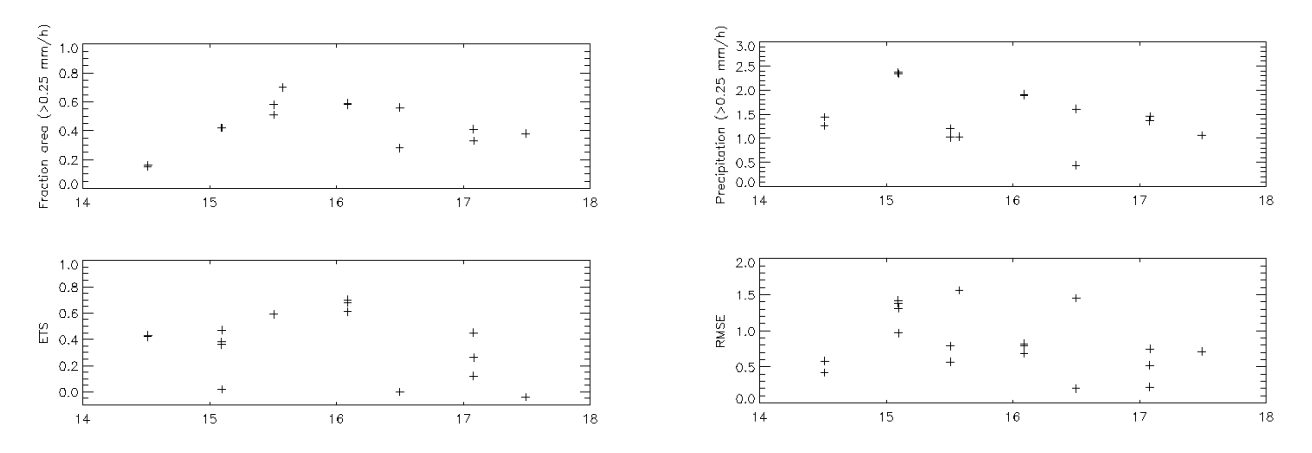


Figure 47 Time evolution of fraction area with rain, average rain rate over this area (threshold 0.25 mm/h), RMSE and ETS during the present case study

### Conclusions

From qualitative and statistics comparison, it appears that for this case study (summer storm characterized by convective rainfall) the h02 product could reproduce the rainfall patterns with quite good confidence, slightly underestimating rainfall amounts.

### 5.2.2 Case study: August 22<sup>th</sup> -24<sup>th</sup>, 2010

#### **Description**

This event has been chosen because thunderstorms with intense precipitation resulted in local flooding in Belgium. The country was at the edge of a large anti-cyclone which was moving away towards South-East (next figure). Warm but humid and unstable air was brought from South-West whereas a cold front was moving from West.

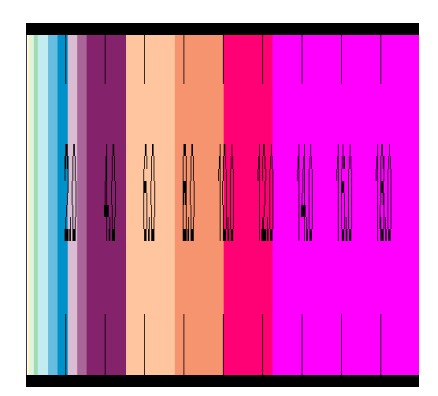


Figure 48 Surface map on 22 August 2010 at 06 UTC (MSLP and synoptic observations)

### Data used



(Product H02 - PR-OBS-2)

Doc.No: SAF/HSAF/PVR-02/1.1 Issue/Revision Index: 1.1

Date: 30/09/2011 Page: 81/177

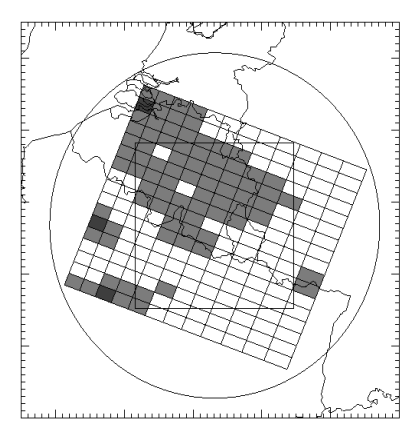
Products (H02) from August 22<sup>th</sup> at 6.00 UTC to August 24<sup>th</sup> at 12.00 UTC have been considered in this study. The total is 12 satellite passages, distributed as follows:

- 4 in the early afternoon of August 22<sup>th</sup>;
- 2 in the early morning of August 23<sup>th</sup>;
- 3 in the early afternoon of August 23<sup>th</sup>;
- 3 in the early morning of August 24<sup>th</sup>.

The ground data used for validation are the Wideumont radar instantaneous measurements, without rain-gauge adjustment. Radar data are available within 5 minutes around the satellite passage.

### Comparison

Here are three examples of H02 files, compared with radar data upscaled to the same grid. The first is in the morning of August 23<sup>th</sup>, the second around noon, and the third one refers to the early morning of August 24<sup>th</sup>.



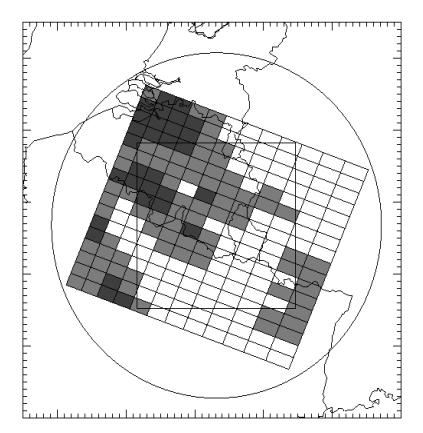
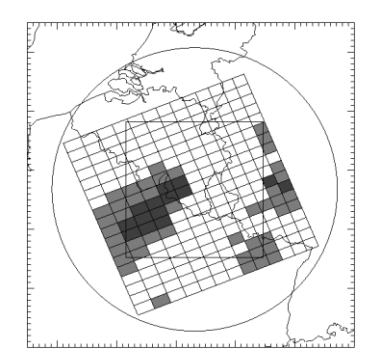


Figure 49 H02 image of August 23th, 2010 at 2.35 (left) compared with upscaled radar at the same time (right). The scale corresponds to thresholds of 0.1, 1., and 10. mm h-1



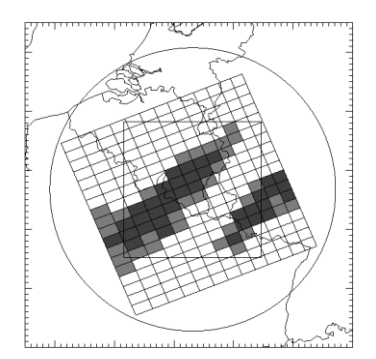


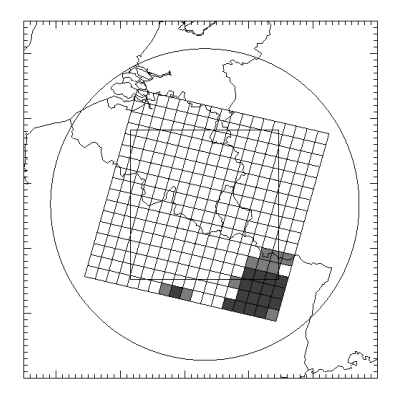
Figure 50 H02 image of August 23th, 2010 at 12.23 (left) compared with upscaled radar at 12.25 (right). The scale corresponds to thresholds of 0.1, 1., and 10. mm h-1



(Product H02 - PR-OBS-2)

Doc.No: SAF/HSAF/PVR-02/1.1 Issue/Revision Index: 1.1

Date: 30/09/2011 Page: 82/177



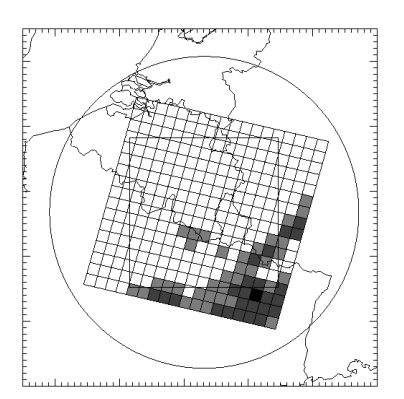


Figure 51 H02 image of August 23th, 2010 at 12.23 (left) compared with upscaled radar at 12.25 (right). The scale corresponds to thresholds of 0.1, 1., and 10. mm h-1

We can see that in all the shown cases the satellite is able to detect the presence of rainfall in the area, but it tends to underestimate the extension and the amount of it.

#### Scores evaluation

The score evaluation results (Table 1) are not as good as the other summer case. They appear more aligned to the ones obtained in the long period analysis, with noticeable underestimation. This might be connected with the fact that in this case, the fraction of area interested by the rainfall is smaller (see Figure 52 and, for comparison, Figure 47).

| Camanala                | 12    |
|-------------------------|-------|
| Sample                  | 12    |
| Mean error*             | -0.72 |
| Standard deviation*     | 1.66  |
| Mean absolute error*    | 1.06  |
| Multiplicative bias     | 0.52  |
| Correlation coefficient | 0.41  |
| Root mean square error* | 1.73  |
| URD-RMSE                | 0.95  |
| POD                     | 0.59  |
| FAR                     | 0.36  |
| CSI                     | 0.44  |

Table 22 Scores obtained with the comparison with radar data (\* in mm h<sup>-1</sup>)

The time evolution of the fraction area with rain, the average rain rate over this area, the Equitable Threat Score (ETS), and the root mean square error (RMSE) is reported in the following figure.



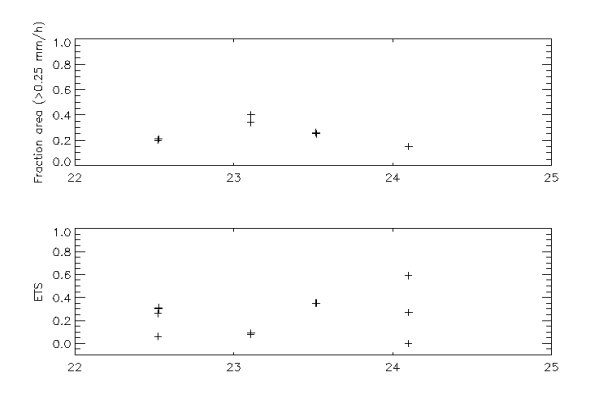


(Product H02 - PR-OBS-2)

Doc.No: SAF/HSAF/PVR-02/1.1 Issue/Revision Index: 1.1

Date: 30/09/2011

Page: 83/177



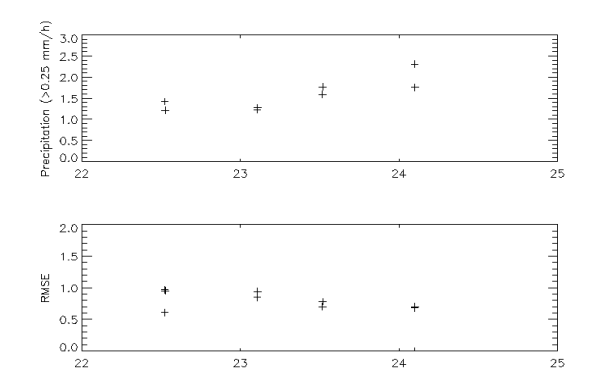


Figure 52 Time evolution of fraction area with rain, average rain rate over this area (threshold 0.25 mm/h), RMSE and ETS during the present case study

### Conclusions

From qualitative and statistics comparison, it appears that for this case study the h02 product could reproduce the rainfall patterns, but regularly underestimating rainfall amounts and areas. The results, aligned with the ones of long period statistics, are sensibly worse than the ones obtained for the other summer case study, occurred just one week before.

### 5.2.3 Case study: November 12<sup>th</sup> - 15<sup>th</sup>, 2010

### Description of the event

A wide area with low pressure extended from Scandinavia to Great Britain and made a very active precipitating perturbation stay over the country during several days (next figure) and result in high

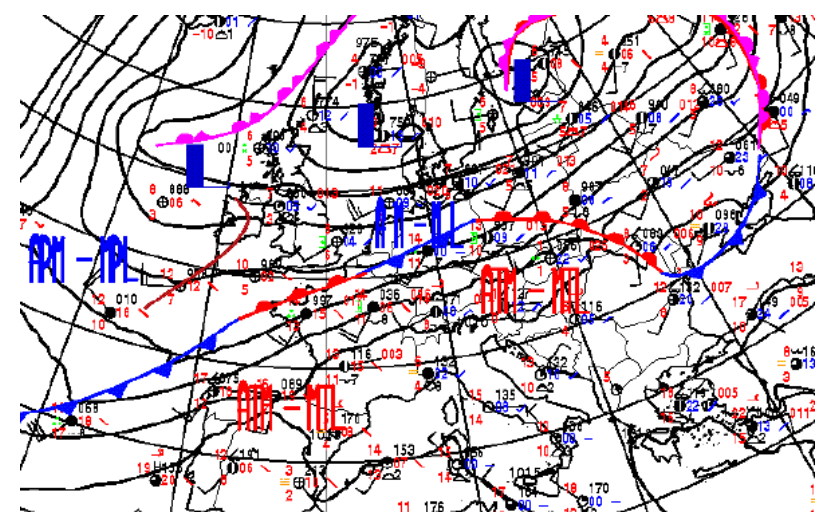


Figure 53 Surface map on 13 November 2010 at 06 UTC (MSLP and synoptic observations)

### Data used

Products (H02) from November 12<sup>th</sup> at 0.00 UTC to November 15<sup>th</sup> at 18.00 UTC have been considered in this study. The total is 58 satellite passages, distributed as follows:



(Product H02 – PR-OBS-2)

Doc.No: SAF/HSAF/PVR-02/1.1 Issue/Revision Index: 1.1

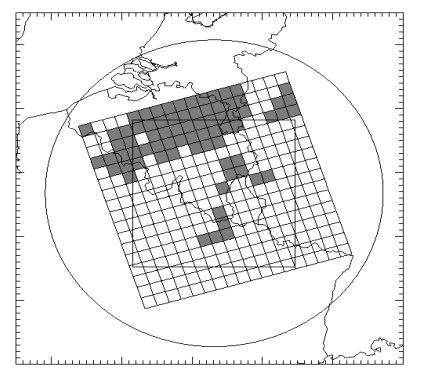
Date: 30/09/2011 Page: 84/177

- 14 in the morning of November  $12^{th}$ ;
- 2 in the early afternoon of November 12<sup>th</sup>;
- 9 in the morning of November 13<sup>th</sup>;
- 6 in the early afternoon of November 13<sup>th</sup>;
- 9 in the morning of November 14<sup>th</sup>;
- 6 in the early afternoon of November 14<sup>th</sup>;
- 7 in the early morning of November 15<sup>th</sup>;
- 5 in the early afternoon of November 15<sup>th</sup>;

The ground data used for validation are the Wideumont radar instantaneous measurements, without rain-gauge adjustment. Radar data are available within t5 minutes around the satellite passage.

### Comparison

Two representative examples of the comparison between H02 and upscaled radar are given.



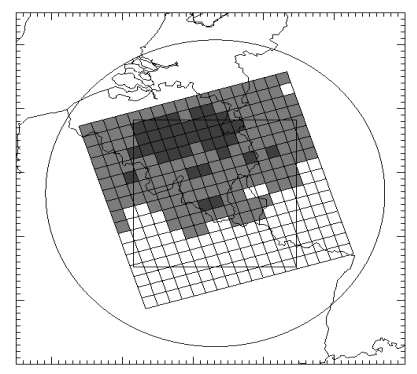
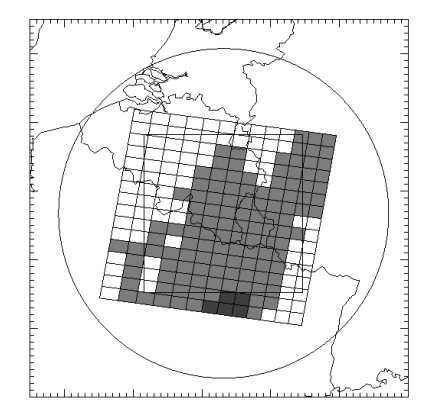


Figure 54 H02 image of November 13th, 2010 at 12.53 (left) compared with upscaled radar at 12.55 (right). The scale corresponds to thresholds of 0.1, 1., and 10. mm h-1



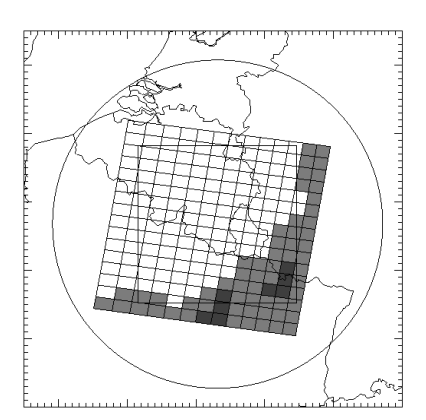


Figure 55 H02 image of November 15th, 2010 at 1.29 (left) compared with upscaled radar at 1.30 (right). The scale corresponds to thresholds of 0.1, 1., and 10. mm h-1

The matching of the precipitation area is very week, and only in one case a cell with rain rate greater than 1 mm h<sup>-1</sup> is detected.



(Product H02 – PR-OBS-2)

Doc.No: SAF/HSAF/PVR-02/1.1 Issue/Revision Index: 1.1

Date: 30/09/2011

Page: 85/177

### Scores evaluation

The statistical scores of the comparison between H02 and upscaled radar data are given on the following table.

| Sample                  | 58    |
|-------------------------|-------|
| Mean error*             | -0.60 |
| Standard deviation*     | 0.49  |
| Mean absolute error*    | 0.64  |
| Multiplicative bias     | 0.20  |
| Correlation coefficient | 0.13  |
| Root mean square error* | 0.80  |
| URD-RMSE                | 0.88  |
| POD                     | 0.19  |
| FAR                     | 0.37  |
| CSI                     | 0.17  |

Table 23 Scores obtained with the comparison with radar data (\* in mm h<sup>-1</sup>)

These results, unlike the summer case, show performances lower than the ones of the long-period analysis, with low probability of detection, high false alarm ratio and large underestimation. It can be added that the radar data cumulated over 24h revealed to be underestimated compared with interpolated rain-gauge data. This of course only worsens the conclusion about the product.

The time evolution of the fraction area with rain, the average rain rate over this area, the Equitable Threat Score (ETS), and the root mean square error (RMSE) is reported in next figure.

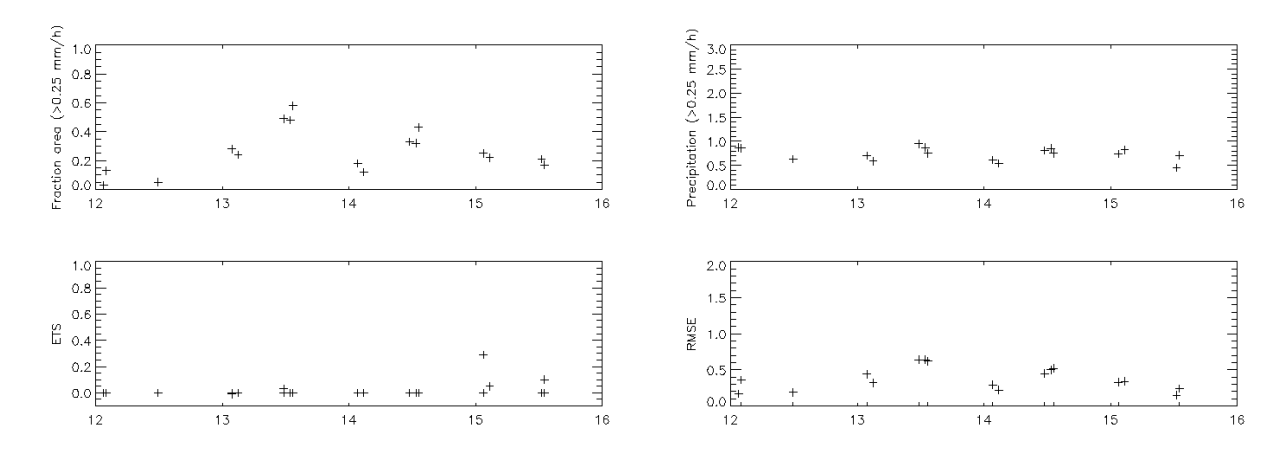


Figure 56 Time evolution of fraction area with rain, average rain rate over this area (threshold 0.25 mm/h), RMSE and ETS during the present case study

### **Conclusions**

From the visual and statistical comparison with radar data, it appears that the H02 product fails to reproduce the rainfall patterns and amount in this winter situation.



(Product H02 - PR-OBS-2)

Doc.No: SAF/HSAF/PVR-02/1.1 Issue/Revision Index: 1.1

Date: 30/09/2011 Page: 86/177

### 5.3 Case study analysis in Germany (BfG)

### 5.3.1 Case study: August 7<sup>th</sup>, 2010 (River Neiße, Oder, Spree and Elbe catchments)

### **Description**

At 7<sup>th</sup> August 2010 there was a baroclinic zone reaching from the Baltic sea across Poland and Czechia until Austria, where sub-tropical air was advected from south to north at the eastern flank of the associated low pressure. During the 7/8<sup>th</sup> August 2010 the precipitation reached about 35 mmh<sup>-1</sup> (150 mm in 48 hours) in parts of Germany, especially in Saxony, causing floods in the upper parts of the rivers Neiße, Spree and Elbe with catastrophic damages.<sup>5</sup>

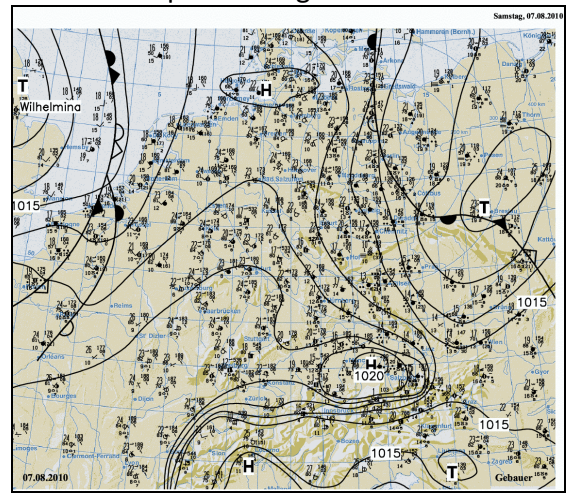


Figure 57 Synopsis for Central Europe for 07th August 2010 (FU Berlin, http://wkserv.met.fu-berlin.de)

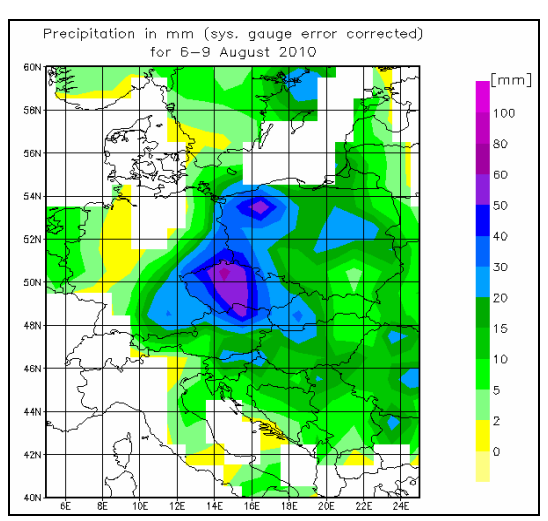


Figure 58 two-day totals (ending at 9th August, 0 UTC) interpolated on a 1°x1° evaluation grid as derived from SYNOP messages (Global Precipitation Climatology Centre, GPCC operated by DWD)

<sup>&</sup>lt;sup>5</sup> Zur Rolle des Starkniederschlages am 7.-9. August 2010 im Dreiländereck Polen, Tschechien, Deutschland bei der Entstehung der Hochwasser von Neiße, Spree und Elbe, Bissolli at all, Rapp, Friedrich, Ziese, Weigl, Nitsche, Gabriele Malitz, Andreas Becker (Floods in Eastern Central Europe in May 2010, FU Berlin 2010).



(Product H02 - PR-OBS-2)

Doc.No: SAF/HSAF/PVR-02/1.1 Issue/Revision Index: 1.1

Date: 30/09/2011 Page: 87/177

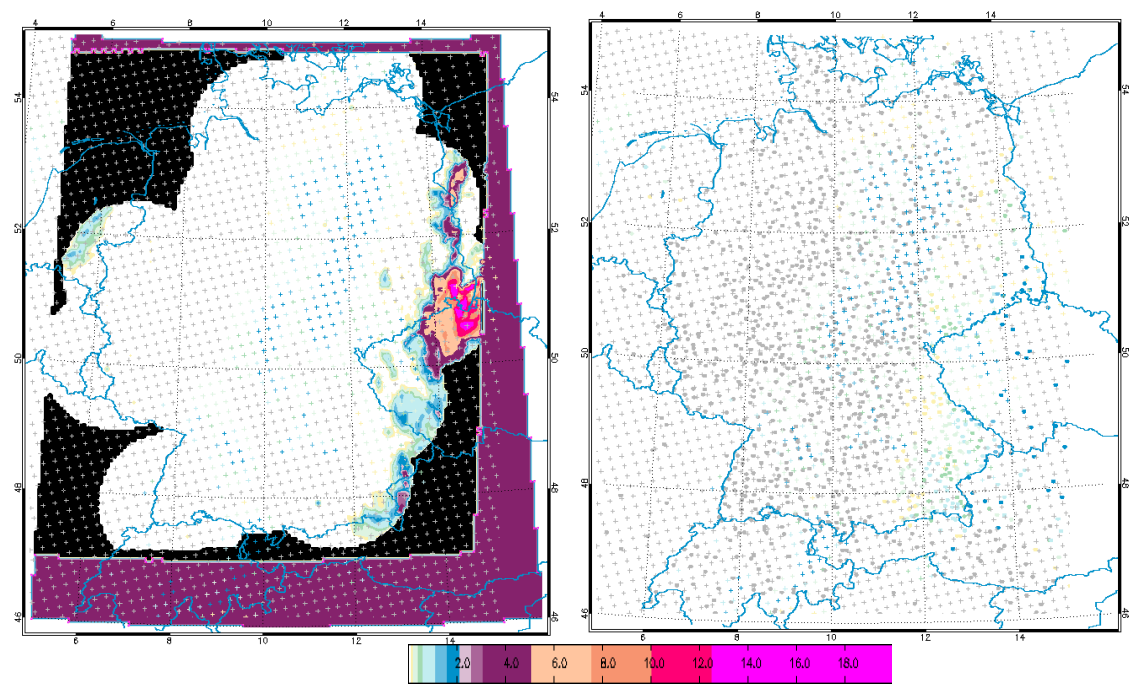


Figure 59 Hourly precipitation sum [mm] for H02 satellite data (crosses, time stamp 2010-08-07 11:58 UTC, station Rome) and for RADOLAN-RW (left, filled raster, 2010-08-07 12:50 UTC) and station data (right, dots, 2010-08-07 13:00 UTC)

### Data used

H02 data for eastern part of Germany in the given period were available for 2:01 UTC (station Athens), 2:02 UTC (station Lannion), 11:51 UTC (station Athens), 11:52 UTC (station Lannion) and 11:58 UTC (station Rome). Only these data are analysed in this case study.

### Comparison

A first look to the results (Figure 59) shows, that rain rates detected by satellite product are in the same area of Germany as those indicated by the ground data.

### Statistical score

In the following two tables the result of the categorical statistic of the validation with both RADOLAN and rain gauge data are listed. The Probability Of Detection (POD) of precipitation >=0.25 mmh<sup>-1</sup> gain for validation with RADOLAN 0.66, with rain gauge 0.54. The different results are due to the fact that RADOLAN data produce more valid pairs of satellite/ground points. A valid pair is given if for a satellite observation point (fixed date/time) at least one ground observation point can be found within an surrounding area formed by a search ellipse of  $\sim$ 2.5 km x  $\sim$ 2.5 km. Also the False Alarm Rate (FAR) is different: for RADOLAN it was 0.49, for rain gauge 0.44 (worse than for whole August 2010). For both kinds of ground data there were no valid pairs in the class RR >= 10 mmh<sup>-1</sup>, so that for this class we have no statement on validation.



(Product H02 - PR-OBS-2)

Doc.No: SAF/HSAF/PVR-02/1.1

Issue/Revision Index: 1.1 Date: 30/09/2011

Page: 88/177

| 7 <sup>th</sup> August 2010 | H02 vs. radar |         |        | H02      | vs. rain gaug | ge      |
|-----------------------------|---------------|---------|--------|----------|---------------|---------|
| [mm/h]                      | RR>=0.25      | RR>=1.0 | RR>=10 | RR>=0.25 | RR>=1.0       | RR>=10  |
| Samples                     | 1133          | 405     | 1      | 288      | 104           | 0       |
| POD                         | 0.66          | 0.37    | 0.00   | 0.54     | 0.35          | 0.00    |
| FAR                         | 0.49          | 0.51    | 1.00   | 0.44     | 0.50          | #DIV/0! |
| CSI                         | 0.41          | 0.27    | 0.00   | 0.38     | 0.26          | 0.00    |

Table 24 Results of the categorical statistic of the validation for 7th August 2010

| August 2010 | H02 vs. radar |         |        | H02      | vs. rain gaug | ge     |
|-------------|---------------|---------|--------|----------|---------------|--------|
| [mm/h]      | RR>=0.25      | RR>=1.0 | RR>=10 | RR>=0.25 | RR>=1.0       | RR>=10 |
| Samples     | 15896         | 7672    | 97     | 3173     | 1019          | 4      |
| POD         | 0.68          | 0.65    | 0.09   | 0.38     | 0.27          | 0.03   |
| FAR         | 0.47          | 0.63    | 0.98   | 0.35     | 0.51          | 0.75   |
| CSI         | 0.43          | 0.31    | 0.02   | 0.32     | 0.21          | 0.03   |

Table 25 Results of the categorical statistic of the validation for whole August 2010

In comparison with categorical statistic of the whole August 2010 we can see, that in case of the 7<sup>th</sup> August we got worse results for POD in all classes for validation with radar data, for validation with gauge data it is the converse. Better results generally were received by validation with radar data. For 7<sup>th</sup> August the validation with both kind of ground data provide a POD in the second class (0.37 radar, 0.35 rain gauge) less than the FAR (0.51 radar, 0.5 rain gauge). The Critical Success Index (CSI) is more stable and differs only by 1-3 percent between the different validation methods. A CSI of 0.41 (0.38) means that 41% resp. 38 % of the predictions (H02) of precipitation (>= 0.25 mmh<sup>-1</sup>) of all predicted/observed rain events are correct.

Next two figures. show the contingency table of four classes. In opposite to results of H01 on validation only for the first class over 50% of the H02 data are in the same class. In higher classes most of H02 data belong to lower classes. That means we have a strong underestimation of all precipitation amounts higher than  $1 \text{ mmh}^{-1}$ .



(Product H02 - PR-OBS-2)

Doc.No: SAF/HSAF/PVR-02/1.1 Issue/Revision Index: 1.1

Date: 30/09/2011

Page: 89/177

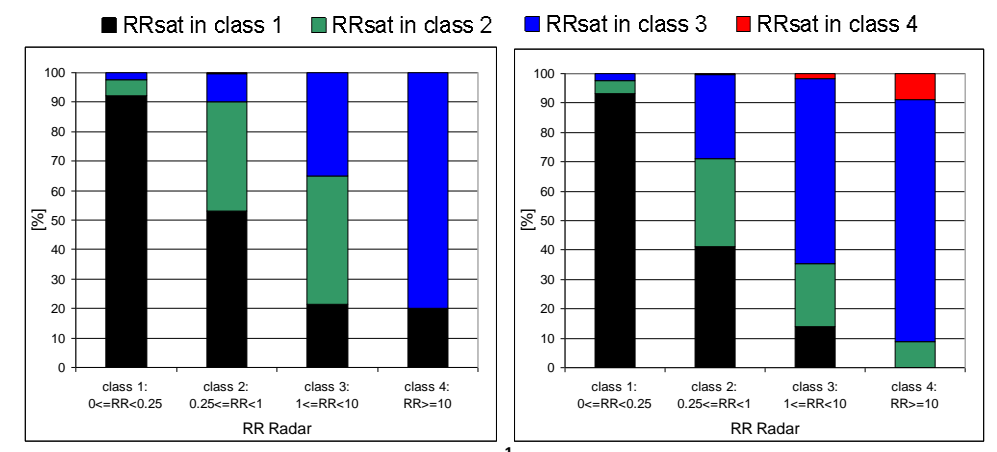


Figure 60 Contingency table statistic of rain rate [mmh h<sup>-1</sup>] for H02 vs. radar data. Left: for 7th August 2010, Right: for whole August 2010

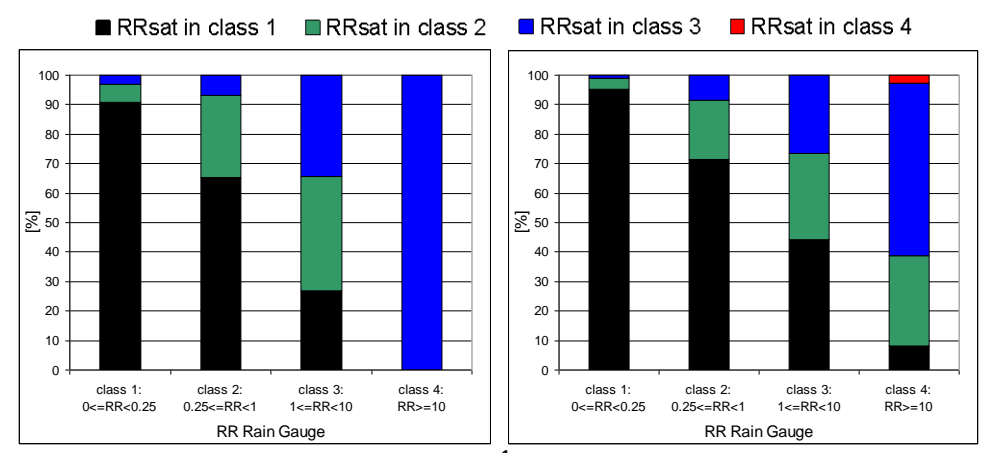


Figure 61 Contingency table statistic of rain Rate [mm h<sup>-1</sup>] for H02 vs. rain gauge data. Left: for 7th August 2010, Right: for whole August 2010

Results of the continuous statistic (next table) show negative mean error (ME) for detection of precipitation (RR >=  $0.25 \text{ mmh}^{-1}$ ), which means, that H-SAF product underestimates the fact of precipitation generally. Standard deviation (SD) with  $0.5 \text{ mmh}^{-1}$  for this class is less than for validation of H01. The correlation coefficient (CC) with 0.61/0.49 is better than that for H01 (0.24/0.46). These facts are due to less samples for H02. Results for whole August are not so clearly better: ME -0.64/0.19 for H02 against -0.25/-0.59 for H01, CC 0.35/0.38 for H02 against 0.32/0.38 for H01.

| RR[mmh <sup>-1</sup> ] | 7 <sup>th</sup> August 2010 |       | August 2010 |            | 7 <sup>th</sup> August 2010 |       | August 2010 |       |
|------------------------|-----------------------------|-------|-------------|------------|-----------------------------|-------|-------------|-------|
|                        | rain                        |       | rain        |            |                             |       |             |       |
|                        | gauge                       | radar | gauge       | radar      | rain gauge                  | radar | rain gauge  | radar |
|                        | 0.25 <= RR < 1              |       |             | RR >= 0.25 |                             |       |             |       |
| ME                     | -0.29                       | -0.18 | -0.21       | 0.41       | -0.84                       | -1.55 | -0.64       | 0.19  |
| SD                     | 0.50                        | 0.81  | 0.76        | 1.32       | 1.44                        | 2.31  | 1.53        | 1.90  |
| MAE                    | 0.47                        | 0.50  | 0.54        | 0.75       | 1.06                        | 1.74  | 0.97        | 1.12  |
| MB                     | 0.46                        | 0.69  | 0.59        | 1.86       | 0.44                        | 0.36  | 0.44        | 1.16  |



(Product H02 - PR-OBS-2)

Doc.No: SAF/HSAF/PVR-02/1.1 Issue/Revision Index: 1.1

Date: 30/09/2011

| Page: 9 | 90/177 |
|---------|--------|
|---------|--------|

| СС   | 0.01         | 0.02  | 0.09  | 0.22  | 0.61   | 0.49  | 0.35   | 0.38  |
|------|--------------|-------|-------|-------|--------|-------|--------|-------|
| RMSE | 0.58         | 0.83  | 0.79  | 1.38  | 1.66   | 2.78  | 1.66   | 1.91  |
|      | 1 <= RR < 10 |       |       |       |        | RR    | >= 10  |       |
| ME   | -1.26        | -2.07 | -1.28 | -0.19 | -11.22 | -9.75 | -11.69 | -8.08 |
| SD   | 1.41         | 1.92  | 1.58  | 2.53  | 0.00   | 1.96  | 2.81   | 5.17  |
| MAE  | 1.52         | 2.18  | 1.61  | 1.75  | 11.22  | 9.75  | 11.69  | 8.88  |
| MB   | 0.45         | 0.35  | 0.40  | 0.92  | 0.24   | 0.20  | 0.17   | 0.40  |
| CC   | 0.52         | 0.42  | 0.28  | 0.22  | -      | -0.04 | 0.58   | 0.14  |
| RMSE | 1.89         | 2.83  | 2.03  | 2.53  | 11.22  | 9.94  | 12.02  | 9.59  |

**Table 26 Continuous statistic** 

#### Conclusions

The results for H02 were worse than for H01. For rain rates greater than 1 mmh<sup>-1</sup> the probability of detection is equal/less than the false alarm rate. All the quantitative precipitation amounts were underestimated.

### 5.3.2 Case study: June 3<sup>rd</sup>, 2010 (River Danube catchment)

### Description

On the beginning of June 2010 the weather was determined by a low pressure area over eastern part of Central Europe. Wet hot air out from Mediterranean Sea was directed around the low-pressure vortex "Bergthora" contraclockwise out from north to Bavaria and arrived overhead the near-ground cold area. By this air advection on 3<sup>rd</sup> of June fell long lasting rain in the catchments of the rivers Regen and Danube and caused a Danube river flood. Precipitation amounts over 24 hours reached between 80 mm and 155 mm and<sup>6</sup>.

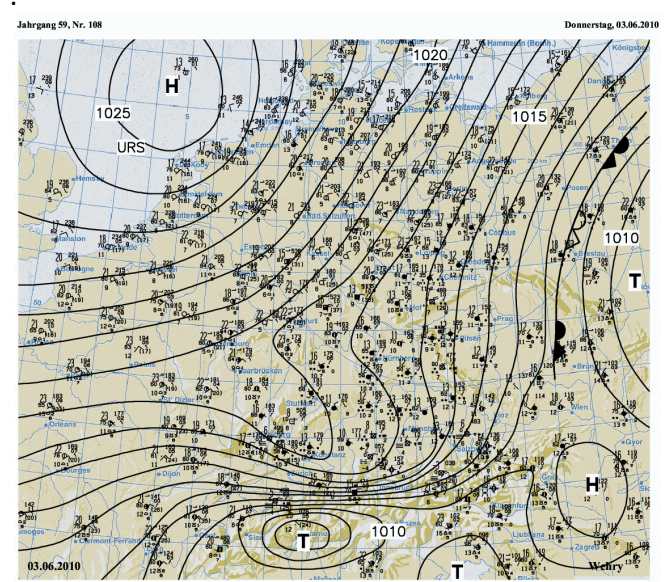


Figure 62 Synopsis for Central Europe for 03rd June 2010 (FU Berlin, http://wkserv.met.fu-berlin.de)

-

<sup>&</sup>lt;sup>6</sup> Gewässerkundlicher Monatsbericht Juni 2010, Bayrisches Landesamt für Umwelt



(Product H02 - PR-OBS-2)

Doc.No: SAF/HSAF/PVR-02/1.1 Issue/Revision Index: 1.1

Date: 30/09/2011 Page: 91/177

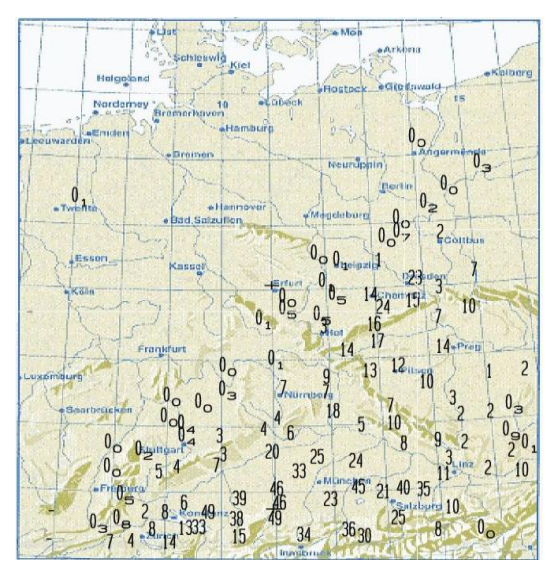


Figure 63 12h totals of precipitation(ending (FU at 3rd June 2010, 7 UTC)

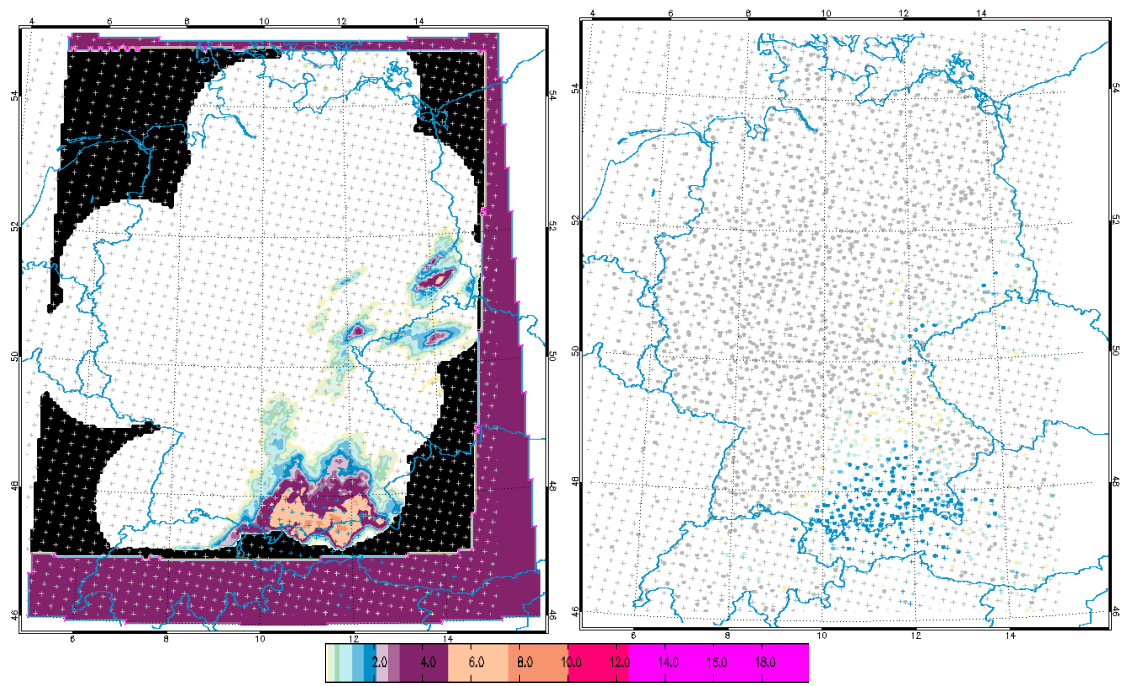


Figure 64 Hourly precipitation sum [mm] for H02 satellite data (crosses, time stamp 2010-06-03 01:50 UTC, station Athens) and for RADOLAN-RW (left, filled raster, 2010-06-03 01:50 UTC) and station data (right, dots 2010-06-03 02:00 UTC)

### Data used

H02 data for Bavaria in the given period were available for 1:30 UTC (Rome), 1:49 UTC (Mos), 1:50 UTC (Athens), 11:42 UTC (Rome), 13:18 UTC (Rome) and 13:22 UTC (Lannion). Only these data are analysed for this case study.

### Comparison

A first look to the results shows, that rain rates detected by satellite product are in the same area of Germany as those indicated by the ground data.



(Product H02 - PR-OBS-2)

Doc.No: SAF/HSAF/PVR-02/1.1 Issue/Revision Index: 1.1

Date: 30/09/2011

Page: 92/177

### Statistical score

In the next two tables the result of the categorical statistic of the validation with both RADOLAN and rain gauge data are listed. The results for validation with radar data for 3<sup>rd</sup> June are worse than for the whole month June: Probability Of Detection of precipitation (RR>=0.25 mmh<sup>-1</sup>) was 0.30 with less False Alarm Rate of 0.13 and Critical Success Index is 0.29. Compared with results of H01 validation the results are much worse for 3<sup>rd</sup> June. Results for H02, 3<sup>rd</sup> June were better than for the whole June. The matter may be the fact, that the rain events were particularly in small point areas, which were not scanned by satellite.

| 3 <sup>rd</sup> June 2010 | Н                       | 02 vs. radar |   | H02      | vs. rain gaug | ge     |
|---------------------------|-------------------------|--------------|---|----------|---------------|--------|
| [mmh <sup>-1</sup> ]      | RR>=0.25 RR>=1.0 RR>=10 |              |   | RR>=0.25 | RR>=1.0       | RR>=10 |
| Samples                   | 206                     | 96           | 0 | 88       | 39            | 3      |
| POD                       | 0.30                    | 0.29         | - | 0.28     | 0.24          | -      |
| FAR                       | 0.13                    | 0.10         | - | 0.14     | 0.18          | 1.00   |
| CSI                       | 0.29                    | 0.28         | - | 0.26     | 0.23          | 0.00   |

Table 27 Results of the categorical statistic of the validation for 3rd June 2010

| June 2010            | Н        | 02 vs. radar          |      | H02 vs. rain gauge |         |        |
|----------------------|----------|-----------------------|------|--------------------|---------|--------|
| [mmh <sup>-1</sup> ] | RR>=0.25 | >=0.25 RR>=1.0 RR>=10 |      |                    | RR>=1.0 | RR>=10 |
| Samples              | 6958     | 2919                  | 29   | 1736               | 594     | 26     |
| POD                  | 0.60     | 0.61                  | 0.22 | 0.39               | 0.31    | 0.29   |
| FAR                  | 0.45     | 0.56                  | 0.62 | 0.43               | 0.54    | 0.85   |
| CSI                  | 0.40     | 0.34                  | 0.16 | 0.30               | 0.23    | 0.11   |

Table 28 Results of the categorical statistic of the validation for whole June 2010

The contingency tables (next two figures) for both kinds of validation data show that only in the lowest class (except for validation with radar data for whole June) more than 50% of H02 data fall in the same class. The results are worse than for H01.

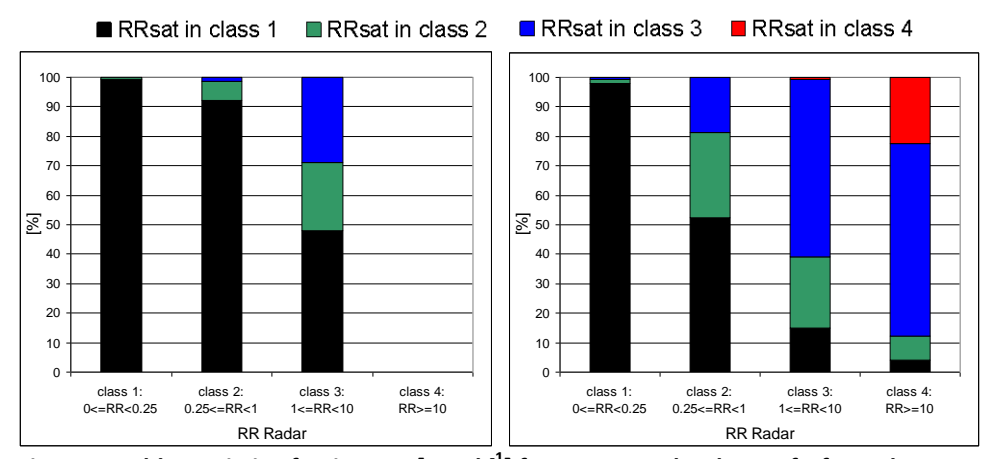


Figure 65 Contingency table statistic of Rain Rate [mm h<sup>-1</sup>] for H02 vs. radar data Left: for 3rd June 2010, Right: for whole June 2010

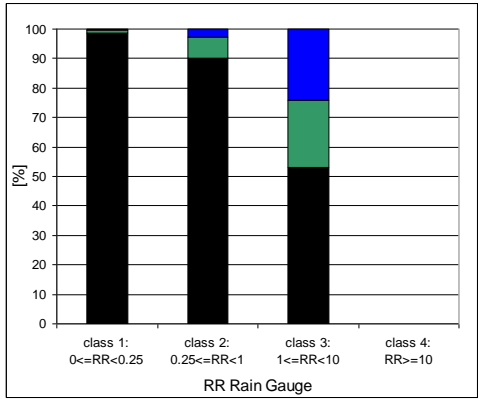


(Product H02 - PR-OBS-2)

Doc.No: SAF/HSAF/PVR-02/1.1 Issue/Revision Index: 1.1

Date: 30/09/2011

Page: 93/177



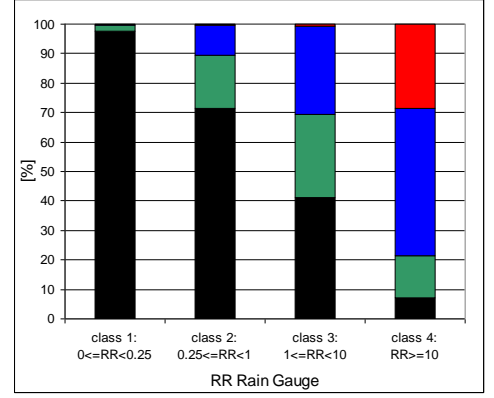


Figure 66 Contingency table statistic of rain rate [mm h<sup>-1</sup>] for H02 vs. rain gauge data. Left: for 3rd June 2010; Right: for whole June 2010

Results of the continuous statistic (next table) show negative Mean Error (ME) in both periods with both kind of ground data in the first class, which means, that H-SAF product underestimates all kind of precipitation amounts. For SD of 0.48 for radar data is the best, analogue to the results for POD (see above). For detection of precipitation RR>=0.25 mmh<sup>-1</sup> there are nearly the same results for both kind of ground data and for both periods, which means the chosen period is representative for June 2010. Standard deviation (SD) with 1.51 mmh<sup>-1</sup> for this class is the highest for validation with RADOLAN for 3<sup>rd</sup> June, nevertheless the correlation coefficient (CC) with 0.62 is the best, analogue to the results for POD (see above).

The better results for CC and RMSE in comparison with that for H01 validation are due to smaller number of samples.

| RR[mmh <sup>-1</sup> ] | 3 <sup>rd</sup> June 20 | 010     | June 201   | June 2010 |            | 3 <sup>rd</sup> June 2010 |            | June 2010 |  |
|------------------------|-------------------------|---------|------------|-----------|------------|---------------------------|------------|-----------|--|
|                        | rain gauge              | radar   | rain gauge | radar     | rain gauge | radar                     | rain gauge | radar     |  |
|                        |                         | 0.25 <= | RR < 1     |           |            | RR >=                     | 0.25       |           |  |
| ME                     | -0.45                   | -0.45   | -0.15      | 0.13      | -1.26      | -1.38                     | -0.55      | -0.11     |  |
| SD                     | 0.54                    | 0.48    | 1.05       | 0.96      | 1.36       | 1.51                      | 1.84       | 1.66      |  |
| MAE                    | 0.57                    | 0.53    | 0.58       | 0.55      | 1.38       | 1.46                      | 1.02       | 0.94      |  |
| MB                     | 0.19                    | 0.15    | 0.71       | 1.28      | 0.27       | 0.28                      | 0.52       | 0.91      |  |
| CC                     | 0.11                    | -0.11   | 0.14       | 0.29      | 0.61       | 0.62                      | 0.32       | 0.50      |  |
| RMSE                   | 0.70                    | 0.65    | 1.06       | 0.97      | 1.85       | 2.05                      | 1.92       | 1.66      |  |
|                        |                         | 1 <= R  | R < 10     |           |            | RR >                      | ·= 10      |           |  |
| ME                     | -2.13                   | -2.33   | -1.19      | -0.47     | -          | -                         | -10.20     | -6.43     |  |
| SD                     | 1.44                    | 1.60    | 1.96       | 2.24      | -          | -                         | 10.48      | 4.53      |  |
| MAE                    | 2.26                    | 2.41    | 1.71       | 1.63      | -          | -                         | 11.66      | 7.11      |  |
| MB                     | 0.29                    | 0.30    | 0.46       | 0.81      | -          | -                         | 0.35       | 0.49      |  |
| СС                     | 0.59                    | 0.56    | 0.22       | 0.25      | -          | -                         | -0.21      | 0.34      |  |
| RMSE                   | 2.57                    | 2.83    | 2.30       | 2.29      | -          | -                         | 14.62      | 7.87      |  |

**Table 29 Continuous statistic** 

### Conclusions



(Product H02 - PR-OBS-2)

Doc.No: SAF/HSAF/PVR-02/1.1 Issue/Revision Index: 1.1

Date: 30/09/2011 Page: 94/177

The results for H02 were worse than for H01. Compared with the case study for August the results were worse. All the quantitative precipitation amounts were underestimated.

### 5.3.3 Case study: December 5<sup>th</sup> /6<sup>th</sup>, 2010 (River Rhine catchment)

### **Description**

Intense rains on 5<sup>th</sup> / 6<sup>th</sup> December 2010 lasting over 72 hours fell along an air mass boundary, lying across France and Germany. It was a result of subtropical air from south west and polar cold air over Central Europe, moving forward to south. First precipitation as snow and rain were observed on 5<sup>th</sup> in relation to the cyclone "Liane" in northern parts of Germany. On the evening the precipitation deflected to the south of Germany. In higher regions of the river Rhine they fell as snow. In the night to 6<sup>th</sup> December in south of river Danube the snow changed to rain.<sup>7</sup>

Over a period of 4 days precipitation sum reached 100 mm. See next figures.

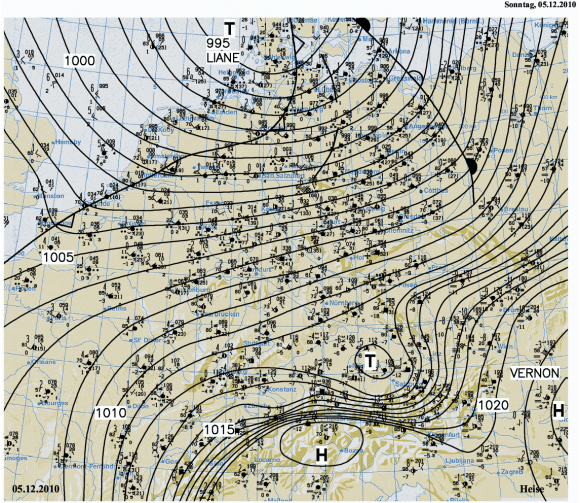


Figure 67 Synopsis for Central Europe for 05th December 2010 (FU Berlin, http://wkserv.met.fu-berlin.de)

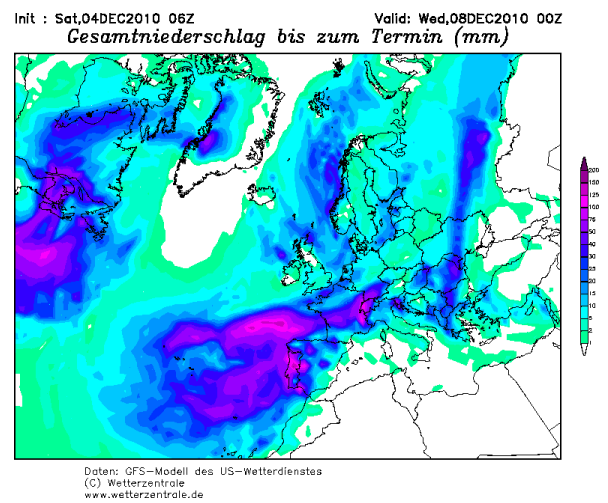


Figure 68 96h totals of precipitation

7

<sup>&</sup>lt;sup>7</sup> Der Wetterservice für NRW und Deutschland, Rückblick Starkniederschläge - Hochwasser - West-, Mitteleuropa 05.12. - 09.12.2010



(Product H02 - PR-OBS-2)

Doc.No: SAF/HSAF/PVR-02/1.1 Issue/Revision Index: 1.1

Date: 30/09/2011 Page: 95/177

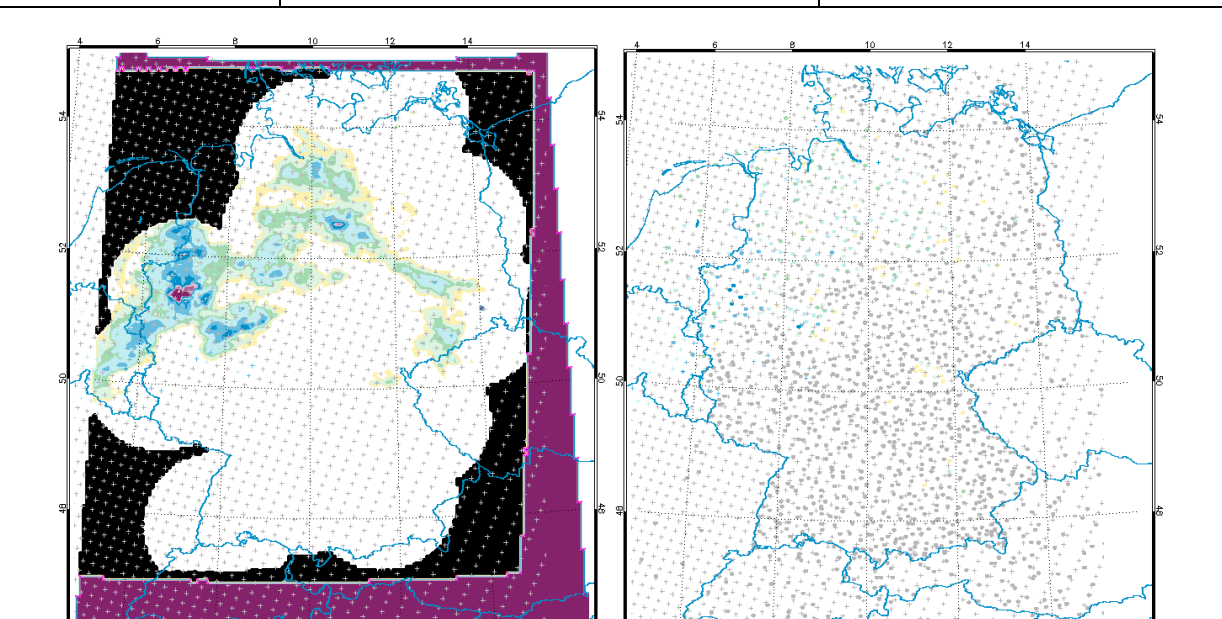


Figure 69 Hourly precipitation sum [mm] for H02 satellite data (crosses, time stamp 2010-12-05 02:29 UTC) and for RADOLAN-RW (left, filled raster, 2010-12-05 02:50 UTC) and station data (right, dots 2010-12-05 03:00 UTC)

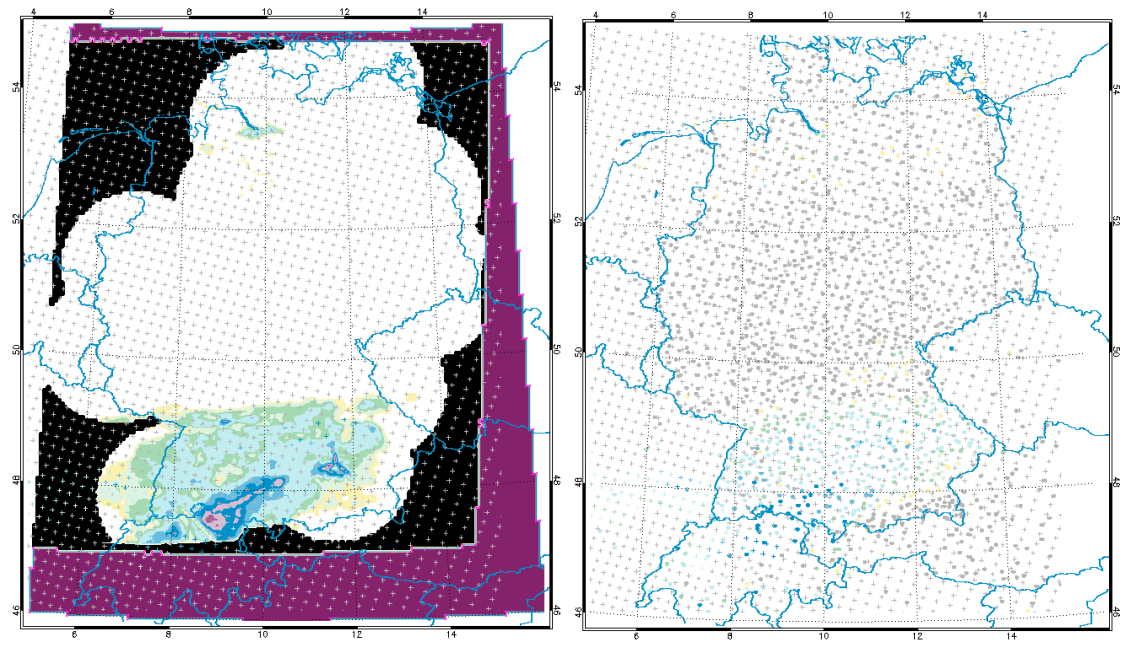


Figure 70 Hourly precipitation sum [mm] for H02 satellite data (crosses, time stamp 2010-12-06 02:18 UTC) and for RADOLAN-RW (left, filled raster, 2010-12-06 02:50 UTC) and station data (right, dots 2010-12-06 03:00 UTC)

### Data used

H02 data for Bavaria in the given period were available for 5<sup>th</sup> December, 1:23, 2:29, 11:51, 12:20 and 12:56 UTC and for 6<sup>th</sup> December, 2:18, 12:09 and 13:50 UTC. Only these data are analysed in this case study.

### Comparison

A first look to the results (previous figures) shows, that rain rates detected by satellite product are in the same two areas of Germany as those indicated by the ground data.



(Product H02 - PR-OBS-2)

Doc.No: SAF/HSAF/PVR-02/1.1 Issue/Revision Index: 1.1

Date: 30/09/2011

Page: 96/177

### Statistical score

In the next two tables the results of the categorical statistic of the validation with both radar and rain gauge data are listed. The results for validation with radar data for 5/6<sup>th</sup> December are worse than for the whole month December: Probability Of Detection of precipitation (RR>=0.25 mmh<sup>-1</sup>) was 0.16 with higher False Alarm Rate of 0.71 and Critical Success Index is 0.11, more worse than summer results.

| 5/6 December<br>2010 | Н        | 02 vs. radar |        | H02      | vs. rain gaug | ge     |
|----------------------|----------|--------------|--------|----------|---------------|--------|
| [mmh <sup>-1</sup> ] | RR>=0.25 | RR>=1.0      | RR>=10 | RR>=0.25 | RR>=1.0       | RR>=10 |
| Samples              | 792      | 504          | 0      | 168      | 108           | 0      |
| POD                  | 0.16     | 0.07         | -      | 0.11     | 0.04          | ı      |
| FAR                  | 0.71     | 0.96         | -      | 0.79     | 0.96          | -      |
| CSI                  | 0.11     | 0.03         | -      | 0.08     | 0.02          | -      |

Table 30 Results of the categorical statistic of the validation for 5/6th December 2010

| December 2010        | H02 vs. radar |         |        | H02 vs. rain gauge |         |        |  |
|----------------------|---------------|---------|--------|--------------------|---------|--------|--|
| [mmh <sup>-1</sup> ] | RR>=0.25      | RR>=1.0 | RR>=10 | RR>=0.25           | RR>=1.0 | RR>=10 |  |
| Samples              | 13082         | 3125    | 4      | 610                | 311     | 1      |  |
| POD                  | 0.49          | 0.23    | -      | 0.08               | 0.09    | 0.00   |  |
| FAR                  | 0.88          | 0.86    | 1.00   | 0.46               | 0.71    | 1.00   |  |
| CSI                  | 0.11          | 0.09    | 0.00   | 0.08               | 0.07    | 0.00   |  |

Table 31 Results of the categorical statistic of the validation for whole December 2010

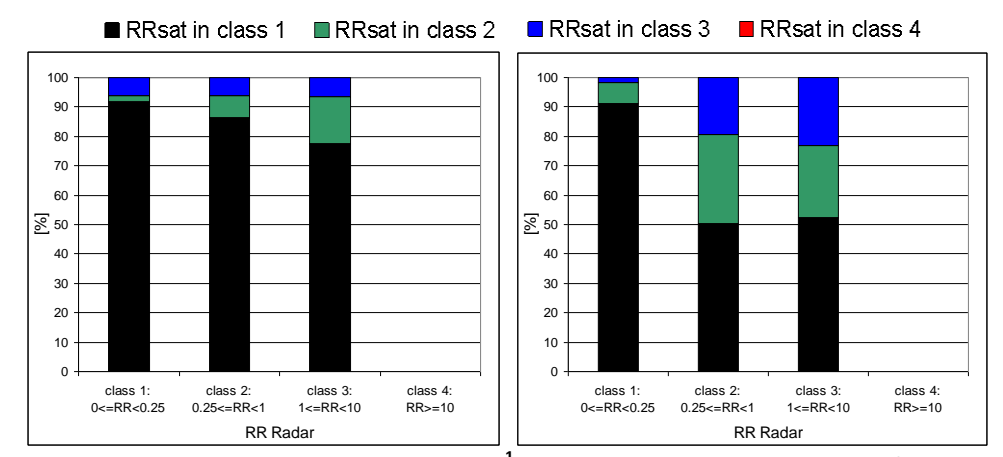


Figure 71 Contingency table statistic of Rain Rate [mm h<sup>-1</sup>] for H02 vs. radar data. Left: for 5/6th December, Right: for whole December 2010

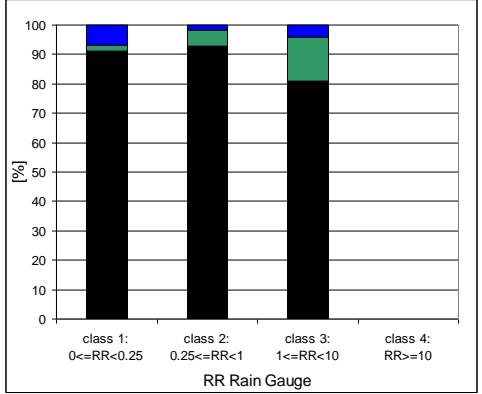


(Product H02 - PR-OBS-2)

Doc.No: SAF/HSAF/PVR-02/1.1 Issue/Revision Index: 1.1

Date: 30/09/2011

Page: 97/177



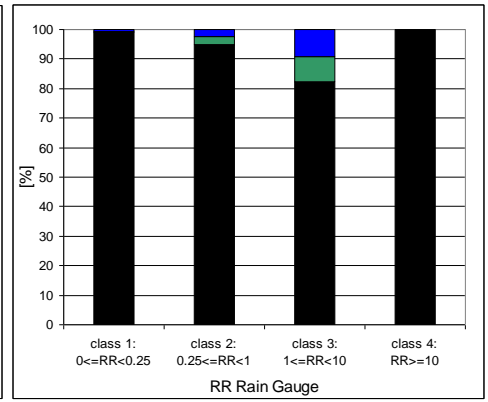


Figure 72 Contingency table statistic of rain rate [mm h<sup>-1</sup>] for H02 vs. rain gauge data. Left: for 5/6th December; Right: for whole December 2010

Results of the continuous statistic (next table) show negative Mean Error (ME) in the period 5/6<sup>th</sup> December with both kind of ground data in all classes, which means, that H-SAF product underestimated precipitation amounts. Standard deviation (SD) with 0.64 mmh<sup>-1</sup> for the class RR>=0.25 mmh<sup>-1</sup> is the highest for validation with radar data for 5/6<sup>th</sup> December, the correlation coefficient (CC) with mostly less than 0.2 is more worse than for results in summer, analogue to the results for POD (see above).

| RR[mmh <sup>-1</sup> ] | 5/6 December 2010 Decemb |         | er 2010    | r 2010 5/6 Decem |            | per 2010 December 2 |            |       |
|------------------------|--------------------------|---------|------------|------------------|------------|---------------------|------------|-------|
|                        | rain<br>gauge            | radar   | rain gauge | e radar          | rain gauge | radar               | rain gauge | radar |
|                        |                          | 0.25 <= | RR < 1     |                  | RR >= 0.25 |                     |            |       |
| ME                     | -0.49                    | -0.40   | -0.46      | -0.09            | -0.70      | -0.58               | -0.70      | -0.77 |
| SD                     | 0.28                     | 0.49    | 0.33       | 0.67             | 0.49       | 0.64                | 0.89       | 1.12  |
| MAE                    | 0.53                     | 0.56    | 0.52       | 0.53             | 0.73       | 0.71                | 0.77       | 1.07  |
| MB                     | 0.10                     | 0.27    | 0.11       | 0.86             | 0.11       | 0.21                | 0.12       | 0.42  |
| СС                     | 0.19                     | -0.03   | 0.12       | 0.04             | 0.22       | 0.03                | 0.14       | 0.16  |
| RMSE                   | 0.57                     | 0.63    | 0.57       | 0.67             | 0.85       | 0.86                | 1.14       | 1.36  |
|                        | 1 <= RR < 10             |         |            | RR >= 10         |            |                     |            |       |
| ME                     | -1.19                    | -1.26   | -1.39      | -1.33            | -          | ı                   | -26.25     | -     |
| SD                     | 0.54                     | 0.68    | 0.97       | 1.10             | -          | -                   | 1.55       | -     |
| MAE                    | 1.21                     | 1.30    | 1.47       | 1.50             | -          | -                   | 26.25      | -     |
| MB                     | 0.11                     | 0.14    | 0.14       | 0.31             | -          | -                   | 0.00       | -     |
| CC                     | 0.16                     | 0.03    | 0.08       | 0.19             | -          | -                   | -          | -     |
| RMSE                   | 1.31                     | 1.43    | 1.69       | 1.73             | -          | -                   | 26.30      | -     |

Table 32 Continuous statistic

### Conclusions

The results for H02 were worse than for H01: the probability of detection was less, the false alarm rate nearly same (higher than POD). All the quantitative precipitation amounts were underestimated.



(Product H02 - PR-OBS-2)

Doc.No: SAF/HSAF/PVR-02/1.1 Issue/Revision Index: 1.1

Date: 30/09/2011 Page: 98/177

### 5.4 Case study analysis in Hungary (OMSZ)

### 5.4.1 Case study: July 18<sup>th</sup>, 2010

### **Description**

At Iceland a cyclone multiple center derives the weather of Europe. Along the front lot of clouds with rain develope, thunderstorms are also observed.

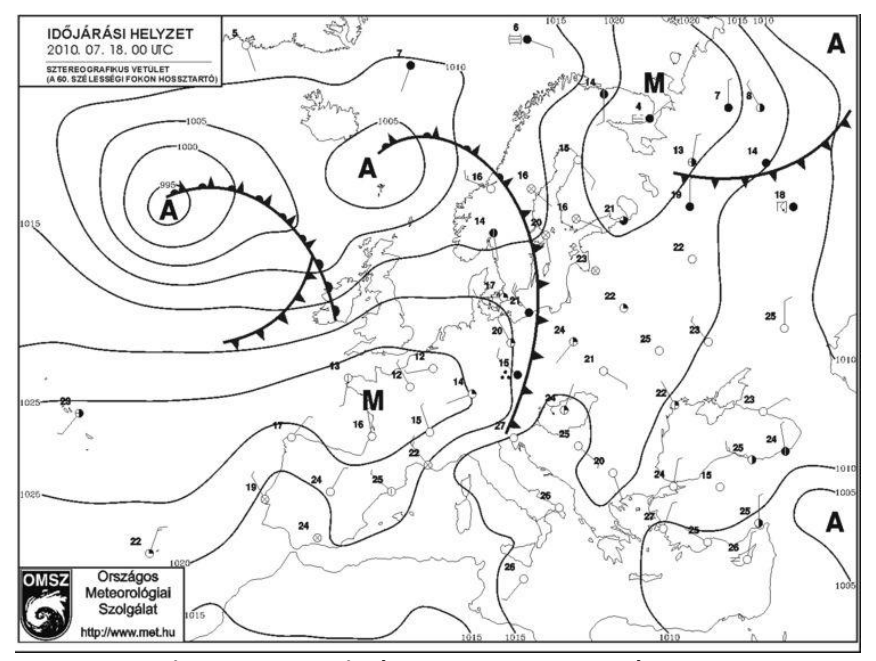
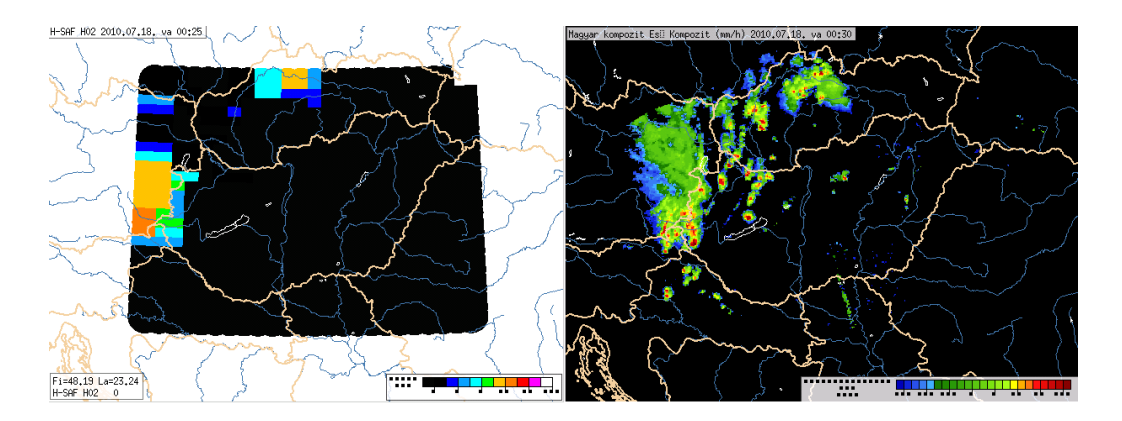


Figure 73 Synoptic chart at 00 UTC on 18 July 2010

### Data used





(Product H02 – PR-OBS-2)

Doc.No: SAF/HSAF/PVR-02/1.1 Issue/Revision Index: 1.1

Date: 30/09/2011

Page: 99/177

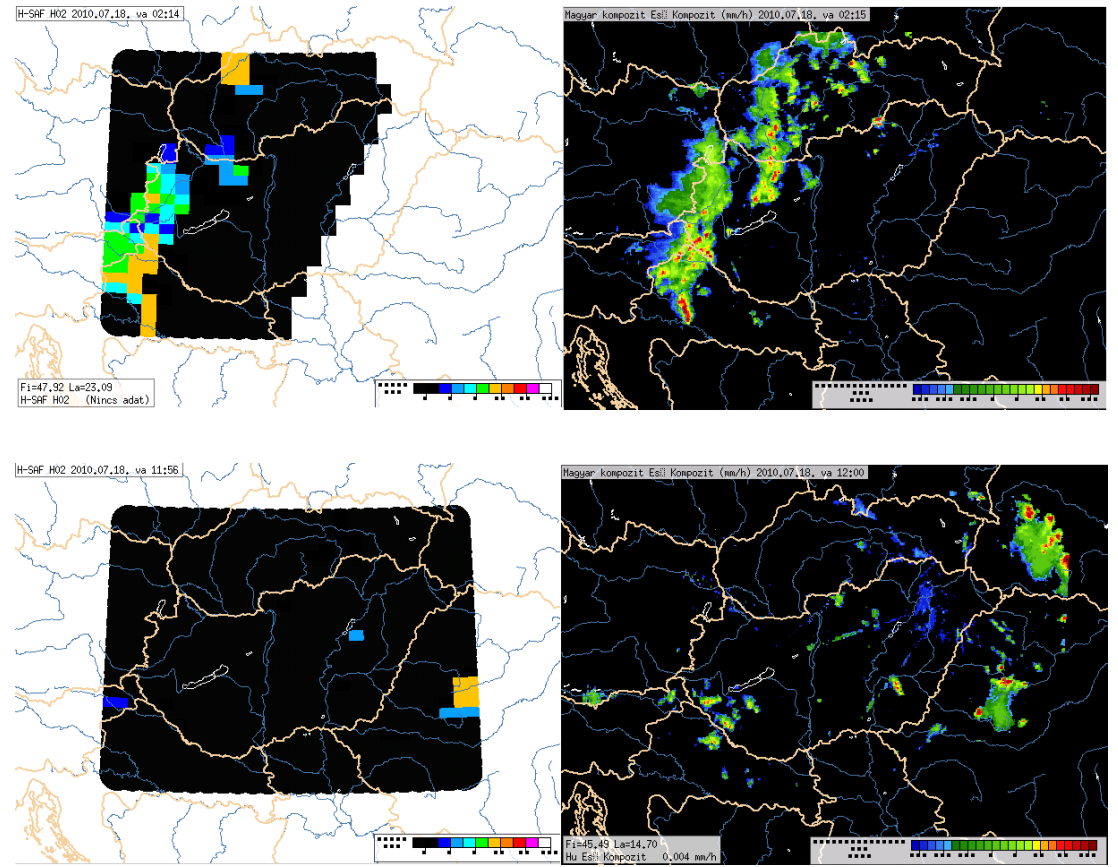


Figure 74 H02 product (left panel), Precipitation rate from the Hungarian radar network at its original resolution (right panel) at 00:30 UTC, at 2:15 UTC and at 12 UTC

### Comparison

In this cold front weather situation during the whole day HO2 did not detected the middle size thunderstorms.

### Conclusions

The H02 in most cases well detects the precipitation area, but the middle size thunderstorms were not detected. Improvement of the H02 spatial resolution would help the detection.

### 5.4.2 Case study: September 2010

### Description

A cyclone over Mediterranean causes precipitation in Central and South Europe. Lot of precipitation was measured mainly in the central part in Hungary.



(Product H02 - PR-OBS-2)

Doc.No: SAF/HSAF/PVR-02/1.1 Issue/Revision Index: 1.1

Date: 30/09/2011 Page: 100/177

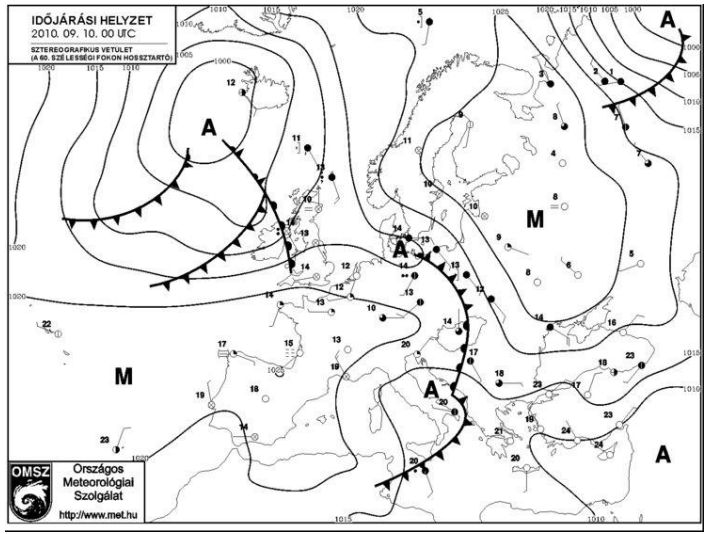


Figure 75 Synoptic chart at 00 UTC on 10 September 2010

### Data used

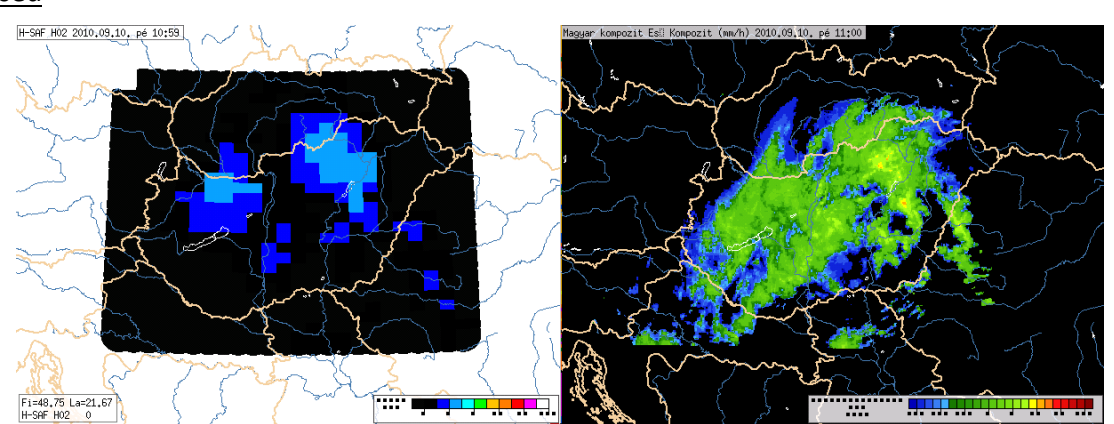


Figure 76 Precipitation rate from the Hungarian radar network at its original resolution at 11 UTC (right panel), H02 product at 11 UTC (left panel)

### Comparison

H02 well detected the precipitation area over the country. H02 derives lower values than the radar measured.

### **Conclusions**

The H02 well detects the precipitation area, but it underestimates the precipitation values.

### 5.5 Case study analysis in Italy (Uni Fe)

### 5.5.1 Case study: July 06<sup>th</sup>, 2010

### **Description**

On July 06 the Azores anticyclone avyected very warm and moist air on the Tyrrhenian coasts, where a weak trough induced cyclonic circulation and instability in the early morning. After 10:00 UTC deep convections initiated in the Po Valley and in central Italy, along the Apennines chain, causing waterspouts along the northern Adriatic coasts, hail falls and supercells storms in Central Italy.

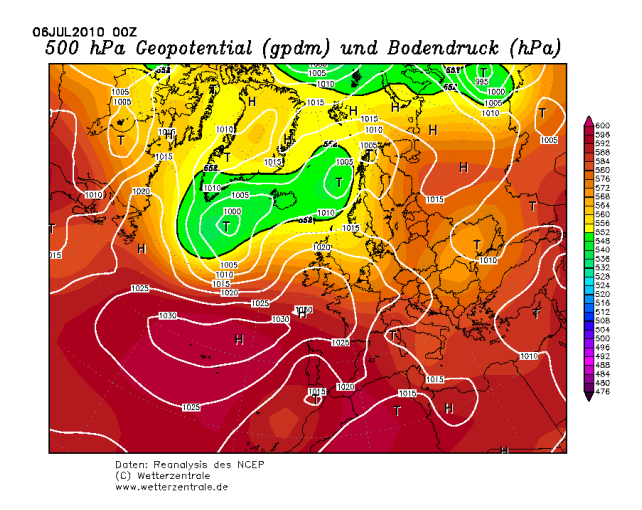


(Product H02 - PR-OBS-2)

Doc.No: SAF/HSAF/PVR-02/1.1 Issue/Revision Index: 1.1

Date: 30/09/2011

Page: 101/177



SEVIRI HR-VIS image at 12:00 on July 06 shows a well developed convective cluster over central Italy, while small-scale, scattered convection is present along the Apennines chain. Some of these small systems are expected to grow in the following hours.



#### Data used

Reference data: Italian hourly raingauges network (provided by DPC)

Ancillary data (used for case analysis):

SEVIRI images (courtesy of University of Dundee – NEODAAS)

Weather charts (courtesy of Wetterzentrale, NCEP and METOFFICE).

### Comparison

This deep convective case has been observed by two different AMSU sensors on board NOAA NP and NOAA NN with a time lag of only 10 minutes. In the figure below the two estimates are presented (top panel) with the hourly cumulated raingauge map at 13:00 UTC (please note: zero rainrate gauges are not shown).

The rain rate patterns in the two estimates are rather similar, but some significant variations in the shape of rain areas and in the rain rate values can be due to the time lag between the images (10 minutes), and to a different viewing angle of the two sensors. The NOAA NP estimate shows higher precipitation rates (close to the end of the scale: 20 mm h<sup>-1</sup>), while the raingauge cumulated maximum value is 34 mm h<sup>-1</sup>. The considered statistical parameters indicate a best matching for the NOAA-NN



(Product H02 - PR-OBS-2)

Doc.No: SAF/HSAF/PVR-02/1.1 Issue/Revision Index: 1.1

Date: 30/09/2011 Page: 102/177

estimate, with the following values: ETS=31 (27), FAR=43 (44), POD=49 (42), HSS=37 (29), where values within brackets refer to the NOAA-NP overpass. Overestimation occurs, for both estimates, around the large convective cells, while underestimation takes place mainly in case of very small structure, not detected by h02 because the rather large IFOV.

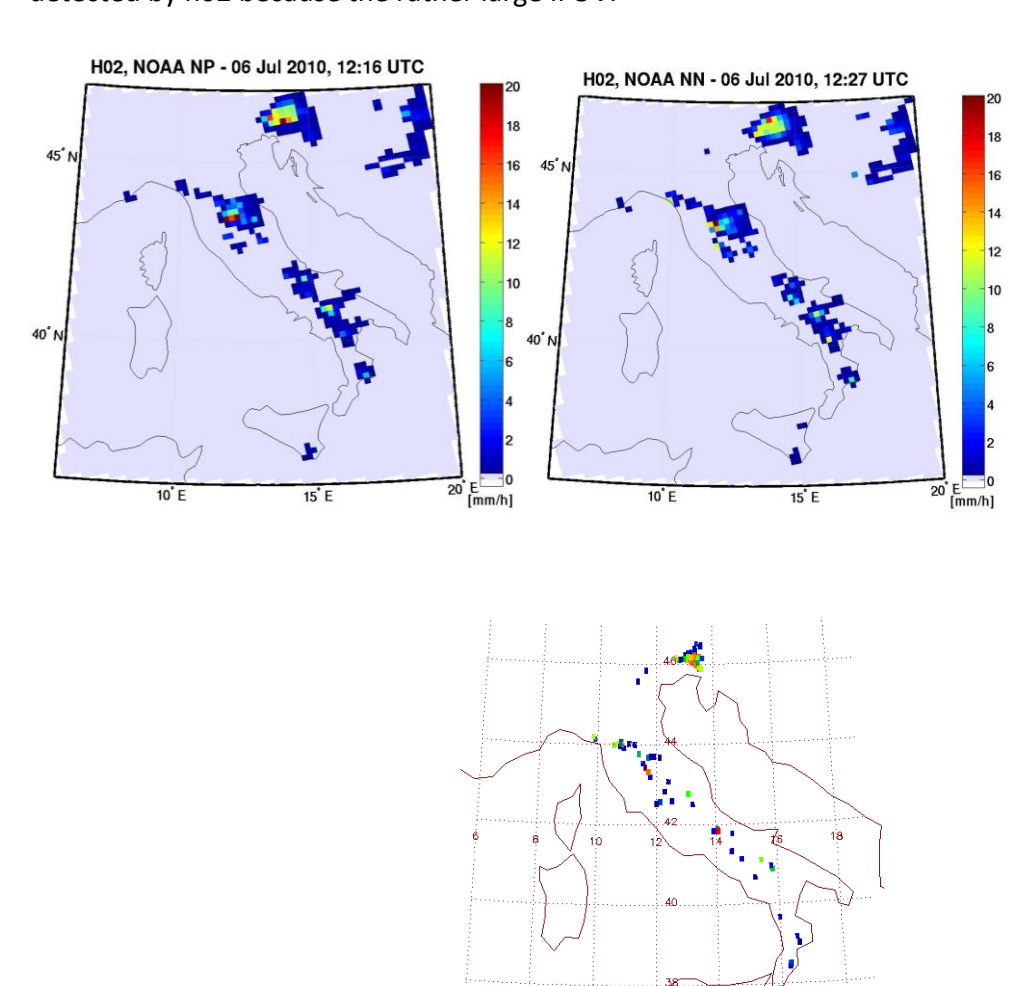


Figure 77 H02 precipitation map at 12:16 UTC (top-left), at 12:27 (top-right) and raingauges hourly precipitation cumulated at 13:00 UTC (bottom panel) of 06 July 2010

Please note different colour scales; zero rainrate gauges are not shown.

### **Conclusions**

For this convective case the performances of h02 are satisfactory, pointing out that no parallax correction is applied and this could be particularly effective in case of small convective structures. This case is also useful to understand the inadequacy of hourly gauge measurements in validating instantaneous satellite snapshots, as in case of h02. As a matter of fact, the variability of the precipitation field, well described by the two overpasses shown above, cannot be caught by hourly integrals provided by the raingauges, especially in case of convective precipitation. The skill score



(Product H02 - PR-OBS-2)

Doc.No: SAF/HSAF/PVR-02/1.1 Issue/Revision Index: 1.1

Date: 30/09/2011 Page: 103/177

values reported above indicate rather different performances between the two satellite overpasses: HSS increases from 29 to 37 in 10 minutes.

It seems the main problem of this technique for convective precipitation is related to the relatively large IFOV of the AMSU data, that prevent the correct retrieval of small (sub-IFOV) precipitation structures. It has also to be mentioned that this case study does not show differences between land and sea algorithms, as it was remarked in the 2009 case study.

### 5.6 Case study analysis in Poland (IMWM)

### 5.6.1 Case study: August 15<sup>th</sup>, 2010

### Description

Significant cloud layer reaching over Lower Silesia region with its upper constituent belongs to developing low pressure centre. That structure is a part of bigger low pressure centre over France and tends to move over Germany to Poland. Stripe of clouds extending from Tunis, through central Italy, Adriatic Sea to Austria is a cold front of Atlantic air which is going to reach Poland on Monday 16<sup>th</sup> of August when bay of low pressure over Germany moves over Poland. Mentioned above bay of low pressure extends further over Balkans with significant wind convergence stimulating convection updrafts with large-scale moves. Moreover the forecast dated on 0000 UTC shows very turbulent night because of development of low pressure centre over Poland.

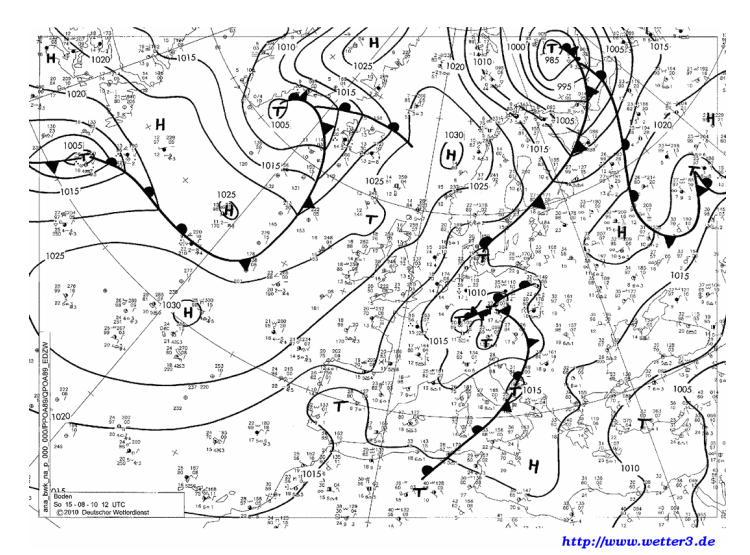


Figure 78 Synoptic chart at 1200 UTC on 15th of August 2010

Convective storms where observed over the country on that day. The precipitation was accompanied by lightning activity. On the next figure, the lightning activity map for half an hour time spam (1145 UTC -1215 UTC) is presented. The map was constructed on the base of data from Polish Lighting Detection System, PERUN.



(Product H02 - PR-OBS-2)

Doc.No: SAF/HSAF/PVR-02/1.1 Issue/Revision Index: 1.1

Date: 30/09/2011 Page: 104/177

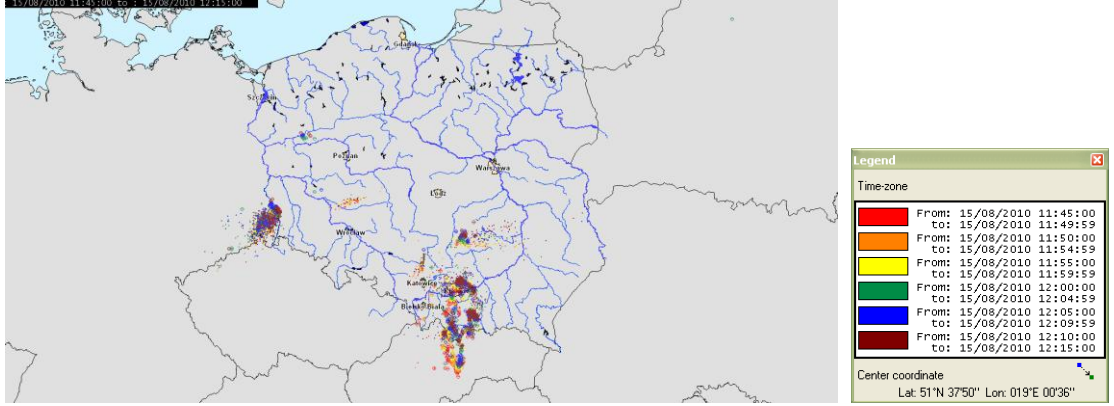


Figure 79 Total lighting map of Poland showing electrical activity between 1145 and 1215 UTC on 15th of August 2010

#### **Comparison**

On the Figure 80 the H02 product is visualized for the noon overpass. For comparison, the distribution of 10 minute precipitation obtained from RG data measured at closest to the given time slot is presented. The RG derived precipitation map was prepared using Near Neighbor method.

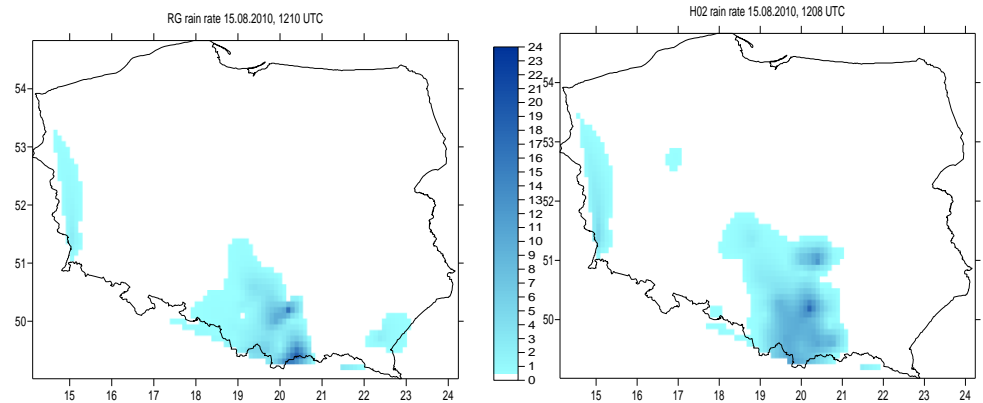


Figure 80 H02 at 1208 UTC on the 15th of August 2010 (right panel) and 10 minute precipitation interpolated from RG data from 1210 UTC (left panel)

On both maps, the precipitating areas reveal the lightning activity seen on the Figure 79, however, the H02 overestimated the precipitation area. This tendency is clearly seen in the Central Poland when H02 reports rainfall, while the ground data doesn't (Figure 80). On the other hand, this precipitating area seen on the satellite derived rainfall map in the Central Poland (Figure 80, right panel) corresponds to lightning activity observed in this region (Figure 79). Fact that this rainfall is not present on the RG map may be explained by the ground network density.

One maximum out of two was properly recognized by satellite product while instead of the second one, the fuzzy area of increased rainfall was obtained (Figure 80).

### Statistical score

Further analysis was performed for all overpasses available for the 15<sup>th</sup> of August 2010. The ability of H02 product to recognize the precipitation was analyzed using dichotomous statistics parameters. The 0.25mm/h threshold was used to discriminate rain and no-rain cases. In the next table the values of Probability of Detection (POD), False Alarm Rate (FAR) and Critical Success Ratio (CSI) are presented.



(Product H02 - PR-OBS-2)

Doc.No: SAF/HSAF/PVR-02/1.1 Issue/Revision Index: 1.1

Date: 30/09/2011

Page: 105/177

| Parameter | Scores |
|-----------|--------|
| POD       | 0.83   |
| FAR       | 0.52   |
| CSI       | 0.44   |

Table 33 Results of the categorical statistics obtained for PR-OBS-1 on the base of all data available on the 15<sup>th</sup>
August 2010

Higher value of POD than the value of FAR indicate that the product ability to recognize the convective precipitation is quite good.

The quality of H02 in estimating the convective precipitation is presented on the next figure. The points on the scatter plot are mostly arranged above and along the diagonal, what indicates that H02 tends to overestimate the precipitation except for the very heavy ones.

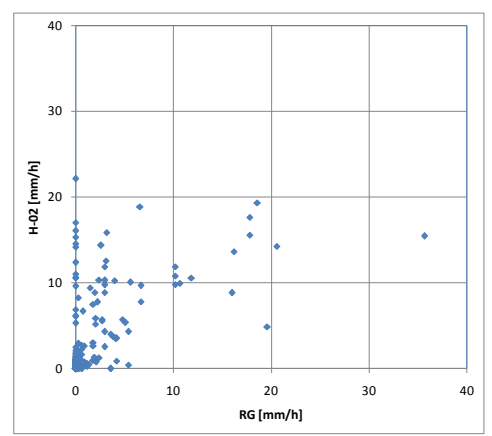


Figure 81 Scatter plot for measured (RG) and satellite derived (H-02) rain rate obtained for all H02 data on the 15<sup>th</sup> of August 2010

Finally, the analysis of rain classes was performed. The categories were selected in accordance with the common validation method. Next figure shows the percentage distribution of satellite derived precipitation categories within each precipitation class defined using ground measurements.

One can easily notice very good ability of H02 to recognize both, no-rain and heavy precipitation situations – respectively, more than 90% and 60% of ground cases was properly allocated by satellite product. The light precipitation is not properly recognized in most cases: it is either overestimated (26% of cases) or missed (36% of cases). When moderate is considered, the H02 quality is better: almost 60% of the observed precipitation in this class is properly recognized.



(Product H02 - PR-OBS-2)

Doc.No: SAF/HSAF/PVR-02/1.1 Issue/Revision Index: 1.1

Date: 30/09/2011 Page: 106/177

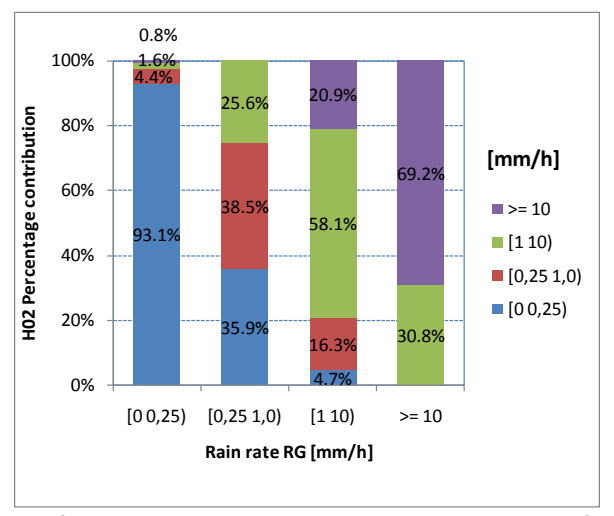


Figure 82 Percentage distribution of H02 precipitation classes in the rain classes defined using rain gauges (RG) data on the 15<sup>th</sup> of August 2010

### **Conclusions**

The analysis performed for situation with convective precipitation showed very good ability of H02 product in recognition of precipitation, especially moderate and heavy ones (rain rate > 10mm/h) while the light precipitation is either overestimated or missed.

The product tends to overestimate the precipitation areas and has some difficulties with proper recognition of rainfall maximum.

### 5.6.2 Case study: September 27<sup>th</sup>, 2010

#### Description

Low pressure centre left Hungary and heading through Slovak Republic entered Poland territory form South and is building up in the centre of the country. However the most rain productive clouds of that low will remain in the SW Poland even when the centre of the low pressure leave NE Poland. According to synoptic charts this low pressure centre will tend to deepen and build up due to feeding with cold air masses from over Barents Sea flowing between low over Scandinavia and above mentioned low pressure centre. This cold air will force up warm air masses. Condensing water vapor will stimulate clouds development and also emitting condensation energy supporting vorticity of the low pressure centre.



(Product H02 - PR-OBS-2)

Doc.No: SAF/HSAF/PVR-02/1.1 Issue/Revision Index: 1.1

Date: 30/09/2011

Page: 107/177

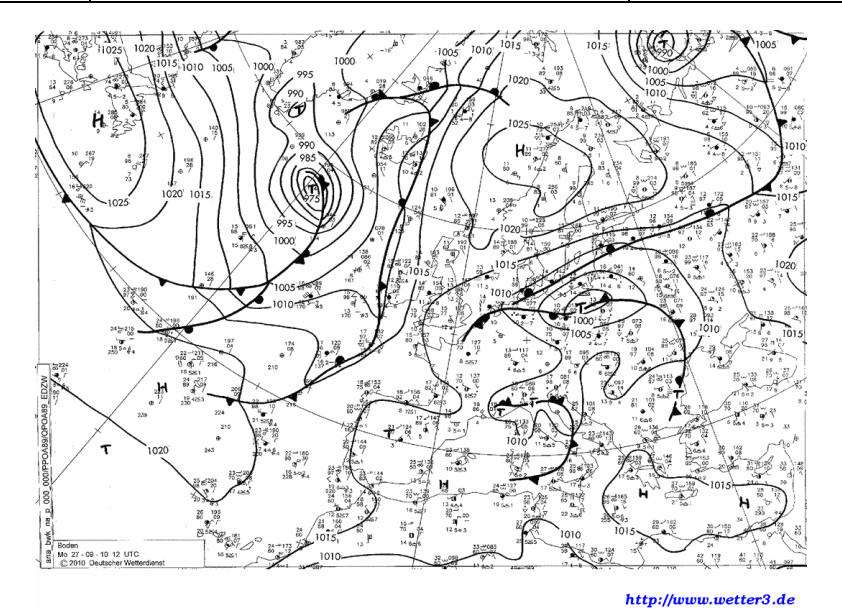


Figure 83 Synoptic chart at 1200 UTC on 27th of September 2010

### Comparison

On the next figure the HO2 product is visualized for the noon overpass. For comparison, the distributions of 10 minute precipitation obtained from RG data measured at closest to the given time slots are presented. The RG derived precipitation maps were prepared using Near Neighbor method.

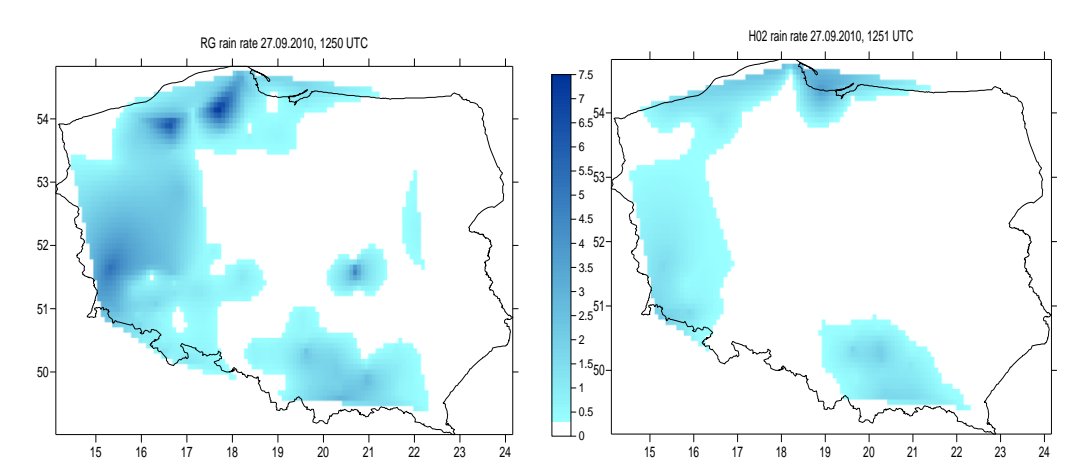


Figure 84 PR-OBS-1 at 1251 UTC on the 27<sup>th</sup> of September 2010 (right panel) and 10 minute precipitation interpolated from RG data from 1250 UTC (left panel)

On the both maps the precipitating area is located along with South, West and North Polish borderlines, however the its spatial distribution is underestimated by H02 product. Moreover, some rainfall observed in the Central Poland was not recognized by satellite product at all. The rainfall maxima measured by ground stations in western and northern Poland were missed by H02, what resulted in more homogenous precipitation distribution obtained for satellite product.

### Statistical score

Further analysis was performed for all overpasses available for the 27<sup>th</sup> of September 2010. The ability of PR-OBS-01 product to recognize the precipitation was analyzed using dichotomous statistics parameters. The 0.25mm/h threshold was used to discriminate rain and no-rain cases. In the next



(Product H02 - PR-OBS-2)

Doc.No: SAF/HSAF/PVR-02/1.1 Issue/Revision Index: 1.1

Date: 30/09/2011 Page: 108/177

table the values of Probability of Detection (POD), False Alarm Rate (FAR) and Critical Success Ratio (CSI) are presented.

| Parameter | Scores |
|-----------|--------|
| POD       | 0.52   |
| FAR       | 0.18   |
| CSI       | 0.47   |

Table 34 Results of the categorical statistics obtained for H02 on the base of all data available on the 27<sup>th</sup> September 2010

Reasonably high value of POD and low value of FAR indicate that the product ability to recognize the stratiform precipitation is rather good.

The quality of H02 in estimating the convective precipitation is presented on the next figure Most of the points on the scatter plot are located under and along with the diagonal what indicates that that H02 tends to underestimate the rain rate rarely exceeding the 4 mm/h value.

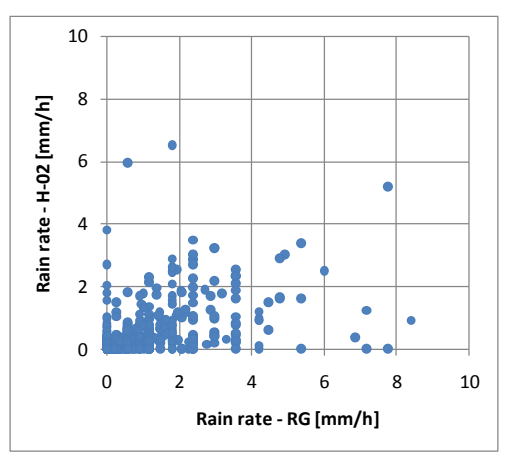


Figure 85 Scatter plot for measured (RG) and satellite derived (H-02) rain rate obtained for all H02 data on the 27<sup>th</sup> of September 2010

Finally, the analysis of rain classes was performed. The categories were selected in accordance with the common validation method. Next figure shows the percentage distribution of satellite derived precipitation categories within each precipitation class defined using ground measurements.

One can easily notice very good ability of H02 to recognize no-rain situations – more than 90% of ground cases was properly allocated by satellite product. The light precipitation is strongly underestimated – 68% of cases is allocated in the no-rain class. Better results were obtained for moderate precipitation: 40% of pixels in this class was properly recognized by H02, however, 34% of cases was overestimated and 27% was underestimated.



(Product H02 - PR-OBS-2)

Doc.No: SAF/HSAF/PVR-02/1.1 Issue/Revision Index: 1.1

Date: 30/09/2011 Page: 109/177

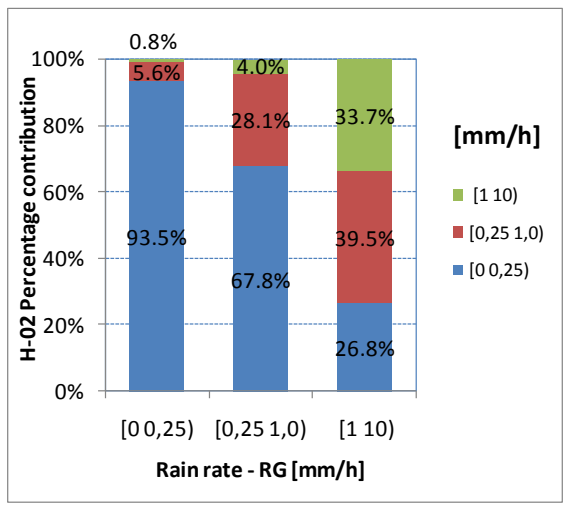


Figure 86 Percentage distribution of PR-OBS-1 precipitation classes in the rain classes defined using rain gauges (RG) data on the 27th of September 2010

### Conclusions

The analysis performed for situation with stratiform precipitation showed reasonably good ability of H02 product in recognition of precipitation, however the product tends to underestimate the precipitation areas and has some difficulties with proper recognition of rainfall maximum.

The stratiform rain rate is underestimated, especially for light precipitation. For the moderate rainfall, the underestimation is not so strong.

## 5.7 Case study analysis in Slovakia

## 5.7.1 Case study: August 15<sup>th</sup>, 2010

### Description

During the day, a cold front was moving over Slovakia territory towards North-East (next figure). The cold front was accompanied by thunderstorms and occasional torrential rainfall causing severe floods in some river catchments in the western half of Slovakia.

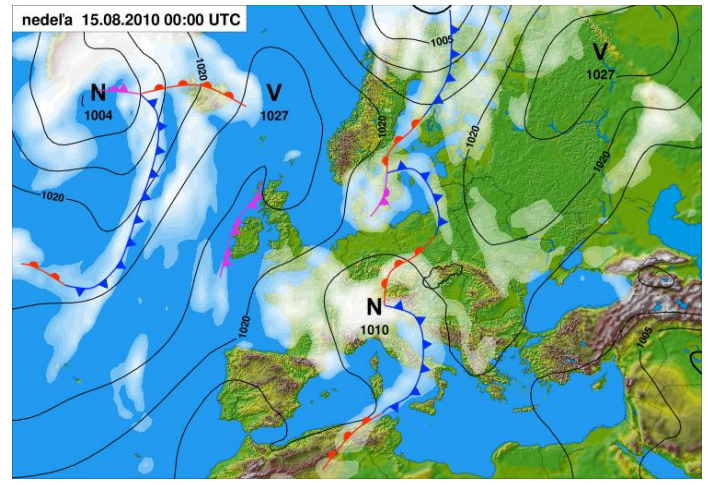


Figure 87 Synoptic situation on 15 August 2010 at 0:00 UTC

### Data used



(Product H02 – PR-OBS-2)

Doc.No: SAF/HSAF/PVR-02/1.1 Issue/Revision Index: 1.1

Date: 30/09/2011 Page: 110/177

The H02 v2.2 data from two temporally close satellite passages over the SHMU validation area on 15 August 2010 have been selected: the NOAA18 observation at 12:07 UTC (average observation time of the SHMU validation area) and the NOAA19 observation at 12:08 UTC.

As ground data the instantaneous precipitation field derived by the SHMU radar network is used. The closest coincident fields (5 min time frequency) to the satellite passages have been selected: from 12:05 UTC and 12:10 UTC.

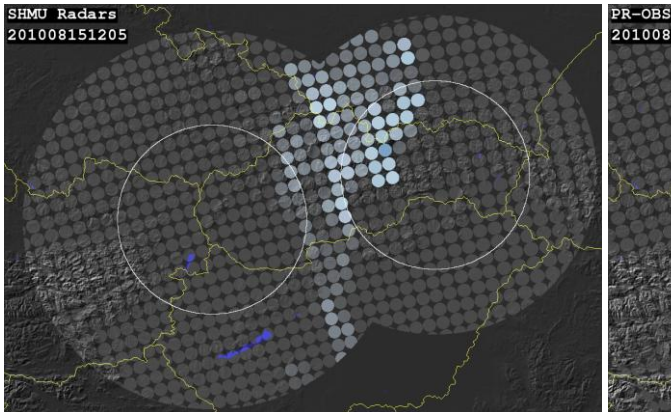
The radar composites used consist of data from two radars: one is situated at Maly Javornik and the second at Kojsovska hola. The rule of maximum value selection is applied in the composition. The original spatial resolution of the radar field is about 1 km but values upscaled into the satellite grid using the IFOV Gaussian filter are presented. For statistical scores computation only the data lying inside the 120 km rain effective range of both radars are considered.

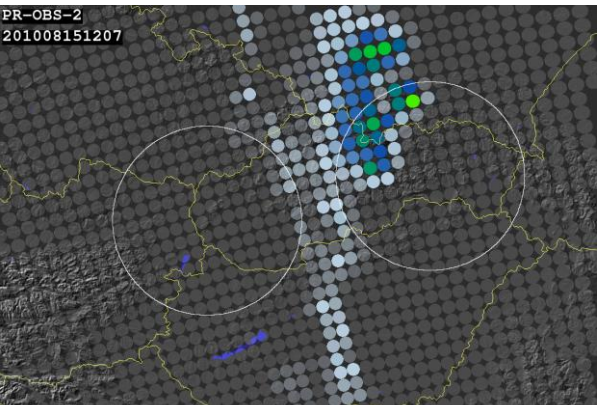
### Comparison

The H02 and upscaled radar precipitation fields for both satellite passages are presented in next figure. In both cases an overestimation of the precipitation by H02 compared to radars can be seen. This is obvious especially in case of higher precipitation intensities. It should be noted that lower radar intensities, especially near the Slovakia-Poland border, could be also caused by the radar beam blockage and/or attenuation in the precipitation.

For the passage of NOAA18 at 12:07 UTC (top row in the figure) the maximum value observed by radars is 7 mm/h while by H02 it is 22 mm/h. For the passage of NOAA19 at 12:08 UTC (second row in the figure) the corresponding maximum value is 3 mm/h and 20 mm/h, respectively. Spatial shift between the maxima in H02 and coincident radar field is about 65 km for the 12:07 UTC passage but only 16 km (1 satellite along-track sampling distance) in case of the 12:08 UTC passage.

Generally, there are slightly smaller differences between higher precipitation rates observed by H02 and radars for the 12:08 UTC passage. This could be a result of larger, closer to the swath edge, IFOVs that smooth more the extremes in precipitation fields. However, observation by different satellites and time lag between the compared fields could also be the reason.







(Product H02 - PR-OBS-2)

Doc.No: SAF/HSAF/PVR-02/1.1 Issue/Revision Index: 1.1

Date: 30/09/2011

Page: 111/177

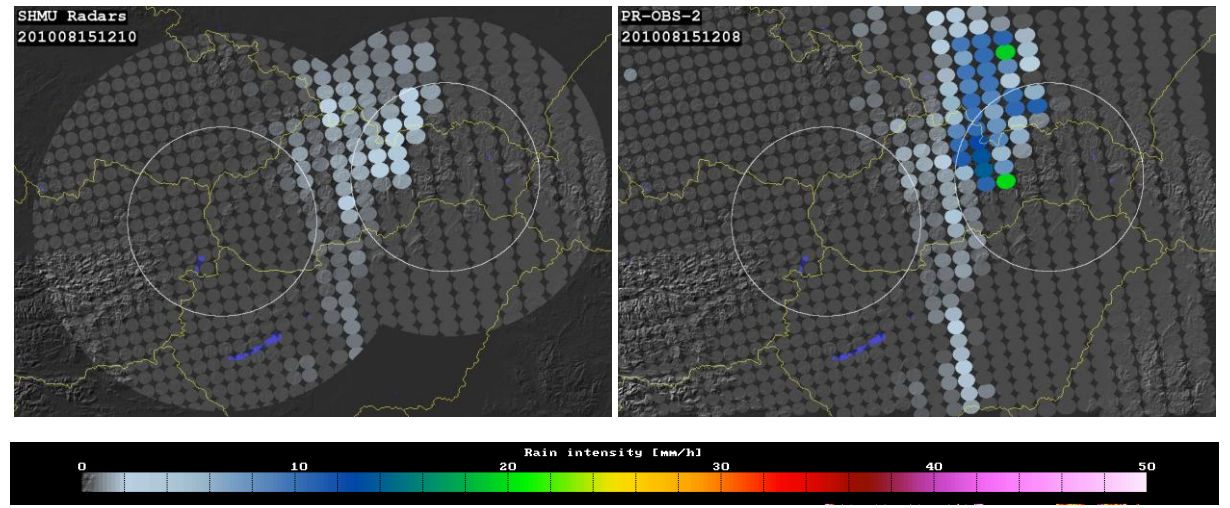


Figure 88 Instantaneous precipitation fields from 15 August 2010 observed by H02 product (left column) and SHMU radar network (right column) corresponding to NOAA18 passage at 12:07 UTC (top row) and NOAA19 passage at 12:08 UTC (second row)

The precipitation values are shown as satellite IFOVs projected over the radar composite domain. White contoured circles represent 120 km rain effective range of the radars inside which data are included in the statistical scores computation.

Despite the H02 overestimation a good spatial consistency between the H02 and radar precipitation fields can be observed. Even the patterns of light precipitation were localized by H02 quite well.

#### Scores evaluation

Statistical scores have been computed separately for each of the two satellite passages but also for common dataset from both passages. Totally 249 radar-satellite pairs from the 12:07 UTC passage and 190 pairs from the 12:08 UTC passage have been included in the computation. Results of the scores for continuous and dichotomous statistics for precipitation threshold of 0,25 mm/h are presented in the next two tables, respectively.

| Satellite passage             | 12:07 UTC<br>NOAA18 | 12:08 UTC<br>NOAA19 | Common |
|-------------------------------|---------------------|---------------------|--------|
| Number of satellite values    | 34                  | 25                  | 59     |
| Number of radar values        | 28                  | 22                  | 50     |
| Mean error (mm/h)             | 5.50                | 5.46                | 5.46   |
| Standard deviation (mm/h)     | 5.67                | 4.93                | 5.34   |
| Mean absolute error (mm/h)    | 5.64                | 5.48                | 5.57   |
| Multiplicative bias           | 3.52                | 4.41                | 3.84   |
| Correlation coefficient       | 0.63                | 0.39                | 0.56   |
| Root mead square error (mm/h) | 7.87                | 7.36                | 7.65   |
| RMSE%                         | 4.01                | 5.60                | 4.77   |

Table 35 Scores for continuous statistics for precipitation threshold of 0,25 mm/h

In agreement with visual comparison of precipitation fields, the scores of continuous statistics (Table 1) as Mean Error and Multiplicative bias exhibit overestimation of the H02 product in this case. The Multiplicative bias and URD-RMSE obtained for the 12:07 UTC passage are better than for the 12:08



(Product H02 – PR-OBS-2)

Doc.No: SAF/HSAF/PVR-02/1.1 Issue/Revision Index: 1.1

Date: 30/09/2011 Page: 112/177

UTC passage. This is in agreement with the observed better consistency of precipitation intensities in the first passage. However other scores such as Mean error do not confirm this observation.

The values of correlation coefficient are relatively high and reflect good spatial consistency of the compared fields. Better values were obtained again for the 12:07 UTC passage.

| Satellite passage | 12:07 UTC<br>NOAA18 | 12:08 UTC<br>NOAA19 | Common |
|-------------------|---------------------|---------------------|--------|
| POD               | 0.93                | 0.96                | 0.94   |
| FAR               | 0.24                | 0.16                | 0.20   |
| CSI               | 0.72                | 0.81                | 0.76   |

Table 36 Scores for dichotomous statistics for precipitation threshold of 0,25 mm/h

The POD (see Table 2) reaches values very close to 1 and the FAR values are on the other hand quite low. This also supports the observed good spatial match between the radar and HO2 fields.

### **Conclusions**

In this event of intense convective precipitation, the H02 product overestimated the precipitation as compared to radars, especially in case of higher precipitation rates. This is not in agreement with results of long-term statistics for August 2010 showing slight underestimation of H02.

The H02 overestimation was slightly lower in case of NOAA19 passage at 12:07 where the IFOVs were larger due to the longer distance from the satellite track compared to NOAA18 passage 1 min later. Thus heavy precipitation in horizontally small convective cells could have been more smoothed by the Gauss filter in the radar field. However, observation by different satellites or time lag between the compared fields could also be the reason of this discrepancy.

Despite the observed H02 overestimation the overall spatial consistency of the H02 and radar fields is satisfactory as confirmed by relatively good results of the correlation coefficient and very good scores of dichotomous statistics (see above).

## 5.8 Case study analysis in Turkey (ITU)

## 5.8.1 Case study: October 20<sup>th</sup>, 2010

#### Description

As it can be seen from next two figures, Turkey is in low pressure area and there are respectively warm and stationary fronts rain bands and precipitation in western part of Turkey on October 20 at 06:00 GMT and 12:00 GMT.

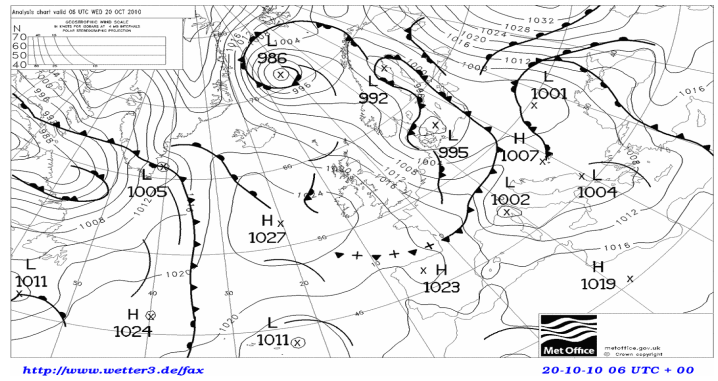


Figure 89 Atmospheric condition (20.10.2010; 06:00 GMT)



(Product H02 - PR-OBS-2)

Doc.No: SAF/HSAF/PVR-02/1.1 Issue/Revision Index: 1.1

Date: 30/09/2011

Page: 113/177

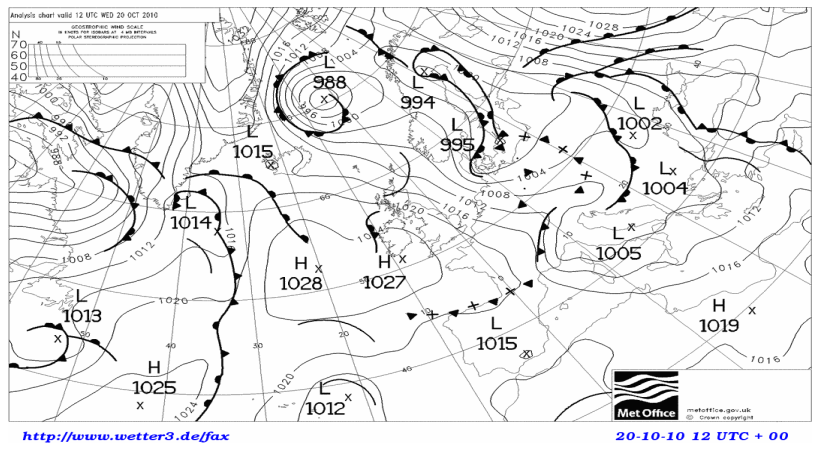


Figure 90 Atmospheric condition (20.10.2010; 12:00 GMT)

## Data used

In this case study, 193 rain gauges, which have specifications as explained in section 4.12, in western part of Turkey has been used. H02 product on October 20 at 10:44 GMT has been compared with gauge observations. Moreover, synoptic cards from UK MetOffice have been taken for understanding the meteorological situation.

### Comparison

Comparison of H02 product and rain gauge can be seen in next two figures. Values of H02 product are between 0.25 to 8.50 mm/h, but they vary from 0.25 to 4.00 mm/h for gauge. Main patterns of product and gauge are similar except western part of product pattern in the following figure.

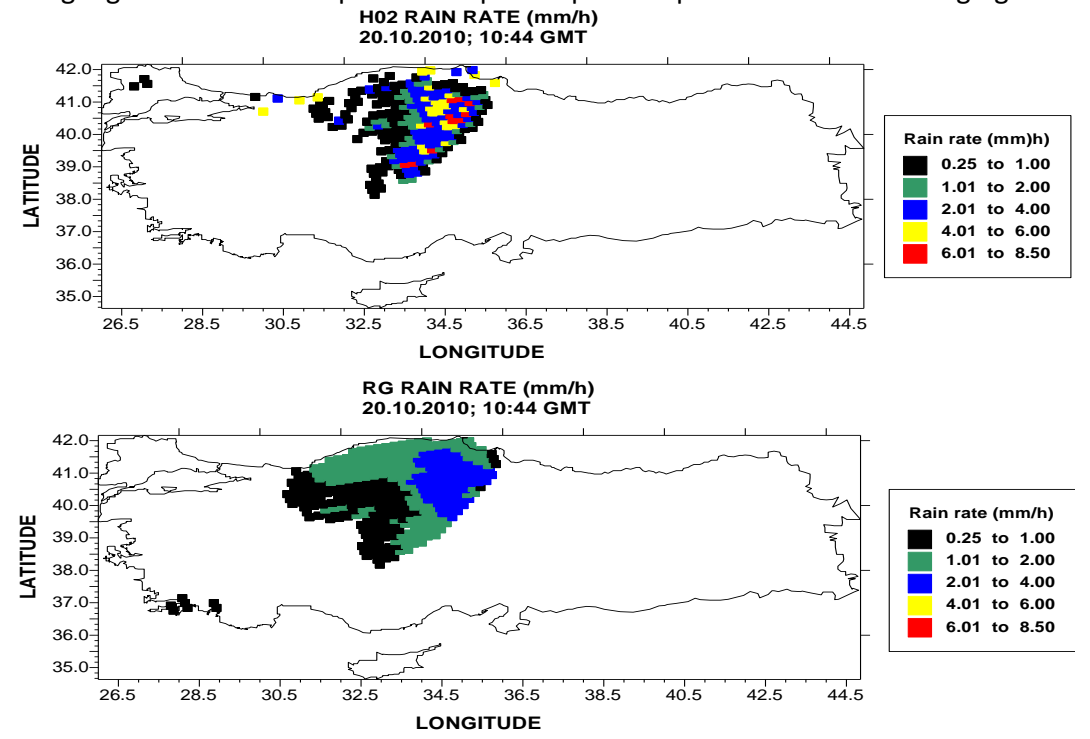


Figure 91 Comparison of H02 product and rain gauge



(Product H02 – PR-OBS-2)

Doc.No: SAF/HSAF/PVR-02/1.1 Issue/Revision Index: 1.1

Date: 30/09/2011 Page: 114/177

According to ME (mean error) score in Table 37, there is no any underestimation or overestimation, but HO2 product has higher rain rate values than rain gauge values in next figure.

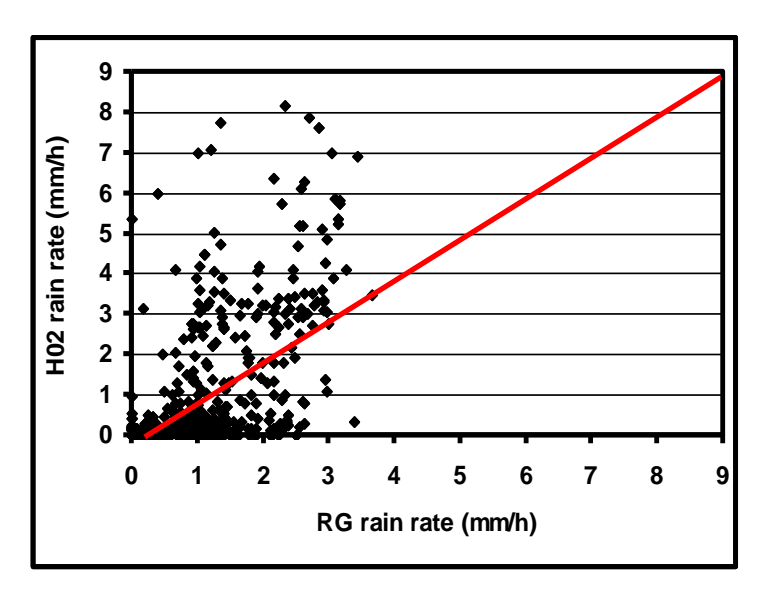


Figure 92 Scatter diagram of rain gauge and H02 product (Red line is 45 degree line)

#### Statistical scores

Statistics scores can be seen from Table 37. Correlation coefficient is 0.54 for H02 product. POD, FAR and CSI are respectively 0.64, 0.04 and 0.62 for this case study.

| NS  | NR  | ME    | SD   | MAE  | MB   | CC   | RMSE | URD  | POD  | FAR  | CSI  |
|-----|-----|-------|------|------|------|------|------|------|------|------|------|
| 494 | 752 | -0.01 | 1.51 | 1.12 | 0.99 | 0.54 | 1.51 | 132% | 0.64 | 0.04 | 0.62 |

**Table 37 Statistic scores for H02** 

### **Conclusions**

H02 product is not well enough to catch rainy area. In other words, frontal system is not well described generally by this product algorithm in terms of areal matching and quantitative estimate.

#### 5.9 Conclusions

Eleven case study analysis of H02 have been here reported for 2010. Stratiform and convective precipitations during summer and winter periods have been analysed in different countries. Rain gauges with 10 minutes refresh time, radar data and nowcasting tools have been used to highlight different characteristics of the satellite product.

The case studies here proposed have pointed out that different statistical score values are obtained during summer and winter period.

In summer, when more convective events occur, all the countries have observed that H02 reproduces the rainfall patterns and amounts with quite good confidence. It has some difficulties with proper recognition of rainfall maximum. About the convective systems it has been observed that H02 did not well detect the small-medium size thunderstorms. This effect is due to a typical size of these convective cells which does not exceed the H02 (AMSU-B and HMS) IFOV. Capturing of convective



(Product H02 - PR-OBS-2)

Doc.No: SAF/HSAF/PVR-02/1.1 Issue/Revision Index: 1.1

Date: 30/09/2011 Page: 115/177

cores by satellite IFOV or in upscaled radar image is strongly dependent on the mutual position of convective core and satellite IFOV centres. Other cases of medium-large size convective cells have showed a general correct qualitative location and estimation of the precipitation by H02, especially moderate and heavy ones (rain rate > 10mm/h) while the light precipitation is either overestimated or missed.

The dichotomous statistical scores evaluated for the summer cases have quite different values, mean values: POD 0.60, FAR 0.40 and CSI 0.40, but there are case studies with POD ranges between 0.8-0.9.

During winter period, when more stratiform events occur, the HO2 product well detects the precipitation area, but it underestimates the precipitation (apart from few cases see Turkish and Polish cases). The satellite product misses or strongly underestimates the rainfall. In general for these events the FAR has an higher value than POD, and the CSI is average 0.15.

Some general satellite product characteristics have been highlighted by the case studies here proposed as that parallax shift is particularly effective in case of small convective structures and that ground data hourly cumulated use is incorrect for H02 validation (see Italian case study). This is due to the variability of the precipitation field, which cannot be caught by hourly integrals provided by the raingauges, especially in case of convective precipitation. It has also to be mentioned that differences between land and sea algorithms have not been observed.

It has been showed a case study (Poland) where the ground data have been unable to catch the precipitation system while the satellite product reproduced more correctly the precipitation area. It is also interesting to stress the German case study where ground data of different sources (rain gauge and radar) have been used for validation exercise over the same region. The statistical scores obtained by rain gauge and radar data validation have very similar values.

## 6 Validation results: long statistic analysis

### 6.1 Introduction

In this Chapter the validation results of the H02 long statistic analysis are reported for the period (1.12.2009 – 31.11.2010). The validation has been performed on the product release currently in force at the time of writing.

Each Country/Team contributes to this Chapter by providing the monthly contingency tables and the statistical scores. The results are showed for radar and rain gauge, land and coast area in the three precipitation classes defined in table 7. The rain rates lower than 0.25 mm/h have been considered as no rain. The precipitation ground networks, instruments and data used for the validation of H02 have been described in Chapter 4.

To assess the degree of compliance of the product with user requirements all the PPVG members provided the long statistic results following the validation methodology reported in Chapter 3. For product H02 the User requirements are recorded in Table 38.

| Precipitation range | threshold | target | optimal |
|---------------------|-----------|--------|---------|
| > 10 mm/h           | 90        | 80     | 25      |
| 1-10 mm/h           | 120       | 105    | 50      |
| < 1 mm/h            | 240       | 145    | 90      |

Table 38 Accuracy requirements for product PR-OBS-1 [RMSE (%)]



(Product H02 – PR-OBS-2)

Doc.No: SAF/HSAF/PVR-02/1.1 Issue/Revision Index: 1.1

Date: 30/09/2011 Page: 116/177

This implies that the main score to be evaluated has been the RMSE%. However, in order to give a more complete idea of the product error structure, several statistical scores have been evaluated as reported: Mean Error, Standard Deviation (SD) and Correlation Coefficient (CC), Probability Of Detection (POD), False Alarm Rate (FAR) and Critical Success Index (CSI). These scores have been defined in Section 3.7.

The long statistic results obtained in Belgium, Hungary, Germany, Italy, Poland, Slovakia and Turkey will be shown in the next sections. The country validation results are here reported in order to respond not only to the question whether the product meets the requirements or not, but also where meets or approaches or fails the requirements.

The average performance of H02 for all sites is presented in a compact, synoptic way in this chapter. The contents of the monthly statistical scores have been provided by the individual Countries/Teams and verified by the Validation Cluster Leader, step by step, as described in the Chapter 3. As stressed in Chapter 4, the average scores reported in the following tables have been obtained on measurements collected in heterogeneous geographical, orographical and climatological conditions.

#### 6.2 The continuous statistic

There are three sets of columns:

- one set for Countries/Teams that has compared satellite data with meteorological radar in inner land areas: Belgium/BE, Germany/DE, Hungary/HU and Slovakia/SL; and their average weighed by the number of comparisons;
- one set for three Countries/Teams that has compared satellite data with rain gauges in inner land areas: Italy/IT, Germany/DE, Poland/PO and Turkey/TU; and their average weighed by the number of comparisons;
- one column for Turkey/TU that has compared satellite data with rain gauges in coastal areas.

In order to highlight the seasonal performances of H02 the statistical scores have been presented not only for yearly average but also for seasons averages. The seasons are reported in table 39.

| Winter:                  | Winter: Spring:  |                       | Autumn:              |
|--------------------------|------------------|-----------------------|----------------------|
| Dec. 2009, Jan. and Feb. | March, April and | June, July and August | Sept., Oct. and Nov. |
| 2010                     | May 2010         | 2010                  | 2010                 |

Table 39 split in four sections, one for each season, reports the Country/Team results side to side



(Product H02 - PR-OBS-2)

Doc.No: SAF/HSAF/PVR-02/1.1

Issue/Revision Index: 1.1

Date: 30/09/2011

Page: 117/177

### 6.2.1The winter period:

| H02       |          | BE    | DE          | HU    | SL    | TOTAL               | IT     | РО    | TU    | DE     | TOTAL               | TU coast            |  |  |
|-----------|----------|-------|-------------|-------|-------|---------------------|--------|-------|-------|--------|---------------------|---------------------|--|--|
|           |          |       | winter 2010 |       |       |                     |        |       |       |        |                     |                     |  |  |
| Version 2 | 2.2      | radar | radar       | radar | radar | radar               | gauge  | gauge | gauge | gauge  | gauge               | gauge               |  |  |
| NS        | <1mm/h   | 1118  | 17006       | 7783  | 1441  | 27348               | 11895  | 378   | 10262 | 449    | 22984               | 663                 |  |  |
| NR        | <1mm/h   | 10828 | 16267       | 25648 | 3279  | 56022               | 131498 | 5850  | 55783 | 6210   | 199341              | 6793                |  |  |
| ME        | <1mm/h   | -0,43 | -0,45       | -0,31 | -0,22 | <mark>-0,37</mark>  | -0,44  | -0,46 | -0,38 | -0,44  | <del>-0,43</del>    | <del>-0,28</del>    |  |  |
| SD        | <1mm/h   | 0,19  | 0,39        | 0,59  | 0,46  | 0,45                | 0,54   | 0,29  | 1,05  | 0,31   | 0,67                | 0,97                |  |  |
| MAE       | <1mm/h   | 0,46  | 0,53        | 0,50  | 0,40  | 0,49                | 0,57   | 0,50  | 0,53  | 0,49   | 0,55                | 0,67                |  |  |
| MB        | <1mm/h   | 0,09  | 0,17        | 0,36  | 0,43  | 0,25                | 0,17   | 0,10  | 0,23  | 0,08   | 0,18                | 0,47                |  |  |
| CC        | <1mm/h   | 0,10  | 0,06        | 0,08  | 0,05  | 0,07                | 0,06   | 0,07  | 0,08  | 0,08   | 0,07                | 0,10                |  |  |
| RMSE      | <1mm/h   | 0,52  | 0,61        | 0,68  | 0,51  | 0,62                | 0,70   | 0,55  | 1,15  | 0,54   | 0,81                | 1,01                |  |  |
| RMSE%     | <1mm/h   | 105%  | 111%        | 152%  | 141%  | 131%                | 132%   | 102%  | 180%  | 107%   | 144%                | 215%                |  |  |
| NS        | 1-10mm/h | 411   | 3932        | 4583  | 557   | 9483                | 19171  | 136   | 5759  | 607    | 25673               | 1753                |  |  |
| NR        | 1-10mm/h | 1502  | 8537        | 5633  | 155   | 15827               | 83347  | 1306  | 20361 | 1391   | 106405              | 3483                |  |  |
| ME        | 1-10mm/h | -1,31 | -1,58       | -1,08 | -0,79 | <mark>-1,37</mark>  | -1,88  | -1,36 | -1,17 | -1,32  | <mark>-1,73</mark>  | <mark>-1,00</mark>  |  |  |
| SD        | 1-10mm/h | 0,62  | 1,03        | 0,97  | 0,59  | 0,97                | 1,80   | 0,73  | 2,10  | 0,98   | 1,83                | 2,88                |  |  |
| MAE       | 1-10mm/h | 1,37  | 1,67        | 1,30  | 0,89  | 1,50                | 2,12   | 1,41  | 1,70  | 1,44   | 2,02                | 2,32                |  |  |
| MB        | 1-10mm/h | 0,16  | 0,15        | 0,36  | 0,41  | 0,23                | 0,17   | 0,09  | 0,36  | 0,15   | 0,21                | 0,53                |  |  |
| CC        | 1-10mm/h | 0,32  | 0,21        | 0,40  | 0,28  | 0,29                | 0,21   | -0,01 | 0,21  | 0,11   | 0,20                | 0,17                |  |  |
| RMSE      | 1-10mm/h | 1,48  | 1,89        | 1,50  | 1,04  | 1,70                | 2,60   | 1,55  | 2,43  | 1,65   | 2,55                | 3,08                |  |  |
| RMSE%     | 1-10mm/h | 92%   | 94%         | 88%   | 74%   | 92%                 | 102%   | 97%   | 145%  | 97%    | 110%                | 150%                |  |  |
| NS        | ≥10mm/h  | 0     | 3           | 0     | 0     | 3                   | 481    | 0     | 118   | 2      | 601                 | 89                  |  |  |
| NR        | ≥10mm/h  | 0     | 3           | 0     | 0     | 3                   | 805    | 0     | 17    | 1      | 823                 | 25                  |  |  |
| ME        | ≥10mm/h  | -     | -11,5       | -     | -     | <mark>-11,50</mark> | -16,03 | - ,00 | -9,83 | -13,80 | <mark>-15,90</mark> | <mark>-12,45</mark> |  |  |
| SD        | ≥10mm/h  | -     | 3,841       | -     | -     | 3,84                | 15,20  | - ,00 | 3,04  | 0,00   | 14,93               | 3,15                |  |  |
| MAE       | ≥10mm/h  | -     | 11,5        | -     | -     | 11,50               | 16,12  | - ,00 | 9,83  | 13,80  | 15,99               | 12,45               |  |  |
| MB        | ≥10mm/h  | -     | 0,076       | -     | -     | 0,08                | 0,09   | - ,00 | 0,16  | 0,00   | 0,09                | 0,00                |  |  |
| CC        | ≥10mm/h  | -     | -0,846      | -     | -     | -0,85               | -0,12  | - ,00 | 0,09  | - ,00  | -0,12               | -0,34               |  |  |
| RMSE      | ≥10mm/h  | -     | 12,125      | -     | -     | 12,13               | 22,44  | - ,00 | 10,21 | 13,80  | 22,17               | 12,83               |  |  |
| RMSE%     | ≥10mm/h  | -     | 91%         | -     | -     | 91%                 | 91%    | 0%    | 87%   | 100%   | 91%                 | 99%                 |  |  |

Table 40 The main statistical scores evaluated by PPVG for H02 during the winter period. The rain rates lower than 0.25 mm/h have been considered as no rain

In Table 40 it can be seen that the scores obtained by radar data are very similar to the scores obtained by rain gauge data for all the precipitation classes. The RMSE % evaluated for light precipitation rain, rate lower than 1mm/h, has the highest value. The difficulty to estimate small precipitation intensities is not only of the satellite product, but also of rain gauge and radar instruments. This aspect has been highlighted also in Section 4.2 and 4.3 on ground data description.

Germany is the only country which has performed the validation using both radar and rain gauge data. The results reported in tab. 40 appear quite similar in particular for precipitation with rain rate lower than 10 mm/h. The difference for the heavy precipitation, rain rate greater than 10 mm/h, is probably due to the small number of samples of this class.

A general precipitation underestimation by H02 is reported in table 40 using both rain gauge and radar data for all the precipitation classes.

The winter average RMSE % evaluated using radar data have been (RMSE% Cl1: 131%, Cl2:92%, Cl3:91%) and using rain gauge (RMSE% Cl1: 144%, Cl2:110%, Cl3:91%).



(Product H02 - PR-OBS-2)

Doc.No: SAF/HSAF/PVR-02/1.1 Issue/Revision Index: 1.1

Date: 30/09/2011

Page: 118/177

A small Mean Error and Mean Absolute errors have been obtained for medium precipitation (rain rate between 1-10 mm/h) with radar (ME: -1,37 mm/h; MAE: 1,5 mm/h) and rain gauge (ME: -1,73 mm/h, MAE: 2,02) with a standard deviation respectively of 0.97 mm/h and 1.83 mm/h.

## 6.2.2 The Spring period

| H02       |          | BE    | DE     | HU    | SL    | тот                | IT     | РО     | TU     | DE     | тот    | TU coast          |
|-----------|----------|-------|--------|-------|-------|--------------------|--------|--------|--------|--------|--------|-------------------|
|           |          |       |        |       |       |                    | spring | 2010   |        |        |        |                   |
| Version 2 | 2.2      | radar | radar  | radar | radar | radar              | gauge  | gauge  | gauge  | gauge  | gauge  | gauge             |
| NS        | <1mm/h   | 3343  | 19496  | 25315 | 9561  | 57715              | 12246  | 2334   | 17105  | 2578   | 34263  | 898               |
| NR        | <1mm/h   | 9850  | 9061   | 40753 | 11495 | 71159              | 57309  | 8886   | 35590  | 7380   | 109165 | 4177              |
| ME        | <1mm/h   | -0,39 | 0,33   | -0,04 | 0,20  | 0,00               | -0,36  | -0,36  | -0,25  | -0,31  | -0,32  | 0,02              |
| SD        | <1mm/h   | 0,20  | 1,12   | 1,73  | 1,09  | 1,34               | 0,80   | 0,66   | 1,09   | 0,65   | 0,88   | 1,41              |
| MAE       | <1mm/h   | 0,47  | 0,67   | 0,60  | 0,55  | 0,58               | 0,59   | 0,52   | 0,58   | 0,50   | 0,57   | 0,85              |
| MB        | <1mm/h   | 0,22  | 1,69   | 0,90  | 1,41  | 0,99               | 0,32   | 0,32   | 0,50   | 0,35   | 0,38   | 1,06              |
| CC        | <1mm/h   | 0,11  | 0,27   | 0,12  | 0,23  | 0,15               | 0,07   | 0,06   | 0,05   | 0,10   | 0,06   | 0,16              |
| RMSE      | <1mm/h   | 0,56  | 1,17   | 1,78  | 1,12  | 1,43               | 0,90   | 0,81   | 1,17   | 0,75   | 0,97   | 1,45              |
| RMSE%     | <1mm/h   | 116%  | 267%   | 444%  | 266%  | <mark>347</mark> % | 164%   | 146%   | 284%   | 155%   | 201%   | <mark>303%</mark> |
| NS        | 1-10mm/h | 1151  | 10450  | 12970 | 3836  | 28441              | 14105  | 1370   | 6974   | 1167   | 23616  | 2039              |
| NR        | 1-10mm/h | 3021  | 3502   | 13741 | 1241  | 21505              | 35710  | 4781   | 11387  | 2296   | 54174  | 2109              |
| ME        | 1-10mm/h | -1,34 | -0,18  | -0,35 | 1,03  | -0,38              | -1,73  | -1,59  | -1,36  | -1,09  | -1,61  | -0,61             |
| SD        | 1-10mm/h | 1,37  | 2,11   | 2,34  | 3,11  | 2,21               | 1,90   | 1,56   | 1,38   | 1,72   | 1,75   | 3,12              |
| MAE       | 1-10mm/h | 1,65  | 1,50   | 1,46  | 1,60  | 1,50               | 2,04   | 1,75   | 1,60   | 1,53   | 1,90   | 2,50              |
| MB        | 1-10mm/h | 0,36  | 0,92   | 0,80  | 1,72  | 0,81               | 0,25   | 0,25   | 0,25   | 0,40   | 0,26   | 0,75              |
| CC        | 1-10mm/h | 0,39  | 0,27   | 0,27  | 0,40  | 0,29               | 0,23   | 0,17   | 0,11   | 0,28   | 0,20   | 0,13              |
| RMSE      | 1-10mm/h | 2,03  | 2,12   | 2,43  | 3,29  | 2,37               | 2,60   | 2,24   | 1,94   | 2,07   | 2,41   | 3,19              |
| RMSE%     | 1-10mm/h | 96%   | 105%   | 165%  | 166%  | 146%               | 113%   | 94%    | 97%    | 117%   | 108%   | 152%              |
| NS        | ≥10mm/h  | 13    | 50     | 354   | 0     | 417                | 418    | 6      | 115    | 22     | 561    | 57                |
| NR        | ≥10mm/h  | 35    | 64     | 40    | 0     | 139                | 533    | 94     | 44     | 9      | 680    | 16                |
| ME        | ≥10mm/h  | -8,61 | -16,89 | -1,27 | -     | -10,31             | -13,82 | -24,96 | -13,38 | -11,06 | -15,30 | -15,14            |
| SD        | ≥10mm/h  | 2,21  | 14,08  | 11,82 | -     | 10,44              | 7,06   | 20,24  | 6,05   | 4,69   | 8,78   | 5,17              |
| MAE       | ≥10mm/h  | 8,73  | 17,15  | 7,45  | -     | 12,24              | 13,89  | 24,96  | 13,38  | 11,06  | 15,35  | 15,14             |
| МВ        | ≥10mm/h  | 0,33  | 0,17   | 0,91  | -     | 0,42               | 0,10   | 0,05   | 0,07   | 0,21   | 0,10   | 0,08              |
| СС        | ≥10mm/h  | 0,56  | -0,35  | 0,07  | -     | 0,00               | -0,04  | 0,09   | 0,21   | -0,02  | -0,01  | -                 |
| RMSE      | ≥10mm/h  | 9,12  | 22,00  | 11,89 | -     | 15,85              | 15,56  | 32,17  | 14,82  | 12,01  | 17,76  | 16,08             |
| RMSE%     | ≥10mm/h  | 71%   | 81%    | 92%   |       | 82%                | 91%    | 93%    | 93%    | 81%    | 91%    | 92%               |

Table 41 The main statistical scores evaluated by PPVG for H02 during the spring period. The rain rates lower than 0.25 mm/h have been considered as no rain

In Table 41 it can be seen that the scores obtained by radar data are quite different from the scores obtained by rain gauge data for light precipitation (rain rate< 1 mm/h). Besides, the RMSE % of this precipitation class has the highest value. This is due to the RMSE% evaluated by Hungary. An investigation on this result is in progress.

The statistical scores evaluated for precipitation classes 2 and 3, using both rain gauge and radar data, are quite similar.

A general precipitation underestimation by H02 is reported in table 42 using both rain gauge and radar data for all precipitation classes.

The spring average RMSE % evaluated using radar data have been (RMSE% Cl1: 347%, Cl2:145%, Cl3:81%) and using rain gauge (RMSE% Cl1: 201%, Cl2:108%, Cl3:91%).



(Product H02 - PR-OBS-2)

Doc.No: SAF/HSAF/PVR-02/1.1 Issue/Revision Index: 1.1

Date: 30/09/2011

Page: 119/177

A small Mean Error and Mean Absolute errors have been obtained for medium precipitation (rain rate between 1-10 mm/h) with radar (ME: -0,38 mm/h; MAE: 1,5 mm/h) and rain gauge (ME: -1,61 mm/h, MAE: 1,9) with a standard deviation respectively of 2.21 mm/h and 1.75 mm/h.

## 6.2.3 The summer period

| H02        |          | BE     | DE    | HU    | SL    | тот         | IT     | РО     | TU    | DE    | тот    | TU coast          |
|------------|----------|--------|-------|-------|-------|-------------|--------|--------|-------|-------|--------|-------------------|
|            |          |        |       | •     |       | summer 2010 |        |        |       |       |        |                   |
| Version 2. | 2        | radar  | radar | radar | radar | radar       | gauge  | gauge  | gauge | gauge | gauge  | gauge             |
| NS         | <1mm/h   | 8105   | 16863 | 24289 | 12951 | 62208       | 7216   | 2785   | 7395  | 4879  | 22275  | 346               |
| NR         | <1mm/h   | 9995   | 18786 | 28570 | 12962 | 70313       | 11803  | 5590   | 13508 | 7290  | 38191  | 2051              |
| ME         | <1mm/h   | -0,19  | 0,27  | 0,01  | 0,54  | 0,15        | -0,18  | -0,11  | -0,11 | -0,15 | -0,14  | 0,27              |
| SD         | <1mm/h   | 0,21   | 1,26  | 1,00  | 1,21  | 0,99        | 1,19   | 0,96   | 1,17  | 0,95  | 1,10   | 2,05              |
| MAE        | <1mm/h   | 0,51   | 0,68  | 0,51  | 0,73  | 0,60        | 0,66   | 0,57   | 0,64  | 0,57  | 0,62   | 1,06              |
| MB         | <1mm/h   | 0,63   | 1,56  | 1,02  | 2,07  | 1,30        | 0,66   | 0,80   | 0,77  | 0,70  | 0,73   | 1,56              |
| CC         | <1mm/h   | 0,12   | 0,23  | 0,23  | 0,33  | 0,23        | 0,07   | 0,14   | 0,11  | 0,09  | 0,10   | 0,08              |
| RMSE       | <1mm/h   | 0,87   | 1,29  | 1,01  | 1,33  | 1,12        | 1,21   | 0,97   | 1,18  | 0,97  | 1,12   | 2,10              |
| RMSE%      | <1mm/h   | 189%   | 289%  | 181%  | 265%  | 226%        | 251%   | 195%   | 254%  | 206%  | 235%   | <mark>521%</mark> |
| NS         | 1-10mm/h | 3879   | 15235 | 14556 | 7575  | 41245       | 5986   | 2733   | 4457  | 2470  | 15646  | 941               |
| NR         | 1-10mm/h | 5938   | 10177 | 16757 | 2869  | 35741       | 12356  | 4777   | 5136  | 3820  | 26089  | 553               |
| ME         | 1-10mm/h | -1,35  | -0,28 | -0,10 | 1,79  | -0,21       | -1,70  | -1,30  | -1,31 | -1,16 | -1,47  | -1,24             |
| SD         | 1-10mm/h | 1,53   | 2,58  | 2,92  | 3,22  | 2,62        | 2,63   | 2,67   | 2,12  | 1,96  | 2,44   | 1,96              |
| MAE        | 1-10mm/h | 1,75   | 1,79  | 1,86  | 2,28  | 1,86        | 2,43   | 2,02   | 1,98  | 1,70  | 2,16   | 2,03              |
| MB         | 1-10mm/h | 0,45   | 0,89  | 0,94  | 2,02  | 0,93        | 0,40   | 0,52   | 0,40  | 0,46  | 0,43   | 0,40              |
| CC         | 1-10mm/h | 0,25   | 0,22  | 0,40  | 0,46  | 0,33        | 0,24   | 0,18   | 0,11  | 0,25  | 0,21   | 0,15              |
| RMSE       | 1-10mm/h | 2,29   | 2,60  | 2,96  | 3,70  | 2,80        | 3,17   | 2,97   | 2,50  | 2,30  | 2,87   | 2,42              |
| RMSE%      | 1-10mm/h | 87%    | 120%  | 133%  | 209%  | 128%        | 108%   | 110%   | 121%  | 101%  | 110%   | 116%              |
| NS         | ≥10mm/h  | 68     | 268   | 1024  | 0     | 1360        | 431    | 97     | 108   | 62    | 698    | 0                 |
| NR         | ≥10mm/h  | 77     | 202   | 359   | 0     | 638         | 584    | 309    | 21    | 80    | 994    | 0                 |
| ME         | ≥10mm/h  | -13,68 | -7,29 | -5,13 | -     | -6,85       | -12,22 | -15,53 | -7,59 | -9,92 | -12,97 | -                 |
| SD         | ≥10mm/h  | 8,27   | 6,65  | 7,31  | -     | 7,22        | 9,31   | 9,88   | 6,70  | 5,83  | 9,15   | -                 |
| MAE        | ≥10mm/h  | 14,28  | 8,89  | 7,61  | -     | 8,82        | 13,12  | 15,57  | 8,63  | 10,75 | 13,60  | -                 |
| MB         | ≥10mm/h  | 0,20   | 0,48  | 0,66  | -     | 0,55        | 0,23   | 0,18   | 0,41  | 0,30  | 0,23   | -                 |
| CC         | ≥10mm/h  | 0,17   | 0,28  | 0,28  | -     | 0,26        | 0,00   | 0,42   | -0,76 | 0,26  | 0,13   | -                 |
| RMSE       | ≥10mm/h  | 16,64  | 9,91  | 9,36  | -     | 10,42       | 15,37  | 18,42  | 10,02 | 11,94 | 15,93  | -                 |
| RMSE%      | ≥10mm/h  | 83%    | 71%   | 59%   | -     | 66%         | 85%    | 84%    | 71%   | 79%   | 84%    | -                 |

Table 42 The main statistical scores evaluated by PPVG for H02 during the summer period. The rain rates lower than 0.25 mm/h have been considered as no rain

In Table 42 it can be seen that the scores obtained by radar data are quite similar to the scores obtained by rain gauge data for all precipitation classes. The RMSE % for the light precipitation has the highest value as during the other seasons.

A general precipitation underestimation by H02 is reported in table 42 using both rain gauge and radar data for rain rate greater than 1 mm/h. Besides a precipitation overestimation by H02 has been found for light precipitation (rain rate< 1mm/h) using radar data.

The spring average RMSE % evaluated using radar data have been (RMSE% Cl1: 226%, Cl2:127%, Cl3:66%) and using rain gauge (RMSE% Cl1: 235%, Cl2:109%, Cl3:84%).

The worst statistical scores during this season have been obtained over coastal areas by Turkey.



(Product H02 - PR-OBS-2)

Doc.No: SAF/HSAF/PVR-02/1.1

Issue/Revision Index: 1.1 Date: 30/09/2011

Page: 120/177

## 6.2.4 The autumn period

| H02       |          | BE    | DE     | HU           | SL           | тот              | IT        | РО     | TU     | DE     | тот                | TU<br>coast |
|-----------|----------|-------|--------|--------------|--------------|------------------|-----------|--------|--------|--------|--------------------|-------------|
|           |          |       |        |              |              | . a              | utumn 201 | 10     |        |        |                    |             |
| Version 2 | 2.2      | radar | radar  | radar        | radar        | radar            | gauge     | gauge  | gauge  | gauge  | gauge              | gauge       |
| NS        | <1mm/h   | 5978  | 20251  | 22648        | 8224         | 57101            | 10554     | 1506   | 12677  | 2857   | 27594              | 578         |
| NR        | <1mm/h   | 11845 | 11886  | 25609        | 9720         | 59060            | 32554     | 4177   | 33369  | 6469   | 76569              | 4514        |
| ME        | <1mm/h   | -0,32 | 0,27   | -0,15        | 0,25         | -0,03            | -0,25     | -0,38  | -0,32  | -0,35  | -0,30              | 0,07        |
| SD        | <1mm/h   | 0,21  | 0,86   | 0,57         | 0,85         | 0,60             | 1,12      | 0,44   | 0,61   | 0,48   | 0,81               | 1,43        |
| MAE       | <1mm/h   | 0,45  | 0,58   | 0,43         | 0,56         | 0,48             | 0,68      | 0,49   | 0,51   | 0,48   | 0,58               | 0,91        |
| MB        | <1mm/h   | 0,38  | 1,59   | 0,70         | 1,52         | 0,95             | 0,54      | 0,30   | 0,37   | 0,32   | 0,44               | 1,12        |
| CC        | <1mm/h   | 0,21  | 0,23   | 0,24         | 0,36         | 0,25             | 0,06      | 0,11   | 0,09   | 0,12   | 0,08               | 0,11        |
| RMSE      | <1mm/h   | 0,56  | 0,91   | 0,59         | 0,89         | 0,70             | 1,17      | 0,58   | 0,70   | 0,59   | 0,88               | 1,44        |
| RMSE%     | <1mm/h   | 107%  | 222%   | 125%         | 202%         | 153%             | 245%      | 106%   | 140%   | 118%   | <mark>181</mark> % | 326%        |
| NS        | 1-10mm/h | 1569  | 11033  | 9541         | 3146         | 25289            | 13241     | 774    | 6808   | 1039   | 21862              | 2645        |
| NR        | 1-10mm/h | 3614  | 3780   | 10123        | 819          | 18336            | 31768     | 2611   | 15989  | 2810   | 53178              | 2815        |
| ME        | 1-10mm/h | -1,13 | -0,52  | -0,55        | 0,45         | -0,61            | -1,90     | -1,42  | -1,36  | -1,28  | -1,68              | -0,32       |
| SD        | 1-10mm/h | 0,72  | 1,51   | 1,18         | 1,42         | 1,17             | 2,44      | 1,33   | 1,93   | 1,20   | 2,17               | 3,27        |
| MAE       | 1-10mm/h | 1,25  | 1,21   | 1,02         | 1,15         | 1,11             | 2,43      | 1,57   | 1,85   | 1,47   | 2,16               | 2,49        |
| MB        | 1-10mm/h | 0,34  | 0,73   | 0,70         | 1,34         | 0,66             | 0,32      | 0,31   | 0,39   | 0,29   | 0,34               | 0,86        |
| CC        | 1-10mm/h | 0,20  | 0,11   | 0,37         | 0,15         | 0,27             | 0,26      | 0,22   | 0,23   | 0,23   | 0,25               | 0,25        |
| RMSE      | 1-10mm/h | 1,45  | 1,62   | 1,31         | 1,53         | 1,41             | 3,11      | 1,95   | 2,37   | 1,76   | 2,76               | 3,29        |
| RMSE%     | 1-10mm/h | 79%   | 83%    | 70%          | 117%         | <mark>77%</mark> | 103%      | 82%    | 98%    | 90%    | 100%               | 162%        |
| NS        | ≥10mm/h  | 0     | 3      | 0            | 0            | 3                | 935       | 0      | 193    | 33     | 1161               | 114         |
| NR        | ≥10mm/h  | 0     | 7      | 0            | 0            | 7                | 1191      | 14     | 256    | 7      | 1468               | 60          |
| ME        | ≥10mm/h  | -     | -12,96 | -            | -            | -12,96           | -12,84    | -13,10 | -10,19 | -13,02 | 72,69              | -8,60       |
| SD        | ≥10mm/h  | -     | 1,28   | -            | -            | 1,28             | 9,97      | 6,04   | 6,63   | 4,58   | 9,33               | 9,26        |
| MAE       | ≥10mm/h  | -     | 12,96  | -            | -            | 12,96            | 13,87     | 13,10  | 11,57  | 13,02  | 13,46              | 11,74       |
| MB        | ≥10mm/h  | -     | 0,04   | -            | -            | 0,04             | 0,25      | 0,04   | 0,26   | 0,11   | 0,25               | 0,43        |
| CC        | ≥10mm/h  | -     | 0,97   | -            | -            | 0,97             | 0,16      | -0,10  | 0,06   | -0,85  | 0,14               | 0,23        |
| RMSE      | ≥10mm/h  | -     | 13,02  | - <u>.</u> , | - <u>.</u> , | 13,02            | 16,40     | 14,43  | 12,54  | 13,97  | 15,69              | 12,59       |
| RMSE%     | ≥10mm/h  | - %   | 97%    | - %          | - %          | 97%              | 84%       | 95%    | 88%    | 90%    | <mark>85%</mark>   | 83%         |

Table 43 The main statistical scores evaluated by PPVG for H02 during the autumn period. The rain rates lower than 0.25 mm/h have been considered as no rain

A general precipitation underestimation by H02 is reported in table 43 using both rain gauge and radar data for all the precipitation classes. The statistical scores obtained during this season with both radar data (RMSE% Cl1: 153%, Cl2:77%, Cl3:97%) and rain gauge (RMSE% Cl1: 181%, Cl2:100%, Cl3:85%) are the best ones of all the year.



(Product H02 - PR-OBS-2)

Doc.No: SAF/HSAF/PVR-02/1.1 Issue/Revision Index: 1.1

Date: 30/09/2011 Page: 121/177

## 6.2.5 The annual average

| PR-OBS-  | -2   | BE  | DE  | ни  | SL  | тот  | IT   | РО  | TU  | DE   | тот  | TU<br>coast   |  |
|--|--|---|---|---|---|--|--|---|---|--|--|---|--|
|  |  |   |   | DIC.09-NOV.10   |   |  |  |   |   |  |  |   |  |
| Version  | 2.2  | radar   | radar   | radar   | radar   | radar  | gauge  | gauge   | gauge   | gauge  | gauge  | gauge   |  |
| NS<br>NR<br>ME<br>SD<br>MAE                            | <1mm/h<br><1mm/h<br><1mm/h<br><1mm/h   | 18544<br>42518<br>-0,33<br>0,20<br>0,47                               | 73616<br>56000<br>0,07<br>0,90<br>0,61                                  | 80035<br>120580<br>-0,11<br>1,07<br>0,52                                | 32177<br>37456<br>0,29<br>1,01<br>0,60                                | 204372<br>256554<br>-0,05<br>0,88<br>0,54                        | 41911<br>233164<br>-0,38<br>0,72<br>0,59                                 | 7003<br>24503<br>-0,33<br>0,60<br>0,52                                | 47439<br>138250<br>-0,31<br>0,97<br>0,55                                | 10763<br>27349<br>-0,31<br>0,61<br>0,51                                | 107116<br>423266<br>-0,35<br>0,79<br>0,57                        | 2485<br>17535<br>-0,05<br>1,32<br>0,82                        |  |
| MB<br>CC<br>RMSE<br>URD                                | <1mm/h<br><1mm/h<br><1mm/h<br><1mm/h   | 0,33<br>0,14<br>0,62<br>128%  | 1,18<br>0,19<br>0,99<br>220%  | 0,77<br>0,16<br>1,11<br>252%  | 1,58<br>0,29<br>1,08<br>238%  | 0,91<br>0,18<br>1,00<br><mark>222%</mark>                        | 0,28<br>0,06<br>0,84<br>162%   | 0,37<br>0,09<br>0,75<br>140%  | 0,39<br>0,08<br>1,05<br>205%  | 0,38<br>0,10<br>0,72<br>149%   | 0,33<br>0,07<br>0,89<br><mark>174%</mark>                        | 0,91<br>0,12<br>1,35<br><mark>300%</mark>                     |  |
| NS<br>NR<br>ME<br>SD<br>MAE<br>MB<br>CC<br>RMSE<br>URD | 1-10mm/h<br>1-10mm/h<br>1-10mm/h<br>1-10mm/h<br>1-10mm/h<br>1-10mm/h<br>1-10mm/h | 7010<br>14075<br>-1,29<br>1,19<br>1,56<br>0,37<br>0,28<br>1,93<br>87% | 40650<br>25996<br>-0,73<br>1,85<br>1,63<br>0,63<br>0,21<br>2,16<br>104% | 41650<br>46254<br>-0,39<br>2,13<br>1,49<br>0,78<br>0,35<br>2,26<br>123% | 15114<br>5084<br>1,31<br>2,83<br>1,89<br>1,79<br>0,39<br>3,17<br>180% | 104458<br>91409<br>-0,53<br>1,95<br>1,56<br>0,73<br>0,30<br>2,23 | 52503<br>163181<br>-1,83<br>2,01<br>2,19<br>0,24<br>0,23<br>2,74<br>105% | 5013<br>13475<br>-1,43<br>1,83<br>1,78<br>0,34<br>0,17<br>2,37<br>98% | 23998<br>52873<br>-1,28<br>1,90<br>1,75<br>0,35<br>0,18<br>2,31<br>118% | 5283<br>10317<br>-1,20<br>1,57<br>1,57<br>0,36<br>0,23<br>2,02<br>101% | 86797<br>239846<br>-1,66<br>1,95<br>2,04<br>0,27<br>0,21<br>2,60 | 7378<br>8960<br>-0,71<br>3,00<br>2,40<br>0,68<br>0,18<br>3,13 |  |
| NS<br>NR   | ≥10mm/h<br>≥10mm/h   | 90<br>112   | 324<br>276  | 1397<br>399   | 0   | 1811<br>787  | 2265<br>3113   | 103<br>417  | 534<br>338  | 119<br>97  | 3021<br>3965   | 260<br>101  |  |
| ME<br>SD<br>MAE  | ≥10mm/h<br>≥10mm/h<br>≥10mm/h  | -12,09<br>6,38<br>12,55   | -9,71<br>8,21<br>10,94  | -4,75<br>7,76<br>7,60   | - ,00<br>- ,00<br>- ,00   | -7,53<br>7,72<br>9,47  | -13,72<br>10,70<br>14,32   | -17,58<br>12,08<br>17,60  | -10,43<br>6,38<br>11,53   | -10,29<br>5,58<br>10,98  | 17,74<br>10,35<br>14,34  | -10,59<br>7,10<br>12,45                                       |  |
| MB<br>CC   | ≥10mm/h<br>≥10mm/h   | 0,24<br>0,30  | 0,39<br>0,14  | 0,68<br>0,26  | - ,00<br>- ,00<br>- ,00   | 0,52<br>0,22   | 0,18<br>0,02   | 0,15<br>0,33  | 0,24<br>0,03  | 0,28<br>0,15   | 0,18<br>0,06   | 0,27  |  |
| RMSE<br>URD  | ≥10mm/h<br>≥10mm/h   | 14,29<br>79%  | 12,82<br>74%  | 9,62<br>63%   | - ,00<br>- %  | 11,40<br><mark>69%</mark>  | 17,62<br>87%   | 21,39<br>87%  | 12,56<br>88%  | 12,11<br>80%   | 17,45<br><mark>87%</mark>  | 13,20<br><mark>88%</mark>                                     |  |

Table 44 The main statistical scores evaluated by PPVG for H02 during one year of data 1<sup>st</sup> December 2009- 30<sup>th</sup>

November 2010 . The rain rates lower than 0.25 mm/h have been considered as no rain

The yearly averages obtained by all the countries using both radar and rain gauge data are similar. The worst RMSE% has been evaluated for light precipitation comparing H02 precipitation estimations with radar data. In this case there is a precipitation overestimation by the satellite product but in general a clear precipitation underestimation by H02 is reported in tab 44.

The yearly averages of RMSE% obtained with radar data (RMSE% Cl1: 222%, Cl2:115%, Cl3:69%) and with rain gauge (RMSE% Cl1: 174%, Cl2:107%, Cl3:87%).

A small Mean Error and Mean Absolute errors have been obtained for medium precipitation (rain rate between 1-10 mm/h) with radar (ME: -0,53 mm/h; MAE: 1,56 mm/h) and rain gauge (ME: -1,66 mm/h, MAE: 2,04) with a standard deviation respectively of 1.95 mm/h and 1.95 mm/h.



(Product H02 - PR-OBS-2)

Doc.No: SAF/HSAF/PVR-02/1.1 Issue/Revision Index: 1.1

Date: 30/09/2011 Page: 122/177

## 6.3 The multi-categorical statistic

Two sets of validation have been performed:

- one set for Countries/Teams that has compared satellite data with meteorological radar in inner land areas: Belgium/BE, Germany/DE, Hungary/HU and Slovakia/SL;
- one set for Countries/Teams that has compared satellite data with rain gauges in inner land areas: Italy/IT, Germany/DE, Poland/PO and Turkey/TU.

Each Country/Team contributes to this Chapter by providing the monthly contingency table and the statistical scores. The Validation Cluster Leader has collected all the validation files, has verified the consistency of the results and evaluated the monthly and yearly contingency tables and the statistical scores.

## 6.3.1 radar validation

|                         | Dec-09 | Jan-10 | Feb10 | Mar10 | Apr10 | May10 | Jun10 | Jul10 | Aug-10 | Sep-10 | Oct-10 | Nov-10 | tot  |
|-------------------------|--------|--------|-------|-------|-------|-------|-------|-------|--------|--------|--------|--------|------|
| POD with RR ≥ 0.25 mm/h | 0,25   | 0,18   | 0,17  | 0,27  | 0,27  | 0,61  | 0,61  | 0,63  | 0,65   | 0,65   | 0,38   | 0,37   | 0,47 |
| FAR with RR ≥ 0.25 mm/h | 0,63   | 0,82   | 0,77  | 0,70  | 0,63  | 0,41  | 0,34  | 0,35  | 0,39   | 0,38   | 0,61   | 0,39   | 0,47 |
| CSI with RR ≥ 0.25 mm/h | 0,18   | 0,10   | 0,11  | 0,17  | 0,18  | 0,43  | 0,47  | 0,47  | 0,46   | 0,47   | 0,24   | 0,30   | 0,33 |
| POD with RR ≥ 1 mm/h    | 0,17   | 0,21   | 0,16  | 0,31  | 0,27  | 0,53  | 0,52  | 0,57  | 0,58   | 0,53   | 0,33   | 0,26   | 0,43 |
| FAR with<br>RR ≥ 1 mm/h | 0,83   | 0,82   | 0,85  | 0,76  | 0,81  | 0,60  | 0,53  | 0,52  | 0,54   | 0,59   | 0,74   | 0,61   | 0,62 |
| CSI with<br>RR ≥ 1 mm/h | 0,09   | 0,11   | 0,08  | 0,15  | 0,13  | 0,29  | 0,33  | 0,35  | 0,35   | 0,30   | 0,17   | 0,19   | 0,25 |

Table 45 The averages POD, FAR and CSI deduced comparing H02 with radar data

|           |               |         | Radar data   |               |          |  |  |  |  |  |  |  |  |
|-----------|---------------|---------|--------------|---------------|----------|--|--|--|--|--|--|--|--|
|           | mm/h          | PR<0.25 | 0.25≤PR<1.00 | 1.00≤PR<10.00 | 10.00≤PR |  |  |  |  |  |  |  |  |
| ta        | PR<0.25       | 98%     | 61%          | 31%           | 5%       |  |  |  |  |  |  |  |  |
| e data    | 0.25≤PR<1.00  | 2%      | 26%          | 26%           | 11%      |  |  |  |  |  |  |  |  |
| Satellite | 1.00≤PR<10.00 | 1%      | 14%          | 42%           | 50%      |  |  |  |  |  |  |  |  |
| Sa        | 10.00≤PR      | 0%      | 0%           | 1%            | 34%      |  |  |  |  |  |  |  |  |

Table 46 The contingency table for the three precipitation classes defined in table 7 evaluated by comparing H02 with radar data

The averages of POD: 0.47, FAR: 0.47 and CSI:0.33 have been obtained using radar data on one year of data 1<sup>st</sup> December 2009- 30<sup>th</sup> November 2010.

In table 46 it is possible to see that 98% of no rain is correctly classified by H02. There is a general precipitation underestimation by H02.



(Product H02 - PR-OBS-2)

Doc.No: SAF/HSAF/PVR-02/1.1 Issue/Revision Index: 1.1

Date: 30/09/2011

Page: 123/177

## 6.3.2 rain gauge validation

|                         | Dec-09 | Jan-10 | Feb10 | Mar10 | Apr10 | May10 | Jun10 | Jul10 | Aug-10 | Sep-10 | Oct-10 | Nov-10 | тот  |
|-------------------------|--------|--------|-------|-------|-------|-------|-------|-------|--------|--------|--------|--------|------|
| POD with RR ≥ 0.25 mm/h | 0,11   | 0,09   | 0,11  | 0,13  | 0,18  | 0,33  | 0,34  | 0,39  | 0,42   | 0,32   | 0,30   | 0,19   | 0,18 |
| FAR with RR ≥ 0.25 mm/h | 0,31   | 0,33   | 0,34  | 0,45  | 0,49  | 0,47  | 0,46  | 0,47  | 0,36   | 0,36   | 0,30   | 0,32   | 0,40 |
| CSI with RR ≥ 0.25 mm/h | 0,10   | 0,08   | 0,11  | 0,12  | 0,15  | 0,26  | 0,26  | 0,29  | 0,34   | 0,27   | 0,27   | 0,17   | 0,16 |
| POD with<br>RR ≥ 1 mm/h | 0,12   | 0,12   | 0,13  | 0,15  | 0,14  | 0,25  | 0,26  | 0,36  | 0,36   | 0,25   | 0,27   | 0,18   | 0,18 |
| FAR with<br>RR ≥ 1 mm/h | 0,50   | 0,50   | 0,46  | 0,57  | 0,66  | 0,59  | 0,57  | 0,53  | 0,43   | 0,48   | 0,44   | 0,43   | 0,52 |
| CSI with<br>RR ≥ 1 mm/h | 0,11   | 0,10   | 0,12  | 0,13  | 0,11  | 0,18  | 0,19  | 0,26  | 0,28   | 0,20   | 0,22   | 0,16   | 0,15 |

Table 47 The averages POD, FAR and CSI deduced comparing H02 with rain gauge data

|          |               | Radar data |              |               |          |  |
|----------|---------------|------------|--------------|---------------|----------|--|
|          | mm/h          | PR<0.25    | 0.25≤PR<1.00 | 1.00≤PR<10.00 | 10.00≤PR |  |
| Ф        | PR<0.25       | 98%        | 88%          | 70%           | 43%      |  |
| data     | 0.25≤PR<1.00  | 1%         | 7%           | 12%           | 13%      |  |
| atellite | 1.00≤PR<10.00 | 1%         | 5%           | 17%           | 35%      |  |
| Sat      | 10.00≤PR      | 0%         | 0%           | 1%            | 9%       |  |

Table 48 The contingency table for the three precipitation classes defined in table 7 evaluated by comparing H02 with rain gauge data

The averages of POD: 0.18, FAR: 0.40 and CSI:0.16 have been obtained using rain gauge data on one year of data  $1^{st}$  December 2009-  $30^{th}$  November 2010.

In table 48 it is possible to see that 98% of no rain is correctly classified by H02. There is a general precipitation underestimation by the satellite product H02.



(Product H02 - PR-OBS-2)

Doc.No: SAF/HSAF/PVR-02/1.1 Issue/Revision Index: 1.1

Date: 30/09/2011 Page: 124/177

## 6.4 User requirement compliance

In table 49 In table 6.9 the statistical scores obtained by the yearly validation of H02 with radar and rain gauge data are reported. The statistical scores reach the thresholds stated in the User Requirements for land areas in all cases using both rain gauge and satellite data as ground reference. Only for precipitation lower than 10 mm/h using rain gauge in coast areas the threshold is not completely reached. This result might be explained by considering the difficulty of rain gauge to evaluate the precipitation in a coastal IFOV with a large part covered by sea.

Between target and optimal Between threshold and target Threshold exceeded by < 50 % Threshold exceeded by ≥ 50 %

| PR-OBS-1 v2.2 |                      |        |         | Annual average of RMSE% |       |       |
|---------------|----------------------|--------|---------|-------------------------|-------|-------|
| Precipitation | Requirement (RMSE %) |        | radar   | gauge                   | gauge |       |
| class         | thresh               | target | optimal | land                    | land  | coast |
| > 10 mm/h     | 90                   | 80     | 25      | 69%                     | 87%   | 88%   |
| 1-10 mm/h     | 120                  | 105    | 50      | 115%                    | 107%  | 152%  |
| < 1 mm/h      | 240                  | 145    | 90      | 222%                    | 173%  | 300%  |

Table 49 User requirement and compliance analysis for product H02

As reported in Annex 8 the results obtained by the current validation procedure represent the convolution of at least three factors: the satellite product accuracy, the accuracy of the ground data used and the limitations of the comparison methodology (e.g., errors of space and time co-location, representativeness changing with scale, etc.). Therefore, the results currently found are by far pessimistic in respect of what is the real product performance.

### 7 Conclusions

### 7.1 Summary conclusions on the status of product validation

The H02 product has been validated by the PPVG on one year of data  $1^{st}$  of December 2009 –  $30^{th}$  of November 2010. Each Country/Team have provided case study and long statistic analysis using radar and rain gauge following the validation methodology reported in Chapter 3.

The results of the Precipitation Validation Programme are reported in this Product Validation Report (PVR). A precipitation product validation section of the H-SAF web page is under development. This validation web section will be continuously updated with the last validation results and studies coming from the Precipitation Product Validation Group (SPVG).

It is well know that radar and rain gauge rainfall estimation is influenced by several error sources that should be carefully handled and characterized before using these data as reference for ground validation of any satellite-based precipitation products. A complete inventory of the precipitation ground networks, instruments and data available inside the PPVG has been provided in Chapter 4 in order to highlight the main error sources and to present possible methodology for selecting the



(Product H02 - PR-OBS-2)

Doc.No: SAF/HSAF/PVR-02/1.1 Issue/Revision Index: 1.1

Date: 30/09/2011 Page: 125/177

ground data more reliable (Annex 1-7). In the last months the first example of precipitation fields integration has been also provided (Section 4.4.3): INCA and RADOLAN products. The INCA system, a tool for the precipitation products validation, is available in Slovakia and Poland, in both countries being run in pre-operational mode. In Germany similar precipitation analysis system called RADOLAN is being run operationally. The study performed in the PPVG (*Annex 5*) showed that the accuracy and reliability of the raingauge stations significantly affect final precipitation analysis of the INCA or INCA-like systems. In order to solve this problem an automated blacklisting technique is going to be developed at SHMÚ (currently blacklisting is used in manual mode).

Eleven case study analysis of H02 have been here reported in Chapter 5. Stratiform and convective precipitations during summer and winter periods have been analysed in different countries. Rain gauges with 10 minutes refresh time, radar data and nowcasting tools have been used to highlight different characteristics of the satellite product. The case studies proposed have pointed out that different statistical score values are obtained during summer and winter period, problems on coast line and parallax shift. It has been also showed a case study (Poland) where the ground data have been unable to catch the precipitation system while the satellite product reproduced more correctly the precipitation area.

In Chapter 6 the validation results of the H02 long statistic analysis obtained for the period (1.12.2009 – 31.11.2010), have been presented. To assess the degree of compliance of the product with user requirements Each Country/Team has provided the monthly contingency tables and the statistical scores. The results have been showed for radar and rain gauge, land and coast area in the three precipitation classes defined in table 7. The rain rates lower than 0.25 mm/h have been considered as no rain.

The statistical scores evaluated by the PPVG reach the thresholds stated in the User Requirements in all cases using both rain gauge and radar data as ground reference. Only for precipitation lower than 1 mm/h using rain gauge in coast areas the threshold is not completely reached. This result might be explained by considering the difficulty of rain gauge to evaluate the precipitation in a coastal IFOV with a large part covered by sea. As reported in Annex 8 the results obtained by the current validation procedure represent the convolution of at least three factors: the satellite product accuracy, the accuracy of the ground data used and the limitations of the comparison methodology (e.g., errors of space and time co-location, representativeness changing with scale, etc.). Therefore, the results currently found are by far pessimistic in respect of what is the real product performance.

### 7.2 Next steps

On the base of the development phase it is possible to say that the ground data error characterization is necessary and that a validation of a common protocol is not enough. Only the use of the same software can guarantee that the results obtained by several institutes are obtained in the same way. To improve the validation methodology and to develop software used by all members of the validation cluster several working groups have been composed during the last Validation Workshop held in Bratislava, 20-22 October 2010 (see annex 1,2,3,4,5,6,7).

On the base of published papers and the characteristics of the ground data available inside the PPVG the main next steps are foreseen in order to improve the validation methodology:



(Product H02 - PR-OBS-2)

Doc.No: SAF/HSAF/PVR-02/1.1 Issue/Revision Index: 1.1

Date: 30/09/2011 Page: 126/177

 quantitative estimation of the errors introduced in the validation procedure comparing the instantaneous satellite precipitation estimation with the rain gauge precipitation cumulated on different intervals;

- definition of a rain gauge and radar data quality check;
- application of the data quality check to all radar and rain gauge data used in the PPVG;
- definition of the optimal and minimal spatial density of rain gauge stations to be representative of the ground precipitation in the view of satellite product comparison;
- development of the three software for raingauges, radar and INCA products up-scaling vs AMSU and MHS grids;
- definition and code implementation of the technique for the temporal matching of satellite rain rate with rain gauge and radar data;
- selection of the appropriate methodology for spatial distribution of precipitation products errors taking into consideration spatial and temporal characteristics of each product for selected areas as test catchments.



(Product H02 - PR-OBS-2)

Doc.No: SAF/HSAF/PVR-02/1.1 Issue/Revision Index: 1.1

Date: 30/09/2011 Page: 127/177

## 8 Annex 1: Status of working group

## Working Group 1: "Rain gauge data"

Coordinator: Federico Porcù (University of Ferrara) supported by Silvia Puca (DPC), Italy.

Proposal completed, first report available.

Participants: Emmanuel Roulin and Angelo Rinollo (Belgium), Gergana Kozinarova (Bulgaria), Claudia Rachimow and Peter Krahe (Germany), Emanuela Campione (Italy), Rafal Iwanski and Bozena Lapeta (Poland), Ibrahim Sonmez and Ahmet Oztopal (Turkey).

## Working Group 2: "Radar data"

Coordinators: Gianfranco Vulpiani (DPC), Italy and Eszter Labo (HMS) Hungary

Proposal completed, first report available.

Participants: Rafal Iwanski (Poland), Emmanuel Roulin and Angelo Rinollo (Belgium)

Marian Jurasek, Luboslav Okon, Jan Kanak, Ladislav Meri (Slovakia), Firat Bestepe and Ahmet Oztopal

(Turkey)

## Working Group 3: "INCA products"

Coordinator: Jan Kanak (SHMU) Slovakia Proposal completed, first report available.

Participants: Claudia Rachimow and Peter Krahe (Germany), Rafal Iwanski and Bozena Lapeta (Poland),

Silvia Puca (Italy)

## Working Group 4: "COSMO grid"

Coordinators: Angelo Rinollo (RMI,) Belgium supported by Federico Porcù (University of Ferrara) and Lucio Torrisi (CNMCA) Italy

Proposal completed, First report available in:

ftp://ftp.meteoam.it/hsaf/WP6000/WP6100/precipitation/WG groups/

software developed, WG CLOSED.

Participants: Emmanuel Roulin, Eszter Labo and Judit Kerenyi

Testing over Belgium successful; procedure already generalized in a way that can be tested and used

by all groups and delivered. Testing by other members in progress

## Working Group 5: "Geographical error map"

Coordinator: Bozena Lapeta (IMGW) Poland

Proposal completed

Participants: Silvia Puca (Italy), Ibrahim Sonmez and Ahmet Oztopal (Turkey)



(Product H02 - PR-OBS-2)

Doc.No: SAF/HSAF/PVR-02/1.1 Issue/Revision Index: 1.1

Date: 30/09/2011 Page: 128/177

## 9 Annex 2: Working Group 1 "Rain gauge data"

#### **PROPOSAL**

The "ground reference" does not exist. The common validation methodology inside the H-SAF project has been based on the "hydrologist reference" (end-users) constituted mainly by rain gauge and then by radar data.

During the Precipitation Product and Hydrological Validation workshop held in Bratislava the 20-22 of October 2010 the Precipitation Product Validation Group (PPVG) has decided to set up a working group for the definition of the correct verification of satellite precipitation product performances using the rain gauges data available inside the PPVG.

The main aims of this working group are:

- to identify the more suitable techniques to compare rain gauge data with satellite precipitation products;
- to analyse the application of these techniques to the rain gauge available inside the PPV;
- to produce a well referenced documentation on the methodology defined;
- to develop the code to be used in the PPVG for a correct verification of satellite precipitation product performances.

## **Activities:**

### **First step** - collect:

• characteristics (telemetric/..., spatial distribution, temporal resolution, quality check applied, instrument sensitivity and saturation value ... and <u>accuracy</u>) of the rain gauge networks which composes the PPVG (Belgium, Bulgaria, Germany, Poland, Italy, Turkey).

Start Time - End time: December 2010 - January 2011

First Report: 31<sup>st</sup> of January 2011

**Second step**- define on the base of published papers and the characteristics of the rain gauge data available inside the PPVG:

- ground data quality check to be applied to all rain gauge data;
- optimal spatial density of rain gauge stations to be representative of the ground precipitation in the view of satellite product comparison;
- optimal time resolution of rain gauge network (15 min, 30 min, 1 h) for a correct comparison with rain rate and cumulated precipitation satellite products;
- raingauges up-scaling techniques vs AMSU-B, SSMI, SEVIRI grids;
- technique for the temporal matching of rain rate and cumulated precipitation satellite products with rain gauge data;

Start Time-End time: January 2011 – July 2011

Second Report: 31<sup>st</sup> of March 2011 Final Report: 31<sup>st</sup> of July 2011

Third step-code (possible Matlab) realization for:

- ground data quality check;
- comparison between rain gauge and satellite products.



(Product H02 - PR-OBS-2)

Doc.No: SAF/HSAF/PVR-02/1.1 Issue/Revision Index: 1.1

Date: 30/09/2011 Page: 129/177

Start Time-End time: June 2011- November 2011

Codes delivery and related documentation: 30<sup>th</sup> of November 2011

## **Composition of the working group:**

Coordinator: Federico Porcù (University of Ferrara) supported by Silvia Puca (DPC), Italy Participants from Belgium, Bulgaria, Germany, Poland, Italy, Turkey.

#### FIRST REPORT

Coordinator: Federico Porcù (University of Ferrara) supported by Silvia Puca (DPC), Italy Participants: Emmanuel Roulin and Angelo Rinollo (Belgium), Gergana Kozinarova (Bulgaria), Claudia Rachimow and Peter Krahe (Germany), Rafal Iwanski and Bozena Lapeta (Poland), Ibrahim Sonmez and Ahmet Oztopal (Turkey), Emanuela Campione (Italy).

### <u>Introduction</u>

This document reports on the outcomes of the inventory completed about the raingauges used as "ground reference" within the validation groups. Moreover, some general conclusion is drawn, based on the raingauges validation activities carried on in the last years by the Validation Group of H-SAF. The inventory was structured in three sections, dealing with the instruments used, the operational network and the approach to match gauge data with the satellite estimates. The results are summarized in the next pages.

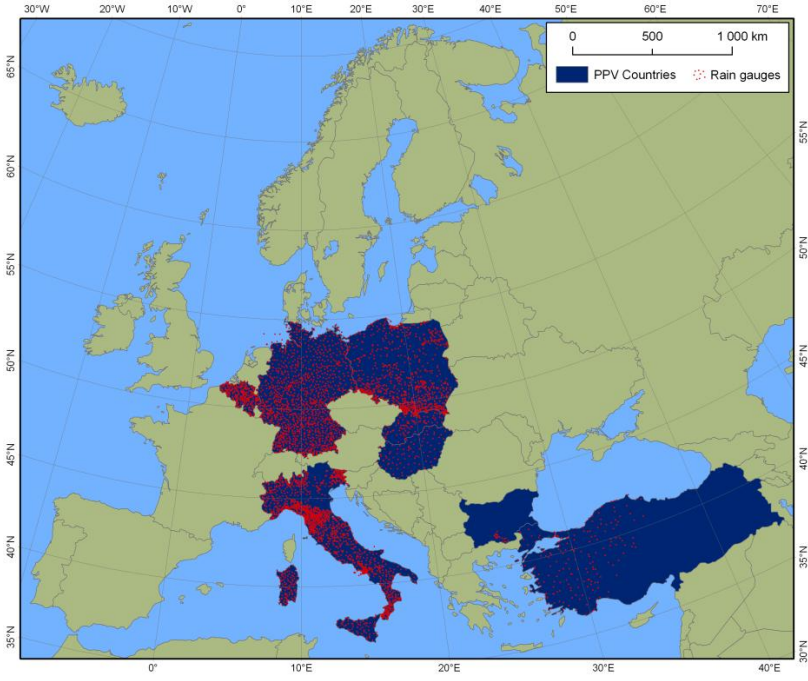


Figure 93 Rain gauge networks in PPVG



(Product H02 – PR-OBS-2)

Doc.No: SAF/HSAF/PVR-02/1.1 Issue/Revision Index: 1.1

Date: 30/09/2011 Page: 130/177

### The Instruments

Most of the gauges used in the National networks by the Precipitation Product Validation Group (PPVG) Partners are of the tipping bucket type, which is the most common device used worldwide to have continuous, point-like rainrate measurement. Nevertheless, several source of uncertainty in the measurements are well known but difficult to mitigate. First, very light rainrates (1 mm h<sup>-1</sup> and less) can be incorrectly estimated due to the long time it takes the rain to fill the bucket (Tokay et al., 2003). On the other side, high rainrates (above 50 mm h<sup>-1</sup>) are usually underestimated due to the loss of water during the tips of the buckets (Duchon and Biddle, 2010). Drifting wind can also greatly reduce the size of the effective catching area, if rain does not fall vertically, resulting in a rainrate underestimation quantitatively assessed in about 15% for an average event (Duchon and Essenberg, 2001).

Further errors occur in case of solid precipitation (snow or hail), when frozen particles are collected by the funnel but not measured by the buckets, resulting in a temporal shift of the measurements since the melting (and the measure) can take place several hours (or days, depending on the environmental conditions) after the precipitation event (Leitinger et al, 2010, Sugiura et al, 2003). This error can be mitigated by an heating system that melts the particles as soon as are collected by the funnel. All these errors can be mitigated and reduced, but in general not eliminated, by a careful maintenance of the instrument.

A number of *a posteriori* correction strategies have been developed in order to correct precipitation data measured by raingauges, but mainly apply at longer accumulation intervals, daily to monthly (Wagner, 2009)

| Country  | Minimum detectable rainrate | Maximum detectable rainrate (mm h <sup>-1</sup> ) | Heating system (Y/N) | cumulation interval (min) |
|----------|-----------------------------|---|----------------------|---------------------------|
| Belgium  | 0.1 mm                      | N/A**   | N                    | 60                        |
| Bulgaria | 0.1 mm                      | 2000  | Υ                    | 120, 1440                 |
| Germany  | 0.05 mm h <sup>-1</sup>     | 3000  | Υ                    | 60                        |
| Italy    | 0.2 mm                      | N/A**   | Y/N*                 | 60                        |
| Poland   | 0.1 mm                      | N/A**   | Υ                    | 10                        |
| Turkey   | 0.2 mm                      | 720   | Υ                    | 1                         |

Table 50 Summary of the raingauge characteristics

Most of these shortcomings could be avoided by using instruments based on different principle or mechanisms. The German network, and a part of the Bulgarian network, as an example, are equipped by precipitation weighting gauges, that allow continuous precipitation (both solid and liquid) measurements with higher accuracy. Other option could be the use of disdrometers, that give more information about the precipitation structure and a more accurate rainrate measure.

In table 53 relevant characteristics of the raingauges used in the different countries are reported.

<sup>\*</sup> only 300 out of 1800 gauges are heated

<sup>\*\*</sup> information not available at the moment: a value about 300 mmh<sup>-1</sup> can be assumed for tipping bucket raingauges.



(Product H02 – PR-OBS-2)

Doc.No: SAF/HSAF/PVR-02/1.1 Issue/Revision Index: 1.1

Date: 30/09/2011 Page: 131/177

### The networks

The validation work carried on with raingauges uses about 3000 instruments across the 6 Countries, as usual, irregularly distributed over the ground. A key characteristic of such networks is the distance between each raingauge and the closest one, averaged over all the instruments considered in the network and it is a measure of the raingauge density. Instruments number and density are summarized in table 55.

The gauges density ranges between 7 (for Bulgaria, where only 3 river basins are considered) to 27 km (for Turkey). These numbers should be compared with the decorrelation distance for precipitation patterns at mid-latitude. Usually the decorrelation distance is defined as the minimum distance between two measures to get the correlation coefficient (Pearson Coefficient) reduced to e<sup>-1</sup>. A recent study on the H-SAF hourly data for Italy, shows this decorrelation distance varies from about 10 km in warm months (where small scale convection dominates) to 50 km in cold months, when stratified and long lasting precipitation mostly occur. In figure 97 the value of the linear correlation coefficient is computed between each raingauge pair in the Italian hourly 2009 dataset, as function of the distance between the two gauges.

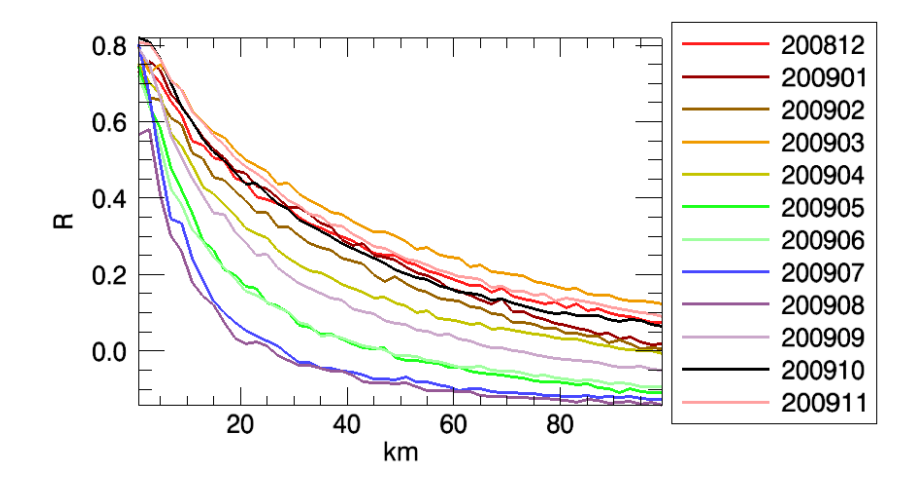


Figure 94 Correlation coefficient between raingauge pairs as function of the distances between the gauges. Colours refer to the months of the year 2009

Assuming these values significant for the other Countries involved in this study, we can conclude the distribution of gauges is capable to resolve the spatial structure of rain patterns only for stratified systems but it is inadequate for small scale convective events.

| Country  | Total number of gauges * | Average minimum distance (km) |
|----------|--------------------------|-------------------------------|
| Belgium  | 89**                     | 11.2                          |
| Bulgaria | 37***                    | 7                             |
| Germany  | 1300                     | 17                            |
| Italy    | 1800                     | 9.5                           |
| Poland   | 330-475                  | 13.3                          |
| Turkey   | 193****                  | 27                            |

Table 51 Number and density of raingauges within H-SAF validation Group



(Product H02 - PR-OBS-2)

Doc.No: SAF/HSAF/PVR-02/1.1 Issue/Revision Index: 1.1

Date: 30/09/2011 Page: 132/177

\* the number of raingauges could vary from day to day due to operational efficiency within a maximum range of 10-15%.

- \*\* only in the Wallonia Region
- \*\*\* only in 3 river basins
- \*\*\*\* only covering the western part of Anatolia

## Data processing

The partners of the Validation Group have been using a variety of different strategies to treat gauge data and to compare them with satellite estimates. Some are using interpolation algorithms to get spatially continuous rainfall maps, while others process directly the measurements of individual gauges. All the data in the network (except for cold months in Poland) are quality controlled: there is no information about the techniques used, but usually quality control rejects data larger than a given threshold and in case of too high rainrate difference (exceeding given thresholds) among neighbouring gauges and between subsequent measures of the same instrument. Table 52 summarizes the data preprocessing performed in different Countries, while Table 53 and Table 54 report the different matching approaches for H01-H02 and H03-H05, respectively.

As for the temporal matching, the used approaches are rather homogeneous within the Groups: instantaneous measurements are matched with next ground cumulated values over the different available intervals, ranging from 1 minute (Turkey) to 1 hour (Italy, Germany). Cumulated estimates, obviously, are compared to ground measured rain amounts over the same cumulation intervals.

As for spatial matching, different approaches are considered, also taking into account the different spatial structure of the satellite IFOVs. Two basic ideas are pursued: pixel-by-pixel matching or ground measure averaging inside satellite IFOV. The second approach seems to be more convenient, especially when the "large" IFOV of H01 and H02 are concerned. Probably it is mandatory for H02 also take into account that the size of the IFOV changes across the track and could become very large. The first approach, e.g. nearest neighbour, can be more effective for H03 and H05 products.

| Country  | Type of interpolation   | Quality control (Y/N)  |
|----------|-------------------------|------------------------|
| Belgium  | Barnes over 5x5 km grid | Υ                      |
| Bulgaria | Co kriging              | Υ                      |
| Germany  | Inverse square distance | Υ                      |
| Italy    | Barnes over 5x5 km grid | Υ                      |
| Poland   | No                      | Y (except cold months) |
| Turkey   | No                      | Υ                      |

**Table 52 Data pre-processing strategies** 

|           | H  | 01  | H02  |   |  |
|-----------|--|---|--|---|--|
| Country   | Spatial matching   | Temporal matching   | Spatial matching   | Temporal matching   |  |
| Belgium*  | N/A  | N/A   | N/A  | N/A   |  |
| Bulgaria* | N/A  | N/A   | N/A  | N/A   |  |
| Germany   | matching gauges are<br>searched on a radius<br>of 2.5 km from the<br>IFOV centre | each overpass is<br>compared to the<br>next hourly rain<br>amount | matching gauges are<br>searched on a radius<br>of 2.5 km from the<br>IFOV centre | each overpass is<br>compared to the<br>next hourly rain<br>amount |  |
| Italy     | mean gauges value<br>over 15x15 km area  | each overpass is compared to the                                  | Gaussian-weighted mean gauges value  | each overpass is compared to the                                  |  |



(Product H02 - PR-OBS-2)

Doc.No: SAF/HSAF/PVR-02/1.1 Issue/Revision Index: 1.1

Date: 30/09/2011

Page: 133/177

|        | centred on satellite | next hourly rain     | centred on satellite | next hourly rain     |
|--------|----------------------|----------------------|----------------------|----------------------|
|        | IFOV                 | amount               | IFOV                 | amount               |
| Poland | mean gauges value    | each overpass is     | mean gauges value    | each overpass is     |
|        | over the IFOV area   | compared to the      | over the IFOV area   | compared to the      |
|        | (rectangular)        | next 10-minutes rain | (rectangular)        | next 10-minutes rain |
|        |                      | amount               |                      | amount               |
| Turkey | weighted mean        | each overpass is     | weighted mean        | each overpass is     |
|        | (semi variogram)     | compared to the      | (semi variogram)     | compared to the      |
|        | gauges value         | corresponding 1-     | gauges value over    | corresponding 1-     |
|        | centred on satellite | minute rain rate     | centred on satellite | minute rain rate     |
|        | IFOV                 |                      | IFOV                 |                      |

Table 53 Matching strategies for comparison with H01 and H02

<sup>\*</sup>Belgium and Bulgaria use raingauges only for cumulated precipitation validation.

|           | H  | 03   | H05  |   |  |
|-----------|--|--|--|---|--|
| Country   | Spatial matching   | Temporal matching  | Spatial matching   | Temporal matching   |  |
| Belgium*  | N/A  | N/A  | Nearest neighbour  | rain amounts in the same number of hours are compared (24 hours)                |  |
| Bulgaria* | N/A  | N/A  | Nearest neighbour  | rain amounts in the<br>same number of<br>hours are compared<br>(3 and 24 hours) |  |
| Germany   | matching gauges are<br>searched on a radius<br>of 2.5 km from the<br>IFOV centre | each overpass is<br>compared to the<br>next hourly rain<br>amount                      | matching gauges are<br>searched on a radius<br>of 2.5 km from the<br>IFOV centre | rain amounts in the same number of hours are compared (3, 6, 12 and 24 hours).  |  |
| Italy     | Nearest neighbour  | the average rainrate<br>over a given hour Is<br>compared to next<br>hourly rain amount | Nearest neighbour  | rain amounts in the same number of hours are compared (3,6,12 and 24 hours).    |  |
| Poland    | mean gauges value over the pixel area  | each overpass is<br>compared to the<br>next 10-minutes rain<br>amount                  | mean gauges value over the pixel area  | rain amounts in the same number of hours are compared(3,6,12 and 24 hours).     |  |
| Turkey    | weighted mean (semi variogram) gauges value centred on satellite IFOV            | each overpass is<br>compared to the<br>corresponding 1-<br>minute rain rate            | weighted mean (semi variogram) gauges value over centred on satellite IFOV       | rain amounts in the same number of hours are compared (3,6,12 and 24 hours).    |  |

Table 54 Matching strategies for comparison with H03 and H05

<sup>\*</sup>Belgium and Bulgaria use raingauges only for cumulated precipitation validation.



(Product H02 - PR-OBS-2)

Doc.No: SAF/HSAF/PVR-02/1.1 Issue/Revision Index: 1.1

Date: 30/09/2011 Page: 134/177

## **Conclusions**

After this inventory some conclusion can be drawn.

First, it seems the raingauge networks used in this validation activities are surely appropriated for the validation of cumulated products (1 hour and higher), while for instantaneous estimates the use of hourly cumulated ground measurements surely introduces intrinsic errors in the matching scores, that can be estimated as very large. The validation of instantaneous estimates should be carried on only when gauges cumulation interval is 10 to 15 minutes (as in Poland). Values cumulated over shorter intervals (5 or even one minute, as it is done in Turkey) are affected by large relative errors in cases of low/moderate rainrates.

Different approaches for the estimates matching are considered, and probably could be a good idea to harmonize them among partners. As an example, for H02 a document was delivered by the developers, where the best estimate-ground reference matching strategy was indicated, and also Angelo Rinollo delivered few years ago the code for the Gaussian weight of the antenna pattern in the AMSU/MHS IFOV.

Anyway, different approaches over different Countries are leading to very similar values in the considered skill scores, indicating probably two things: 1) none of the considered approaches can be considered as inadequate and (more important) 2) the differences between ground fields and satellite estimates are so large that different views in the data processing do not results in different numbers.

### References

- Duchon, C.E. and G.R. Essenberg, G. R., 2001, Comparative rainfall observations from pit and aboveground gauges with and without wind shields, *Water Resour. Res.*, **37**, 3253–3263.
- Duchon, C.E. and C.J. Biddle, 2010, Undercatch of tipping-bucket gauges in high rain rate events. *Adv. Geosci.*, **25**, 11–15.
- Leitinger, G., N. Obojes and U. Tappeiner, 2010, Accuracy of winter precipitation measurements in alpine areas: snow pillow versus heated tipping bucket rain gauge versus accumulative rain gauge, EGU General Assembly 2010, held 2-7 May, 2010 in Vienna, Austria, p.5076.
- Sevruk, M. Ondrás, B. Chvíla, 2009, The WMO precipitation measurement intercomparisons, *Atmos. Res.*, **92**, 376-380.
- Sugiura, K., D. Yang, T. Ohata, 2003, Systematic error aspects of gauge-measured solid precipitation in the Arctic, Barrow, Alaska. *Geophysical Research Letters*, **30**, 1-5.
- Schutgens, N.A.J. and R.A. Roebeling, 2009, Validating the validation: the influence of liquid water distribution in clouds on the intercomparison of satellite and surface observations, *J. Atmos. Ocean. Tech.*, **26**, 1457-1474
- Tokay, A., D.B. Wolff, K.R. Wolff and P. Bashor, 2003, Rain Gauge and Disdrometer Measurements during the Keys Area Microphysics Project (KAMP). *J. Atmos. Oceanic Technol.*, **20**, 1460-1477.
- Wagner, A., 2009, Literature Study on the Correction of Precipitation Measurements, FutMon C1-Met-29(BY), 32 p. available at www.futmon.org.



(Product H02 - PR-OBS-2)

Doc.No: SAF/HSAF/PVR-02/1.1 Issue/Revision Index: 1.1

Date: 30/09/2011 Page: 135/177

## 10 Annex 3: Working Group 2 "Radar data"

#### **PROPOSAL**

Radar rainfall estimation is influenced by several error sources that should be carefully handled and characterized before using it as a reference for ground validation of any satellite-based precipitation products.

The main issues to deal with are:

- 1. system calibration,
- 2. contamination by non-meteorological echoes, i.e. ground clutter, sea clutter, "clear air" echoes (birds, insects), W-LAN interferences,
- 3. partial or total beam shielding,
- 4. rain path attenuation,
- 5. wet radome attenuation,
- 6. range dependent errors (beam broadening, interception of melting snow),
- 7. contamination by dry or melting hail ("hot spots"),
- 8. variability of the Raindrop Size Distribution (RSD) and its impact on the adopted inversion techniques

Some of them are typically handled by resorting to standard procedures, some others requires the availability of dual-polarized observations. Generally speaking, there are not correction methodologies applicable worldwide. The knowledge of the radar system and the environmental conditions makes the difference when approaching such problems.

During the Precipitation Product and Hydrological Validation workshop held in Bratislava the 20-22 of October 2010 the Precipitation Product Validation Group (PPVG) has decided to set up a working group on the radar data use in the validation procedures. This WG is not aimed at promoting the acceptance of shared data processing chain.

What really matter for us is the characterization of the error sources through the construction of appropriate "quality maps".

As requested by the hydro-meteorological community, many operational institutions already provide such information, others are currently working on this task.

The main aims of this WG are:

- to describe the characteristics and generated products of PPVG radar networks;
- to produce a referenced documentation on minimal requirements for certifying the radar products quality, radar rainfall products testing and the procedure for satellite products validation;
- to develop the code to be used in the PPVG for satellite products validation.

## **Activities:**

#### First step - collect:

- characteristics ((polarization, beam width, maximum range, range, resolution, scan frequency, geographical coordinates, scan strategy[elevations], number of integrated samples, etc.) of the radar networks which composes the PPVG
- adopted processing chain;



(Product H02 - PR-OBS-2)

Doc.No: SAF/HSAF/PVR-02/1.1 Issue/Revision Index: 1.1

Date: 30/09/2011 Page: 136/177

• generated products (including the quality map, if any); **Start Time - End time :** December 2010 - February 2011

First Report: 10<sup>th</sup> of Febrary 2011

**Second step**- define on the base of published papers and studies of the characteristics of the radar data available inside the PPVG:

- minimal requirements for certifying the radar products quality;
- radar rainfall products testing;
- identification of the test bed scenario for satellite products validation.

Start Time-End time: January 2011 – July 2011

Second Report: 31<sup>st</sup> of March 2011 Final Report: 31<sup>st</sup> of July 2011

Third step-code (possible Matlab) realization for:

 comparison between radar data and satellite products on SSMI, AMSU-B and SEVIRI satellite grid.

Start Time-End time: June 2011- November 2011

Codes delivery and related documentation: 30<sup>th</sup> of November 2011

## Composition of the working group:

Coordinators: Estezr Labo (HMS) Hungary and Gianfranco Vulpiani (DPC), Italy

Participants: Belgium, Germany, Hungary, Italy, Slovakia, Turkey.

### FIRST REPORT AND SECOND REPORT

Reported by Eszter Lábó, Hungarian Meteorological Service

Contributors: Gianfranco Vulpiani (DPC, Italy), Angelo Rinollo (Belgium), Jan Kanak and Luboslav Okon (Slovakia), Firat Bestepe (Turkey), Rafal Iwanski (Poland), Claudia Rachimow (Germany)

## **Description of tasks:**

In the HSAF project, satellite-based precipitation estimations are compared regularly with the radarderived precipitation fields. However, radar rainfall products are influenced by several error sources that should be carefully analyzed and possibly characterized before using it as a reference for validation purposes.

However, we have to emphasize that the radar data used for validation purposes is not developed by the validation groups themselves. They are developed within specialized radar working teams in many of the countries. Therefore, it should not be the aim of the work of the Radar WG to improve the radar data used; however, it is specifically expected from the current activities to characterize radar data and error sources of the ground data coming from the radar networks of the Precipitation Validation Group (PPVG).



(Product H02 - PR-OBS-2)

Doc.No: SAF/HSAF/PVR-02/1.1 Issue/Revision Index: 1.1

Date: 30/09/2011 Page: 137/177

Main error sources of radar rainfall estimations are listed in the Radar Working Group description document:

- 1. system calibration,
- 2. contamination by non-meteorological echoes, i.e. ground clutter, sea clutter, "clear air" echoes (birds, insects), W-LAN interferences,
- 3. partial or total beam shielding,
- 4. rain path attenuation,
- 5. wet radome attenuation,
- 6. range dependent errors (beam broadening, interception of melting snow),
- 7. contamination by dry or melting hail ("hot spots"),
- 8. variability of the Raindrop Size Distribution (RSD) and its impact on the adopted inversion techniques

Moreover, several studies have been on radar quality assessments like *S'* alek *M*, Cheze J-L, Handwerker J, Delobbe L, Uijlenhoet R. 2004.: Radar techniques for identifying precipitation type and estimating quantity of precipitation. COST Action 717, Working Group 1 – A review. Luxembourg, Germany; or Holleman, I., D., Michelson, G. Galli, U. Germann and M. Peura, Quality information for radars and radar data, Technical rapport: 2005, EUMETNET OPERA, OPERA\_2005\_19, 77p.

Our main purpose for the first step was to collect characteristics (polarization, beam width, maximum range, range, resolution, scan frequency, geographical coordinates, scan strategy [elevations]...) of the radar networks which composes the PPVG adopted processing chain; and the generated products (including the quality map, if any). This report is intended to present the results of the overview of different radar capacities and instruments in each of the participating countries.

#### Radar sites and radars:

In the PPVG group, we have all together 54 radars used, or in the plan to be used. Their distribution in the countries is:

- Belgium (1 radar)
- Germany (16 radars not BfG products)
- ➤ Hungary (3 radars)
- > Italy (18 radars)
- Slovakia (2 radars)
- Poland (8 radars)
- Turkey (6 radars)

These radars cover wide range of geographical area: from the longitude 5.50562 in Wideumont, Belgium to the most Eastern area with longitude 32°58'15" in Ankara, Turkey; and from the Northern latitude of 54°23′03,17" in Gdańsk, Poland to the latitude of 36°53'24" in Mugla, Turkey and lat 37,462 in Catania, Italy.

Radars are built at different elevations above the sea level. In mountainous countries, they are placed at elevations more than 1000m above sea level; whereas in flat countries like Hungary or Belgium, their height position is not exceeding 400m. This information collected will be useful in the future steps of the Working Group to assess the partial or total beam shielding by mountains in the propagation way of the radar signals.

All radars are C-band radars, working at frequency in C-band, at 5.6 GHz. This is important to know that our radar system is comparable.



(Product H02 - PR-OBS-2)

Doc.No: SAF/HSAF/PVR-02/1.1 Issue/Revision Index: 1.1

Date: 30/09/2011 Page: 138/177

All radars are equipped by Doppler capacity which means that ground clutters can be removed from the radar data measurements effectively; however, not all of them have dual polarization which would be important to correct rain path attenuation.

#### Scan strategies:

We have explored the scan strategy for each of the radars used. In this matter, all countries have shared their information on the number of elevations, minimum and maximum elevations, scan frequency, maximum nominal range distance, and range resolution.

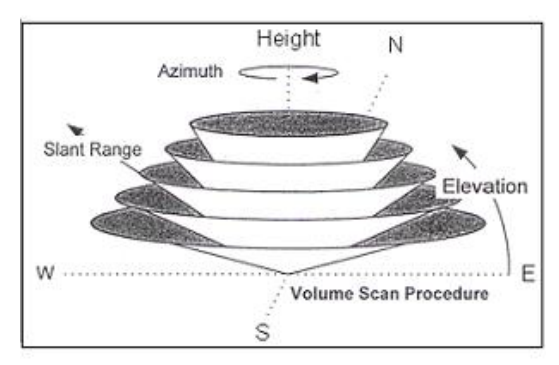


Figure 95 Volume scan procedure

We can conclude that the scan frequency ranges from 5 minutes in Belgium, Germany and Slovakia to 10 minutes in Turkey and Poland, and 15 minutes in Hungary; and varying frequency for Italian radars. The number of elevation stays between 4 and 15, in average around 10.

The range distance used is 240 km in general. But in some places in Italy, and for the Turkish radars, the maximum range distance used is 120 km, or even less, e.g. 80 km.

Range resolution is 250 m in Belgium, 250, 340, 225, and sometimes 500 m for the Italian radars, 500 m for one of the Hungarian radars, and 250m for the other two, Polish radars can work with 125 m and 250 m resolution, and in Turkey it is 250 m for all the radars.

All in all, the scan strategies within the PPVG countries are well-balanced and similar to each other; though they vary from one radar to the other, even within countries.

All radars are regularly maintained and calibrated, which is a good indicator of the continuous supervision of quality of radar data, and the important element to sustain radar data quality.

## Overview of radar products used for validation in the HSAF project:

The Table at the end of the report is provided to summarize the available products generated from radar measurements, and the processing chain used to generate them. Finally, the list of the radar products used for the validation work is included in the last row.

Radar rainfall products are obtained after processing the measured radar reflectivity at different elevations of the radar scan strategy. After each elevation, the PPI (Plan Position Indicator) products and the CAPPI (Constant Altitude PPI) products are calculated. PPI is the measurement of the radar antenna rotating 360 degrees around the radar site at a fixed elevation angle. CAPPI products are derived from this, by taking into account the radar displays which give a horizontal cross-section of data at constant altitude. The CAPPI is composed of data from several different angles that have measured reflectivity at the requested height of CAPPI product.

The PPVG group uses mostly CAPPI products for calculation of rainfall intensities; except for Hungary, which uses the CMAX data (maximum radar reflectivity in each pixel column among all of the radar



(Product H02 - PR-OBS-2)

Doc.No: SAF/HSAF/PVR-02/1.1 Issue/Revision Index: 1.1

Date: 30/09/2011 Page: 139/177

elevations) for deriving rainfall intensities. However, the rest of the countries have also chosen different elevation angles for the CAPPI product which provides the basis for rain rate estimations. Additionally, we have to say that the countries apply different techniques of composition of radar data that were not specified in this questionnaire. The composition technique is important in areas which are covered by more than one radar measurements. Also, the projection applied is varying from one country to the other.

To sum up, the radar products used are not harmonized, different techniques are applied. However, each of them is capable to grasp rainfall and to estimate rainfall intensity.

As for the accumulated products, we see that Belgium uses 24-hourly accumulations, with rain gauge correction, Italy uses 3, 6, 12, 24h accumulations without gauge-correction; in Hungary 3, 6, 12, 24h data is used, but only the 12h and 24 hourly accumulations are corrected by rain gauges, in Poland and Slovakia no rain gauge correction is applied. Poland has only 6, and 24 hourly data. Turkey has 3,6,12,24h data, and applies rain gauge correction for 1 hourly data. It is important to note that techniques used for accumulation are numerous, even within the same country the can differ from one accumulation period to another. E.g. in Hungary, the 3,6h accumulations are derived from summing up the interpolation of the 15minute-frequent measurements into 1 minute-intervals; whereas the 12, and 24 h accumulations are summed up from 15 minute measurements, but corrected with rain gauge data.

All above implies that more probably the quality and error of rainfall and rain rate accumulations is differing from one country to another; and cannot be homogeneously characterized.

### Conclusion of the questionnaire:

### Maintenance

All the contributors declared the system are kept in a relatively good status.

### Correction factors for error elimination:

These correction factors are diverse in the countries, not homogeneous distribution of correction methods:

- > all contributors compensate for non-meteorological echoes (Clutter)
- RLAN interferences implemented in Hungary, Slovakia- in development.
- Poland and Slovakia correct attenuation. In other countries, it is not accounted for.
- Some of the countries are testing new procedures for dealing with VPR (Italy) and Partial Beam Blockage, PBB effects. VPR (Vertical Profile of Reflectivity) used in Turkey.

This means that the corresponding rainfall estimates are diverse, and the estimation of their errors cannot be homogenized.

However, each county can provide useful information of the error structure of its rainfall products based on its own resources: e.g. if they have already defined Quality Indicators, or estimations of errors based on studies of comparison of radar and rain gauge data in the country itself.

In the future, possible separation of reliable and quasi-reliable radar fields would be possible. Separation would be based on radar site/geographical areas/event type/radar products. Selected cases will be suitable enough to be used as a reference for the H-SAF products validation.

Satellite product testing will be carried out in areas with higher reliability. Statistical results will be



(Product H02 - PR-OBS-2)

Doc.No: SAF/HSAF/PVR-02/1.1 Issue/Revision Index: 1.1

Date: 30/09/2011 Page: 140/177

evaluated and compared to previous data. As such, the accuracy of statistical results of PPVG with radar data as ground reference will be able to be established.

#### References

References have been collected from each country describing radar data, radar data quality, and radar data quality estimation techniques. This list will be the baseline for further work of the Radar WG.

The following list of references has been set up:

### **Belgium**

Goudenhoofdt, E. and Delobbe, L.: Evaluation of radar-gauge merging methods for quantitative precipitation estimates, Hydrol. Earth Syst. Sci., 13, 195-203, doi:10.5194/hess-13-195-2009, 2009. http://radar.meteo.be/en/3302595-Publications.html

Berne, A., M. ten Heggeler, R. Uijlenhoet, L. Delobbe, Ph. Dierickx, and M. De Wit, 2005. A preliminary investigation of radar rainfall estimation in the Ardennes region. Natural Hazards and Earth System Sciences, 5, 267-274. <a href="http://radar.meteo.be/en/3302595-Publications.html">http://radar.meteo.be/en/3302595-Publications.html</a>

### Italy

Fornasiero A., P.P. Alberoni, G. Vulpiani and F.S. Marzano, "Reconstruction of reflectivity vertical profiles and data quality control for C-band radar rainfall estimation", Adv. in Geosci., vol. 2, p. 209-215, 2005. <a href="http://www.adv-geosci.net/2/index.html">http://www.adv-geosci.net/2/index.html</a>

R. Bechini, L. Baldini, R. Cremonini, E. Gorgucci . Differential Reflectivity Calibration for Operational Radars, Journal of Atmospheric and Oceanic Technology, Volume 25, pp. 1542-1555, 2008. http://journals.ametsoc.org/doi/pdf/10.1175/2008JTECHA1037.1

Silvestro, F., N. Rebora, and L. Ferraris, 2009: An algorithm for real-time rainfall rate estimation using polarimetric radar: Rime. J. Hydrom., 10, 227–240.

Vulpiani, G., P. Pagliara, M. Negri, L. Rossi, A. Gioia, P. Giordano, P. P. Alberoni, Roberto Cremonini, L. Ferraris, and F. S. Marzano, 2008: The Italian radar network within the national early-warning system for multi-risks management. Proceed. of 5th European Radar Conference (ERAD), Helsinki (Finland); <a href="http://erad2008.fmi.fi/proceedings/extended/erad2008-0184-extended.pdf">http://erad2008.fmi.fi/proceedings/extended/erad2008-0184-extended.pdf</a>

Vulpiani, G., M. Montopoli, L. Delli Passeri, A. Gioia, P. Giordano and F. S. Marzano, 2010: On the use of dual-polarized C-band radar for operational rainfall retrieval in mountainous areas. submitted to J. Appl. Meteor and Clim. <a href="http://www.erad2010.org/pdf/oral/tuesday/radpol2/5">http://www.erad2010.org/pdf/oral/tuesday/radpol2/5</a> ERAD2010 0050.pdf Hungary

Péter Németh: Complex method for quantitative precipitation estimation using polarimetric relationships for C-band radars. Proceed. of 5th European Radar Conference (ERAD), Helsinki (Finland); <a href="http://erad2008.fmi.fi/proceedings/extended/erad2008-0270-extended.pdf">http://erad2008.fmi.fi/proceedings/extended/erad2008-0270-extended.pdf</a>

#### Slovakia

D. Kotláriková, J. Kaň ák and I. Strmiska: Radar horizon modelling as a requirement of SHMI radar network enhancement, Physics and Chemistry of the Earth, <u>Volume 25, Issues 10-12</u>, 2000, Pages 1153-1156

First European Conference on Radar Meteorology, doi:10.1016/S1464-1909(00)00170-2

### **Poland**



(Product H02 - PR-OBS-2)

Doc.No: SAF/HSAF/PVR-02/1.1 Issue/Revision Index: 1.1

Date: 30/09/2011

Page: 141/177

Szturc, J., Ośródka, K., and Jurczyk, A., 2008. Parameterization of QI scheme for radar-based precipitation data. Proceedings of ERAD 2008.

http://erad2008.fmi.fi/proceedings/extended/erad2008-0091-extended.pdf

Szturc, J., Ośródka, K., and Jurczyk, A., 2009. Quality index scheme for 3D radar data volumes, 34<sup>th</sup> Conf. on Radar Meteorology. Proceedings. AMS, 5-9.10.2009, Williamsburg VA, USA;

Katarzyna Osrodka, Jan Szturc, Anna Jurczyk, Daniel Michelson, Gunther Haase, and Markus Peura: Data quality in the BALTRAD processing chain., Proceed. of 6th European Radar Conference (ERAD 2010), Sibiu (Romania);

## http://www.erad2010.org/pdf/oral/wednesday/dataex/06\_ERAD2010\_0240.pdf

Szturc, J., Ośródka, K. and Jurczyk, A. , Quality index scheme for quantitative uncertainty characterization of radar-based precipitation. Meteorological Applications, 2010 (doi: 10.1002/met.230)

|   | BELGIUM  | ITALY  | HUNGARY   |
|---|--|--|---|
| List of<br>Available<br>Products.   | Rain rate 240 Km;<br>rain rate 120 Km;<br>velocity (120 Km);<br>MAX (240 Km);<br>VVP2 Windprofiles;<br>Hail Probability;<br>Hail Probability 24h<br>Overview;<br>1, 3, 24 Hr Rainrate<br>accumulation; |  | CMAX, PPI, CAPPI(2.5 km), VIL, ETops, Base, HailProbability   |
| Is any quality map available?   | NO   | YES  | NO  |
| Processing chain  | Clutter removal (time-domain Doppler filtering and static clutter map); Z-R: a=200, b=1.6  | Clutter suppression by Fuzzy Logic scheme using Clutter map, Velocity, Texture.  Z-R: a=200, b=1.  VPR correction under testing.     | RLAN(wifi) filter; Clutter removal; attenuation correction + beam blocking correction => next Year (2012) VPR => No Z-R: a=200, b=1.6     |
| Description of instantaneous radar product used in HSAF Validation Activities | PCAPPI-1500m<br>Cartesian grid,<br>600m resolution   | Nationale composite:<br>CAPPI 2 km, CAPPI 3 km,<br>CAPPI 5 km, VMI, SRI<br>Projection: Mercator<br>Resolution: 1 km<br>Threshold: No | National composite,<br>(CMAX)<br>Projection:<br>stereographic (S60)<br>Resolution: 2 km<br>Threshold: 7dBZ<br>No rain gauge<br>correction |
| Description of accumulated radar product used in HSAF Validation              | 24-h accumulation with range-dependent gauge adjustment, Cartesian grid, 600m resolution   | Acc. periods: 1, 3, 6, 12, 24h Projection: Mercator Resolution: 1 km Threshold: No   | Acc.periods: 3,6,12,24h National composite, (CMAX) Projection:  |



(Product H02 – PR-OBS-2)

Doc.No: SAF/HSAF/PVR-02/1.1

Issue/Revision Index: 1.1

Date: 30/09/2011 Page: 142/177

| Activities | No r | ain gauge correction | stereographic (S60)   |
|------------|------|----------------------|-----------------------|
|            |      |                      | Resolution: 2 km      |
|            |      |                      | Threshold: 7dBZ       |
|            |      |                      | Rain gauge correction |
|            |      |                      | applied for 12, 24    |
|            |      |                      | hourly data           |

|                | POLAND                   | SLOVAKIA                              | TURKEY                 |
|----------------|--------------------------|---------------------------------------|------------------------|
| List of        | PPI, PCAPPI, RHI, MAX,   | CAPPI 2 km,                           | MAX,                   |
| Available      | EHT, SRI, PAC, VIL, VVP, | Etops,                                | PPI,                   |
| Products.      | HWIND, VSHEAR,           | PPI 0.2,                              | CAPPI,                 |
|                | HSHEAR, LTB, SWI,        | Base,                                 | VIL,                   |
|                | MESO, WRN.               | Cmax,                                 | ETOPS,                 |
|                | List of non-operational  | Hmax,                                 | EBASE,                 |
|                | products: LMR, CMAX,     | VIL,                                  | RAIN Accumulation      |
|                | UWT, VAD, SHEAR, SWI,    | Precip. Intensity, 1h-,               | (1,3,6,12,24h)         |
|                | MESO, ZHAIL, RTR, CTR,   | 3h-, 6h-, 24h-acc.                    |                        |
|                | WRN.                     | precip., 1h-acc.                      |                        |
|                |                          | SRI 1km, 2km agl                      |                        |
| Processing     | Doppler method clutter   | Clutter filtering:                    | Clutter Removal, VPR   |
| chain          | removal; attenuation     | frequency-domain IIR                  | Correction, Z-R:       |
|                | correction - yes;        | filter;                               | A=200 b=1.6            |
|                | VPR => No                | Atmospheric attenuation               |                        |
|                | Z-R: a=200, b=1.6        | correction;                           |                        |
|                |                          | Z-R: a=200, b=1.6                     |                        |
|                |                          | RLAN filtering in                     |                        |
|                |                          | development                           |                        |
| Is any quality | NO, in development       | NO                                    | NO                     |
| map available? |                          |                                       |                        |
| Description of | National composite,      | National composite                    | CAPPI, Projection:     |
| instantaneous  | (SRI); Projection:       | CAPPI 2 km                            | Azimuthal Equidistant  |
| radar product  | azimutal equidistant     | Projection: Mercator                  | Resolution: 250 m      |
| used in HSAF   | (standard: elipsoid);    | Resolution: 1 km                      | Threshold: ? Rain      |
| Validation     | Resolution: 1 km;        | Threshold: -31.5 dBZ                  | Gauge Correction (with |
| Activities     | Threshold: 5 dBZ; No     | No rain gauge correction              | limited number of      |
|                | rain gauge correction.   |                                       | gauges)                |
| Description of |                          | · · · · · · · · · · · · · · · · · · · | Acc.periods:           |
| accumulated    | National composite       | 24h                                   | 1,3,6,12,24h           |
| radar product  | (PAC), Projection:       | National composite                    | Projection: Azimuthal  |
| used in HSAF   | azimuthal equidistant    | CAPPI 2 km                            | Equidistant            |
| Validation     | (standard: elipsoid);    | Projection: Mercator                  | Resolution: 250 m      |
| Activities     | Resolution: 1 km;        | Resolution: 1 km                      | Threshold: ?           |
|                | Threshold: 0,1 mm; No    | Threshold: -31.5 dBZ                  | Rain gauge correction  |
|                | rain gauge correction    | No rain gauge correction              | applied for 1h Rain    |
|                |                          | 55 List of products used              | Acc.                   |



(Product H02 - PR-OBS-2)

Doc.No: SAF/HSAF/PVR-02/1.1 Issue/Revision Index: 1.1

Date: 30/09/2011 Page: 143/177

# 11 Annex 4: Study on evaluation of radar measurements quality indicator with regards to terrain visibility

Ján Kaňák, Ľuboslav Okon, SHMÚ

For validation of H-SAF precipitation products it is necessary to know errors distribution of used ground reference. In this case precipitation intensity or accumulated precipitation measured by SHMÚ radar network is considered as a ground reference. To find distribution of errors in radar range next steps must be done:

- simulations of terrain visibility by radar network using 90m digital terrain model
- statistical comparison of radar data against independent rain gauge data measurements
- derivation of dependence (regression equation) describing the errors distribution in radar range with regard to terrain visibility, based on rain gauge and radar data statistical evaluation
- computation of error distribution maps using regression equation and terrain visibility

24-hour cumulated precipitation measurements from 68 automatic precipitation stations from the period 1 May 2010 – 30 September 2010 were coupled with radar based data. Distribution of gauges according their elevation above the sea level is shown in next figure.

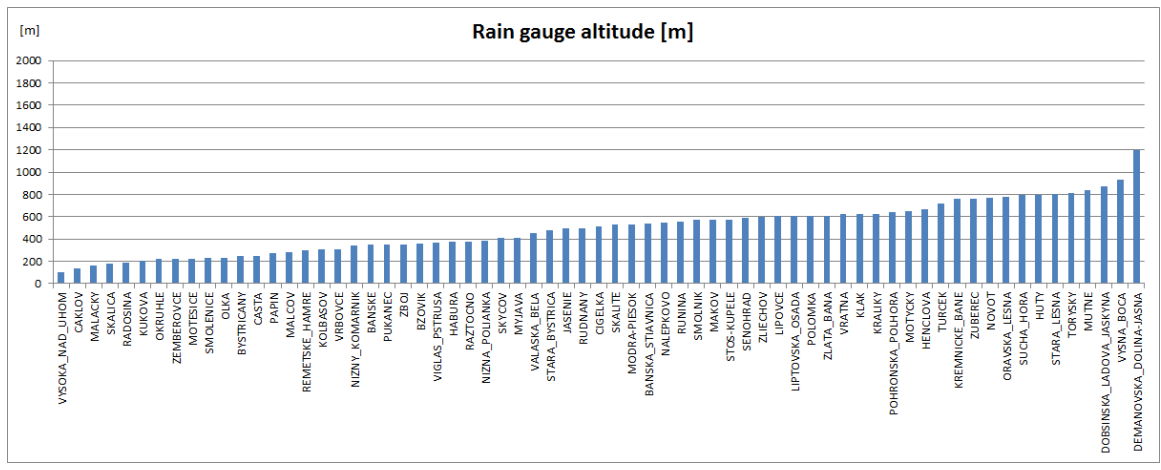


Figure 96 Distribution of rain gauges according their altitude above the sea level

To simulate terrain visibility by meteorological radars Shuttle Radar Topography Mission (SRTM) data were used as an input into radar horizon modeling software developed in SHMÚ. Details about SRTM can be found at <a href="http://en.wikipedia.org/wiki/Shuttle Radar Topography Mission">http://en.wikipedia.org/wiki/Shuttle Radar Topography Mission</a> or directly at <a href="http://www2.jpl.nasa.gov/srtm/">http://en.wikipedia.org/wiki/Shuttle Radar Topography Mission</a> or directly at <a href="http://www2.jpl.nasa.gov/srtm/">http://en.wikipedia.org/wiki/Shuttle Radar Topography Mission</a> or directly at <a href="http://www2.jpl.nasa.gov/srtm/">http://en.wikipedia.org/wiki/Shuttle Radar Topography Mission</a> or directly at <a href="http://www2.jpl.nasa.gov/srtm/">http://www2.jpl.nasa.gov/srtm/</a> SRTM model provides specific data set of terrain elevations in 90 m horizontal resolution in the whole HSAF area where HSAF validation by radars is performed. Modelling software parameters were adjusted for single radar according real scanning strategy:

| Radar Site          | Malý Javorník             | Kojšovská hoľa            |
|---------------------|---------------------------|---------------------------|
| Tower height        | 25m                       | 25m                       |
| Range               | 1200 pixels / 240 km      | 1200pixels/200km          |
| Resulted resolution | 200m/pixel                | 166,67m/pixel             |
| Min elevation       | -0,1 deg                  | -0,8 deg                  |
| Refraction          | 1,3 (standard atmosphere) | 1,3 (standard atmosphere) |
| Elevation step      | 0,01 deg                  | 0,01 deg                  |



(Product H02 - PR-OBS-2)

Doc.No: SAF/HSAF/PVR-02/1.1 Issue/Revision Index: 1.1

Date: 30/09/2011 Page: 144/177

 Azimuth step
 1/40 deg
 1/40 deg

 Layer minimum
 500 m
 500 m

 Layer maximum
 1000 m
 1000 m

 Max displayed height
 5000 m
 5000 m

Radar horizon model provides the following outputs (maps of radar range):

- terrain elevation
- minimum visible height above the sea level
- minimum visible height above the surface
- Layer visibility (defined by minimum and maximum levels)

Results of the horizon model for Malý Javorník and Kojšovská hoľa radar sites are shown on Figure 97. To evaluate the radar visibility over the whole radar network composite picture of minimum visible height above the surface was created and is shown on Figure 98.

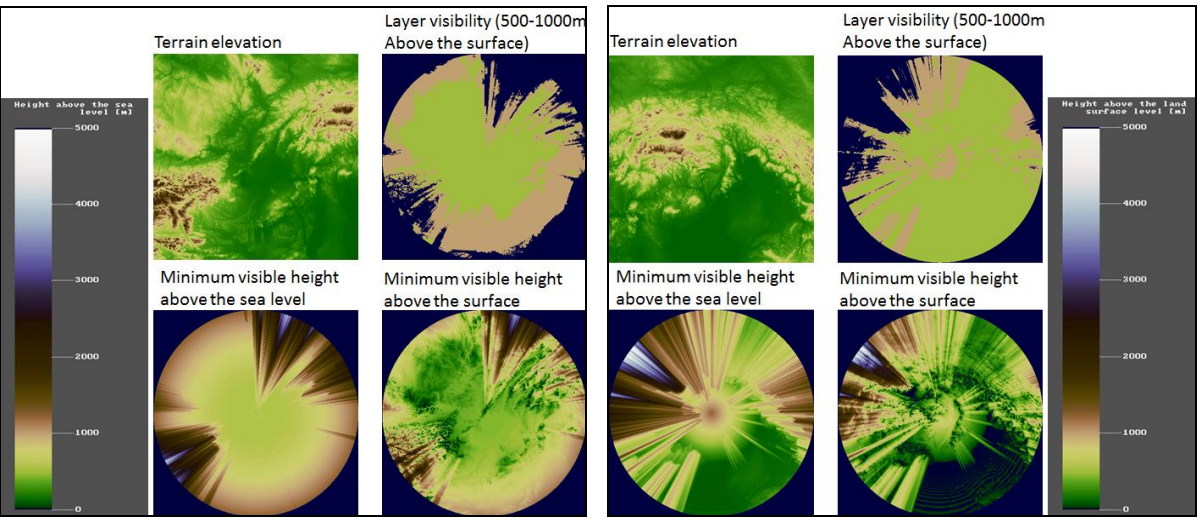


Figure 97 Radar horizon model output for Malý Javorník (left) and Kojšovská hoľa (right) radar sites

Colour scale on left corresponds to the products showing heights above the sea level, scale on right corresponds to the products showing heights above the surface.



(Product H02 - PR-OBS-2)

Doc.No: SAF/HSAF/PVR-02/1.1 Issue/Revision Index: 1.1

Date: 30/09/2011 Page: 145/177

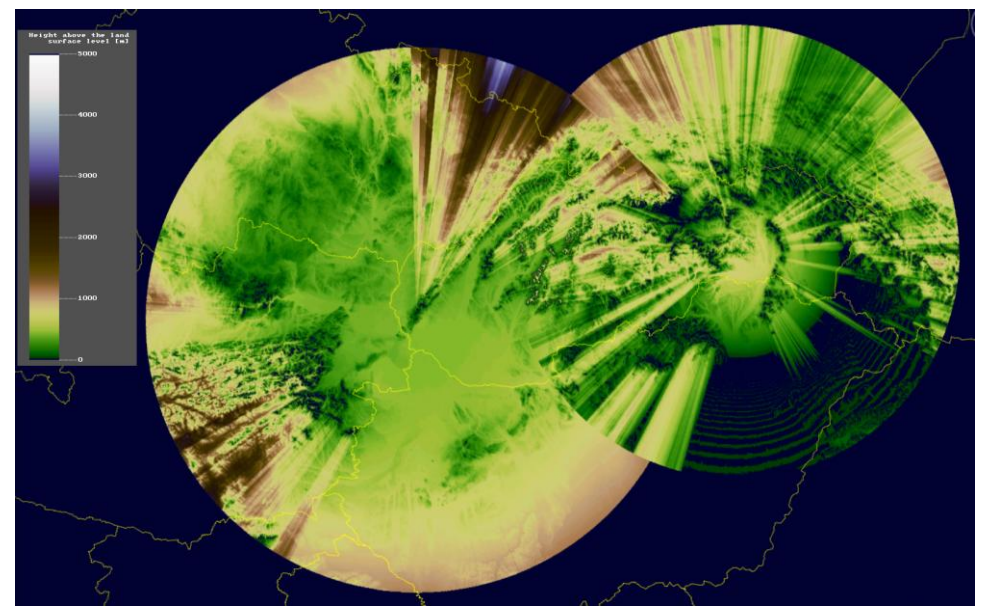


Figure 98 Composite picture of minimum visible height above the surface over the whole radar network.

Compositing algorithm selects the minimum value from both radar sites

In next step minimum visible heights above the rain gauge stations were derived from the composite picture. Distribution of rain gauges according to the minimum visible height of radar beam is shown on next figure. It should be noted that while radar beam elevation is reaching 3000m in northern central part of composite picture, no rain gauge station was available in this region. Only rain gauge stations with minimum visible heights in the interval (0m; 1100m) were available in this study.

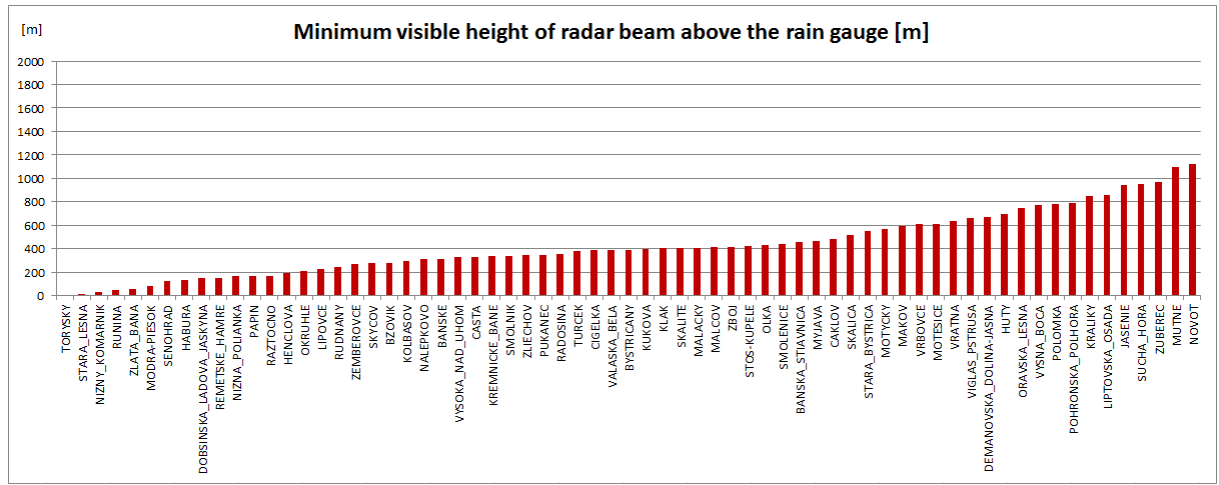


Figure 99 Distribution of rain gauges according to the minimum visible height of radar beam

To understand dependence of radar precipitation estimations and rain gauge values on gauge altitude above the sea and on radar beam altitude the scatterplots of log(R/G) versus station altitude shown on next figure and log(R/G) versus radar beam altitude shown on Figure 101 were generated. Quite wide scattering can be observed but quadratic polynomial trend lines indicate that in general radar underestimates precipitation and this underestimation is proportional to station elevation and radar beam elevation.



(Product H02 - PR-OBS-2)

Doc.No: SAF/HSAF/PVR-02/1.1 Issue/Revision Index: 1.1

Date: 30/09/2011 Page: 146/177

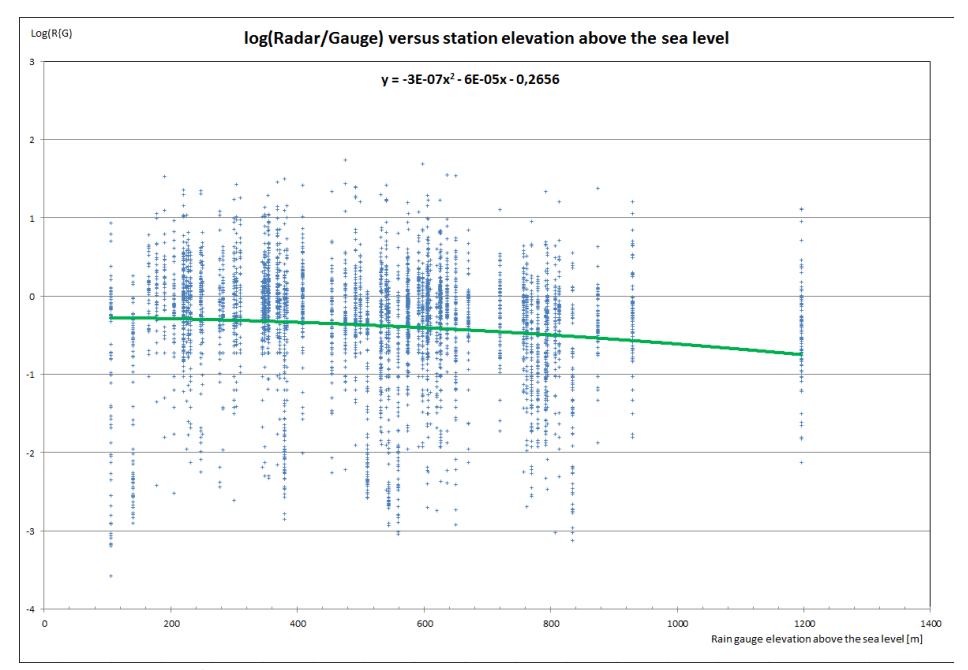


Figure 100 Scatterplot of log(R/G) versus station altitude shows general underestimation of precipitation by radar

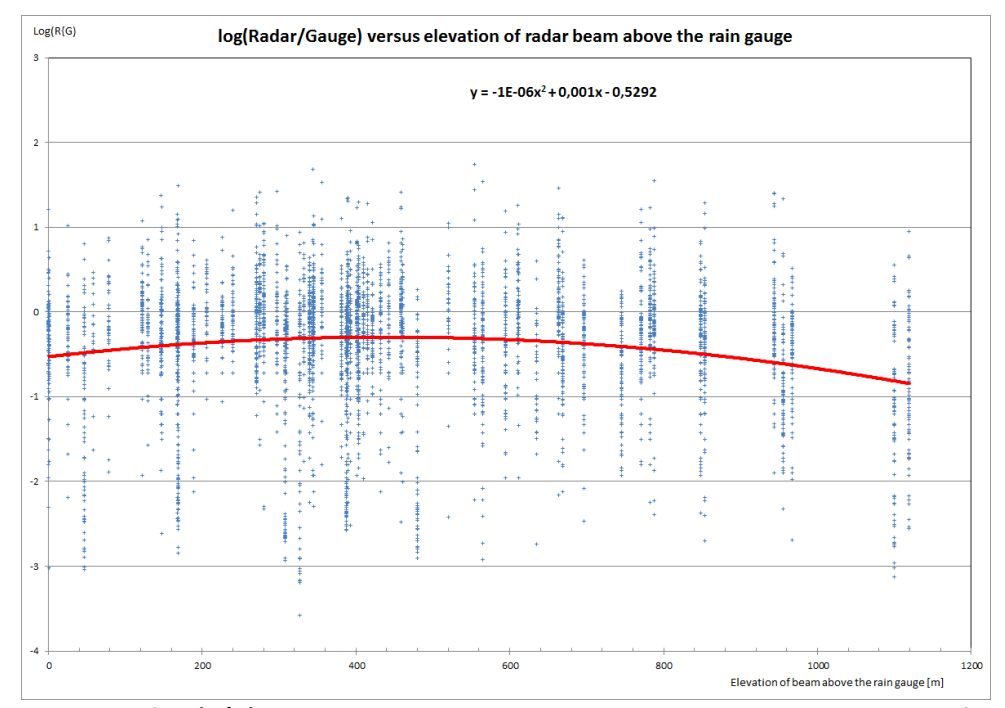


Figure 101 Scatterplot of log(R/G) versus radar beam altitude shows increased underestimation of radar for high and close to zero radar beam elevations

Polynomial trend line on the Figure 98 differs from trend line of Figure 101. While in case of rain gauge altitudes the lowest underestimation by radar can be observed for the lowest rain gauge altitudes, in case of radar beam altitudes the lowest underestimation by radar is observed for radar beam elevation about 500m. Stronger underestimation for rain gauges with close to zero radar beam elevation can be explained by partial signal blocking by terrain obstacles. These are the cases when rain gauge station is close to the top of terrain obstacle.



(Product H02 - PR-OBS-2)

Doc.No: SAF/HSAF/PVR-02/1.1 Issue/Revision Index: 1.1

Date: 30/09/2011 Page: 147/177

Finally set of statistical parameters for each single rain gauge station was computed: mean error, standard deviation, mean absolute error, multiplicative bias, correlation coefficient, RMSE and relative RMSE. Relative RMSE and Mean Error were selected to be specified for radar precipitation measurement over the whole radar range. For this purpose quadratic or linear polynomial trend lines were created as is shown on next figure.

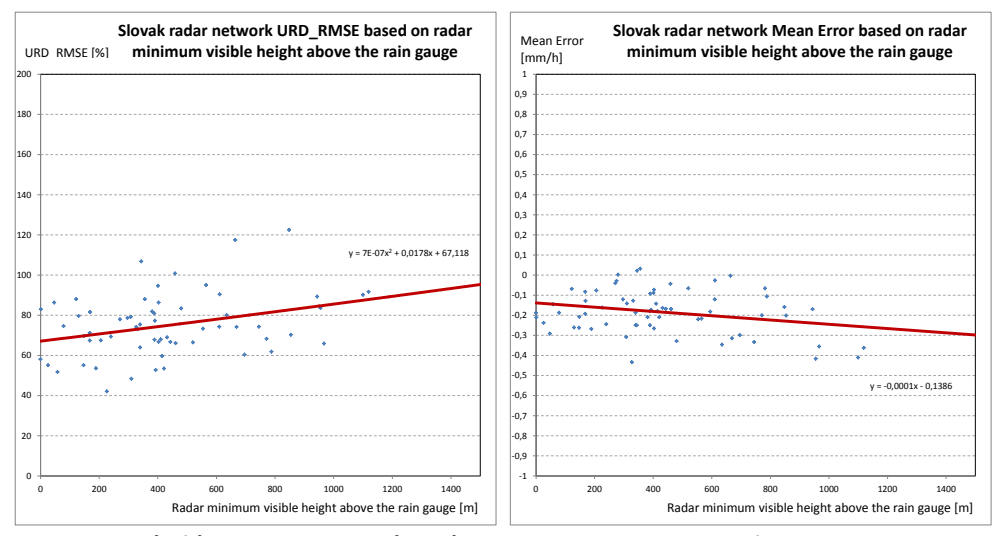


Figure 102 Relative RMSE (left) and Mean Error (right) computed independently for each rain gauge station in radar range and corresponding trend lines extrapolated for beam elevation up to 1500m

Relative RMSE and Mean Error can be specified for each pixel of radar network composite map using regression equations which describe dependence on minimum radar beam elevation above the surface. This can be considered as quality indicator maps of radar measurements with regard to terrain visibility by current radar network of SHMÚ as is shown in next two figures.

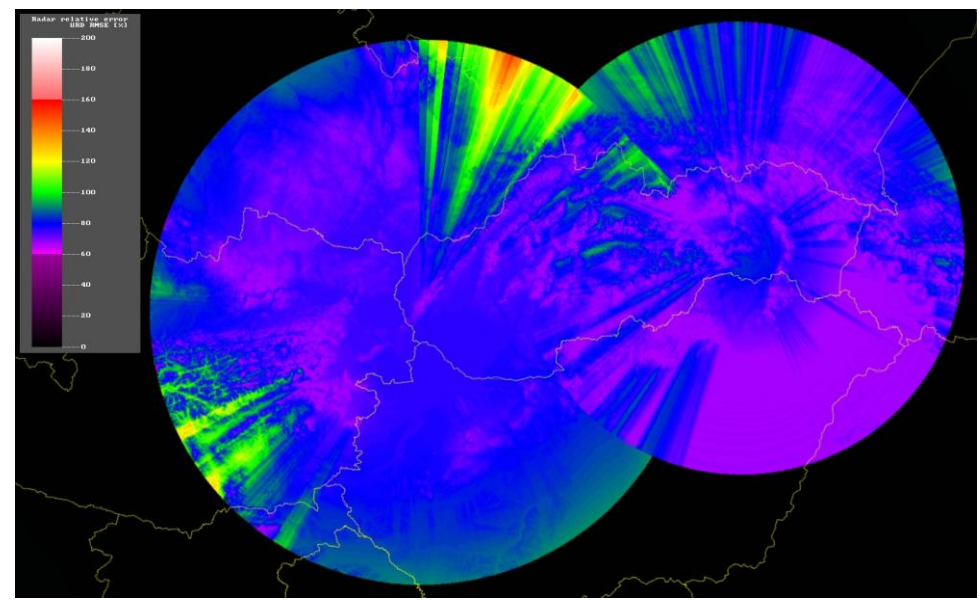


Figure 103 Final relative root mean square error map of radar measurements with regard to terrain visibility by current radar network of SHMÚ



(Product H02 - PR-OBS-2)

Doc.No: SAF/HSAF/PVR-02/1.1 Issue/Revision Index: 1.1

Date: 30/09/2011 Page: 148/177

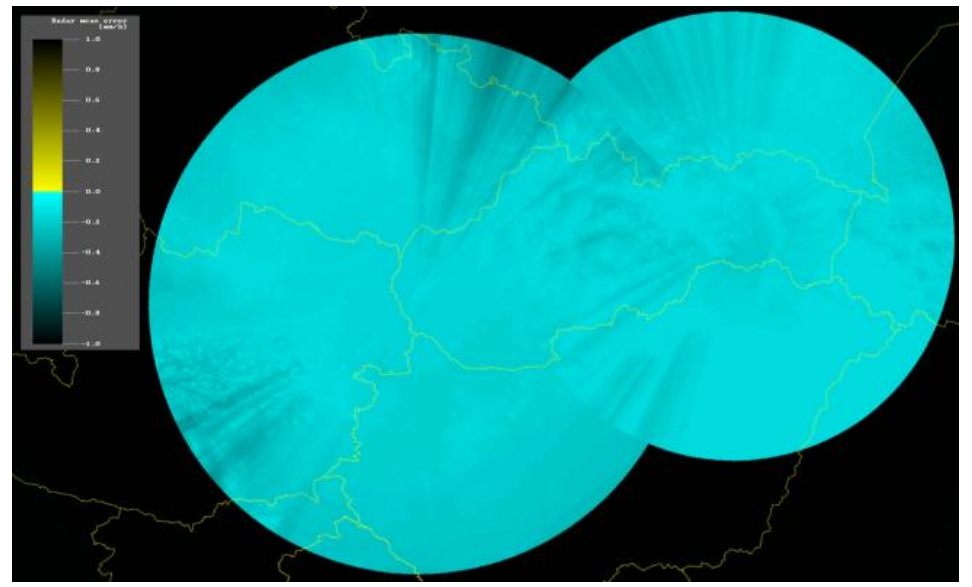


Figure 104 Final mean error map of radar measurements with regard to terrain visibility by current radar network of SHMÚ. General underestimation of precipitation by radars is observed

#### Conclusions

Considering the fact that reference precision of rain gauges used in this study is not sufficient and they do not reflect real ground reference of precipitation fields, obtained results can be considered as a ceiling guess of radar measurements quality indicator with regards to terrain visibility. This result includes also the error of rain gauge network itself.

Also averaged mean error, root mean square error and relative root mean square error values were computed for 68 rain gauge stations located in radar horizons:

Averaged mean error: -0,184 mm/h for instantaneous or -4,42 mm for 24 hours cumulated precipitation

Averaged RMSE: 0,395 mm/h for instantaneous or 9,48 mm for 24 hours cumulated precipitation Averaged URD\_RMSE: 69,3 % for 24 hours cumulated precipitation

It should be noted that all computations in this study were based on 24 hour cumulated precipitation and only re-calculated into instantaneous precipitation. Values of errors in case of instantaneous precipitation can be significantly higher because of short time spacing. Therefore it is planned in the future to calculate errors of radar measurements separately for instantaneous and for cumulated precipitation.



(Product H02 - PR-OBS-2)

Doc.No: SAF/HSAF/PVR-02/1.1 Issue/Revision Index: 1.1

Date: 30/09/2011 Page: 149/177

#### 12 Annex 5: Working Group 3 "INCA Precipitation for PPV"

#### **PROPOSAL**

The "precipitation ground reference" can be only based on certain conceptual models. The validation activity inside H-SAF project is composed by hydrological and product validations. Precipitation captured by river basin is transformed by set of processes into the river discharge. This set of processes is described by hydrological discharge models and by river discharges measured by hydrological equipments. Moreover validation of precipitation products cannot be overcasted by only an evaluation of methods describing transformation of precipitation into river discharge. For this reason a common validation methodology to compare satellite precipitation estimations with ground data (radar and rain gauge) inside the H-SAF project has been defined. The validation of precipitation field is a difficult task and a continuous study of possible validation methodology improvement is necessary. The Precipitation Product Validation Group decided during the last internal workshop held in Bratislava from 20-22 of October 2010 to set up various working groups for the investigation of possible improvement of the validation methodology. One of these working groups is "INCA precipitation for PPV" group.

Definition of INCA Precipitation Products: INCA system consists of computational modules which enable us to integrate various sets of precipitation data sources – raingauge network, radar network, NWP models outputs and climatological standards into common precipitation product, which can describe well the areal instantaneous and cumulated precipitation fields.

The main aims of INCA precipitation for PPV group are:

- to identify the INCA precipitation products which can be considered as "precipitation ground reference" and used for validation of H-SAF products, both instantaneous and cumulated precipitation fields
- to identify the techniques of comparison the INCA precipitation products with satellite precipitation products;
- to develop the code to be used in the PPVG for a correct verification of satellite precipitation product performances with INCA;
- to produce a well referenced documentation on the methodology defined;
- to perform H-SAF products validation based on these techniques and INCA precipitation products;

#### **Activities:**

#### First step:

- identify experts/contact persons inside INCA community which can provide information on INCA system, like methods of precipitation data integration, product formats, data coverage, products availability and quality;
- collect and study INCA methods and products, and to consider how these methods meet requirements of H-SAF precipitation products validation;



(Product H02 – PR-OBS-2)

Doc.No: SAF/HSAF/PVR-02/1.1 Issue/Revision Index: 1.1

Date: 30/09/2011 Page: 150/177

 compare precipitation field reconstructed using radar data, raingauges data, and INCA products for some case studies;

**Start Time-End time:** December 2010 – March 2011

First Report: 31<sup>st</sup> of March 2011

Second step:

- develop common upscaling software tools for proper upscaling of identified INCA products into native H-SAF product's grids;
- select extreme weather events and make case studies on comparison the INCA and H-SAF relevant precipitation products;
- in case of positive case studies to perform batch validation of H-SAF products and provide standard validation statistical outputs (continuous and multicategorical statistics);

**Start Time-End time:** April 2011 – November 2011

Second Report: 31<sup>st</sup> of July 2011 Final Report: 30<sup>th</sup> of November 2011

#### Composition of the working group:

Coordinator: Jan Kanak (SHMU)

Participants: members of H-SAF consortium, which are in parallel involved in development of INCA

products – Belgium, Germany, Italy, Hungary, Slovakia, Turkey.

#### FIRST REPORT

Coordinator: Ján Kaňák (Slovakia)

Participants: Claudia Rachimow and Peter Krahe (Germany), L'uboslav Okon, Jozef Vivoda and Michal

Neštiak (Slovakia), Rafal Iwanski and Bozena Lapeta (Poland), Silvia Puca (Italy)

#### Introduction

This report presents outcomes of the initial activities performed within the "INCA products" working group. In the first part information on the INCA or INCA-like systems available in the participating countries are summarized. The second part of the report presents several case studies comparing precipitation fields estimated by radars, raingauges and the INCA system. Results of the statistical comparison of the PR-OBS-2 product with the different reference fields for selected precipitation events are also included.

#### Summary of the INCA system survey

As a first step of survey experts/contact persons were identified inside the INCA group community as listed in the following table.



(Product H02 - PR-OBS-2)

Doc.No: SAF/HSAF/PVR-02/1.1 Issue/Revision Index: 1.1

Date: 30/09/2011 Page: 151/177

| Country  | Contact person/expert           | E-mail address                                 |
|----------|---------------------------------|--|
| Slovakia | Jozef Vivoda<br>Michal Neštiak  | jozef.vivoda@shmu.sk<br>michal.nestiak@shmu.sk |
| Poland   | Rafal Iwanski                   | rafal.iwanski@imgw.pl                          |
| Germany  | Claudia Rachimow<br>Peter Krahe | rachimow@bafg.de<br>krahe@bafg.de              |

**Table 56 List of contact persons** 

Within the participating countries there are two types of systems providing precipitation analyses usable for H-SAF validation: **INCA** (developed by ZAMG, Austria) and **RADOLAN** (DWD, Germany). The INCA system is currently under development as INCA-CE (Central Europe) and is used in preoperational mode in Slovakia and Poland. The RADOLAN system is used in Germany operationally and is already utilized for the H-SAF products validation.



Figure 105 Coverage of Europe by the INCA and RADOLAN systems

Here below a brief description of the INCA and RADOLAN systems follows. More information on both systems can be found in the documentation which is available on the H-SAF ftp server: /hsaf/WP6000/precipitation/WG\_groups/WG3-inca/documentation

#### Brief description of the INCA system

The INCA (Integrated Nowcasting through Comprehensive Analysis) analysis and nowcasting system is being developed primarily as a means of providing improved numerical forecast products in the nowcasting and very short range forecasting. It should integrate, as far as possible, all available data sources and use them to construct physically consistent analyses of atmospheric fields. Among the input data sources belong:

- NWP model outputs in general (P, T, H, clouds ...)
- Surface station observations (T, precipitation)
- Radar measurements (reflectivity, currently 2-d, 3-d in development)
- Satellite data (CLM, Cloud type, in development for use in precipitation analysis)



(Product H02 - PR-OBS-2)

Doc.No: SAF/HSAF/PVR-02/1.1 Issue/Revision Index: 1.1

Date: 30/09/2011 Page: 152/177

• Elevation data (high resolution DTM, indication of flat and mountainous terrain, slopes, ridges, peaks)

#### The INCA system provides:

- High-resolution analyses interest of validation WG-3
- Nowcasts
- Improved forecasts

#### of the following variables:

- Temperature (3-d field)
- Humidity (3-d)
- Wind (3-d)
- Precipitation (2-d) interest of validation WG-3
- Cloudiness (2-d)
- Global radiation (2-d)

The INCA precipitation analysis is a combination of station data interpolation including elevation effects, and radar data. It is designed to combine the strengths of both observation types, the accuracy of the point measurements and the spatial structure of the radar field. The radar can detect precipitating cells that do not hit a station. Station interpolation can provide a precipitation analysis in areas not accessible to the radar beam.

The precipitation analysis consists of the following steps:

- i. Interpolation of station data into regular INCA grid (1x1 km) based on distance weighting (only nearest 8 stations are taken into account to reduce bull-eyes effect)
- ii. Climatological scaling of radar data by means of monthly precipitation totals of raingauge to radar ratio (partial elimination of the range dependence and orographical shielding)
- iii. Re-scaling of radar data using the latest rain gauge observations
- iv. Final combination of re-scaled radar and interpolated rain gauge data
- v. Elevation dependence and orographic seeding precipitation

In the final precipitation field the raingauge observations are reproduced at the raingauge station locations within the limits of resolution. Between the stations, the weight of the radar information becomes larger the better the radar captures the precipitation climatologically.

Important factor affecting the final precipitation analysis is accuracy and reliability of the raingauge stations. In order to eliminate the influence of raingauge stations providing evidently erroneous data, the SHMÚ is developing the blacklisting technique which temporarily excludes such stations from the analysis. Currently, the stations can be put into the blacklist only manually but development of the automated blacklisting is expected in near future.

#### **Brief description of the RADOLAN system**

RADOLAN is a routine method for the online adjustment of radar precipitation data by means of automatic surface precipitation stations (ombrometers) which has started on a project base at DWD in



(Product H02 - PR-OBS-2)

Doc.No: SAF/HSAF/PVR-02/1.1 Issue/Revision Index: 1.1

Date: 30/09/2011 Page: 153/177

1997. Since June 2005, areal, spatial and temporal high-resolution, quantitative precipitation data are derived from online adjusted radar measurements in real-time production for Germany.

The data base for the radar online adjustment is the operational weather radar network of DWD with 16 C-band sites on the one hand, and the joined precipitation network of DWD and the federal states with automatically downloadable ombrometer data on the other hand. In the course of this, the precipitation scan with five-minute radar precipitation data and a maximum range of 125 km radius around the respective site is used for the quantitative precipitation analyses. Currently, from more than 1000 ombrometer station (approx. 450 synoptic stations AMDA I/II-and AMDA III/S-of DWD; approx. 400 automatic precipitation stations AMDA III/N of DWD; approx. 150 stations of the densification measurement network of the federal states) the hourly measured precipitation amount is used for the adjustment procedure.

In advance of the actual adjustment different preprocessing steps of the quantitative radar precipitation data are performed. These steps, partly already integrated in the offline adjustment procedure, contain the orographic shading correction, the refined Z-R relation, the quantitative composite generation for Germany, the statistical suppression of clutter, the gradient smoothing and the pre-adjustment. Further improvements of these procedures are being developed.

Precipitation distribution of the rain gauge point measurements Precipitation distribution of the areal original radar measurements RADOLAN precipitation product

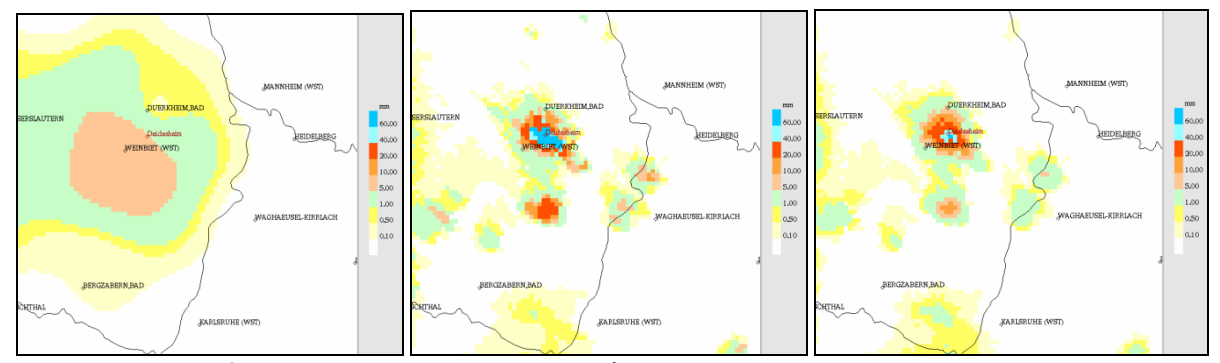


Figure 106 Procedure of the RADOLAN online adjustment (hourly precipitation amount on 7 August 2004 13:50 UTC)

In order to collect more detailed information about both types of systems a questionnaire was elaborated and completed by Slovakia, Poland and Germany. The questionnaire provided details such as geographical coverage (see Figure 105) input data inventory or availability of different instantaneous and cumulated precipitation products.

The final version of the questionnaire is shown in the next table and is also available on the H-SAF ftp server: /hsaf/WP6000/precipitation/WG\_groups/WG3-inca/questionnaire.



(Product H02 - PR-OBS-2)

Doc.No: SAF/HSAF/PVR-02/1.1

Issue/Revision Index: 1.1

Date: 30/09/2011

Page: 154/177

|   | 1   |   |  | T  |  |
|---|---|---|--|--|--|
| Group of information  | ltem  | GERMANY   | POLAND                                   | SLOVAKIA domain1                               | SLOVAKIA domain2                               |
| Availability of documentation for INCA or similar (German) system [Yes/No]      | If possible please attach link or documentation   | Dokumentation received during Helsinki validation meeting | Documentation available from ZAMG        | Documentation available from ZAMG              | Documentation should be issued in future       |
| Definition of geographical area covered by INCA or similar (in Germany) system  | Grid size in pixels   | 900x900   | 741x651                                  | 501x301  | 1193x951                                       |
|   | Min longitude   | 3.5943 E  | 13.82 E                                  | 15.99231 E                                     | 8,9953784943 E                                 |
|   | Max longitude   | 15.71245 E  | 25.334 E                                 | 23.09630 E                                     | 25,9996967316 E                                |
|   | Min latitude  | 46.95719 N  | 48.728 N                                 | 47.13585 N                                     | 45,0027313232 N                                |
|   | Max latitude  | 54.73662 N  | 55.029 N                                 | 50.14841 N                                     | 53,000579834 N                                 |
|   | Space resolution  | 1 km  | 1 km                                     | 1 km   | 1 km   |
| Input data  | Number of radars in network   | Composite of 16 national radars                           | Composite of 8 national radars           | Composite of 2 national radars                 | Composite of 5 international radars            |
|   | Number of precipitation stations  | 1300  | 475 (Poland only)                        | 397 (SHMU, CHMI, ZAMG,<br>IMWM)                | TBD  |
|   | Blacklist for precipitation stations [Yes/No]   | ?   | Yes                                      | Yes  | Yes  |
| Density of raingauge stations   | Map of density of precipitation stations [Yes/No]   | ?   | TBD                                      | TBD  | TBD  |
| Output data   | Instantaneous precipitation based only<br>on raingauge network, time resolution,<br>timelines               | 5 min   | No                                       | Yes, 15 min                                    | Yes, 15 minute                                 |
|   | Instantaneous precipitation based only<br>on radar network, time resolution,<br>timelines                   | 5 min   | No                                       | Yes, 5 minute                                  | Yes, 5 minute                                  |
|   | Instantaneous precipitation based on<br>combined raingauge and radar<br>network, time resolution, timelines | 5 min   | Yes, 10 minutes                          | Yes, 5 minutes                                 | Yes, 5 minutes                                 |
|   | Cumulative precipitation based only on<br>raingauge network, time intervals,<br>timelines                   | 5 min, 1,3,6,12,18,24 hours                               | No                                       | Yes, min 5 min, available<br>1,3,6,12,24 hours | Yes, min 5 min, available<br>1,3,6,12,24 hours |
|   | Cumulative precipitation based only on radar network, time intervals, timelines                             | 5 min, 1,3,6,12,18,24 hours                               | No                                       | Yes, min 5 min, available<br>1,3,6,12,24 hours | Yes, min 5 min, available<br>1,3,6,12,24 hours |
|   | Cumulative precipitation based on combined raingauge and radar network, time intervals, timelines           | 5 min, 1,3,6,12,18,24 hours                               | Yes, min 10 minutes, available in future | Yes, min 5 min, available<br>1,3,6,12,24 hours | Yes, min 5 min, available<br>1,3,6,12,24 hours |
| Dates for selected case studies   | Case 1  | will be set   | No                                       | 29.3.2009                                      |  |
|   | Case 2  |   | No                                       | 13.6.2010                                      |  |
|   | Case 3  |   | No                                       | 20.6.2010                                      |  |
|   | Case 4  |   | No                                       | 1516.8.2010                                    |  |
|   | Case 5  |   | No                                       |  |  |
| Availability of own software for upscaling INCA data into native satellite grid | Н01   | yes   | No                                       | No   | No   |
|   | H02   | yes   | No                                       | No   | No   |
|   | ноз   | yes   | No                                       | No   | No   |
|   | Н04   | no  | No                                       | No   | No   |
|   | но5   | yes   | No                                       | No   | No   |
|   | H06   | yes   | No                                       | No   | No   |

**Table 57 Questionnaire** 

#### **Case studies**

Several case studies comparing the INCA analyses with their source precipitation fields from radars and raingauges and with selected H-SAF products have been elaborated at SHMÚ. The precipitation fields from individual observations have been compared visually but have also been used as a "ground reference" for statistical analysis of the PR-OBS-2 product during selected precipitation events.

#### Case study PR-OBS-1 vs. INCA,15 August 2010 15:00 UTC

This is the first case study elaborated at SHMÚ which compares the PR-OBS-1 product with precipitation fields produced by the INCA system. In order to make precipitation fields from the microwave instruments and ground observations at 1 km resolution comparable, the INCA precipitation fields have been upscaled into the PR-OBS-1 native grid using the Gaussian averaging method.



(Product H02 - PR-OBS-2)

Doc.No: SAF/HSAF/PVR-02/1.1 Issue/Revision Index: 1.1

Date: 30/09/2011 Page: 155/177

Ellipses in next figure represent the satellite instrument IFOVs with colour corresponding to the upscaled radar, rain-gauge and INCA analysis rain-rate value in case of next figure a), b) and c), respectively, or the satellite rain-rate value in case of next figure, part d).

As can be seen in next figure, part b) the rain-gauge network captured intense precipitation near the High Tatras mountain in the northern part of Slovakia where only low precipitation rates were observed by radars (next figure, part a) The resulting INCA analysis is shown in next figure, part c).

The corresponding PR-OBS-1 field (next figure, part d)) shows overestimation even when compared with the rain-gauge adjusted field of the INCA analysis.

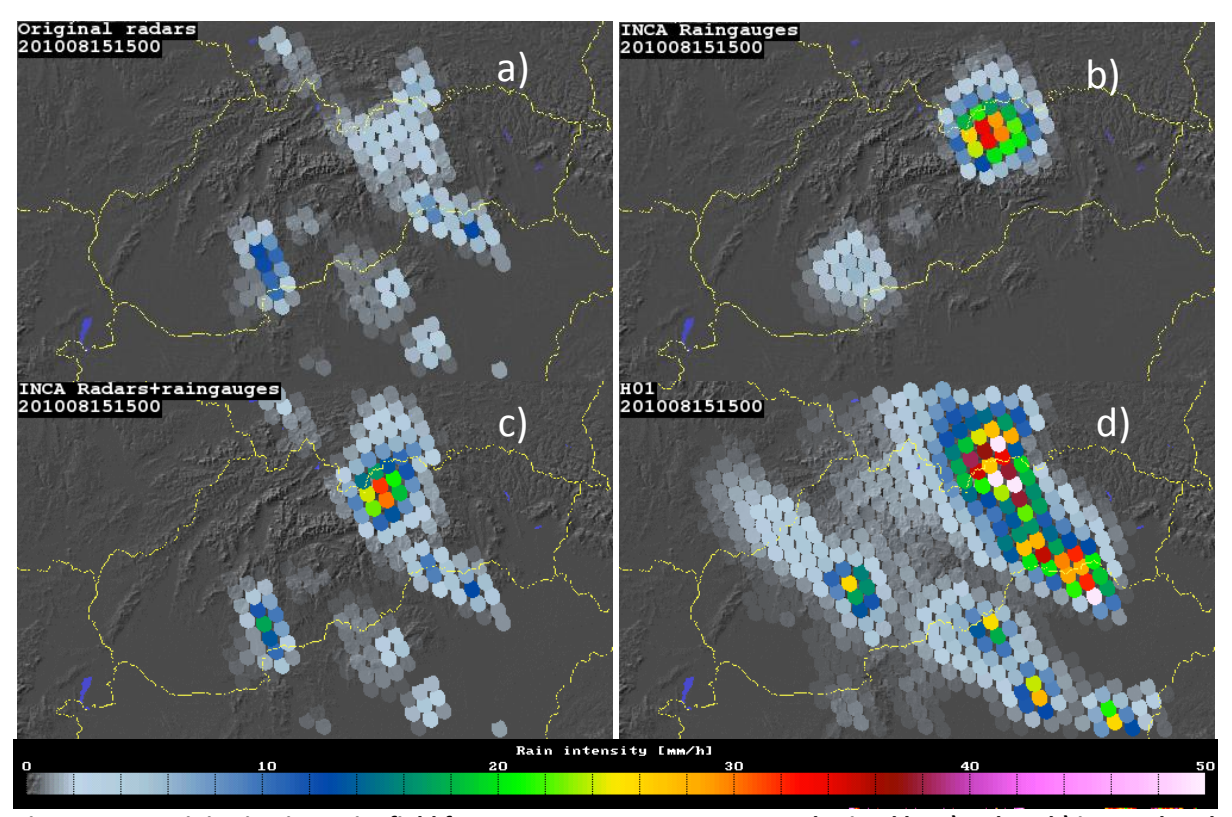


Figure 107 Precipitation intensity field from 15 August 2010 15:00 UTC obtained by a) radars, b) interpolated raingauge data, c) INCA analysis and d) PR-OBS-1 product

#### Visual comparison of the precipitation fields

In this section two case studies from 15 August 2010 focused on performance of the INCA analyses are presented.

#### 15 August 2010, 06:00 UTC

This case illustrates potential of the INCA system to correct errors in radar precipitation measurements due to radar beam attenuation in heavy precipitation. As can be seen in Fig. 3a) the radar measured precipitation near centre of the circled area was relatively weak. However, as Fig. 3c) suggests, the precipitation was probably underestimated by radars because an intense convective cell occurred directly in path of the radar beam (dashed line in Figure 108 part c). The raingauge network (Figure 108 part b) captured the intense precipitation underestimated by radars and improved the INCA analysis (Figure 108 part c).



(Product H02 - PR-OBS-2)

Doc.No: SAF/HSAF/PVR-02/1.1 Issue/Revision Index: 1.1

Date: 30/09/2011

Page: 156/177

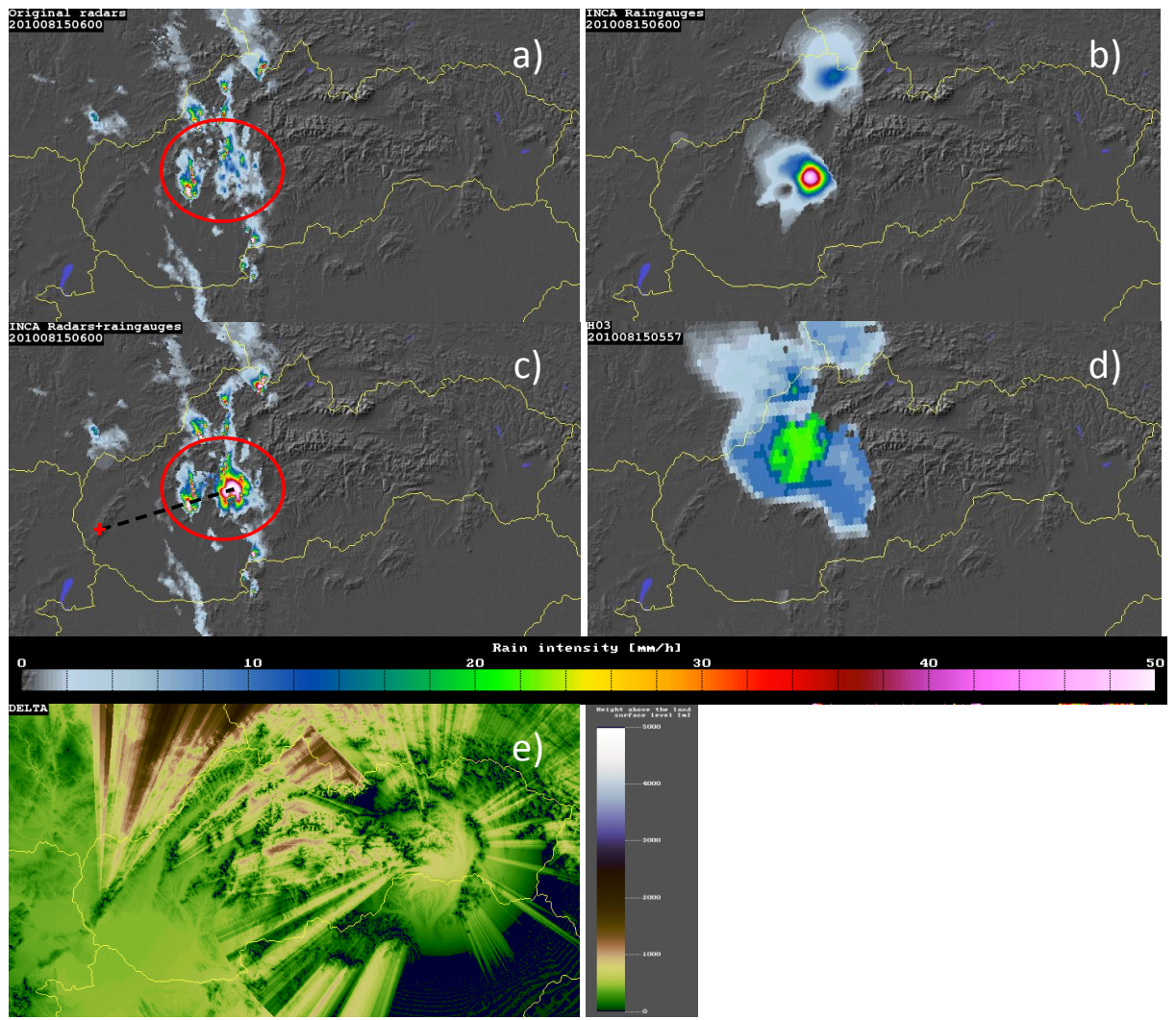


Figure 108 Precipitation intensity field from 15 August 2010 6:00 UTC obtained by a) radars, b) interpolated raingauge data, c) INCA analysis and d) PR-OBS-3 product (5:57 UTC) supplemented with map of minimum visible height above surface level (SHMU radar network)

#### 15 August 2010, 08:00 UTC

The case from 08:00 UTC (Figure 109) gives an example of partial correction of radar beam orographical blocking by the INCA analysis. The radar precipitation field in the north-western part of Slovakia (Figure 109a) is affected by orographical blocking as indicated by relatively high minimum elevations of radar beam above this location in Figure 109e). Also in this case information from raingauge network (Figure 109b) supplemented the radar field in the resulting INCA analysis (Figure 109c).



(Product H02 – PR-OBS-2)

Doc.No: SAF/HSAF/PVR-02/1.1 Issue/Revision Index: 1.1

Date: 30/09/2011 Page: 157/177

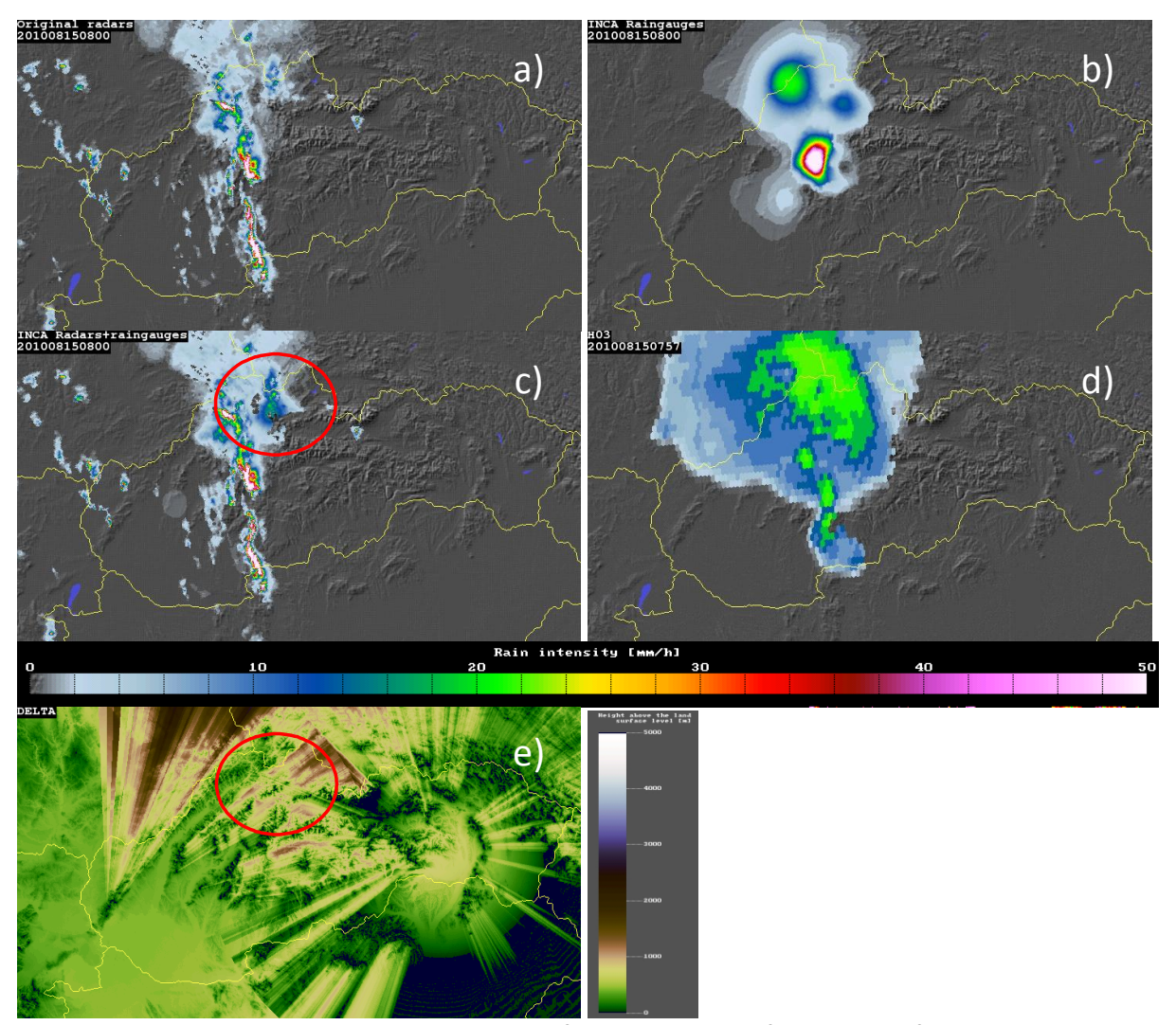


Figure 109 Precipitation intensity field as in previous figure, except for 8:00 UTC

#### Statistical analysis of the PR-OBS-2 product on selected precipitation events

As a first step towards utilizing the INCA precipitation analyses for the H-SAF validation, it has been decided to perform at SHMÚ a statistical analysis of the H-SAF products using the precipitation fields from INCA, radars and raingauges as a "ground reference" data for selected precipitation events. Since this task required modification of the SHMÚ software currently used for upscaling radar data, until now results for the PR-OBS-2 product are only available.

In order to eliminate interpolation artefacts in the areas outside the raingauge network occurring in the INCA analyses, only the PR-OBS-2 data falling inside the Slovakia territory were taken into account in the statistical analysis.

Overall five precipitation events with different prevailing type of precipitation have been selected for the statistical analysis as listed in next table.



(Product H02 – PR-OBS-2)

Doc.No: SAF/HSAF/PVR-02/1.1 Issue/Revision Index: 1.1

Date: 30/09/2011

Page: 158/177

| Event | Period (UTC)                 | Precipitation type |
|-------|------------------------------|--------------------|
| 1     | 15 August 2010 00:00 - 21:00 | convective         |
| 2     | 16 August 2010 06:00 - 23:45 | convective         |
| 3     | 15 September 2010 15:00 -    | mixed              |
|       | 18 September 2010 09:00      |                    |
| 4     | 21 November 2010 20:00 -     | stratiform         |
|       | 22 November 2010 23:45       |                    |
| 5     | 28 November 2010 15:00 -     | stratiform         |
|       | 29 November 2010 10:00       |                    |

Table 58 List of precipitation events selected for statistical analysis

For each precipitation event and each "ground reference" data a set of continuous and dichotomous statistical scores was computed. The scores and thresholds of the precipitation classes were adopted from the H-SAF common validation methodology.

As an example, the results of selected statistical scores obtained with different reference data for the event 1 and 4 are shown in next two figures respectively.

Due to the small number of compared PR-OBS-2 observations during the selected precipitation events (overall convective: 1864 observations, stratiform: 2251, mixed: 3409) the obtained results may not be representative enough. Therefore it is questionable if any conclusion about dependence of the investigated "ground reference" data on the long-term validation results can be made. It is proposed that statistical analysis using longer validation period will have to be performed.



(Product H02 - PR-OBS-2)

Doc.No: SAF/HSAF/PVR-02/1.1

Issue/Revision Index: 1.1 Date: 30/09/2011

Page: 159/177

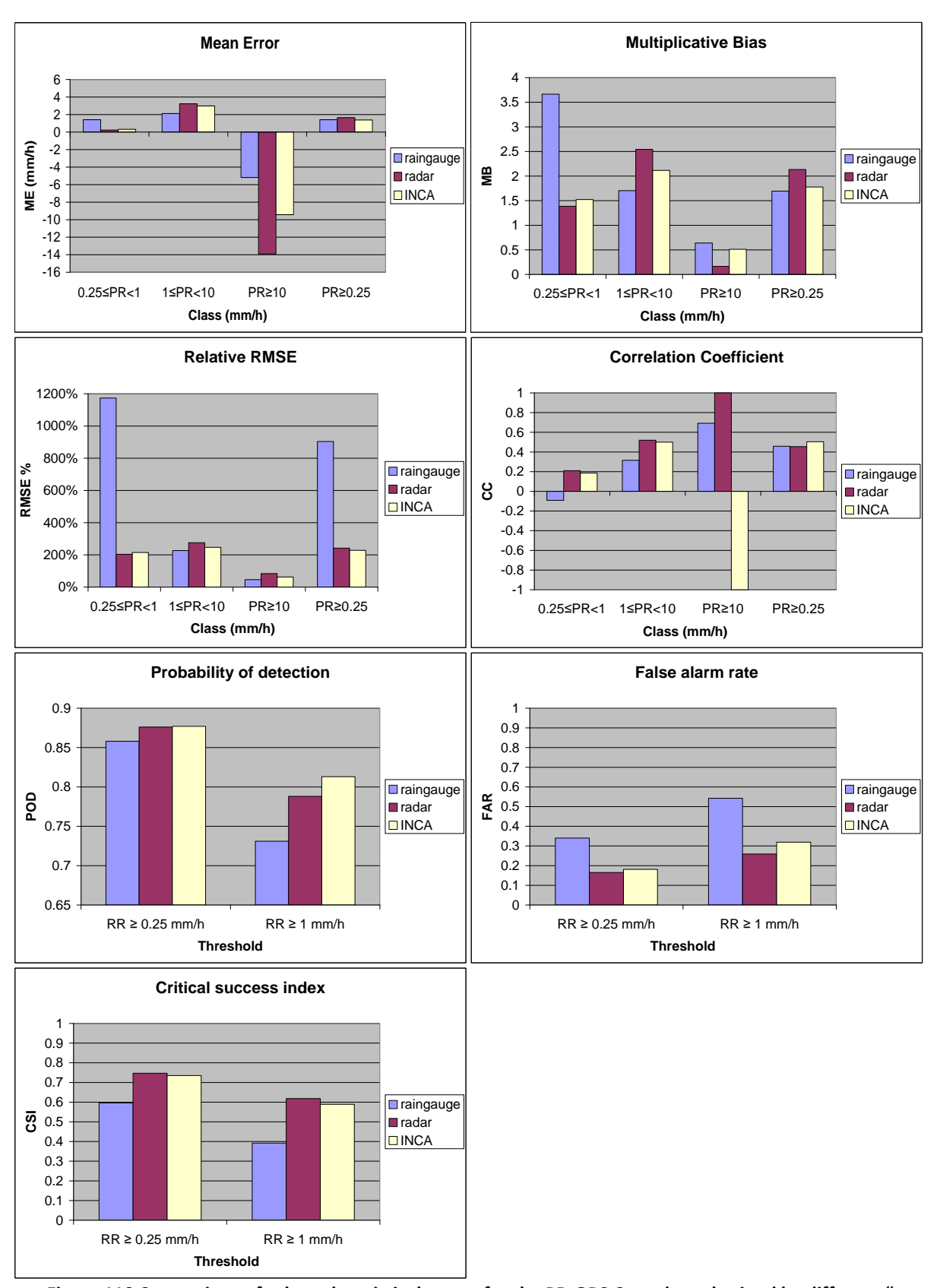


Figure 110 Comparison of selected statistical scores for the PR-OBS-2 product obtained by different "ground reference" data; valid for event 1 (convective)



(Product H02 - PR-OBS-2)

Doc.No: SAF/HSAF/PVR-02/1.1

Issue/Revision Index: 1.1 Date: 30/09/2011

Page: 160/177

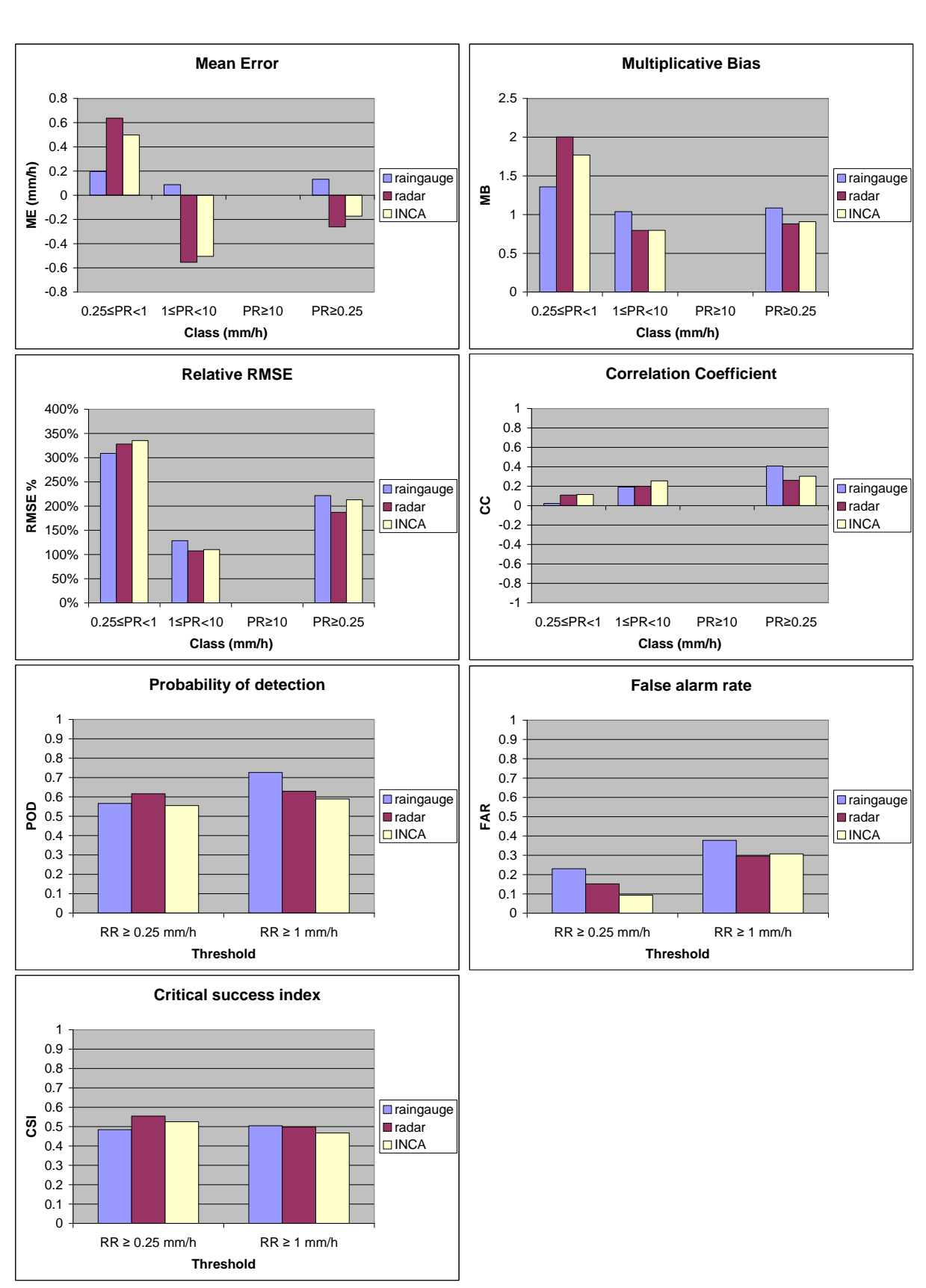


Figure 111 Comparison of selected statistical scores for the PR-OBS-2 product as in previous figure except for event 4 (stratiform)



(Product H02 - PR-OBS-2)

Doc.No: SAF/HSAF/PVR-02/1.1 Issue/Revision Index: 1.1

Date: 30/09/2011 Page: 161/177

#### Conclusion

The INCA system as a potential tool for the precipitation products validation is available in Slovakia and Poland, in both countries being run in pre-operational mode. It is still relatively new system undergoing continuous development. More sophisticated algorithms of the precipitation analysis (e.g. assimilation of the 3-D radar data) can be expected from its development in frame of the ongoing INCA-CE project.

In Germany similar precipitation analysis system called RADOLAN is being run operationally. This tool is already used for validation of the H-SAF precipitation products in this country.

The accuracy and reliability of the raingauge stations significantly affect final precipitation analysis of the INCA or INCA-like systems and therefore need to be checked. In order to solve this problem an automated blacklisting technique is going to be developed at SHMÚ (currently blacklisting is used in manual mode).

The case studies presented in the report comparing the INCA analyses with corresponding input precipitation fields from radars and raingauges pointed out the benefits of the INCA system. It has been shown that the system has potential to compensate errors due to effects like radar beam orographical blocking but also to correct instantaneous factors affecting radar measurement quality like radar beam attenuation in heavy precipitation what cannot be achieved by standard methods of climatological radar data adjustment.

First attempts to utilize the INCA analyses as a "ground reference" data for the H-SAF products validation have been done by statistical analysis of the PR-OBS-2 product during selected precipitation events.

The software for upscaling the INCA precipitation field into the H-SAF products grid will have to be developed. Since the grids of INCA and RADOLAN have similar horizontal resolution to the common radar grid, the radar upscaling techniques can be applied also on the INCA or RADOLAN data. In frame of the unification of the validation methodologies the same common upscaling software could be shared between both radar (WG2) and INCA (WG3) working groups in the future.

#### References:

T.Haiden, A. Kann, G. Pistotnik, K. Stadlbacher, C. Wittmann: Interated Nowcasting through Comprehensive Analysis (INCA) System description. ZAMG, Vienna, Austria, 4 January 2010 André Simon, Alexander Kann, Michal Neštiak, Ingo Meirold-Mautner, Ákos Horváth, Kálmán Csirmaz, Olga Ulbert, Christine Gruber: Nowcasting and very short range forecasting of wind gusts generated by deep convection. European Geosciences Union General Assembly 2011, Vienna, Austria, 03 - 08 April, 2011

Ingo Meirold-Mautner, Benedikt Bica, Yong Wang: INCA-CE: A Central European initiative in nowcasting applications. Central Institute for Meteorology and Geodynamics, Hohe Warte 38, 1190 Vienna, Austria

Ingo Meirold-Mautner, Yong Wang, Alexander Kann, Benedikt Bica, Christine Gruber, Georg Pistotnik, Sabine Radanovics: Integrated nowcasting system f or the Central European area: INCA-CE. Central Institute for Meteorology and Geodynamics (ZAMG), Hohe Warte 38, 1190 Vienna, Austria



(Product H02 - PR-OBS-2)

Doc.No: SAF/HSAF/PVR-02/1.1 Issue/Revision Index: 1.1

Date: 30/09/2011 Page: 162/177

### 13 Annex 6: Working Group 4 "PR-ASS-1 (COSMO grid) validation"

#### **PROPOSAL**

The aim of the group is to find, in cooperation with the developing team of PR-ASS-1, the most reliable way to validate the PR-ASS-1 product, which is provided on the COSMO model grid in a rotated coordinate system, and to develop software tools for a common validation methodology of the product.

#### **Activities:**

**First step** – defining the best validation strategy for PR-ASS-1, depending on the resolution of the ground data used. Implementation of prototype softwarefor grid-cutting and ground data up-scaling in the COSMO grid (with the help of Lucio Torrisi, CNMCA).

Start Time - End time: November 2010 - December 2010

First Report: 20<sup>th</sup> of December 2010

**Second step**- up-scaling software tools dissemination and checks by the different validation teams.

Eventual improving and refining if needed.

Start Time-End time: January 2011 – February 2011

Final Report: 28<sup>th</sup> of February 2011

Codes delivery and related documentation: 28<sup>th</sup> of February 2011

#### **Composition of the working group:**

Coordinator: Angelo Rinollo (RMI, Belgium) supported by Federico Porcù (University of Ferrara, Italy)

and Lucio Torrisi (CNMCA, Italy)

Participants: Belgium, Bulgaria, Germany, Italy, Hungary, Slovakia, Turkey.



(Product H02 – PR-OBS-2)

Doc.No: SAF/HSAF/PVR-02/1.1 Issue/Revision Index: 1.1

Date: 30/09/2011 Page: 163/177

#### **REPORT**

H-SAF project – WP 6100 - Working Group 4: Development of a common procedure for validation of PR-ASS-1 in the native COSMO model grid

A.Rinollo (RMI, Belgium), F.Porcu' (Università di Ferrara, Italy), L.Torrisi (CNMCA, Italy)

#### Validation technique depends on data resolution

The task of the present group is to develop a common validation procedure for the PR-ASS-1 product, characterized by the COSMO model native grid, which is built up in a rotated coordinate system. Depending on the resolution of the ground data, we decided to suggest two different approaches:

-in case of ground data with a spatial sampling similar to the one of COSMO (that is the typical case of raingauge networks), the nearest-neighbor approach is suggested. In this case, no upscaling is needed.

-in case of a resolution of the ground data much finer than the one of COSMO (that is the case of many radar products), then the upscaling to the native COSMO grid is recommended. For this case, we are currently working on a common upscaling procedure.

#### Methodology

The main issue in this task is the fact that PR-ASS-1 is based on the rotated coordinate system of the source model (COSMO), while the ground observations are normally based on geographical coordinates.

For this reason, in case upscaling is needed, a regular portion (i.e. a fixed number of rows and columns) is extracted from the COSMO grid. Then all the coordinates of the ground data are converted in the rotated system, and associated to the grid cell in which they fall in.

At this stage, upscaling technique is straightforward: the upscaled value associated to every grid cell is simply the arithmetical average of all the ground observations falling into that cell.

#### Software development: extraction of a regular subset in the PR-ASS-1 files

The first program we developed, useful to all groups (with both the validation approaches) allows to select a fixed number of rows and columns in the PR-ASS-1 files, given the geographical extremes of the chosen validation area. In this way, it's possible to process uniquely the data falling in and around the region of interest.

#### Software development: upscaling of fine-resolution data to the COSMO grid

A prototype version of the upscaling procedure has been developed and successfully tested over Belgium. It consists of two programs: the first creates a "lookup table", a file which states a correspondence between every point of the observational grid (radar in this case) and the corresponding cell of the chosen subsection of the COSMO grid in which it falls. The second upscales every observational file to the COSMO grid, given the lookup table, and it is part of the Belgian validation procedure previously developed by E. Roulin (RMI, Belgium).

#### **Preliminary testing results**



(Product H02 - PR-OBS-2)

corresponding upscaled images. The images appear correctly upscaled.

Doc.No: SAF/HSAF/PVR-02/1.1 Issue/Revision Index: 1.1

Date: 30/09/2011 Page: 164/177

Here are the preliminary results obtained by testing the upscaling procedure over Belgium. On the left the original images (from Wideumont radar, RMI, Belgium) and on the right the

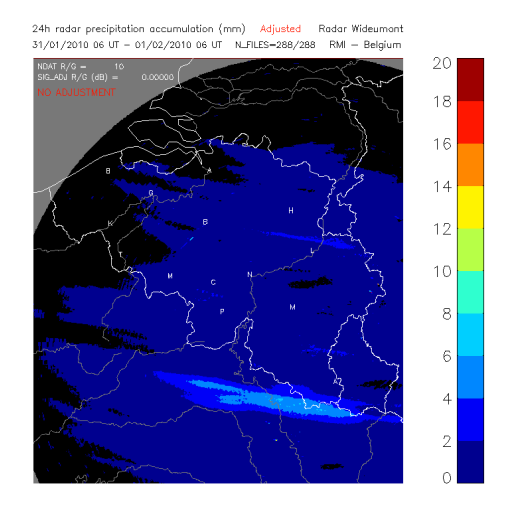


Figure 112 The Wideumont radar image of 1/2/2010 (cumulated rainfall in the previous 24 hours, raingauge-adjusted)

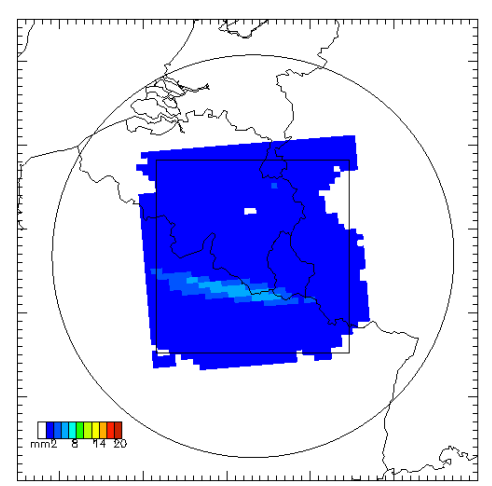


Figure 113 The Wideumont radar image of 1/2/2010 upscaled to the COSMO grid

.



(Product H02 - PR-OBS-2)

Doc.No: SAF/HSAF/PVR-02/1.1 Issue/Revision Index: 1.1

Date: 30/09/2011

Page: 165/177

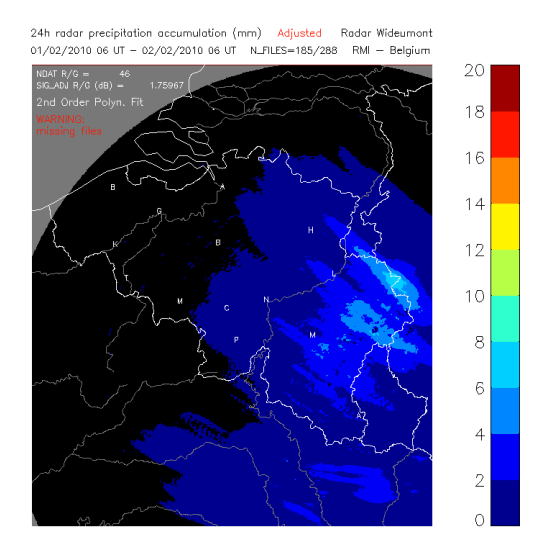


Figure 114 The Wideumont radar image of 2/2/2010 (cumulated rainfall in the previous 24 hours, raingauge-adjusted)

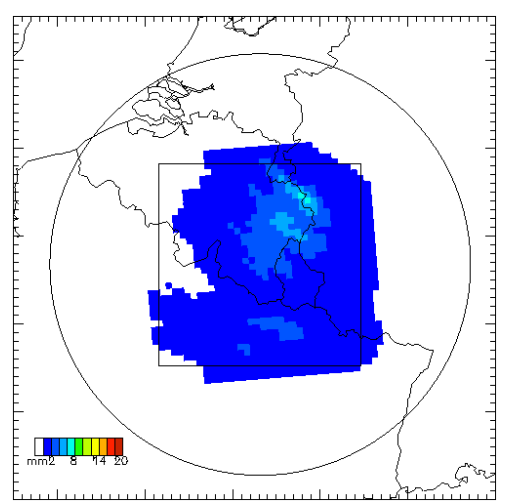


Figure 115 The Wideumont radar image of 2/2/2010 upscaled to the COSMO grid

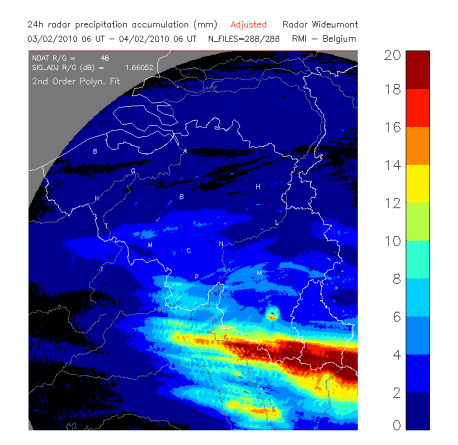


Figure 116 The Wideumont radar image of 4/2/2010 (cumulated rainfall in the previous 24 hours, raingauge-adjusted)



(Product H02 - PR-OBS-2)

Doc.No: SAF/HSAF/PVR-02/1.1 Issue/Revision Index: 1.1

Date: 30/09/2011 Page: 166/177

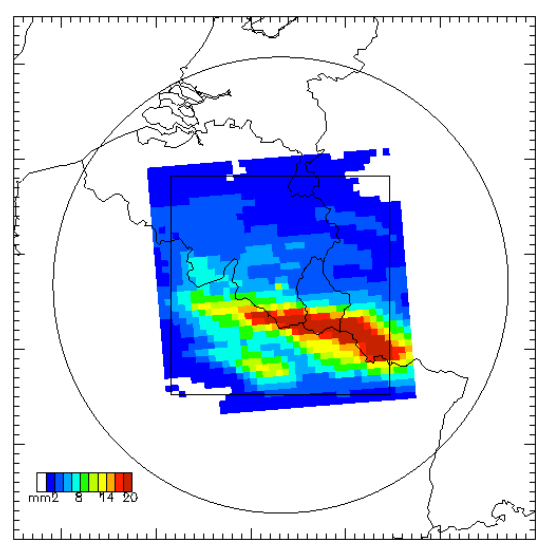


Figure 117 The Wideumont radar image of 4/2/2010 upscaled to the COSMO grid

#### Adaption of the software to all the groups and delivery for testing: present status

After successful testing over Belgium, the software has been adapted for common use by all the other groups, and then delivered for testing. Some feedback from Hungary and Slovakia has already been received and used for improvements. The testing by all the groups is still in progress.

#### References

About the COSMO model rotated grid, see:

http://www.cosmo-model.org/content/model/documentation/core/cosmoDyncsNumcs.pdf pages 21-27.



(Product H02 - PR-OBS-2)

Doc.No: SAF/HSAF/PVR-02/1.1 Issue/Revision Index: 1.1

Date: 30/09/2011 Page: 167/177

#### 14 Annex 7: Working Group 5 "Geographical maps – distribution of error"

#### **PROPOSAL**

Validation activities performed during Development Phase for land and coast areas showed the difference in H-SAF precipitation products quality depending on geographical localisation. Those first achievements as well as the request from Hydrological Validation Group to provide the error characteristic of precipitation products for test catchments made Precipitation Validation Group to set up a Working Group for creating geographical maps of error distribution. The main goals of this working group are:

- to investigate the opportunity to create geographical maps of error distribution for H-SAF validation;
- to define (if necessary) the methodology for spatial representation of precipitation products errors;
- to produce a well referenced documentation on the methodology defined;
- to produce two short reports on the results obtained (first: by 31<sup>st</sup> of March 2011 and second by 30<sup>th</sup> of November 2011);
- to develop if necessary the code to be used in the PPVG for a correct generation of the defined geographical maps of error distribution.

#### **Activities:**

First step – to define the methodology

- selection of the appropriate methodology for spatial distribution of precipitation products errors taking into consideration spatial and temporal characteristics of each product;
- first study performed for selected Polish test catchments as well as Polish territory;

Start Time - End time : December 2010 - March 2011

First Report: 31st of March 2011

#### **Second step**

To define the precipitation products errors maps for country – members of PPVG.

- collection of collocated ground data and satellite products for selected period (possibly through 6300);
- creation of the error maps for territory of PPVG country members for selected period;
- analysis of the achieved results emphasizing the errors distribution obtained for test catchments;
- analysis of the possible solutions for operational creation of the error maps and selection of the best one;
- creation the software (if necessary).

Start Time-End time: March 2011 – November 2011

Second Report: 30<sup>th</sup> of November 2011

Coordinator: Bozena Lapeta (IMGW, Poland) Members: Ibrahim Somnez (ITU, Turkey)



(Product H02 - PR-OBS-2)

Doc.No: SAF/HSAF/PVR-02/1.1 Issue/Revision Index: 1.1

Date: 30/09/2011 Page: 168/177

H-SAF project – Validation Programme- WP 6100 – Working Group 5: Geographical maps – distribution of error *Bozena Lapeta (IMGW, Poland)* 

First report – March 31<sup>st</sup>, 2011

#### Introduction

The Working Group 5 aims at creating geographical maps of H-SAF products' error and analyzing its usefulness for H-SAF validation. The idea of this work stemmed from hydrological validation community that is interested in distribution of the error over the catchments. In this report the results obtained during the first step of WG5 activities aiming at selection of the best method for mean error specialization are presented.

#### Selection of spatialisation algorithm – first results

The most important issue in creating geographical distribution of any parameter is the algorithm for spatial interpolation. As there is no universal spatial interpolation method that can be applied for any parameters, the first step in the creation of maps of H-SAF precipitation products error was the selection of the interpolation algorithm. Commonly used Ordinary Kriging, Inverse Distance Weighted and Natural Neighbour methods were tested firstly. The analysis was performed for monthly average mean error of H-05 3 h cumulated precipitation for selected months. In the analysis data from Polish rain gauges were used. In the next figure the example mean error maps for July 2010 obtained using three mentioned above algorithms are presented.

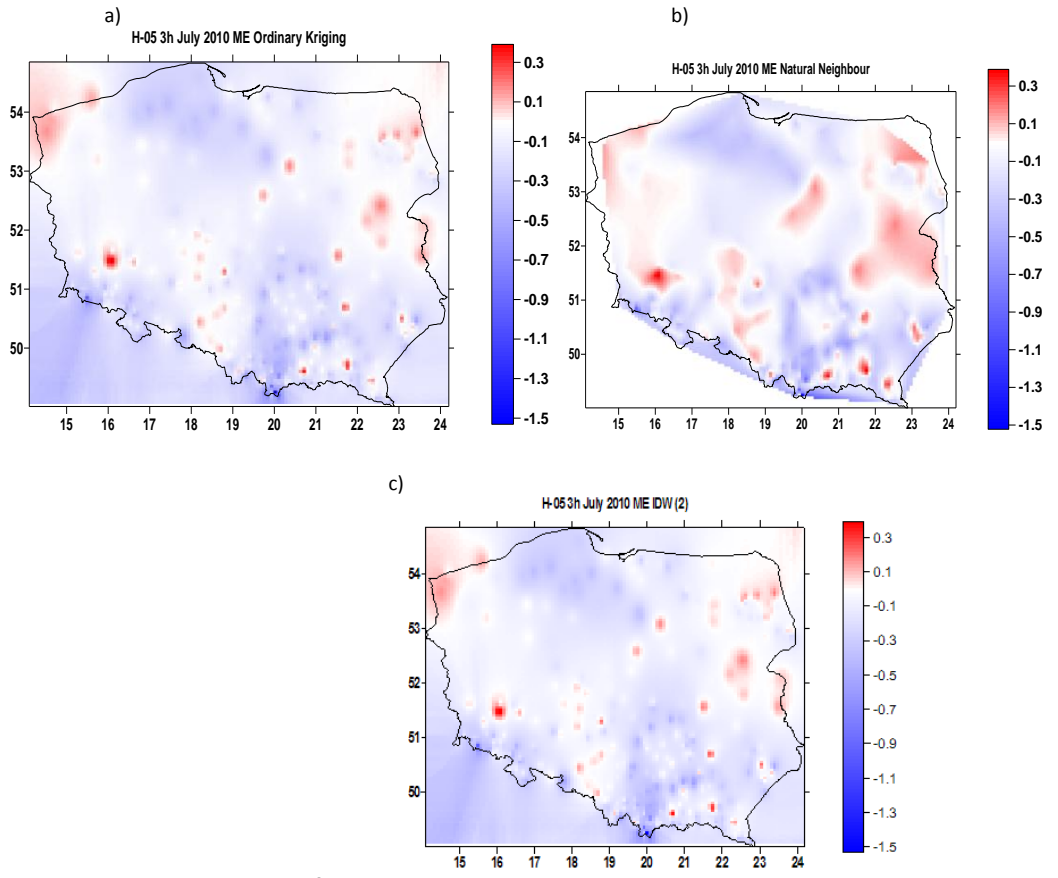


Figure 118 Distribution of the monthly average H-05 3 h cumulated precipitation Mean Error calculated for July 2010 using three methods: a) Ordinary Kriging, b) Natural Neighbour, and c) IDW (2)



(Product H02 - PR-OBS-2)

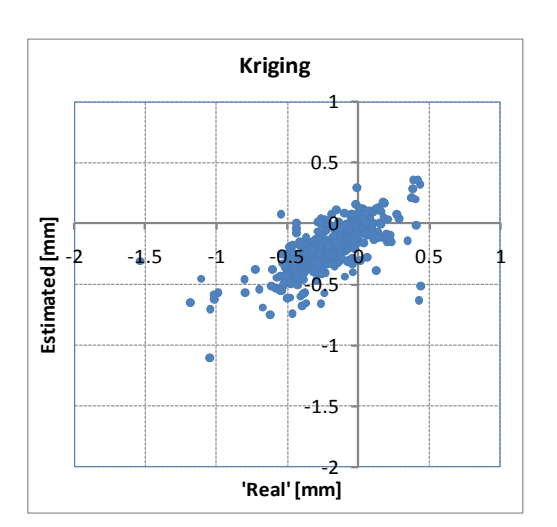
Doc.No: SAF/HSAF/PVR-02/1.1 Issue/Revision Index: 1.1

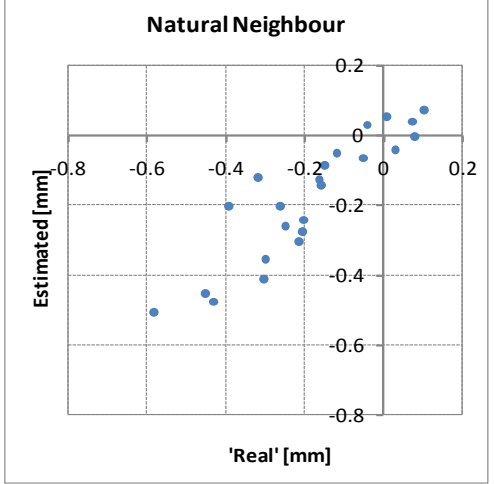
Date: 30/09/2011

Page: 169/177

One can see that the obtained maps do not differ significantly, however, for the map created with the use of Natural Neighbour method, the maximum and minimum values are less pronounced that on the other two maps. Moreover, application of Natural Neighbour method does not allow for extrapolating the distribution beyond the area defined by stations.

In order to evaluate the quality of the error distribution, the cross validation was performed and the results are presented on the next figure.





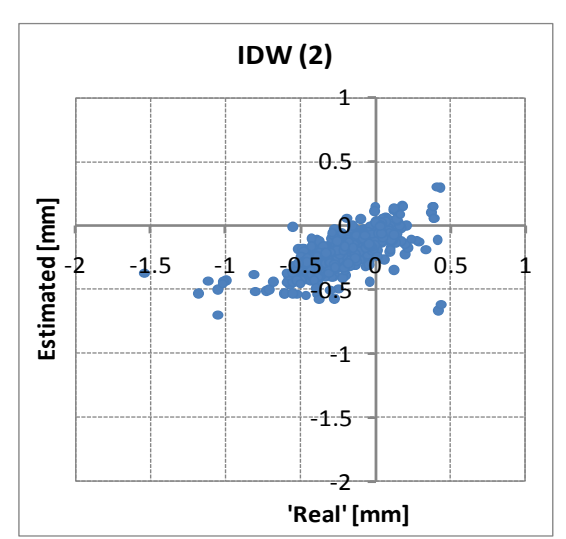


Figure 119 Cross validation results obtained for three different methods for spatial interpolation

For all methods, the results are similarly scattered around the perfect estimation, however, for IDW(2) some underestimation was found for negative ME values. The values of Mean Residual and Mean Absolute Residual defined as mean and mean absolute difference between Estimated and Real values of ME are presented in the next table.



(Product H02 - PR-OBS-2)

Doc.No: SAF/HSAF/PVR-02/1.1

Issue/Revision Index: 1.1

Date: 30/09/2011

Page: 170/177

|                   | Mean Residual | Mean Absolute Residual |
|-------------------|---------------|------------------------|
| Kriging           | -0.004        | 0.09                   |
| Natural Neighbour | 0.007         | 0.06                   |
| IDW(2)            | -0.009        | 0.10                   |

Table 59 Mean Residual and Mean Absolute Residual values obtained for three algorithms for spatial interpolation using cross-validation approach

The lowest value of Mean Absolute Residual was found for Natural Neighbour method, what indicates that application of this algorithm may allow for minimizing the systematical error introduced by spatialisation method. Therefore this method seems to be the best for creating the geographical distribution of H-SAF products error for countries characterized by terrain geographical configuration similar to the Polish one.

#### **Conclusions**

The analysis performed for ME of H-05 3 h cumulated product obtained using data from Polish network of rain gauges showed that Natural Neighbour interpolation method seems to be the best one for creating maps of H-SAF products error. However, application of Natural Neighbour method does not allow for extrapolating the distribution beyond the area defined by stations, what is a disadvantage of these methods.

As the maps are to be created for the whole H-SAF domain, presented above results should be verified over other countries. Therefore, in the next step of WG5 activities the study will be performed for other countries and for the errors calculated using radar data.



(Product H02 – PR-OBS-2)

Doc.No: SAF/HSAF/PVR-02/1.1 Issue/Revision Index: 1.1

Date: 30/09/2011 Page: 171/177

# 15 Annex 8: Comments on the Validation Results for Products PR-OBS-1, PR-OBS-2 And PR-OBS-3

Casella F. \*, Dietrich S. \*, Levizzani V. \*, Mugnai A. \*, Laviola S. \*, Petracca M. \*\*\*, Sanò P. \* , F.

Zauli \*\*

\* CNR-ISAC, \*\* CNMCA, \*\*\*VS EUMETSAT

The results of WGs said that is not possible to consider radar and raingauge fields like the reference and the accuracy indicated in the table 63, RMSD, is the degree of closeness of measurements of a quantity to its actual reference value. The reference value of precipitation fields is not available, and the measurement available are a limited picture of the reference. Then it is important to evaluate which are the limits of "available reference" and then to understand the sources of errors of data used to evaluate the satellite outputs. Taking in account this consideration a direct comparison of the requirements with the result of validation is not correct, since they have different meanings:

- the requirements indicate what *error* is allowed by the user to the satellite product to be significantly useful (*threshold*), or to produce a step improvement in the application (*target*) or to produce the maximum improvement before entering saturation (*optimal*); it is the RMSE of satellite v/s reference.
- the result of validation activities indicate the *difference* between the satellite measurement and the ground measurement utilized as a reference; it is the RMSD of satellite v/s reference.

| Retween target and ontima | Between threshold and target | Threshold exceeded by < 50 %     | Threshold exceeded by ≥ 50 %     |
|---------------------------|------------------------------|----------------------------------|----------------------------------|
| Detween target and optima | Detween unconord and target  | Till colloid exceeded by 4 00 70 | Till collola checcaca by = 00 /0 |

| PR-OBS1                  | F         | Result of |         |            |
|--------------------------|-----------|-----------|---------|------------|
| PR-OBST                  | threshold | target    | optimal | validation |
| Accuracy RMS (> 10 mm/h) | 30 %      | 20 %      | 10 %    | 89 %       |
| Accuracy RMS (1-10 mm/h) | 60 %      | 40 %      | 20 %    | 117 %      |
| Accuracy RMS (< 1 mm/h)  | 200 %     | 100 %     | 50 %    | 232 %      |

Table 1 - Simplified compliance analysis for product PR-OBS-1

| PR-OBS2                  | F         | Result of |         |            |
|--------------------------|-----------|-----------|---------|------------|
| FR-0B32                  | threshold | target    | optimal | validation |
| Accuracy RMS (> 10 mm/h) | 50 %      | 30 %      | 15 %    | 87 %       |
| Accuracy RMS (1-10 mm/h) | 60 %      | 40 %      | 20 %    | 115 %      |
| Accuracy RMS (< 1 mm/h)  | 120 %     | 80 %      | 40 %    | 202 %      |

Table 2 - Simplified compliance analysis for product PR-OBS-2

| PR-OBS3                  | F         | Result of |         |            |
|--------------------------|-----------|-----------|---------|------------|
| PR-OBS3                  | threshold | target    | optimal | validation |
| Accuracy RMS (> 10 mm/h) | 80 %      | 40 %      | 20 %    | 92 %       |
| Accuracy RMS (1-10 mm/h) | 160 %     | 80 %      | 40 %    | 106 %      |
| Accuracy RMS (< 1 mm/h)  | 320 %     | 120 %     | 80 %    | 195 %      |

Table 60 Simplified compliance analysis for product PR-OBS 1-2-3

Obviously, it is RMSD > RMSE, since RMSD is inclusive of:



(Product H02 – PR-OBS-2)

Doc.No: SAF/HSAF/PVR-02/1.1 Issue/Revision Index: 1.1

Date: 30/09/2011 Page: 172/177

- the error of satellite measurements RMSE<sub>sat</sub> (that is what we would like to know from validation);
- the error of ground measurements RMSE<sub>ground</sub> (that should be known by the owners of the stations);
- the error of the comparison methodology RMSEcomparison (that should be estimated by metrologists).

Then we should consider It should be: RMSD = (RMSEsat<sup>2</sup> + RMSEground<sup>2</sup> + RMSEcomparison<sup>2</sup>)<sup>1/2</sup>

In the final part of the H-SAF Development Phase attempts have been made to evaluate RMSEground.

All validation groups (not only for precipitation, but also for soil moisture and snow) have been requested to quote figures to characterise the errors of the ground reference that they used. The various team did this after consultation with the operational units in charge of the observing networks in their institutes. For precipitation the following figures were quoted.

| Unit        | Ground system             | Rain rate                           | 24-h accumulated |
|-------------|---------------------------|-------------------------------------|------------------|
| UniFerrara  | Rain gauge                | 50 %                                | 25 %             |
| UniFerrara  | Radar                     | 100 %                               | 50 %             |
| BfG         | Rain gauge                | 5 ÷ 35 %                            | 5 ÷ 35 %         |
| SHMÚ        | Radar                     | 100 % or 15 mm/h (for RR > 10 mm/h) | 50 ÷ 100 %       |
| OMSZ        | Radar                     | 100 %                               | 50 %             |
| IRM         | Rain gauge (interpolated) |                                     | 70 ÷ 100 %       |
| IKWI        | Gauge-adjusted radar      |                                     | 50 %             |
| IMWM        | Gauge                     | 30 %                                |                  |
| TSMS        | Gauge                     | 25 %                                | 10 %             |
| F           | Gauge                     | 5 <b>+</b> 50 %                     | 5 + 100 %        |
| Error range | Radar                     | 50 ÷ 150 %                          | 50 ÷ 100 %       |

Table 61 Errors of the ground reference provided by all validation groups

The values of table 64, apart from details, indicates that the errors due to the ground reference are of the same order than the threshold requirements. It is interesting to note that the validation activity has indicated that the results from rain gauge and radar are comparable, whereas the error of radar

should be definitively higher. This means that radar is favored in the third error type, RMSEcomparison.

RMSE<sub>comparison</sub> is in reality a composition of several errors. It refers to the limitations of the comparison method that, in spite of all efforts envisaged and implemented by the validation teams, has left residual errors difficult to be further reduced, but needing evaluation by in-depth investigation. A short list is:

- upscaling/downscaling processes to make compatible the instrument resolution and the ground station representativeness have been applied, for instance by applying Gaussian filters, but the statistics of residual errors are not available; this problem affects radar to a minor extent than raingauge, that may explain why comparisons with radar finally are not worse than with rain gauge;
- the raingauge's representativeness of IFOV;



(Product H02 - PR-OBS-2)

Doc.No: SAF/HSAF/PVR-02/1.1 Issue/Revision Index: 1.1

Date: 30/09/2011 Page: 173/177

- pixel geolocation is retrieved by using the information made available by satellite owners, and it is not perfect; it is necessary to evaluate how much mislocations impact on the accuracy of the comparison. The effect is clearly larger for convective precipitation. This may explain why product PR-OBS-3 is apparently performing better than PR-OBS-1 and PR-OBS-2: the high resolution minimizes mislocation errors.

- similarly, time mismatching is a source of error, more effective for convective precipitation, hence the advantage of PR-OBS-3; and also of radar, contributing to reduce the effect of intrinsic lower accuracy.
- parallax errors introduce mislocation of satellite precipitation, with associated comparison errors, larger for convective precipitation because of deeper penetration in the upper troposphere.

These (and maybe other) error sources need to be analyzed in detail in order to determine their contribution to the overall RMSEcomparison. WG and VS started to evaluate the sources of errors, awaiting the final results is it possible to reconsider the requirements like to understand the thresholds of requirements in table 63. Then it is need to anticipate the likely size of these errors. The very low POD values and very high FAR values, as well as the invariably poor values of the correlation coefficient, indicate that RMSEcomparison could be dominant in the error partitioning with RMSEsat and RMSEground. An estimate of the errors due to the various effects impacting the RMSEcomparison is not difficult. It is not necessary to build a large statistics, but just perform experiments using a few campaigns carried out over one dense rain gauge network, and one well-calibrated radar. In fact, the purpose is simply to evaluate the size of RMSEcomparison, not to reduce it (that would require a large effort, probably improductive).

For the sake of providing an example, it is noted that, if the three contributions RMSE<sub>sat</sub>, RMSE<sub>ground</sub> and RMSE<sub>comparison</sub> were of comparable size, equipartitioning of the error would improve the RMSD by a factor  $3^{1/2} = 1.7$ , and the figures resulting from the current validation would match at least the threshold requirements.

In order to obtain an estimate of RMSE $_{comparison}$  and then a more accurate estimation of RMSE $_{sat}$ , CNR-ISAC performed an experiment based on its polarimetric C-band radar (Polar~55C) located close to Rome, surrounded by a network of 14 rain gauges in an area of 14 km  $\times$  14 km (approximately the pixel of SSM/I at 85.5 GHz and of AMSU-B/MHS) generally used for the radar calibration. Assuming Polar 55C as "reference", the the spread of rain gauge measurements resulted as follows:

 $RR > 10 \text{ mm/h} : 50 \% 1 < RR \le 10 \text{ mm/h} : 80 \% RR < 1 \text{ mm/h} : 150 \%$ 

A similar experiment, with 2 rain gauges in reduced area of 5 km  $\times$  5 km (approximately the pixel of SEVIRI at middle latitude), shows similar results. That's means that

In order to obtain an estimate of upscaling / downscaling and interpolation process theoretical experiment of some methodologies has been implemented. Hypothetic perfect fields are been defined and a grid of perfect measurements has been defined. The experiment assumed different typologies of precipitation field respect the variance of precipitation intensity in the field. To obtain the field of perfect measurements some grid points from the precipitation field are been



(Product H02 - PR-OBS-2)

Doc.No: SAF/HSAF/PVR-02/1.1 Issue/Revision Index: 1.1

Date: 30/09/2011 Page: 174/177

removed. The experiment removed the perfect rain gauge long a regular grid to simulate an unreal distribution of non realistic rain gauges.

The sampling has been done at different grid spacing (2, 3 and 4 time the perfect field) to obtain new data at different spatial density. Then, the algorithm performances of up/down scaling procedure to reproduce the original field are been evaluated. The work has been implemented for 4 different algorithms: Barnes, Inverse Distance Squared (IDS), kriging and Nearest Neighbor (NN).

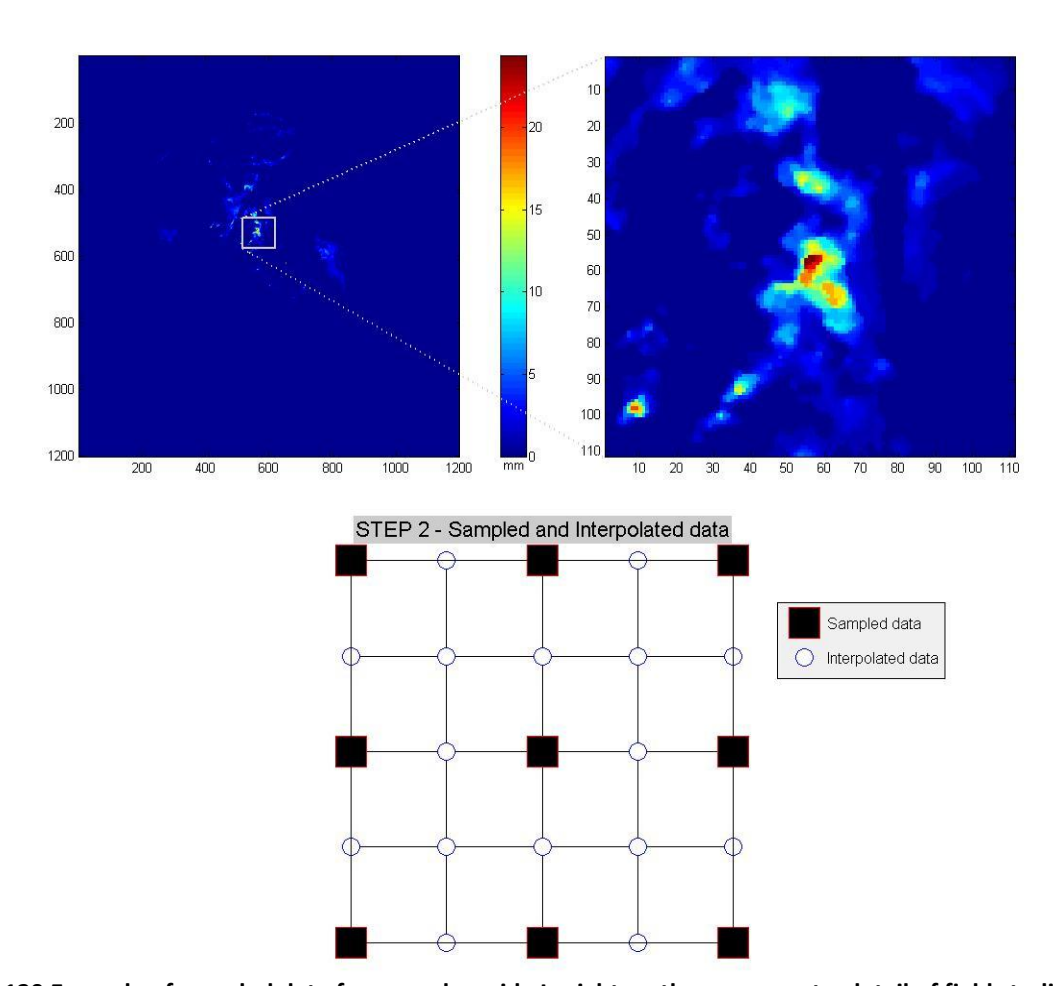


Figure 120 Example of sampled data for a regular grid. In right on the upper part a detail of field studied, below the original grid of field for step 2. From the field the white circles mean the data removed from the map. The black squares mean the position of perfect measurement. The techniques of up/down scaling reproduce the field only from the perfect measurements

The algorithms used in the validation group are similar to the Barnes algorithm. This like-Barnes algorithm creates a grid of regular step where each node contains the data calculated from all data weighted by distance from the node itself. The calculation is done several times (through successive iterations) in order to minimize errors in the precipitation field.

In the following table 65 are reported the values of RMSE were sat<sub>i</sub> is the sampled and captioned data and reference<sub>i</sub> is the value of perfect field.



(Product H02 – PR-OBS-2)

Doc.No: SAF/HSAF/PVR-02/1.1 Issue/Revision Index: 1.1

Date: 30/09/2011 Page: 175/177

$$RMSE\% = \sqrt{\frac{1}{N} \sum_{i=1}^{N} \frac{(sat_i - true_i)^2}{true_i^2}} * 100$$

N is the total number of pairs data in which the reference value is different by 0.

| Algorithms | Step 2    | Step 3    | Step 4        |  |
|------------|-----------|-----------|---------------|--|
|            |           |           |               |  |
| Barnes     | 32 ± 11 % | 52 ± 34 % | $68 \pm 43\%$ |  |
| Kriging:   | 35 ± 12 % | 58 ± 36 % | 77± 62 %      |  |
| NN:        | 56 ± 20 % | 77 ± 45 % | 96 ± 50 %     |  |
| IDS:       | 63 ± 37 % | 71 ± 41 % | 81.± 43 %     |  |

Table 62 RMSE% and standard deviation of interpolation algorithms for 3 different regular grids

In the cases studied, Barnes appears to be the algorithm with the lower mean value of RMSE% and their standard deviation than the other interpolation algorithms, and the error of interpolation can be evaluated in the 30% for the step 2 that means an ideal condition were the rain gauge are disposed long a regular grid with a distance that the half of phenomenon length. The structure of precipitation depends from precipitation typology, time and spatial resolution, therefore phenomenon length cannot be considered absolute.

An irregular distribution of perfect measurements has been considered also. For each step the number of perfect measurement has been redistribuited randomly to simulate the raingauge network. In the figure 124 below the white circles mean the position of perfect measurement points. In the figure 124 below the white circle mean the position of perfect measurement points in the best case (step 2). The results shown again the Barnes tecnique the best choice to reproduce the field.

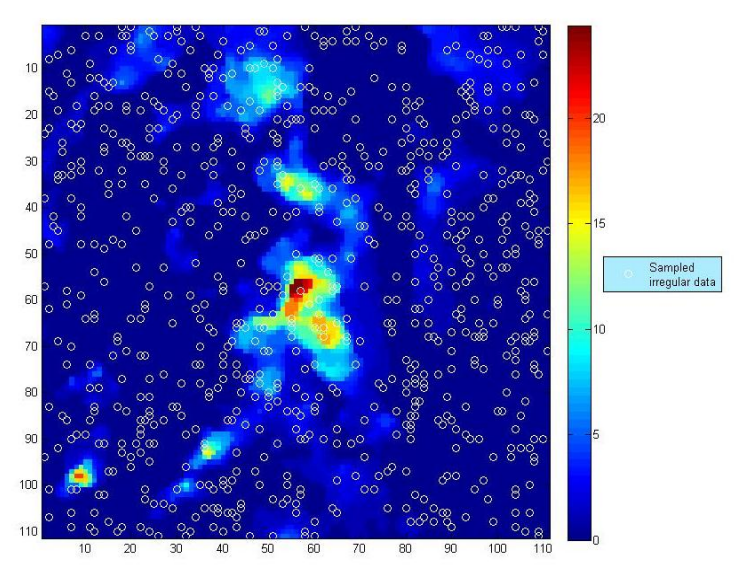


Figure 121 randomly distribution of perfect measurement to remap the field on a regular grid

Assuming the best condition (step 2 for the regular grid), an evaluation of spread of RMSE respect the structure of precipitation field has been done. In the figure 125 below the Barnes and Kriging



(Product H02 - PR-OBS-2)

Doc.No: SAF/HSAF/PVR-02/1.1 Issue/Revision Index: 1.1

Date: 30/09/2011 Page: 176/177

tecniques show a low dependence from the standard deviation of field, ie the level of inomogeneity of field. The performance of up/down scaling tecniques are reported in table below:

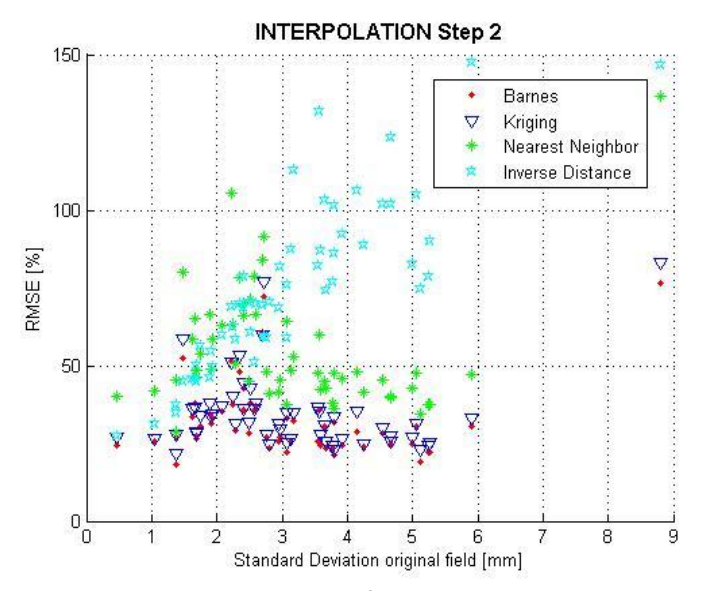


Figure 122 STD vs. RMSE% for interpolations by step 2

Taking into account the results discussed before is possible to define a range of uncertainty that is necessary to consider when comparing the results of validation with operational requirements. More effort has to be done to understand if exist a link between the error of remap procedure and precipitation intensity, but the preliminary study shows that in the best case an error of 30% has to be considered for the up/down scaling remapping procedure.

Using the previous equation we can derive: RMSE<sub>sat</sub> = (RMSD<sup>2</sup> - RMSE<sub>ground</sub><sup>2</sup> - RMSE<sub>comparison</sub><sup>2</sup>)<sup>1/2</sup> where, RMSD is provided by the validation activity, RMSE<sub>ground</sub> is provided by tab. 64 using the University of Ferrara numbers. At the moment for the RMSE<sub>comparison</sub> is assumed: equal to three values resulting from the ISAC study for validation w.r.t. rain gauges, and equal zero for validation w.r.t. radar, plus a 30% for the remapping procedure.

#### **Conclusions:**

1) It is believed that the results of the validation activity cannot be substantially improved: they are

most probably consistent with the size of the error sources (satellite, ground stations and comparison method). This needs to be confirmed by evaluating the size of the error associated with the limits of the comparison technique.

2) It must be considered that the total RMSD is affected by other-than-satellite terms, one of which

RMSEground, very difficult to be reduced, and the other one, RMSEcomparison, possibly dominant (and also very difficult to be reduced). This tells us that the validation figures have a large component, which is independent from the structure of the algorithm.

3) However, the case for continuing algorithm improvement is very strong. Data are produced for being used, and the better the quality, the higher the impact. The fact that the current validation



(Product H02 - PR-OBS-2)

Doc.No: SAF/HSAF/PVR-02/1.1 Issue/Revision Index: 1.1

Date: 30/09/2011 Page: 177/177

methodology cannot completely evaluate the intrinsic error of satellite data is regrettable, but should not prevent a better representation of the physics in the retrieval model.

4) The case for continuing the validation activity essentially as it is now, or improving it if considered cost-effective, is also very strong since it is necessary to continuously watch that the product generation chain works correctly.